Environmental influences on polyphosphate accumulation in microalgae: an investigation into species differences and transcriptional responses.

A thesis presented in partial fulfilment of the requirements for the degree of

Doctor of Philosophy

In

Engineering

at Massey University, Manawatū, New Zealand.

Alexander Cliff

2022

In loving memory of my father

Graham Stephen Cliff

10 April 1947 – 5 September 2022

Abstract

Many species of microalgae can store phosphorus (P) as polyphosphate (polyP) granules during the process of 'luxury uptake', a term describing intracellular P accumulation above levels required for normal metabolism (0.2 – 1% P by dry weight). Environmental conditions can influence P luxury uptake but it is not known whether the effects of environmental conditions on luxury P uptake are the same for all microalgae or whether all microalgae can in fact store P as polyP.

The broad aim of the work described in this thesis was to extend the current knowledge of polyphosphate (polyP) synthesis in microalgae, enabling improved exploitation of their ability to sequester P from water sources and enhance recovery of a vital nutrient. Specifically, the mechanisms by which environmental conditions influence luxury uptake and potential species differences need to be studied to better understand observations at the population level and make informed decisions in the design of treatment processes.

The experimental work was therefore divided into two main objectives:

Objective 1 sought to determine whether there were in fact differences in luxury uptake 'abilities' between species. In Chapter 3, this is explored through the use of genetic database searches, biochemical assays, and protein modelling.

Objective 2 examined the effects of environmental factors known to influence luxury uptake. In Chapter 4, the responses of the microalgae *Chlamydomonas reinhardtii* and *Chlorella vulgaris* to P repletion were studied in a range of conditions to identify similarities and differences in environmental influences. Chapter 5 sought to determine whether the observed differences could be due to responses at the genetic level, by comparing the gene expression levels of P-related genes in *C. reinhardtii* under selected sets of conditions from the previous chapter. An additional experiment was conducted, to examine gene expression without inducing 'noise' through changes in growth conditions, and this is discussed in Chapter 6.

Using protein sequence homology searches, phylogenetic tree generation, protein structure modelling, and biochemical assays (using the chlorophytes *C. reinhardtii*, *C. vulgaris*, *Desmodesmus* cf. *armatus*, *Gonium pectorale*, *Pediastrum boryanum*, and the cyanobacterium *Microcystis aeruginosa*), it was shown that the ability to store P as polyP is common among microalgae, as implied by the broad conservation of the polyP polymerase VTC4, but luxury uptake abilities vary between species. All six tested microalgae responded to P addition following a period of P depletion by accumulating P as granular polyP. Under the conditions tested, the total P assimilated over 24 hours was similar for five of the microalgae tested (2.6 – 3.6% P by dry weight) but *C. vulgaris* assimilated considerably less P (~1.2% P) than the others.

The effects of environmental conditions on P uptake and polyP accumulation were assessed by triggering luxury uptake in *C. vulgaris* and *C. reinhardtii* in different conditions of light supply, temperature, and pH, with different P repletion doses following different P depletion times.

P uptake and polyP accumulation were influenced by light supply, P depletion time, and P repletion dose in both microalgae but P dose had the strongest influence in *C. reinhardtii* versus light supply in *C. vulgaris*. PolyP was still accumulated by these two species in conditions suppressing growth and severely repressing metabolism (10 °C and darkness), evidencing that P uptake and polyP synthesis do not require light energy.

The model alga *C. reinhardtii* was then used to evaluate, for the first time, whether the differences in P uptake and polyP accumulation observed with respect to differences in environmental conditions were associated with differences in gene expression.

Although the genes assessed were downregulated (relative to controls) 24 hours after P repletion, as expected, in all experimental conditions, changing conditions at the start of the experiment also caused changes in gene expression in controls, making it hard to distinguish responses to P repletion from ‘global’ responses to changing conditions. Another experiment was therefore performed where temperature and light intensity were maintained constant before and after P

repletion. The results confirmed that increased P repletion dose and P depletion time were associated with increased P uptake and polyP accumulation over 24 hours.

The results evidenced the expected downregulation of *PSR1*, *VTC4*, *VTCX*, and *PTB5* after 1 hour of P repletion, but this response was much more salient after 7 days of P depletion (compared to 3 days). Changes in gene expression were also associated with P repletion dose, but only after 7 days of P depletion. This showed that the response to P repletion is stronger after a longer P depletion time but the observed expression changes did not support the hypothesis that these changes were the reason for the higher observed P uptake and polyP accumulation.

For the first time, it has been systematically shown that the ability to accumulate P as polyP is widespread among microalgae but that the kinetics of P accumulation vary between species and this species-dependence is influenced by environmental factors. These factors engender differences at the level of gene expression, involving both components of the VTC complex and phosphate transporters. However, the differences in P uptake and polyP accumulation may be better understood by investigating the structural differences and changes in activity of relevant proteins.

Acknowledgments

I would like to start by acknowledging my supervisors, Prof. Benoit Guieysse, Dr Maxence Plouviez, and Dr Nicola Brown, for their patience, wisdom, and guidance throughout this work. Their feedback has been instrumental to ensuring the quality and consistency of my writing. The training on laboratory procedures, by Dr Plouviez, has been invaluable and his encouragement throughout has been profoundly helpful.

I am very grateful to Prof. Peter Lockhart from the School of Natural Sciences at Massey University and Prof. Eric Dubreucq from L'Institut Agro, Monpellier, France for their guidance and contributions to Chapter 3.

I also greatly appreciate the advice I have received from Trish McLenachan from the School of Natural Sciences and Dr Matthew Sells from the School of Food and Advanced Technology, Massey University.

I would like to thank Massey University, the technical and administrative staff of the School of Food and Advanced Technology, my colleagues, friends, and family for all their support.

Lastly, I wish to thank the Royal Society for providing the funding that enabled me to undertake this work.

Table of Contents

Table of Figures

Table of Tables

Abbreviations

ADP	Adenosine 5′-diphosphate
AISP	Acid-insoluble polyphosphate
ASP	Acid-soluble polyphosphate
ATP	Adenosine 5′-triphosphate
cDNA	Complementary DNA
CO_2	Carbon dioxide
CPC	Cellular phosphorus content
C_q	Quantification cycle (also C_T or C_p)
DAPI	4′,6-diamidino-2-phenylindole
DNA	Deoxyribonucleic acid
DW	Dry weight
EBPR	Enhanced biological phosphorus removal
MM	Minimal medium
N	Nitrogen
OD	Optical density
P	Phosphorus
PAR	Photosynthetically active radiation
PCR	Polymerase chain reaction
P_i/PO_4^{3-}	Inorganic phosphate
PolyP	Inorganic polyphosphate
PPK	Polyphosphate kinase
PPN	Endopolyphosphatase
PPX	Exopolyphosphatase
RNA	Ribonucleic acid
RT-qPCR	Reverse transcription quantitative (real-time) PCR
sp.	Species (singular)
spp.	Species (plural)
VTC	Vacuolar transporter chaperone
WSP	Waste stabilization pond

Chapter 1 Introduction

Phosphorus (P) is involved in many biochemical processes (Schindler & Vallentyne, 2008) and forms the backbone of biological compounds such as nucleic acids (genetic material), phospholipids (cell structure), and ATP[1] (metabolism). Life-sustaining terrestrial and aquatic phosphorus stores originate from the erosion of rock phosphate – the accumulation of igneous rock and sedimentary rock pushed up from the ocean floor by tectonic processes. Much biological material is ultimately washed into the oceans, where it decays in the sediment layer and remains there until brought to the surface by plate tectonics, thus completing a cycle on a geological time scale (Solovchenko et al., 2016).

Intensification of agriculture has led to the increased use of mineral resources as fertilizer to supplement nutrient-depleted soils and maintain high levels of crop production. However, the over-application of fertilizers causes nutrients such as P to leach into waterways where they can harm aquatic ecosystems. An additional nutrient burden comes from inefficient wastewater treatment processes: chemical precipitation can be cost-prohibitive for treatment plants in small communities and typically produces aluminium-contaminated sludge which must be disposed of in landfills at additional cost. P removal by biological means promises the recovery of bioavailable P for use as fertilizer but recovery rates are often low, resulting in undesirable levels of P discharge into receiving waters.

Algae are employed widely in waste stabilization ponds (WSP) for their ability to grow under a range of conditions, using energy from sunlight and nutrients from wastewater to produce biomass. This simple and low-cost treatment method enables the recovery of nutrients through assimilation into biomass but removal rates can be sub-optimal. P assimilation in microalgae is sometimes greater than the cell's immediate metabolic needs and results in storage of P for later use, a mechanism known as 'luxury uptake' (Levin & Shapiro, 1965). Although observed in many

[1] ATP: Adenosine 5′-triphosphate, the 'energy currency' of cellular metabolism.

microalgal species, and potentially providing a way to improve nutrient removal in WSP, luxury uptake is not well understood at the cellular level. Recent studies have identified several environmental conditions influencing luxury uptake in microalgae (Powell et al., 2008; Sells, Brown, & Shilton, 2018) but a review of the literature suggests that the responses to changes in P availability are species-dependent and selection of appropriate species for P removal processes could be critical to their success (Lavrinovičs et al., 2021).

Considering the fast depletion of rock phosphate (currently the main source of P fertilizer), and the increased attention on the degradation of river water quality, this new knowledge would have broad implications for the agricultural, environmental, and biotechnological sectors.

Following a review of the literature (Chapter 2), the following hypotheses have been formulated:

I. The ability of microalgae to perform luxury uptake is widely observed because it is innate to all microalgae and is due to conservation of the genes encoding polyP polymerases.

II. The amount of polyP accumulated in microalgae is species-dependent but differences depend on environmental conditions (more favourable to one species than another).

III. The influences of environmental conditions on polyP accumulation are the result of different gene expression responses (within the polyP pathway) in different conditions.

Chapter 2 Literature Review

2.1 Environmental impacts of phosphorus use

Phosphorus (P) is considered a limiting nutrient in many aquatic ecosystems, particularly in freshwater environments (González-Gil et al., 1998; Kulakova et al., 2011). Increased nitrogen (N) and P concentrations in waterways often result from human activities (e.g., farm runoff, urban stormwater contamination, or inadequate wastewater treatment) and are known to contribute to eutrophication[2]. Eutrophic conditions can cause overgrowth of microalgae, causing adverse effects for other aquatic species. Some microalgae, particularly cyanobacteria, also produce toxins that make waterways unsafe for fishing, recreational activities, and water supply (Solovchenko et al., 2016).

Algal blooms, the most salient indicators of eutrophication, typically occur during the warmer months, when conditions are favourable for plant growth and water flows are low (Nazari-Sharabian, Ahmad, & Karakouzian, 2018). However, the occurrence of microalgal blooms can be difficult to predict as, counter-intuitively, the phosphorus concentration of the water is usually low prior to their onset (Schindler & Vallentyne, 2008).

Reduction of P and N discharges from point sources such as wastewater treatment plants is critical for reducing eutrophication downstream (Nazari-Sharabian et al., 2018). The traditional approach to treatment processes, focused on increasing water clarity, paradoxically promotes microalgal growth through increased light penetration (Levin & Shapiro, 1965). Consequently, authorities responsible for treating wastewater must broaden the range of treatment processes to increase nutrient removal and reduce eutrophication. Furthermore, the introduction of P and N from non-point sources, such as farm runoff, still presents problems. It has been estimated that inefficient use of P results in 80% losses (Solovchenko et al., 2016), much of it due to over-fertilization of

[2] Eutrophication: Abnormally high nutrient levels which lead to overgrowth of microalgae and aquatic plants and result in the lowering of dissolved oxygen concentrations, through aerobic degradation of decaying biomass and nocturnal respiration (Craggs, 2006), which can be detrimental to aquatic ecosystems.

farmland. Mitigation of pastural nutrient losses (and their impacts on the environment) may be achieved through better fertilizer management (Monaghan et al., 2007), the use of slow-release fertilizers such as wastewater-derived struvite (Talboys et al., 2016), riparian planting, and enhanced plant uptake via the use of soil microbes (Susser, Pelini, & Weintraub, 2020), and manipulation of plant P-scavenging genes (Gaxiola, Edwards, & Elser, 2011).

2.2 Phosphorus: A limited and vital natural resource

Global phosphate mining was estimated at 270 million metric tons in 2018, while total stocks were estimated at 70 billion metric tons in 2019 (USGS, 2019). Phosphate rock is now considered a critical raw material (Egle et al., 2016) and, at the current rate, economically-viable rock phosphate for fertilizer is predicted to be exhausted within 50 to 100 years (Cordell, Drangert, & White, 2009). Although some estimates suggest a longer lifetime, they may not have taken into account the increasing costs of extraction and decreasing quality of remaining stocks (Cordell et al., 2009), or may assume that those mineral stocks presently uneconomical to extract may be accessible in the future, as technology advances. Rock phosphate stocks are largely located in a few countries (Gilbert, 2009) and global supply chains may be vulnerable to regional political instability (Hutching, 2018) and fossil fuel price rises (Cordell et al., 2009).

The diminishing availability of phosphorus (P) poses a serious threat to agriculture worldwide as the use of fertilizers accounts for up to 50% of crop yields (Stewart & Roberts, 2012). The global population is steadily rising and expected to reach 9.3 billion by 2050 (Stewart & Roberts, 2012), yet the need to ensure future P supply to produce sufficient food for this growing population has not been adequately addressed (Cordell et al., 2009).

2.3 The economic potential of phosphorus recovery

For countries dependent on agriculture for export earnings, such as New Zealand, rising commodity prices can severely impact the bottom line for farmers and the fertilizer industry. In 2019, 154,000 tonnes of P were sold as fertilizer in New Zealand alone (Stats NZ, 2021b). In the

same year, 71,000 tonnes of P were applied to farmland as superphosphate and 42,000 tonnes as diammonium phosphate (Stats NZ, 2021b). At current prices (Ballance, 2022; Ravensdown, 2022), the cost of these fertilizers would be around NZ$600 – 700 million and this does not include other P-containing fertilizers.

In New Zealand, P losses from fertilizer runoff are estimated to be between 1 and 10 kg per hectare per year for dairy-dominated land and 0.1 – 2.2 kg P per hectare per year for sheep and beef (McDowell & Nash, 2012). As of 2019, approximately 9 million hectares of farmland were used for sheep and cattle farming in New Zealand (Stats NZ, 2021a) and the estimated P losses through runoff could be worth millions of dollars (Table 1) without including other agricultural and horticultural activities and the costs associated with transport and land application. Clearly, there is economic benefit in reducing costs due to P losses.

Table 1. New Zealand land usage for sheep and cattle and estimated P losses through runoff.

Land use type	**Area (million ha)** [a]	**P losses (kg P·ha^{-1}·y^{-1})** [b]		**P losses (kT P·y^{-1})**		**Cost of losses (million NZ$·y^{-1})** [c]	
		Low	High	Low	High	Low	High
Sheep	4.1	0.1	2.2	0.4	9.0	1.7	53.0
Beef	2.7	0.1	2.2	0.3	5.9	1.1	34.9
Dairy	2.2	1	10	2.2	22	9.1	129.3
Total	9.0					11.9	217.3

[a] Stats NZ (2021a)

[b] McDowell and Nash (2012)

[c] Costs were calculated based on the range of 2022 prices for superphosphate fertilisers (Ballance, 2022; Ravensdown, 2022).

Besides the cost of resource wastage, the effects of eutrophication also have a financial impact. It has been estimated that these costs may amount to billions of dollars annually in the United States (Dodds et al., 2009).

2.4 Current technologies for phosphorus recovery

The recovery of phosphorus in a bioavailable form presents an opportunity for mitigating environmental effects and simultaneously reaping economic benefits (see Section 2.3). P recovered from domestic wastewater has the potential to replace 15-30% of the global demand for rock phosphate (Yuan, Pratt, & Batstone, 2012), but this might be increased significantly if P could also be recovered from industrial and agricultural wastewater. The phosphorus concentration in domestic wastewater is typically below 11 mg $P \cdot L^{-1}$ (Tchobanoglous, Burton, & Stensel, 1991), meaning P must be concentrated to make recovery feasible using existing technologies (Yuan et al., 2012). In comparison, industrial wastewaters may contain up to 100 mg $P \cdot L^{-1}$ and livestock effluent, even higher concentrations (Yuan et al., 2012).

Current technological approaches to removing P from wastewater, as discussed below, are mainly based on adsorption, precipitation, and sedimentation, and assimilation into biomass (Craggs, 2006).

2.4.1 Chemical/physical processes

Although P may be present in insoluble particulate or colloidal form in wastewater, its major form is dissolved phosphate (Craggs, 2006; Dueñas et al., 2003). Phosphate precipitation can occur naturally, depending on the prevailing conditions, or can be triggered by chemical addition (Serafim et al., 2002). Natural phosphate precipitation is primarily triggered by high pH. During wastewater treatment in waste stabilisation ponds, this is often a consequence of CO_2 removal by photosynthetic microorganisms (Hemens & Mason, 1968), but lower pH at night, when photosynthesis is absent, may result in re-solubilization of P from the sludge layer[3] (Crimp, 2015). Nutrient release from settled sludge can reduce removal efficiency (Craggs, 2006), but this can be reduced by regular de-sludging, albeit at considerable cost.

[3] Sludge layer: Layer of solid material formed at the bottom of a treatment tank, basin, or pond, by settling.

Wastewater treatment plants serving larger municipalities frequently remove dissolved phosphorus during the post-biological stages by precipitation using soluble salts such as aluminium sulphates (alum), iron sulphate, iron chloride, or calcium oxide (lime) (Dueñas et al., 2003). These chemicals react with phosphate to form insoluble salts that precipitate as a sludge that is subsequently removed (Pratt et al., 2012). The efficacy of these salts may be enhanced by the addition of polymers, which bind small particles in highly settleable flocs (Pratt et al., 2012).

P may also be precipitated in the form of minerals such as struvite ($NH_4MgPO_4 \cdot 6H_2O$), which serves as an effective fertilizer, but its formation often requires magnesium addition (Craggs, 2006) and a P concentration higher than is normally found in domestic wastewater (Yuan et al., 2012). Struvite can also be formed biologically, although the potential for this mechanism for P removal from wastewater has not been widely explored (Pratt et al., 2012).

Insoluble (particulate) material cannot be chemically precipitated but can be removed through sedimentation by applying appropriate design considerations or may be adsorbed to material in the sludge layer of treatment ponds (Craggs, 2006). Adsorption may also be effected through the addition of nanomaterials and polymers (Pratt et al., 2012).

2.4.2 Biological processes

Biological processes can effect phosphorus removal through assimilation into biomass. However, efficient P removal by assimilation requires that conditions are suitable for growth and that the population density is sufficiently high. The typical N:P ratio of domestic wastewater is around 4:1, which is lower than that required by most organisms, so P removal through biomass growth is generally limited by N availability (Craggs, 2006).

However, many microorganisms are able to store phosphorus at levels greater than those required for normal metabolic function, a phenomenon which has been termed ‘luxury uptake’ (Harold, 1966). This phosphorus is primarily stored as inorganic polyphosphate (polyP; see Box 1).

Box 1: Polyphosphate – structure and natural occurrence

Inorganic polyphosphate (polyP) is a condensed polymer of a few to many thousands of phosphate residues linked by high-energy phosphoanhydride bonds (Ault-Riché et al., 1998; Kulaev & Vagabov, 1983; Kulaev, Vagabov, & Kulakovskaya, 2004). Although described primarily as a linear polymer (e.g. Akiyama, Crooke, & Kornberg, 1992; Docampo & Moreno, 2011), having the general form $M_{(n+2)}P_nO_{(3n+1)}$, where M is a cation (Kulaev et al., 2004), they also exist in cyclic or branched forms (Christ et al., 2020). The cyclic 'metaphosphates' are typically shorter-chain polymers with the much simpler general form MPO_3 (Kulaev et al., 2004).

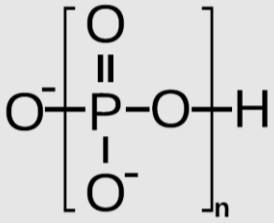

Figure 1: Molecular structure of polyP.

PolyP has been identified in all organisms in which it has been sought out, from bacteria to mammals, and is believed to have pre-dated life itself (Kornberg, Rao, & Ault-Riche, 1999). Its presence has been reported in many species of algae (Keck & Stich, 1957; Sommer & Thomas, 1938), bacteria (Clark, Beegen, & Wood, 1986), protozoa (Ruiz, Rodrigues, & Docampo, 2001), archaea (Serrano et al., 2004), yeasts (Wiame, 1949), fungi (Ashford, Ryde, & Barrow, 1994; Callow et al., 1978), amoebae (Gezelius, 1974), plants (Seufferheld & Curzi, 2010), and mammals (Kumble & Kornberg, 1995; Ruiz et al., 2004).

When luxury uptake occurs as the result of microorganisms acclimatized to P deficiency being abruptly P-enriched, the rapid accumulation of polyP that results is described as 'polyphosphate overplus' (Harold, 1964), 'over-compensation' (Aitchison & Butt, 1973), or 'overshoot' (Cembella et al., 1984) and can be used in laboratory settings to trigger luxury uptake on demand.

This process may represent an adaptive strategy for coping with intermittent P supply by storing as much P as possible when the opportunity presents itself. There is a great deal of interest in understanding this process as it has potential for improving the efficiency of the biological removal of P from wastewater (Solovchenko et al., 2016). Increasing the P-storing ability of microorganisms could reduce the land area required for treatment processes that use photosynthetic organisms (Shilton, Powell, & Guieysse, 2012). However, although there is clear evidence that luxury uptake can occur in wastewater environments, the P concentrations in WSP are not typically growth-limiting (Powell et al., 2008), so it is unlikely that luxury uptake in these situations is the result of the overplus response (Brown & Shilton, 2014).

2.4.2.1 Enhanced biological phosphorus removal

The P accumulation abilities of bacteria are used in a modified activated sludge process[4] specifically designed for P removal: enhanced biological phosphorus removal (EBPR). This is a two-phase biological treatment process in which polyP and organic compounds are alternately stored within the cells, resulting in a net increase in assimilated P (Dueñas et al., 2003; Yuan et al., 2012). Wastewater bacteria have been reported to store polyP at up to 30% of their dry biomass weight (Docampo, 2006; Kulaev, Vagabov, & Kulakovskaya, 1999). Consequently, this process is quite efficient, removing more than 90% of influent P from a variety of sources, and increasing the P concentration of sludge to 5-7% (Yuan et al., 2012). This high-P sludge is an effective substitute for P fertilizer although the low N:P ratio in EBPR biosolids is unfavourable for plant growth and therefore requires additional N fertilizer application (Yuan et al., 2012). Consideration must also be given to removal, transport, and storage/disposal of sludge, particularly the timely removal of biomass to avoid sludge degradation leaching P back into the treated water (Brown & Shilton, 2014; Powell et al., 2011b).

[4] Activated sludge process: Biological wastewater treatment process in which a fraction of the biomass-laden sludge removed is returned to the reactor to maintain the waste-degrading microbial population (Tchobanoglous et al., 1991).

Although the use of EBPR technology has increased in recent years, it is not appropriate for many small communities due to high capital and operating costs and the requirement for on-site operator control (Brown & Shilton, 2014; Powell et al., 2009; Sells et al., 2018). Furthermore, P removal may be hampered by competition between the so-called phosphorus-accumulating organisms and glycogen-accumulating organisms for carbon substrates (Pratt et al., 2012; Yuan et al., 2012). In the event of reactor failure, which may occur without an obvious cause (Blank, 2012), it is difficult to prepare an inoculum for replacement, as these organisms are not typically lab-culturable (Keasling et al., 2000), making them difficult to isolate and selectively enrich.

2.4.2.2 Waste stabilization ponds

For many farms and small communities, appropriateness of wastewater treatment technology means simplicity, low cost, and low maintenance requirements. For this reason, waste stabilization ponds (WSP) are a popular solution utilizing naturally occurring microbial populations, including microalgae and bacteria, to break down waste. However, although these ponds are effective for the removal of pathogens and organic carbon (Brown & Shilton, 2014), they are not designed for nutrient removal, which limits their perceived usefulness and potential future uptake as a treatment technology in the face of increasingly stringent regulations (Craggs, 2006).

WSPs account for a high proportion of wastewater treatment processes in New Zealand, but there has been limited research into the potential for these to effect P removal through luxury uptake (Brown & Shilton, 2014). The cellular phosphorus content (CPC) of microalgae, as required for normal metabolism, is typically around 0.2 – 1% of biomass by weight (Plouviez et al., 2021; Powell et al., 2009), but luxury uptake can increase this to over 3% (Powell et al., 2008). However, the minimum phosphorus content can vary between species (Schmidt, Gagnon, & Jamieson, 2016) and may change at different life cycles stages (Crimp, Brown, & Shilton, 2018); therefore, CPC may be an inconsistent metric for P removal efficiency.

2.4.2.3 Factors influencing luxury uptake in microalgae

It has been observed that polyP accumulation is enhanced in conditions less favourable for growth (Aitchison & Butt, 1973), suggesting that there is competition for resources between polyP synthesis and growth. According to Harold (1963), a reciprocal relationship exists between the formation of polyP and that of nucleic acids, due to competition for intracellular P, so increased growth is liable to reduce the production of polyP.

Using laboratory-scale simulations of waste stabilization ponds, several conditions influencing luxury uptake by microalgae have recently been identified (Powell et al., 2009; Powell et al., 2008; Sells et al., 2018). Light intensity, temperature, organic loading, pH, influent P concentration, and mixing influence the degree of luxury uptake by microalgae (Table 2).

P concentration and light intensity

Powell et al. (2008) found that the influent P concentration alone did not have a significant effect on luxury uptake, even though higher P availability might be expected to result in higher P storage. However, cellular P content was higher when both P concentration and light intensity were both increased, consistent with an earlier observation by Kuhl (1962) that P uptake is correlated with P concentration in the light but not in the dark. The effect of light intensity on its own appears to vary, as shown in Table 2. Although light might promote P uptake, it also provides energy for cell growth, and the overall effects on cellular P content will depend in part on the rate of growth. Also, consumption of polyP stores may provide an alternative source of P for growth when light intensity is high and exogenous P supply is limited, which might explain the negative correlation between light intensity and luxury uptake observed by Powell et al. (2008). At low light levels, the rate of polyP consumption is reduced, resulting in a higher degree of accumulation (Brown & Shilton, 2014). Although light may stimulate increased luxury uptake, it is not necessary for polyP formation (Harold, 1966; Healey, 1973).

The internal P concentration (or ‘P quota’) is also influential on the rate of P uptake and has been incorporated into uptake rate models such as the well-established model of Droop (1973). The

kinetics of P uptake have also been described as being those of non-competitive enzyme inhibition (Rhee, 1973), in which the concentrations of internal P-containing compounds (including polyP) can influence the activity of the enzymes responsible for transporting P into the cell.

Prior P depletion

The 'overplus' phenomenon demonstrates that prior P depletion[5] enhances luxury uptake but the mechanisms underlying this enhancement are unclear. Growth and P uptake are considerably enhanced when P repletion[6] is preceded by a P-depletion period. However, an extended period of P depletion can inhibit growth and P uptake in some species (Hernandez, de-Bashan, & Bashan, 2006; Lavrinovičs, Mežule, & Juhna, 2020). On the other hand, insufficient P-depletion time results in cultures being 'incompletely starved' at the time of P repletion (Lavrinovičs et al., 2021).

Lavrinovičs et al. (2021) found that P uptake was enhanced by a prior P depletion period of 3 – 5 days, and was influenced by the duration of P depletion, but the timing varied between species. Effects on polyP accumulation were not clear in all cases, due to polyP reserves being detected even after 5 days P depletion.

In experiments using the green microalga *Chlorella vulgaris*, Aitchison and Butt (1973) found that the amount of polyP accumulated via luxury uptake increased with the duration of phosphate starvation but decreased in proportion to the concentration of polyP within the cells prior to refeeding.

Mixing

Adequate mixing is important to maximize the uptake of P by microalgae, by increasing exposure to nutrients and influencing the diffusion gradient across the boundary layer (Grobbelaar, 2004; Sells et al., 2018). Although Sells et al. (2018) found that mixing reduced luxury uptake, no

[5] Reduction of available extracellular P, by replacing the growth medium with a P-free medium or allowing the culture to exhaust extracellular P through normal metabolism.

[6] Addition of a bioavailable form of P to the growth media to restore growth conditions.

correlation was observed at mixing rates greater than those required to just suspend the microalgae. Additionally, while mixing had a positive effect on P uptake, the effect on growth was greater, resulting in the observed net overall CPC reduction. Mixing is also important for increasing light availability, particularly in dense populations where cells are subject to mutual shading (Powell et al., 2009).

Organic loading

Sells et al. (2018) demonstrated that reducing influent organic loading, thereby limiting heterotrophic growth, can increase luxury uptake by microalgae. However, changing the organic loading did not have an effect on P assimilation but reduced luxury uptake by 'diluting' intracellular P when higher organic loading led to higher growth.

Cations

The presence of cations is associated with polyP accumulation in both prokaryotes and eukaryotes, as polyP is a polyanionic compound which complexes with cations (Kulaev et al., 2004). Therefore, the availability of cations could be important for polyP synthesis. It is worth noting that while Sells et al. (2018) found no effects of calcium (Ca^{2+}), magnesium (Mg^{2+}), and potassium (K^{+}) concentrations on polyP synthesis at the typical cation concentrations found in wastewater, Siderius et al. (1996) demonstrated a positive correlation between Ca^{2+} concentration and polyP synthesis at a higher concentration. Furthermore, Peverly, Adamec, and Parthasarathy (1978) observed that *Chlorella pyrenoidosa* cells were unable to accumulate polyP in the absence of K^{+}, but were not affected by the absence of Ca^{2+} of Mg^{2+}.

Temperature

Temperature was positively correlated with luxury uptake above 15 °C (Powell et al., 2009; Powell et al., 2008), although other researchers found no correlation at lower temperatures (Crimp et al., 2018; Schmidt et al., 2016). Powell (2008) also found significant negative interaction effects (i.e., the effect of one of the variables is diminished by an increase in the other) on luxury uptake,

occurring between temperature and P concentration, and between light intensity and temperature. These effects are difficult to interpret and suggest that the effects of light intensity and temperature on growth metabolism may obscure concurrent effects on P uptake when changes in cellular P content are used as the primary metric for luxury uptake.

Nutrient ratio

Lavrinovičs et al. (2020) compared the P uptake, growth, and polyP accumulation of three microalgal species grown in primary and secondary wastewaters with N:P ratios of 3:1 and 1:1, respectively (and equal P concentrations). These authors found that all three species assimilated more P and accumulated more polyP in the primary wastewater. They also noted that higher growth of *Desmodesmus communis* and *Tetradesmus obliquus* in the secondary wastewater resulted in a greater pH increase and consequent P precipitation.

pH

Increasing acidity has been shown to decrease polyP accumulation (Docampo, Ulrich, & Moreno Silvia, 2010). This effect is believed to be linked to the changes in ionic speciation of phosphate with changing pH and selective absorption, as well as effects on membrane-bound enzymes (Cembella, Antia, & Harrison, 1982; Kuhl, 1962).

Species

Using data collected from laboratory-scale simulations and novel image-processing method for quantifying polyP granules in microalgal cells, Sells (2019) established a regression equation for predicting luxury P uptake from environmental parameters in mixed cultures. This equation has an excellent predictive ability but was improved by using coefficients specific to the microalgal genus, raising the possibility of species-specific responses to the environmental parameters.

Although many microalgal species have been described as capable of P luxury uptake in the literature, differences in the response to P repletion with or without prior P depletion have been

observed at the genus level (Lavrinovičs et al., 2020; Lavrinovičs et al., 2021) and even between species of the same genus (Hernandez et al., 2006). However, there is currently a need for more work examining the effects of a range of important parameters at the genus or species level (Brown & Shilton, 2014).

2.4.2.4 Enhanced phosphorus removal by microalgae

The potential for P removal by microalgae may be higher than the removal efficiency currently achieved in ponds if conditions can be optimized, but it is important to take a holistic approach by considering how changes in metabolism to achieve high P assimilation may impact on other aspects of the treatment process.

Maximal P uptake is achieved by combining factors favourable to P uptake and high cell density, although the latter may also impact nutrient transport and light availability. Higher levels of luxury uptake can be obtained by limiting growth, but reduced growth may be detrimental to COD removal. A 'luxury uptake pond' system has been proposed to maximize the potential of microalgal ponds (Powell et al., 2009; Sells et al., 2018). The first stage is an anaerobic pond to reduce organic load (with limited P removal). This stage is followed by a well-mixed aerobic pond in which P would be assimilated and stored as polyP. The third stage, essentially a 'growth pond', allows biomass to grow at the expense of polyP stores. P-depleted microalgae from this stage would be recycled to the second stage, ready to assimilate more P. The remaining biomass is harvested for disposal.

The biomass must be efficiently harvested in order to prevent large-scale settling and resolubilization of assimilated nutrients, but few ponds currently employ harvesting of microalgae (Shilton et al., 2012). The technology to achieve this will, ideally, need to be simple, low-maintenance, and cost-effective, to be appropriate for remote and small communities. Harvesting algal biomass may be facilitated by selective breeding of highly settleable species and enhanced floc formation (Park, Craggs, & Shilton, 2011; Smith & Davis, 2012) However, it is important to note that microalgae may be prone to predation by unwanted species (such as rotifers),

unfavourable climatic conditions, and shifts in population dominance. These could have negative effects on P removal efficiency if species selection is critical to the process.

Disposal of the biomass may present logistical challenges. As a rich source of P, as well as other essential nutrients, the most obvious use for the microalgal biomass is as a fertilizer (Brown & Shilton, 2014). Direct application may be possible, and is clearly desirable, but some processing may be required to address problems of nutrient imbalance, organic micropollutants, pathogenicity, and accumulation of heavy metals. Heavy metals are likely to exist at very low concentrations in farm effluents; however, any trace quantities may, through land application, lead to accumulations in the soil at levels of concern over time. These metals may then be taken up by plants and consumed by farm animals.

If direct land application is to be used, it is also important that the P inside the biomass is available to plants. PolyP is readily degraded in soils (Dick & Tabatabai, 1986); however, the rates of degradation of microalgae and release of polyP may require further investigation.

The key next step is to better understand the process of polyP accumulation and how it affects population dynamics in WSP. Previous investigations have treated microalgal polyP synthesis as a ‘black box’ process (Brown & Shilton, 2014) manipulated through external factors. While the conditions favouring the process in WSP populations are now better known, these are complex communities and likely involve numerous interactions between species.

While some researchers have characterized phosphorus uptake by single species and mixed microalgal cultures, results can be difficult to compare because experiments are not performed in identical conditions and the observed kinetics of mixed populations may conflate the underlying kinetics of several different species. Therefore, a comparison between a variety of microalgal species, using the same protocol and well-defined experimental conditions, would help to identify differences in phosphorus metabolism between species. Furthermore, our understanding of the role of polyP in defining the species composition of microalgal communities is limited.

Table 2: Factors reported to influence phosphorus luxury uptake by microalgae.

Factor	Range	Effect on luxury uptake
Light intensity	10 – 200 µmol photons·$m^{-2}s^{-1}$	Negative [a]
	60 – 150 µmol photons·$m^{-2}s^{-1}$	Negative [b]; Positive [c]
	100 – 150 µmol photons·$m^{-2}s^{-1}$	Positive [d]
	280 – 1650 µmol photons·$m^{-2}s^{-1}$	NS [e]
Temperature	15 – 25 °C	Positive [b,c]
	10 – 15 °C	NS [d]
	4 – 28 °C	NS [e]
pH	6.6 – 9.8	NS [e]
	≥ 7	Positive [f]
Influent P concentration	5 – 30 mg·L^{-1}	Positive [c]
	7.5 – 15 mg·L^{-1}	Positive [d]
	0.5 – 8.6 mg·L^{-1}	Positive [e]
Organic load (COD)	0 – 2140 mg·L^{-1}	Negative [f]
Ca^{2+} concentration	0 – 40.0 mg·L^{-1}	Positive [g]
	15 – 30 mg·L^{-1}	NS [f]
Mg^{2+} concentration	0 – 24.3 mg·L^{-1}	NS [g]
	4 – 8 mg·L^{-1}	NS [f]
K^{+} concentration	0 – 39.1 mg·L^{-1}	NS [g]
	33 – 66 mg·L^{-1}	NS [f]
Mixing intensity	0 – 500 min^{-1}	Negative [f]
N:P ratio	1:1 – 3:1	Positive [h]

[a] Hessen, Færøvig, and Andersen (2002)

[b] Powell et al. (2008)

[c] Powell et al. (2009)

[d] Schmidt et al. (2016)

[e] Crimp et al. (2018)

[f] Sells et al. (2018)

[g] Siderius et al. (1996)

[h] Lavrinovičs et al. (2020).

NS: No significant effect.

Interest in condensed phosphates was initially spurred by the discovery of nucleotide phosphates as the backbone of genetic material (DNA and RNA) and as a vehicle for biological energy transfer (ATP). Studies of inorganic polyphosphate (polyP) have increased in frequency due to its ubiquity in nature (Ault-Riché et al., 1998) and the wide variety of biological activities in which it participates.

2.4.3 Physiological aspects of polyP

PolyP is found in many different organisms (see Box 1) and has been shown to account for over 20% of total cellular phosphorus in certain microbes exposed to high extracellular P levels (Aitchison & Butt, 1973).

Eukaryotes have a more complex internal structure than prokaryotes and their polyP is found within many organelles (Kulaev & Kulakovskaya, 2000). In yeast, polyP was first found in high concentrations within granules and known as ‘volutin’ or ‘metachromatic granules’ due to their colour-changing reaction with certain basic dyes (Widra, 1959). The polyP in yeast granules forms a complex with proteins and metal ions (Jacobson, Halmann, & Yariv, 1982), and the amount of polyP increases with the accumulation of these ions (Kulaev & Kulakovskaya, 2000).

The use of ^{32}P radioisotope-tagged P_i has shown that, following a spike in P availability, primarily short-chain polyP is formed in cultures previously grown under conditions of constant P sufficiency, whereas long-chain polyP is formed before short-chain polyP in cultures temporarily moved to P-free media before the P addition, as long-chain polyP replenishes the depleted polyP stores (Niemeyer, 1976). Clark et al. (1986) also showed that the substrate used for heterotrophic growth may influence the formation of polyP as bacterial cells grown on glucose contained significantly less long-chain polyP, and more short-chain polyP, than cells grown on lactate. The absence of granules in the glucose-grown cells would therefore suggest that polyP granules are stores of long-chain polyP.

Although polyP has been found to exist in the cytosols of bacteria (Klauth et al., 2006) and microalgae (Keck & Stich, 1957), its cytosolic accumulation may be toxic to yeast (Gerasimaitė et al., 2014).

In bacteria and some lower eukaryotes, polyP has been found in acidic calcium-rich vacuoles known as acidocalcisomes (Docampo, 2006). These are membrane-bounded and contain various ion pumps, including Ca^{2+} transporters, a vacuolar proton pyrophosphatase (V-H^+-PPase), and a vacuolar proton ATPase (V-H^+-ATPase) (Lander et al., 2016). Under electron microscope, acidocalcisomes appear as electron-dense spherical regions (Docampo, 2006). Acidocalcisomes also contain a number of other mono- or divalent cations, including Mg^{2+}, sodium (Na^+), K^+, zinc (Zn^{2+}), and iron (Fe^{2+}) (Moreno & Docampo, 2013) and basic amino acids (Docampo et al., 2010).

In green microalgae, polyP has been found to be largely located in vacuoles similar to acidocalcisomes. Using energy-dispersive analysis of X-rays (EDAX) and nuclear magnetic resonance (^{31}P-NMR), Komine et al. (2000) showed that granules of *Chlamydomonas reinhardtii* mainly contained polyP, Mg^{2+} and Ca^{2+}.

The insolubility of high molecular weight polyP in cold acids (Noegel & Gotschlich, 1983), and their solubility in alkalis, has been widely used as the basis for methods to chemically fractionate polyP. The shorter-chain ‘acid-soluble polyphosphate’ (ASP) is believed to be used as short-term P storage and involved in metabolism, while the longer-chain ‘acid insoluble polyphosphate’ (AISP) is thought to be used as long-term phosphorus storage (Brown & Shilton, 2014; Miyachi et al., 1964). AISP may be bound with proteinaceous material (Juni et al., 1947; Komine et al., 2000), suggesting that it is stored in granules. Other researchers have employed more complex extraction procedures, further separating polyP into three (Clark et al., 1986) or more fractions (Kanai, Aoki, & Miyachi, 1965). Although the differences in extractability of different types of polyP may be due to differences in their affinity for the extracting agent(s), there is evidence to support the hypothesis that these molecules are separately compartmented within the cell and metabolically distinct (Kulaev & Vagabov, 1983; Widra, 1959).

2.4.4 Functions of polyP

PolyP is believed to be involved in many metabolic processes such as energy storage (Achbergerová & Nahálka, 2011), osmoregulation (Docampo et al., 2010), the chelation of divalent cations (Kornberg, 1995), protection from heavy metals (Keasling, 1997), quorum sensing and biofilm formation (Rashid et al., 2000), parasitic virulence (Rao, Gómez-García, & Kornberg, 2009), the formation of ion channels for DNA competence (Reusch, 1999), the storage of phosphorus (Kornberg et al., 1999), adaptations in the stationary phase (Rao & Kornberg, 1996), and involvement in mitosis (Lindegren, 1947). Evidence has been found for several of these functions in microalgae (Table 3).

Table 3: Potential functions of polyphosphate in microalgae.

Function	**Reference(s)**
Phosphorus reservoir	Jensen and Sicko (1974); Miyachi and Tamiya (1961)
Energy reservoir	Miyachi et al. (1964)
Heavy metal tolerance/sequestration	Nishikawa et al. (2006); Samadani and Dewez (2018a, 2018b); Twiss and Nalewajko (1992)
Involvement in cell division	Werner, Amrhein, and Freimoser (2007)
Response to osmotic shock/stress/desiccation	Bock et al. (1996); Leitão et al. (1995); Pick, Zeelon, and Weiss (1991); Seufferheld and Curzi (2010)
Iron storage	Seufferheld and Curzi (2010)
Regulation of growth rate	Rhee (1973)
Protection against alkaline stress	Pick et al. (1991); Seufferheld and Curzi (2010)
Buoyancy regulation	Romans, Carpenter, and Bergman (1994)

Although there are indications that polyP may have been used as a source of energy earlier in microbial evolution (Kornberg, 1995), the hypothesis that polyP is used as an energy store has encountered opposition due to observations that polyP is not degraded in bacterial and fungal cells when energy is limited (Harold, 1966), and that polyP would only be capable of providing the energy needed for a very short time (Kornberg et al., 1999).

It has also been suggested that excess P (beyond that required for metabolism) is accumulated as polyP to serve as a P store to maintain essential metabolic processes, such as the production of essential compounds such as genetic material, when P subsequently becomes unavailable (Harold, 1966). Shirahama et al. (1996) demonstrated that yeast lacking the ability to synthesize polyP (due to an absence of vacuoles) ceased growing when deprived of external phosphorus, whereas those containing polyP continued growing and consumed their granules.

The formation of polyP may also be useful as a strategy for reducing negative effects of high cytosolic phosphate concentration (Bruna et al., 2021) and maintaining ATP homeostasis[7] (Plouviez et al., 2021; E. Sanz-Luque et al., 2020). High levels of intracellular phosphate may cause osmotic stress, whereas polyP is an osmotically neutral form of phosphorus (Kornberg, 1995; Kulakovskaya, Pavlov, & Dedkova, 2016) and this has been suggested as the cause of polyP accumulation in bacteria under osmotic stress (Ault-Riché et al., 1998). It follows that, during periods of P abundance, a beneficial strategy would be to store as much P as possible as 'inert' polyP for later use.

As a polyanionic compound, polyP can bind divalent cations such as toxic heavy metals and nitrogen-rich amino acids in the vacuole (Allan & Miller, 1980; Nishikawa et al., 2003; Samadani & Dewez, 2018b). In bacteria, the degradation of vacuolar polyP yields orthophosphate which is complexed with metals and transported out of the cell (Keasling, 1997). This might explain why, although the accumulation of polyP may enable heavy metal sequestration, the amount of polyP in algae has been experimentally shown to decrease following exposure to heavy metals, such as cadmium (Nishikawa et al., 2003; Samadani & Dewez, 2018a), mercury (Samadani & Dewez, 2018b), and copper and zinc (Nishikawa et al., 2003).

PolyP may also have an important role in governing gene expression in bacteria (Kulaev & Vagabov, 1983) and eukaryotes (Kulaev et al., 2004) as well as maintaining exponential phase growth in microalgae (Rhee, 1973). The intracellular concentration of polyP changes with growth

[7] A self-regulating process to maintain optimal levels of ATP for normal cell function.

phases, appearing to be higher in actively growing cells (Keck & Stich, 1957). The presence of polyP stores has been used to explain the continued exponential growth of microalgae after external phosphate has been exhausted (Rhee, 1973).

In bacteria, polyP is essential for adaptation to the stationary phase and its accompanying stress factors (Kornberg et al., 1999). PolyP also interacts with bacterial second messengers involved in stress responses, such as guanosine 3,5-bispyrophosphate (ppGpp), which has been found in the microalgae *Chlamydomonas* and *Euglena* (Cembella et al., 1984). There may be a similar function in lower eukaryotes, involving messenger compounds such as phosphoinositides and highly phosphorylated nucleotides (Kulaev et al., 2004).

2.4.5 PolyP metabolism

While polyP has been identified in virtually all cells examined for its presence (Kornberg, 1995), the mechanisms of its biosynthesis are still unclear in many organisms. The isolation and characterization of enzymes from bacteria and yeasts have revealed that polyP is synthesized almost exclusively by the transfer of the terminal phosphate group of ATP to a growing polyP chain (see Box 2). Microalgal polyP metabolism is however poorly understood but the knowledge gleaned from other organisms, particularly bacteria and yeast, may guide research into microalgal polyP synthesis/metabolism.

2.4.5.1 PolyP synthesis

In most prokaryotes and a small number of eukaryotes, polyP is synthesized by polyphosphate kinase (PPK) enzymes. Cyanobacteria also produce polyP using PPK (Dyhrman, 2016) but the bacterial-type PPK genes are largely absent from eukaryotic genomes (Kulaev et al., 2004), and those few that have been found are believed to be either artefacts due to contamination or the result of horizontal gene transfer (Whitehead, Hooley, & Brown, 2013). Consequently, different enzymes are responsible for polyP synthesis in most eukaryotes. In the model yeast, *Saccharomyces cerevisiae*, this function is performed by the vacuolar transporter chaperone

(VTC) complex, a group of protein subunits referred to as VTC1 through VTC4 (Hothorn et al., 2009). This complex is bound to the vacuolar membrane and endoplasmic reticulum, and comprises VTC1, VTC4, and either VTC2 or VTC3, depending on the location of the complex. An additional VTC component, VTC5, is believed to influence the rate of polyP synthesis by the VTC complex but is not significantly regulated during P depletion (Desfougeres et al., 2016). It has been suggested that, in yeast, polyP chains are translocated into the vacuole as they are formed in order to prevent their toxic build-up in the cytoplasm (Gerasimaitė et al., 2014).

The genome of the model microalga *Chlamydomonas reinhardtii* contains genes encoding proteins similar to the *S. cerevisiae* VTC1 and VTC4 proteins and both of these are required for polyP synthesis in *C. reinhardtii* (Aksoy, Pootakham, & Grossman, 2014; Grossman & Aksoy, 2015; Plouviez et al., 2021). Genes encoding proteins homologous to the *C. reinhardtii* VTC1 and VTC4 proteins have been identified in the genomes of other microalgae (Table 4). However, it has not yet been established whether these enzymes are ubiquitous in microalgae, or whether they are universally required for polyP synthesis.

2.4.5.2 PolyP degradation

In bacteria, polyP is degraded by PPK (by reversing the synthesis reaction) or by exopolyphosphatases (PPX), which both remove the terminal phosphate of polyP by hydrolysis. PolyP may also be used as a donor to phosphorylate glucose, adenosine monophosphate, or nicotinamide adenine dinucleotide (Kulaev et al., 2004). In the yeast *S. cerevisiae*, polyP degradation is performed by either PPX enzymes or endopolyphosphatases (PPN), which cleave the polyP chain into shorter subunits (see Box 2).

It is currently not known how polyP is degraded in microalgae. Cordeiro et al. (2019) identified a pair of Nudix hydrolase enzymes with polyphosphatase activity in the protozoan *Trypanosoma brucei* and Plouviez et al. (2021) have suggested that a homologous protein may be responsible for polyP degradation in *C. reinhardtii*.

Table 4. Eukaryotic microalgal species reported to harbour genes encoding potential VTC components and PPK-type polyP polymerases.

VTC1	**VTC4**	**PPK**
	Aureococcus anophagefferens [b]	
	Bathycoccus prasinos [c]	*Bathycoccus prasinos* [c]
Chlamyodonomas reinhardtii [a,c]	*Chlamyodonomas reinhardtii* [c,d]	
Chlorella sp. NC64A [c]	*Chlorella* sp. NC64A [c]	
Chlorella variabilis [a]		
		Chondrus crispus [c]
Coccomyxa subellipsoidea [c]	*Coccomyxa subellipsoidea* [c]	
Cyanidioschyzon merolae [c]		*Cyanidioschyzon merolae* [c]
	Cyanophora paradoxa [c]	
Dunaliella salina [c]	*Dunaliella salina* [c]	
	Ectocarpus siliculosus [c]	
Emiliana huxleyi [c]	*Emiliana huxleyi* [b,c]	
Fragilariopsis cynindrus [c]	*Fragilariopsis cynindrus* [c]	
Galdieria sulphuraria [c]		*Galdieria sulphuraria* [c]
Guillardia theta [c]	*Guillardia theta* [c]	
		Klebsormidium flaccidum [c]
	Micromonas pusilla CCMP1545 [c]	
	Micromonas pusilla RCC299 [c]	
Nannochloropsis gaditana [c]	*Nannochloropsis gaditana* [c]	
	Ostreococcus lucimarinus [c]	*Ostreococcus lucimarinus* [c]
	Ostreococcus tauri [c]	*Ostreococcus tauri* [c]
Phaeodactylum tricornutum [c]	*Phaeodactylum tricornutum* [c]	
	Thalassiosira oceanica [c]	
Thalassiosira pseudonana [c]	*Thalassiosira pseudonana* [b,c]	
Volvox carteri [a,c]	*Volvox carteri* [c]	

[a] Aksoy et al. (2014)

[b] Dyhrman (2016)

[c] Blaby-Haas and Merchant (2017)

[d] Grossman and Aksoy (2015)

No other genes or proteins related to polyP degradation (e.g. PPX, PPN) have been identified in microalgae to date but Nguyen, Ezawa, and Saito (2022) recently demonstrated the reversibility of the VTC4 protein (i.e., it can be used to degrade polyP) present in the arbuscular mycorrhizal fungus *Rhizophagus irregularis*.

Box 2: Enzymatic mechanisms of polyP synthesis/degradation in bacteria and yeast.

Polyphosphate kinase (PPK) – reversibly transfers phosphate from ATP to polyP (primarily in the direction of synthesis) (Ahn & Kornberg, 1990).

$$ATP + polyP_n \overset{\text{PPK}}{\longleftrightarrow} ADP + polyP_{n+1}$$

Exopolyphosphatase (PPX) – liberates the terminal phosphate group by hydrolysis (Akiyama, Crooke, & Kornberg, 1993).

$$polyP_{n+1} + H_2O \overset{\text{PPX}}{\longrightarrow} polyP_n + P_i$$

Endopolyphosphatase (PPN) – breaks the polyP chain into smaller fragments (Sethuraman, Rao, & Kornberg, 2001).

$$polyP_n + (a + b - 1)H_2O \overset{\text{PPN}}{\longrightarrow} a(polyP_{60}) + b(polyP_3)$$

Ruiz, Marchesini, et al. (2001) showed that the vacuoles (acidocalcisomes) of *Chlamydomonas* cells also contain membrane-bound V-H^+-PPases (pyrophosphatases) and V-H^+-ATPases similar to those found in acidocalcisomes of other lower eukaryotes. V-H^+-ATPases are responsible for maintaining the electrochemical potential across the vacuolar membrane and this potential provides the proton motive force essential for transporting polyanionic compounds such as polyP into the vacuole (Gerasimaitė et al., 2014; Ogawa, DeRisi, & Brown, 2000). The acidocalcisome V-H^+-PPases of microalgae are responsible for acidification of these organelles (Docampo & Huang, 2016; Seufferheld et al., 2004).

2.5 PolyP in the microbial environment

Microbial communities are frequently subjected to selective pressures promoting evolutionary adaptation. Since phosphorus is needed for many essential metabolic processes, the ability to store excess P provides an ecological advantage by allowing for growth when P is scarce. It is not unusual for microalgae to store excess P as polyP under normal conditions, and this store is sufficient to sustain growth for several cell divisions (Powell et al., 2009).

When many organisms are reliant on the same limited resources, such as P, any physiological or metabolic adaptations that enhance resource uptake may lead to dominance through starvation of slow competitors (de Mazancourt & Schwartz, 2012; Donald et al., 1997). However, those advantageous functions may only prove effective under certain conditions, and seasonal variations in populations are often observed (Pearson, 2006).

2.5.1 In natural environments

Organisms found in oligotrophic environments (low trophic status)[8], such as many lakes and seas, must be equipped to optimally utilize available resources. As aquatic microorganisms vary in their nutrient requirements, particularly N and P (but also silicon, Si, in the case of siliceous diatoms), the ratio of these key nutrients in the environment may play an important role in promoting dominance (Blackburn, 2004; Sommer, 1996). An interesting observation is that significant amounts of polyP have been found in plankton inhabiting oligotrophic environments, where luxury uptake is unlikely to occur (Martin et al., 2014).

2.5.2 PolyP in engineered environments

Engineered environments, such as WSP, differ from natural environments in their much higher and relatively constant concentrations of phosphate. Seasonal variations in environmental conditions, including light, temperature, and organic loading, can lead to continuously-changing

[8] The trophic state index (TSI) describes the level of biological productivity a body of water can sustain.

species dominance (Pearson, 2006). The same concept of competitive advantage holds in these environments, as in natural ecosystems. However, mechanical mixing (for instance, in high rate algal ponds) may negate the advantages otherwise experienced by motile species, leading to different species dominance profiles to those in natural environments (Pearson, 2006).

2.6 Examining polyP in microalgal cultures

Our understanding of the roles of polyP in organisms is limited by a lack of suitable methods for its quantification (Kulakova et al., 2011; Lee et al., 2017; Moudříková et al., 2017). Many analytical methods have been employed with varying levels of success and each has its own advantages and disadvantages (Table 5). Where accurate quantification of polyP is required, the choice of protocol is very important as it may cause significant variability between results (Bru et al., 2017; Kumble & Kornberg, 1995). Because there is no reference method which can be used to confirm complete extraction (Christ & Blank, 2018a), it is important to optimize the selected protocol for the type of sample to be processed. Simplicity is highly desirable as it improves the likelihood of repeatability and restricts opportunities for losses that may lead to underestimation (Kulakova et al., 2011).

Early methods of quantifying polyP in biological samples involved the extraction of unbound P-containing compounds followed by acid hydrolysis to orthophosphate (P_i) and quantification of P_i by colorimetry, such as the molybdenum blue assay (Ota & Kawano, 2017). Extraction may be as simple as boiling (Fitzgerald & Nelson, 1966), may utilize nucleic acid extraction methods such as organic solvent (phenol-chloroform) partitioning (Leitão et al., 1995), or involve the separation of polyP pools (see 2.4.3) through multiple extraction steps with strong acids and bases (Aitchison & Butt, 1973; Kanai et al., 1965; Powell et al., 2008). Computer-aided microscopy, using images cells stained to show polyP granules, can be used for estimating granular polyP content by image analysis (Sells, 2019). Table 5 provides a summary of the quantification methods reported in the literature.

Table 5: Methods reported in the literature for the quantification of polyphosphate in microalgae/phytoplankton.

Method	**Advantages**	**Limitations**
Metachromasy (TBO, methylene blue)	Can be used in vivo[9].	Poor detection of short-chain polyP; prone to interference by other anions; depends on ionic strength and pH (Lorenz & Schröder, 1999).
Fluorometry (DAPI, fura-2, tetracycline, JC-D7/JC-D8)	Can be used in vivo.	Potential interferences (can be mitigated). Linearity may be limited by signal saturation.
Acid hydrolysis to P_i	Can be combined with acid extraction.	Background P_i must be accurately measured. Low specificity.
Enzymatic (PPK, PPX)	High substrate specificity, sensitivity (Kumble & Kornberg, 1995), and linearity (Bru et al., 2017).	Enzymes are expensive and difficult to source. Chain length specificity. PPK assay requires excess ADP in reaction mix.
^{31}P-NMR	Can be used in vivo.	Cannot detect low concentrations (Kornberg, 1995). Low temporal resolution.
Raman spectroscopy	Subcellular localization of compounds.	Strong chlorophyll autofluorescence. Interference from compounds of same bond class. Requires specialized equipment.
Microscopy and image analysis	Rapid post hoc measurement.	Only measures granular polyP. Requires species-specific parameters.

[9] In vivo: Quantification is performed in live cells.

Additional pre-treatment steps may facilitate polyP extraction. Physical disruption of microalgal cells may be enhanced by the use of boiling (Martin & Van Mooy, 2013) or sonication and bead beating (Moudříková et al., 2017). Detergents (such as SDS, CTAB, and Triton X-100) can be used to permeabilize membranes (Moudříková et al., 2017), the chaotropic agent guanidinium isothiocyanate (GITC) disrupts proteins to reduce binding of granular polyP (Nishikawa et al., 2006), and the chelating agent EDTA binds divalent cations which may otherwise complex with polyP and reduce its solubility (Christ & Blank, 2018a; Oh-hama et al., 1986). Extraction methods using acids, bases, or alkaline hypochlorite may result in inaccurate estimation of polyP due to degradation of polyP (Bru et al., 2017; Mullan, Quinn, & McGrath, 2002) or other P-containing compounds (Serafim et al., 2002).

PolyP can also be visualized (when concentrated in granules) and quantified, without degrading it to P_i, using metachromatic reactions with dyes, such as toluidine blue (Leitão et al., 1995). 4′,6-diamidino-2-phenylindole (DAPI), a fluorescence dye previously used to detect DNA (Bru et al., 2017) also binds to polyP producing a distinct response (Allan & Miller, 1980). Excited by light at a wavelength of 360 nm, the excitation peak of DAPI is shifted from 475 nm to 525 nm in the presence of polyP (Diaz & Ingall, 2010). The fluorescence intensity can be used to quantify polyP (using suitable standards for calibration) but may be confounded by interferences due to the presence of other anionic compounds such as DNA (for which the dye is commonly used), which exhibits a fluorescence peak at approximately 460 nm (Omelon, Georgiou, & Habraken, 2016). Lipids fluoresce similarly to polyP when bound to DAPI, but this fluorescence fades rapidly (Streichan, Golecki, & Schön, 1990).

An improved protocol developed by Aschar-Sobbi et al. (2008) avoids many of these interferences by changing the excitation and emission wavelengths used to 415 nm and 550 nm, respectively, thereby improving the specificity of the dye for polyP. However, DAPI binding to inositol phosphates (phosphorylated sugars involved in cellular signalling) may lead to polyP overestimation (Kolozsvari, Parisi, & Saiardi, 2014).

Although protocols have been developed for in situ[10] quantification (Gomes et al., 2013; Kulakova et al., 2011), they have not been validated using microalgae. If this approach can be shown to reliably estimate cellular polyP content, it might allow for rapid quantification using spectrofluorometry and with minimal sample processing.

Although the incubation period required for DAPI to bind to polyP potentially limits the temporal resolution of measurements (that is, in experiments where the polyP concentration changes quickly, the time course of polyP formation would be difficult to obtain), it may be possible to freeze samples and measure polyP after thawing.

The polyP-binding fluorescence characteristics of other compounds, including Fura-2 (Ruiz, Rodrigues, et al., 2001), tetracycline (Günther et al., 2009), and JC-D7/JC-D8 (Angelova et al., 2014), have been used to identify polyP in various organisms in situ but, to our knowledge, these methods have not yet been validated in microalgae.

The expression of the polyphosphate enzymes PPK and PPX in the bacterium *Escherichia coli* or the yeast *Saccharomyces cerevisiae* and isolation of these enzymes from lab cultures have led to the development of enzymatic methods for quantifying polyP (Moudříková et al., 2017; Nishikawa et al., 2006).

Briefly, the method using PPK relies on the high specificity of the enzyme for polyP as substrate. The amount of ATP produced is then assayed by the light-producing enzyme luciferase (Ault-Riché et al., 1998; Nishikawa et al., 2006) or by radioisotope labelling (Crooke et al., 1994; Kumble & Kornberg, 1995).

The PPX method relies on the enzyme (normally ScPPX isolated from *S. cerevisiae*) to completely hydrolyze polyP, so that it can be quantified by the amount of P_i liberated. It has been noted, however, that PPX is only able to reduce polyP to a chain length of 2 and therefore complete hydrolysis to P_i requires a second enzyme such as inorganic pyrophosphatase (Christ &

[10] In situ: Quantification without first extracting the material from the cell.

Blank, 2018b). Enzymatic quantification methods are noted for their high specificity and sensitivity, but the enzymes can be cost prohibitive.

Methods for indirect identification and/or quantification of polyP include nuclear magnetic resonance (NMR) (Bental et al., 1991; Elgavish & Elgavish, 1980; Oh-hama et al., 1986; Sianoudis et al., 1986), Fourier-transform infrared (FTIR) spectroscopy (Wang, Schröder, & Müller, 2018), and Raman spectroscopy (Moudříková et al., 2017; Solovchenko et al., 2019). These methods are particularly useful for identifying the subcellular location of polyP stores but require specialized equipment. Accurate measurements using NMR may be hindered by low natural polyP concentrations and high abundance of other P-containing compounds with the same bond class as polyP (Diaz & Ingall, 2010; Sanz-Luque, Bhaya, & Grossman, 2020).

Two approaches are possible for measuring polyP synthesis kinetics in cell cultures: samples can be taken at time intervals, or measurements can be made in vivo. The latter allows for observations to be made over time and in the same sample, potentially aiding in the visualization of metabolic processes in real time.

2.7 Responses to phosphorus deficiency

Besides storing P as polyP granules for later consumption, strategies for coping with periodic shortages of exogenous P include enhanced scavenging, recycling of intracellular compounds, sparing, use of alternative substrates, and inter-specific competition.

2.7.1 Competition and cooperation

When essential nutrients are limited, organisms within the same habitat may be forced to compete for them, and this competition can impact species dominance and diversity. The ability of a species to access available nutrients more readily than others may confer better survival and serve as an evolutionary driver.

Bacteria are known to use quorum sensing to coordinate activities for community-scale benefits. While some cyanobacteria have been shown to use quorum sensing to regulate phosphate uptake by other bacteria (Van Mooy et al., 2012), it is not known whether eukaryotic microalgae utilize a similar strategy. However, there is evidence that quorum sensing does play a part in microalgal-bacterial interactions (Zhou et al., 2017; Zhou et al., 2016).

Within the same ecosystem, microalgae and bacteria can exist in a symbiotic relationship: photosynthesizing microalgae produce oxygen, and this oxygen can be used by heterotrophic aerobic bacteria. By degrading organic material, these heterotrophic bacteria produce carbon dioxide and nutrients, and these substrates can in turn be used by the microalgae. Some bacteria can promote the growth of microalgae through nutrient transport and disease control (Crimp, 2015) and can assist with P acquisition through enzymatic degradation of compounds not bioavailable to microalgae (Solovchenko et al., 2016).

On the other hand, bacteria and microalgae may compete for common resources, such as phosphorus (Rhee, 1972). Resource competition has also been identified as a key driver of species dominance between microalgae (Titman, 1976) and luxury uptake may be a strategy that gives some species an advantage over others (de Mazancourt & Schwartz, 2012).

2.7.2 Phosphorus sensing

Responses to changes in P availability begin with sensing of external P levels and activation of signalling pathways which mediate metabolic responses. In bacteria, such as *E. coli*, extracellular concentrations (around 4 µM) of inorganic phosphate (P_i) are sensed by the Pho regulon, which regulates the expression of genes to produce proteins involved in P_i uptake (Kornberg et al., 1999; Rao & Kornberg, 1999) including an inducible alkaline phosphatase (Torriani, 1960).

In yeast, responses to changes in extracellular P_i are governed by the PHO regulatory system, which in/activates several genes encoding phosphatases and P_i transporters (Ogawa et al., 2000; Oshima, 1997). The production of inducible phosphatases is controlled by PhoB in response to

external P_i (Rao & Kornberg, 1999). PHO84 and PHO5, encoding a P_i transporter and an acid phosphatase, respectively, are both up-regulated[11] in low P_i conditions (Ogawa et al., 2000).

The phosphorus sensing mechanism of microalgae is not as well understood but may be similar to that of higher eukaryotes such as plants. Some microalgal VTC proteins (see 2.4.5) contain SPX domains, which are involved in plant phosphorus homeostasis and may be regulated by signalling compounds such as inositol phosphates (Wild et al., 2016). Named after the yeast proteins SYG1 and Pho81, and the human protein XPR1, SPX domains have been found in all major eukaryotes (Secco et al., 2012) but not in prokaryotes (Qi et al., 2016). This hydrophilic domain is found at the N-terminal of proteins and consists of three well-conserved sub-domains, separated by low-similarity regions of varying length (Secco et al., 2012). The SPX domain is involved in P sensing, signalling (through involvement with inositol polyphosphates, InsPs), and P_i homeostasis and may physically interact with other proteins (Qi et al., 2016; Secco et al., 2012; Wild et al., 2016). Extracellular phosphate concentrations are also sensed by the Phosphorus Starvation Response transcription factor, PSR1, which is activated during low P_i conditions and regulates several genes involved in P metabolism in *Chlamydomonas* (Shimogawara et al., 1999; Wykoff et al., 1999). During P_i sufficiency, the PSR1 homologue found in plants, PHR1, complexes with the InsP-bound SPX domains of other proteins, leading to a reduction in expression of starvation-induced genes under the control of PHR1 (Ried et al., 2021; Wild et al., 2016).

2.7.3 Scavenging

Phosphorus is primarily found in the form of organic phosphate esters (also known as organophosphates) in the environment. These compounds must be de-esterified for the phosphate they contain to be imported into the cell (Quisel, Wykoff, & Grossman, 1996). In *C. reinhardtii*, this function is performed by phosphatase enzymes enabling access to a range of phosphorus

[11] Up-regulation: Increase in the transcription of a gene, to increase the number of proteins produced.

sources (Patni, Dhawale, & Aaronson, 1977). The phosphatases of *C. reinhardtii* are a mixture of constitutive and repressible enzymes[12] (Loppes & Matagne, 1973) and may be classified as acid or alkaline phosphatases depending on their optimum pH (Quisel et al., 1996). Phosphatase activity in the medium increases as the culture ages (Patni et al., 1977), reflecting increasing pressure to acquire P.

Free phosphate is imported into the cell by phosphate transporters. High affinity transporters have a low Michaelis-Menten constant (K_m) and are generally produced when exogenous phosphate is scarce, whereas low affinity transporters have a high K_m and are constitutive. Phosphate transport in *E. coli* is mediated by high-affinity phosphate-specific transporters (Pst) or, when the external concentration is high, low-affinity transporters such as PitA and PitB (Blank, 2012; Rao et al., 2009). Within the *C. reinhardtii* genome, 10 genes encode PTB-type (Na^+/P_i) phosphate symporters[13], 4 genes encode PTA-type (H^+/P_i) phosphate symporters, and one gene encodes the low-affinity phosphate transporter PTC1 (Grossman & Aksoy, 2015).

2.7.4 Recycling and sparing

Internal phosphorus pools may also be utilized to provide P for microalgal growth in P-limited conditions. For example, P may be recycled from non-vital RNA (Harold, 1960) or chloroplast DNA (Yehudai-Resheff et al., 2007) and membrane phospholipids may be replaced by sulfolipids and galactolipids (Bajhaiya et al., 2016; Martin et al., 2014; Riekhof et al., 2003).

2.7.5 Alternative substrates

A considerable advantage may be experienced by some species (particularly in marine environments) which have developed the ability to utilize P-containing substrates, such as

[12] Constitutive enzymes are produced constantly by constitutive (always expressed) genes whereas the production of repressible/inducible enzymes may be suspended in certain conditions (e.g., P sufficiency).

[13] Symporters transport two compounds (such as two ions of opposite charge) in the same direction across a membrane.

phosphonates (compounds with a phosphate group bonded directly to a carbon moiety), as P sources (Dyhrman et al., 2006). Some microalgae have been reported to utilize polyphosphates, glucose-6-phosphate, AMP, α-glycerophosphate, and phosphorus-based detergents (Kuhl, 1974). Patni et al. (1977) reported differences in growth rates of *Chlamydomonas* supplied various organic phosphate substrates, although it is not known whether the availability of different substrates influences the ability/propensity of microalgae to synthesize polyP.

2.7.6 Transcriptional changes

The transcriptional response[14] to P depletion involves the differential regulation of numerous genes encoding proteins related to P metabolism. As shown in Table 6, genes encoding phosphatases, phosphate transporters, and sulfolipid synthases (involved in P sparing) are typically upregulated during P depletion. Within the first 24 hours following P repletion (i.e., restoration of P sufficiency), the same genes are downregulated. Several of these genes are under the control of the regulatory protein PSR1, as evidenced by the lack of their expression in mutants lacking the *PSR1* gene (Bajhaiya et al., 2016; Moseley, Chang, & Grossman, 2006). Differential gene regulation in response to changing P availability is discussed further in Chapter 5.

2.8 Summary of findings

Phosphorus (P) is a vital natural resource but stocks are finite and much P is lost to the environment where it can harm aquatic ecosystems. Wastewater treatment using microalgae is low-cost but P removal efficiencies are low. P removal might be improved through microalgal luxury uptake in which P is stored as the highly condensed polymer polyphosphate (polyP).

[14] Transcription is the first step in gene expression, involving the copying of genetic information from DNA to mRNA. The second step is translation, in which the mRNA is used produce proteins.

Table 6. Differential expression reported in the literature for genes related to P metabolism.

Protein function	**Gene(s)**	**Expression changes during P depletion**	**Expression changes following P repletion [e]**
PolyP polymerase	*VTC4*		Down
VTC complex component	*VTC1*	Up [c]	Down
Unknown	*VTCX*		Down
P stress response regulator	*PSR1*	Up [a,b,c,d]	Down
Alkaline phosphatase	*PHOX* *	Up [a,b,c]	Down
	PHO1		Down
	PHOD		Down
Metallophosphoesterase	*MPA1*		Down
	MPA2		Down
	MPA8		Down
H^+/P_i symporter	*PTA1* *	Down [a]; NS [c]	Up
	PTA2	Up [a]; NS [c]	Up
	PTA3 *	Down [a]; Up [c]	Down
	PTA4	Up [c]	Down
Na^+/P_i symporter	*PTB2* *	Up [a,c]	Down
	PTB3 *	Up [a,c]	Down
	PTB4 *	Up [a,b,c]	NS
	PTB5 *	Up [a,c]	NS
	PTB6	Up [a]	
	PTB7 *	Up [a]	NS
	PTB8 *	Up [a]	Down
	PTB12 *	Up [a]	Down
Low affinity P_i transporter	*PTC1*		Up
Cation antiporter[15]	*CAX1*	Up [b,c]	Down
	CAX5		Down
Sulfolipid synthase	*SQD1*	Up [b]	NS
	SQD2		Down
	SQD3	Up [b]	
Light-harvesting complex protein	*LHCBM3*		Down

[a] Wang et al. (2020)

[b] Bajhaiya et al. (2016)

[c] Moseley et al. (2006)

[d] Wykoff et al. (1999)

[e] Plouviez et al. (2021)

*Not differentially regulated, or significantly less so, in *psr1* mutants

NS: no significant change

[15] Antiporters exchange two compounds in different directions across the cell membrane.

While many species of microalgae are capable of synthesizing polyP, there is currently limited understanding of the function of polyP in microalgal communities. In microalgae, polyP synthesis is influenced by external factors such as light intensity, temperature, and external phosphorus concentration, and this knowledge may be used to increase the level and consistency of P removal from water in engineered environments. However, the mechanisms of this process are not well understood and observations are often counter-intuitive: for example, if the mechanisms responsible for polyP synthesis are triggered by P starvation, we would not expect to find polyP granules in WSP microalgae when there is typically a constant P supply.

Responses to phosphorus depletion involve changes in gene transcription associated with P uptake, including increased production of extracellular phosphatases, activation of high-affinity phosphate transporters, and production of VTC enzymes. The vacuolar transporter chaperone (VTC) complex is involved in polyP synthesis in the model microalga *Chlamydomonas reinhardtii*.

However, we do not know:

1. Whether the ability to accumulate polyP in response to P repletion is innate to all species of microalgae.
2. Whether the VTC complex is highly conserved among microalgae.
3. Whether the response to P repletion is species-dependent with respect to environmental conditions.
4. Whether the different responses to P repletion with respect to changes in environmental conditions are due to gene expression, protein activity, or changes in growth metabolism.

Further research in this area will improve on current knowledge regarding polyP synthesis in microalgae, potentially contributing to improved practices in biotechnology, wastewater treatment, and resource management.

Chapter 3 The species-dependence of responses to P repletion

3.1 Preface

In ‘The paradox of the plankton’, G. E. Hutchinson (1961) asked why so much species diversity is observed within natural ‘homogeneous’ environments that should favor a smaller number of ‘best-suited’ species. Responses to changes in availability of the growth-limiting nutrient phosphorus (P) may help us to understand the role of this nutrient in supporting species diversity.

In this chapter, we seek to investigate whether the ability to sequester P as polyP is highly conserved among microalgae by: (i) searching genetic databases for microalgal species potentially able to synthesize polyP, (ii) selecting species for experimentation based on literature and database searches, (iii) comparing kinetics of polyP metabolism in the selected species in identical experimental conditions, and (iv) modelling the physical structure of the predicted proteins.

3.2 Introduction

When exogenous P is readily available, microalgae can assimilate far more P than immediately needed for normal metabolism and this process is known as luxury P uptake. P accumulated through luxury uptake is primarily stored as polyphosphate (polyP) located in specialized acidocalcisome-like vacuoles (Ruiz, Marchesini, et al., 2001). Within these vacuoles, polyP is found as electron-dense granules originally described in yeast as ‘volutin’ (Nagel, 1948) and colocalized with high concentrations of mono- and divalent cations (Tsednee et al., 2019).

Under conditions of P sufficiency, microalgae contain around 0.2 – 1 % P by dry cell weight (Plouviez et al., 2021). Luxury P uptake increases this cellular P content considerably (see Table 7) and P which is not immediately needed is stored primarily as polyP.

Table 7. Some maximum cellular P content (%P) values for microalgae reported in the literature.

Reference	**Maximum %P**	**Community profile**
Powell et al. (2008)	3.16%	Mixed culture dominated by *Scenedesmus* spp.
Powell et al. (2011a)	3.85%	WSP sample
Schmidt et al. (2016)	3.3%	Mixed culture of *C. reinhardtii* and *C. vulgaris*
Crimp et al. (2018)	3.8%	WSP sample
Solovchenko et al. (2019)	5%	*C. vulgaris* and *Parachlorella kessleri*
Plouviez et al. (2021)	2.64%	*C. reinhardtii*

WSP: waste stabilization ponds.

Numerous species of microalgae have been reported in the literature as being able to perform luxury P uptake but, to the best of our knowledge, no studies have attempted to compare polyP accumulation between species to identify similarities and differences.

In eukaryotes, such as yeast (Hothorn et al., 2009) and trypanosomes (Lander, Ulrich, & Docampo, 2013), polyP is synthesized by components of the membrane-bound vacuolar transporter chaperone (VTC) complex using ATP as substrate and this synthesis is concurrent with polyP translocation across the vacuole membrane (Gerasimaitė et al., 2014; Tsednee et al., 2019). The function of the VTC complex in polyP metabolism has been studied in the yeast *Saccharomyces cerevisiae*, in which the complex is made up of three subunits: VTC1, VTC4, and either VTC2 or VTC3, depending on the subcellular localization of the complex, as well as the more recently identified VTC5 (Desfougeres et al., 2016). In *C. reinhardtii*, both VTC1 and VTC4 proteins contain a transmembrane domain (Hothorn et al., 2009). VTC4 additionally contains an N-terminal SPX domain (Pfam accession PF03105), involved in regulating phosphate homeostasis (Hürlimann et al., 2009), and a catalytic tunnel domain (Hothorn et al., 2009).

To date, little is known about the prevalence of VTC proteins among microalgae or phenotypic variation in polyP synthesis between microalgal species but *VTC1* and *VTC4* genes have been identified as essential for polyP synthesis in the model microalga *Chlamydomonas reinhardtii* (Aksoy et al., 2014; Plouviez et al., 2021).

In this part of the thesis, a database search was conducted to assess the degree of conservation of potential VTC4-encoding genes in microalgae. Differences in polyP synthesis kinetics among selected microalgal species were then investigated using a laboratory protocol triggering luxury P uptake. Finally, protein homology modelling was used to generate the first models of the microalgal polyP polymerase, VTC4, in three species.

3.3 Methodology

3.3.1 VTC protein homology search

Algal species containing genes sequences which potentially encode proteins homologous to the polyP polymerase subunit of the *C. reinhardtii* VTC complex, CrVTC4 (Cre09.g402775), were identified using the Basic Local Alignment Search Tool (BLAST) (Altschul et al., 1990) within the NCBI non-redundant protein database (Pruitt, Tatusova, & Maglott, 2007). Sequences were aligned using Clustal Omega 1.2.2 (Sievers et al., 2011). A phylogenetic tree was generated from this sequence alignment using the Geneious Prime version 2022.0 tree builder (Biomatters).

3.3.2 P assimilation and storage in six species of microalgae

3.3.2.1 Strains and cultivation conditions

Six species of microalgae were selected for their relevance to New Zealand ecosystems, their prevalence in waste stabilization ponds (WSP) and harmful microalgal blooms, and the availability of existing knowledge surrounding their P metabolism (Table 8). One of these species was isolated from a WSP and initially identified as a member of the genus *Scenedesmus*. Transcriptomic sequence data from RNAseq (see 3.3.4) were searched for the 18S ribosomal RNA and the resulting sequence was used to search the NCBI nucleotide collection for homologues using Megablast in Geneious Prime version 2022.0.1. Our 1,273 bp partial sequence matched that of *Desmodesmus armatus* (KF673362) with 2 mismatches and a 99.9% grade. Therefore, this organism was provisionally identified as *Desmodesmus* cf. *armatus*. The

remaining five species were acquired from The University of Texas at Austin (UTEX) Culture Collection of Algae and The Chlamydomonas Resource Centre.

It should be noted that, as a cyanobacterium, *Microcystis aeruginosa* contains a different regulatory network for maintaining P homeostasis, compared to the eukaryotic species. This includes the polyP polymerase, PPK, found in prokaryotic organisms.

Table 8. Microalgal species selected for comparative experiments with induced luxury P uptake.

Species (and strain)	**Order**	**Relevance**
Chlamydomonas reinhardtii (CC-1690)	Chlamydomonadales	Model organism (Harris, 2001; Salomé & Merchant, 2019). Genome fully sequenced (Merchant et al., 2007).
Chlorella vulgaris (UTEX 259)	Chlorellales	Well-studied polyP metabolism (Aitchison & Butt, 1973). *Chlorella* spp. are commonly used in wastewater treatment (Hernandez et al., 2006).
Desmodesmus cf. *armatus*	Sphaeropleales	Isolated from a New Zealand WSP and initially identified as '*Scenedesmus* sp.'.
Gonium pectorale (UTEX 2582)	Chlamydomonadales	PolyP ability unknown but closely related to *C. reinhardtii*.
Pediastrum boryanum (UTEX 471)	Sphaeropleales	Potential for use in WSP (Park, Craggs, & Shilton, 2015).
Microcystis aeruginosa (UTEX 2385)	Chroococcales	Prevalent in microalgal blooms (Jacobson & Halmann, 1982).

The selected microalgae species were cultivated axenically on low-phosphorus (1 mg $P \cdot L^{-1}$) liquid minimal medium (7.48 mM $NaNO_3$; 0.41 mM $MgSO_4 \cdot 7H_2O$; 0.34 mM $CaCl_2 \cdot 2H_2O$; 21.1 µM K_2HPO_4; 10.8 µM KH_2PO_4; Hutner's trace elements, prepared per Hill and Kafer (2001) at 1 mL/L^{-1}) under continuous illumination at 29 µmol photons$\cdot m^{-2}s^{-1}$ provided by six 18 W Gro-Lux fluorescent tubes (Sylvania, Wilmington, MA). Temperature was maintained at 25 °C, air within the incubator was supplemented to 1.0 ± 0.1% (v/v) with CO_2, and mixing was effected by continuous orbital agitation at 165 min^{-1} in a Minitron incubator (Infors, Bottmingen, Switzerland). Cultures were reinoculated on the same medium, at a ratio of 15-25 mL culture to

100 mL medium in 250 mL Erlenmeyer (E-) flasks plugged with cotton wool, after five days growth. For long-term maintenance, *C. reinhardtii*, *C. vulgaris*, *D. armatus*, and *G. pectorale* were also maintained axenically on solid medium (the above minimal medium, with the phosphate concentration increased to 10 mM P, solidified with 1.6% (w/v) agar) and re-plated monthly.

3.3.2.2 Experimental protocol

To prepare biological replicates for the experiment, cultures were reinoculated on the same medium in six E-flasks and grown for five days in the same conditions (described above). After this time, 25 mL was taken from each replicate for initial measurements. Three of the replicate cultures, designated 'treatments', were supplied with a phosphate dose equivalent to a final concentration of 10 mg $P \cdot L^{-1}$, using a 1 M stock solution of phosphate (46 g $KH_2PO_4 \cdot L^{-1}$ and 115 g $K_2HPO_4 \cdot L^{-1}$). The remaining unaltered cultures were designated 'controls'. The cultures were returned to the incubator to continue growing under the same conditions in which they were maintained (i.e., 29 µmol photons$\cdot m^{-2}s^{-1}$, 25 °C, 1.0 ± 0.1% (v/v) CO_2, and continuous mixing at 165 min^{-1}). Additional 10 mL samples were taken from all six cultures 1, 5, and 24 (final) hours after the P-addition time. A 24-hour growth period has previously been shown to be sufficient to demonstrate polyP accumulation, using the same protocol outlined here (Plouviez et al., 2021).

3.3.2.3 Measurements

Light intensity was measured using a LI-COR LI-250A handheld photometer equipped with a LI-190/R Quantum Sensor (LI-COR Biosciences, Lincoln, NE, U.S.A.).

Optical density (OD) was determined as light absorbance at 683 nm using a UV-1800 spectrophotometer (Shimadzu, Kyoto, Japan). Dry weight (DW) was determined by filtering 5 mL of sample, followed by 5 mL MilliQ water to elute salts, through a pre-weighed 47 mm glass-fibre filter (1.2 µm), drying overnight at 105 °C, and reweighing. These measurements were performed in triplicate.

Extracellular phosphate-P (P_{ext}) was measured by ion chromatography (Plouviez et al., 2017). Total phosphorus (P_{tot}) was quantified colorimetrically, using low-range (0.5 – 1.5 mg $P \cdot L^{-1}$) test tube kits (Hach, TNT843) and a DR3900 spectrophotometer (Hach, Loveland, CO). Polyphosphate granules were stained using the lead sulfide procedure of Bolier et al. (1992). For each sample, 300 µL of culture was pipetted onto a glass slide and dried at 105 °C. This was then wetted with a 25 g/L solution of lead nitrate in 5% (w/v) nitric acid and left for five minutes. The slide was rinsed off using reverse osmosis purified (RO) water, wetted with 20% ammonium sulfide, and left for 10 seconds before rinsing again with RO water. Slides were dried again at 105 °C and examined using a BX53 light microscope (Olympus) at 100× magnification. Images were captured using a XC50 digital camera (Olympus) and cellSens Dimension v. 1.5 software (Olympus). The cellular phosphorus content (CPC or %P) was determined from the difference between total and extracellular P ($P_{tot} - P_{ext}$) as a fraction of dry weight (DW).

Multiple experimental runs were conducted for some species and the data from separate experimental runs were pooled. The total number of replicates for each species is indicated on Figure 5 in the Results section.

Statistical significance of differences in measurements was established by performing t-tests between groups of biological replicates and deeming differences significant where $p < 0.05$.

3.3.3 RNA extraction

Samples of *C. vulgaris* and *D. armatus* (approximately 50 mL) were centrifuged and the cell pellet was stored at -80 °C. Total RNA was extracted using a Plant and Fungi Mini Kit (Macherey-Nagel, item number 740120.50). The manufacturer's protocol was followed except that the lysis step was performed by resuspending the thawed pellet in lysis buffer, transferring to a tube containing 10 – 15 zirconia/silica beads (2.3 mm diameter BioSpec no. 11079125), and homogenizing for 60 seconds at 5000 rpm using a MagNA Lyser bead mill (Roche).

3.3.4 Transcriptome assembly

Extracted RNA was sequenced using an Illumina NovaSeq 6000 system with NovaSeq S4 flow cell, producing 60-80 million 150 nt paired-end reads per sample. RNA-seq data were uploaded to the public Galaxy server (Afgan et al., 2018) at https://usegalaxy.org for analysis. Contigs (~0.18 to 35 kbp) were assembled using Trinity 2.9.1 (Grabherr et al., 2011).

3.3.5 Protein sequence prediction

Protein sequences were predicted from the contigs using Transdecoder 5.5.0 (Haas et al., 2013). Local BLAST databases were created from the candidate protein sequences and searched for homologs of CrVTC4, as described in Section 3.3.1.

3.3.6 Protein structure prediction and substrate docking

The putative VTC4 protein sequences obtained from RNA-seq data (for *C. vulgaris* and *D. armatus*) and the protein sequence for CrVTC4 (Cre09.g402775) were used to generate structural models of the proteins so that comparisons could be made regarding the structures of their key domains and affinities for polyP.

Models of the predicted VTC4 proteins from *C. reinhardtii*, *C. vulgaris* and *D. armatus* were obtained by two approaches : (i) homology modelling based on *Saccharomyces cerevisiae* domain structures from the Protein Data Bank (3G3Q: VTC domain from VTC4; 5IIQ: SPX domain from VTC4) using the Phyre2 server (Kelley et al., 2015) and (ii) using DeepMind's neural network-based AlphaFold2 structure prediction model (Jumper et al., 2021).

The predicted VTC4 models were then further refined by structure equilibration and minimization in a TIP3 water box using NAMD v2.14 (Phillips et al., 2020).

Autodock Vina v1.2.0 (Trott & Olson, 2010) was used for ligand docking and UCSF ChimeraX v1.3 (Pettersen et al., 2021) was used to visualize and analyze molecular structures and related data.

3.4 Results and Discussion

3.4.1 Phylogeny of microalgal VTC4 protein sequences

To identify potential VTC4 proteins encoded in the genomes of other microalgae, the NCBI protein database was searched for sequences with similarity to the complete *C. reinhardtii* protein sequence for the polyP polymerase VTC4. The results of the database search were manually purged of sequences not belonging to microalgae and one sequence was rejected due to low similarity, leaving 48 sequences with percentage identity ranging from 38.96% to 96.82%. These sequences were aligned using Clustal Omega 1.2.2 to identify similarities in conserved regions. Inspection of the alignment revealed that several sequences appeared to be incomplete due to the absence of one or more of the three conserved domains (SPX, VTC, and DUF202) found in VTC4 proteins (Emanuel Sanz-Luque et al., 2020). The SPX domain (PFAM accession PF03105) was absent from the entries for *Guillardia theta* (XP_00582982.1), *Raphidocelis subcapitata* (GBG00374.1), *Ostreobium quekettii* (CAD7705264.1), and *Thalassiosira pseudonana* (XP_002295322.1). However, the sequence from *T. pseudonana* begins near the C-terminal end of the SPX domain and Blaby-Haas and Merchant (2017) previously noted that the sequence model had been incorrectly truncated by misinterpreting the start codon as coding for a methionine residue. It is not clear whether this is also the case for the other species mentioned above but may have resulted from insufficient sampling depth or poor-quality sequencing leading to erroneous transcriptome assembly. Sequences for *Haematococcus lacustris* (GFH07673.1, GFH26351.1), *Volvox reticuliferus* (GIL87349.1), *Dunaliella salina* (KAF5830825.1), and *G. theta* (as above) were missing the DUF202 domain (PFAM accession PF02656) found in both VTC4 and VTC1 proteins. These sequences were removed from the alignment[16] and the 40 remaining sequences were realigned against the *C. reinhardtii* VTC4 protein sequence.

[16] Incomplete sequences may still indicate VTC4 proteins but could bias the assessments of sequence relatedness.

The phylogenetic structure derived from the sequence differences between all the putative VTC4 proteins (Figure 2) demonstrates consistency with the current taxonomic relationships (Guiry, 2022) between these species. Protein sequences from *Auxenochlorella protothecoides*, *Micractinium conductrix*, *Volvox reticuliferus*, and *Haematococcus lacustris* appear to represent isoforms originating from a single gene for each species. Species of Chlorellales form two clades, one of which is more closely related to the remaining Chlorophyta sequences than the other clade. The differences between the sequences in these two clades lie primarily in the DUF202 transmembrane domain.

Species of *Phaeodactylum*, *Thalassiosira*, *Nannochloropsis*, *Chlorella*, *Trebouxia*, *Scenedesmus*, and *Chlamydomonas* have been shown to be capable of luxury uptake and/or polyP granule accumulation (Dyhrman et al., 2012; Fisher, 1971; Keck & Stich, 1957; Leitão et al., 1995; Mühlroth et al., 2017; Rhee, 1973).

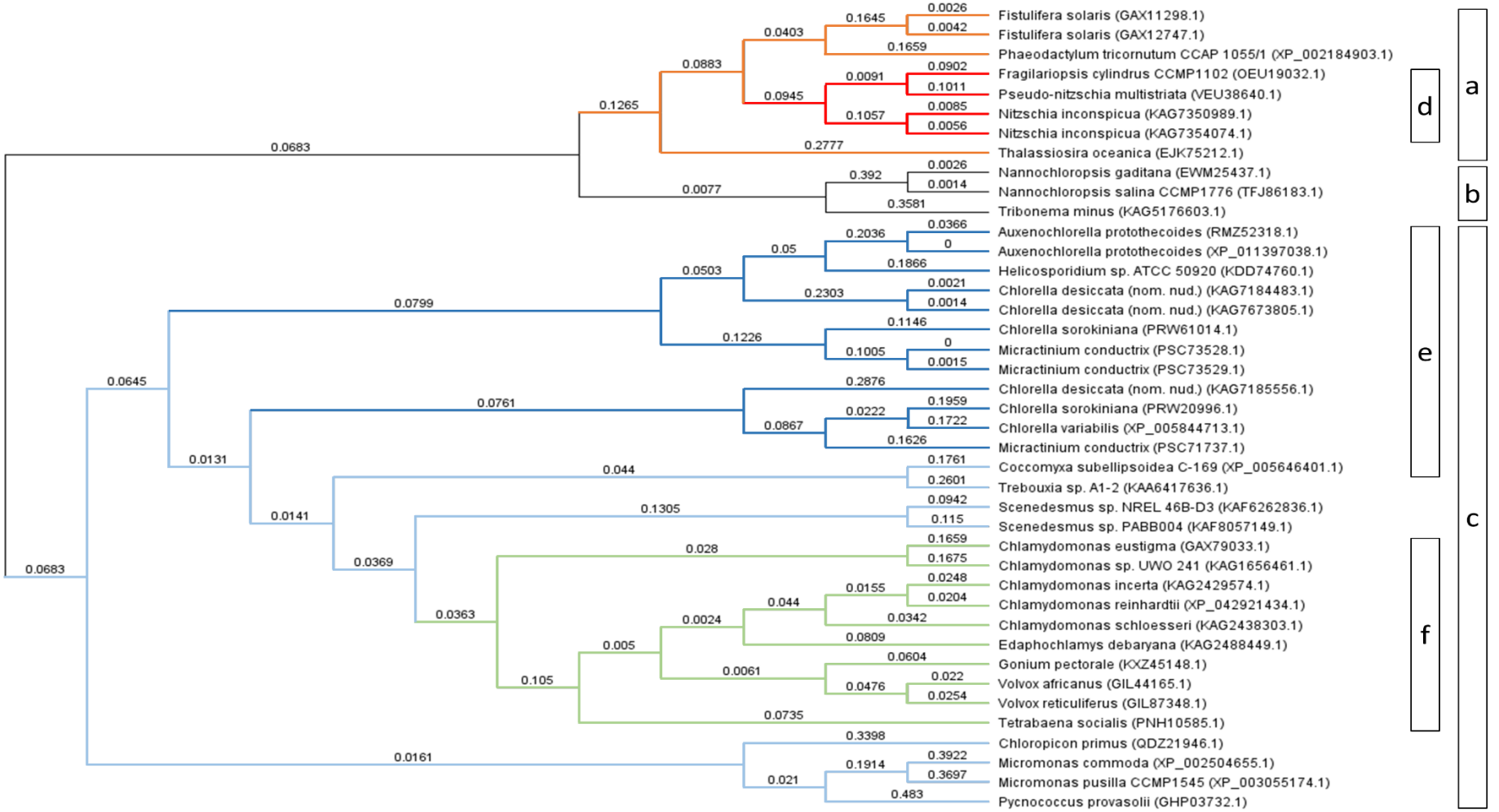

Figure 2. Cladogram showing relatedness of putative VTC4 protein sequences (accession numbers in parentheses) found through a BLAST search for proteins with similarity to CrVTC4 (Cre09.g402775), showing clades corresponding to groupings by phyla (a: Bacillariophyta; b: Ochrophyta; c: Chlorophyta) and orders containing more than three results (d: Bacillariales; e: Chlorellales; f: Chlamydomonadales).

The microalgal species identified in the search are known to inhabit marine, freshwater, and terrestrial environments, suggesting that the luxury uptake trait is not limited to a specific niche but the phylogeny of the putative VTC4 protein sequences indicates that the genes have evolved to suit the needs of different species and provides evidence for the necessity of polyP synthesis for survival. PolyP synthesis has also been observed in eukaryotic microalgae inhabiting arctic regions (Barcytė et al., 2020), hot springs (Nagasaka & Yoshimura, 2008), and acidic environments (Nishikawa et al., 2006).

The presence of potential VTC genes within species from different phyla suggests that the function they perform is ancient and likely universal among microalgae but it is yet to be confirmed experimentally that the other genera identified in the BLAST search are actually capable of polyP accumulation. Evidence of this relatedness between the presence of VTC genes and the ability to sequester P as polyP is important to demonstrate that functionality of the VTC complex has been preserved throughout evolution.

It is important to note that these results do not provide an exhaustive list of microalgal VTC proteins, as other researchers have uncovered evidence of VTC genes within the transcriptomes of other microalgae (Dyhrman et al., 2012; Solovchenko et al., 2019).

3.4.2 P assimilation and storage in six species of microalgae

A biochemical assay involving addition of phosphate to P-depleted cultures was used to trigger luxury uptake in *C. reinhardtii* and five other microalgae, to compare the potential of these species to assimilate and store P as polyP.

Cytological staining confirmed the formation of polyP granules in *C. reinhardtii* as previously observed (Plouviez et al., 2021) as well as in all the other species examined (Figure 3 andFigure 4). PolyP accumulation by *Gonium pectorale* is reported here for the first time, confirming the ability hypothesized based on the presence of a VTC protein.

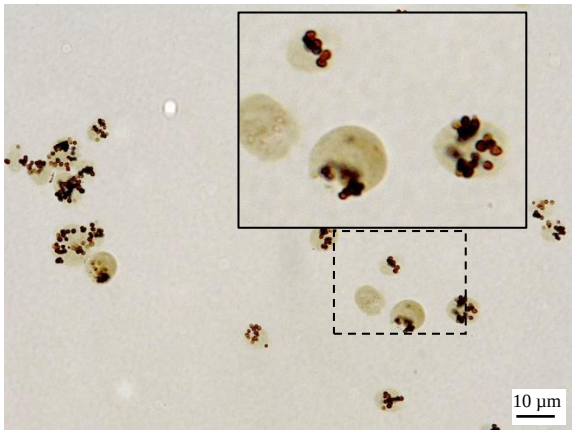

Chlamydomonas reinhardtii

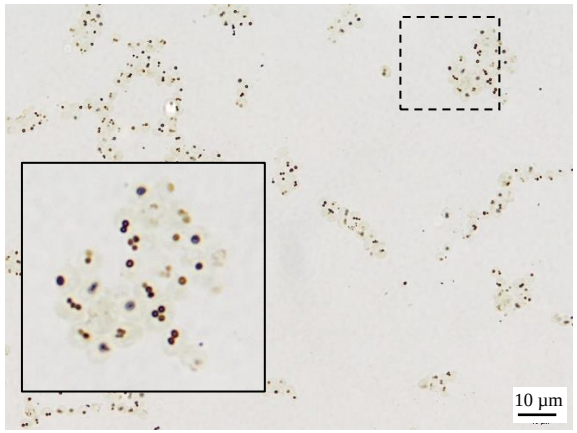

Chlorella vulgaris

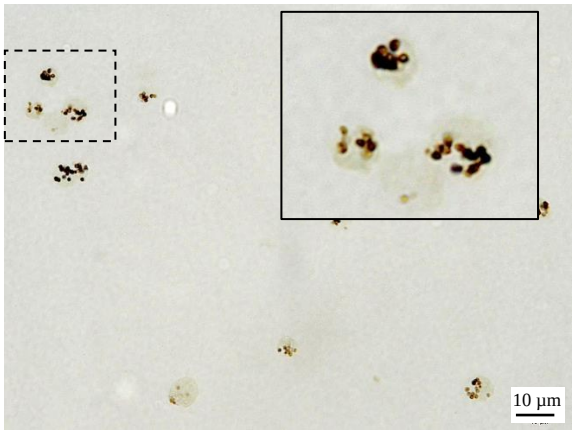

Gonium pectorale

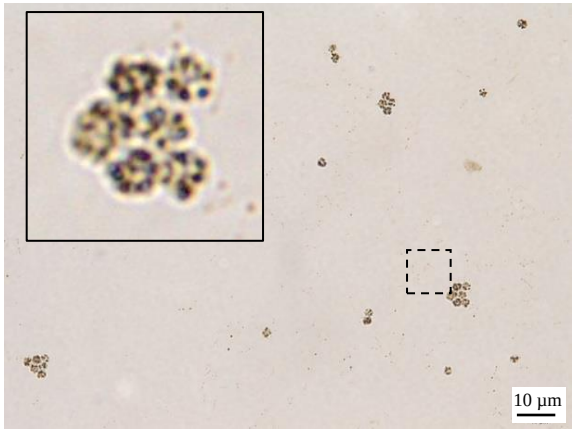

Microcystis aeruginosa

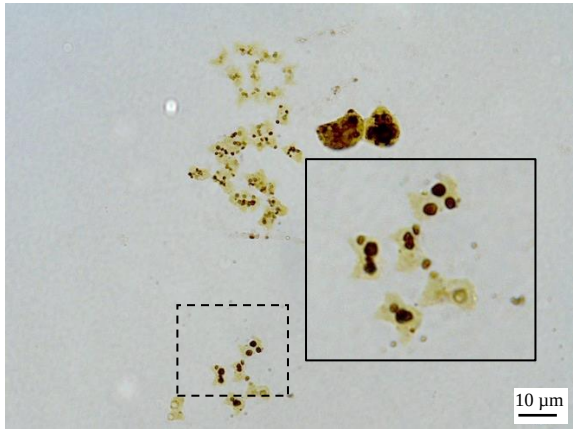

Pediastrum boryanum

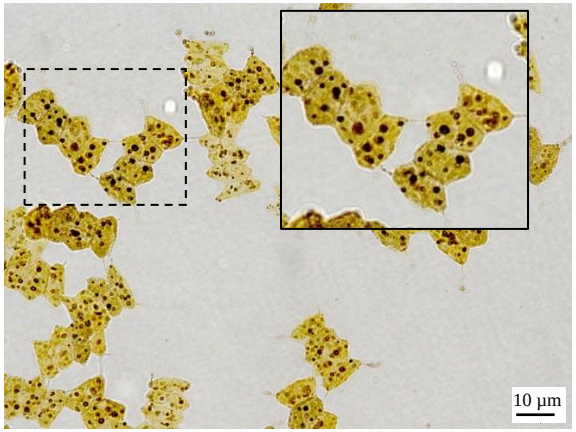

Desmodesmus cf. *armatus*

Figure 3. Examples of granules stained with lead sulfide after 24 hours* following phosphate addition. *Images for *C. vulgaris* were taken from 5-hour samples since granules were most abundant at this time point. Inset images show magnifications of regions bounded by dashed lines.

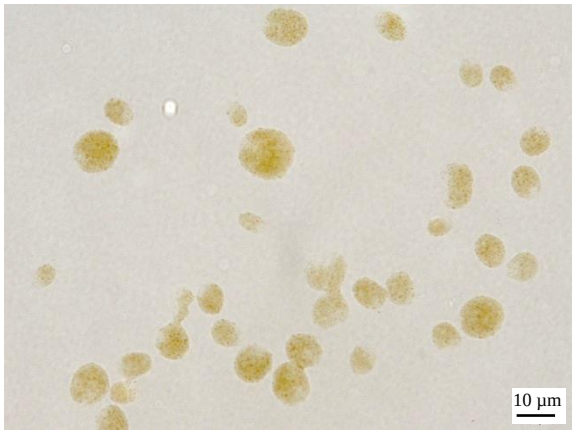

Chlamydomonas reinhardtii

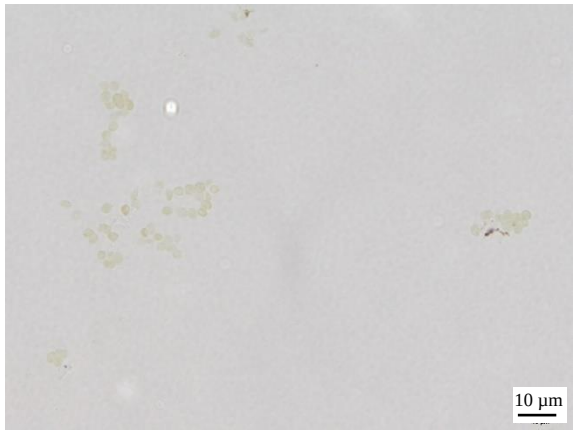

Chlorella vulgaris

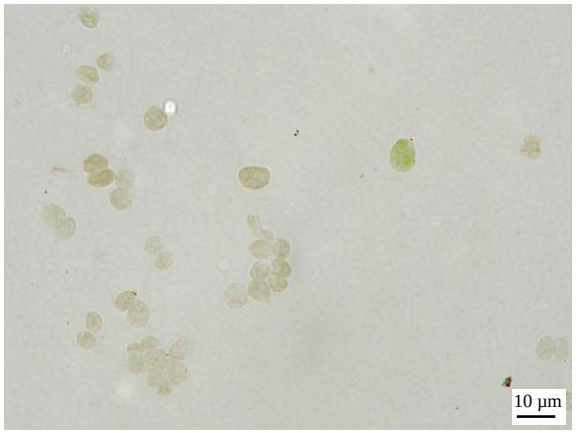

Gonium pectorale

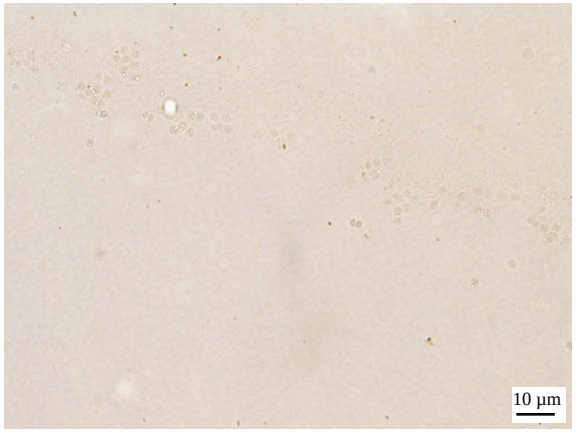

Microcystis aeruginosa

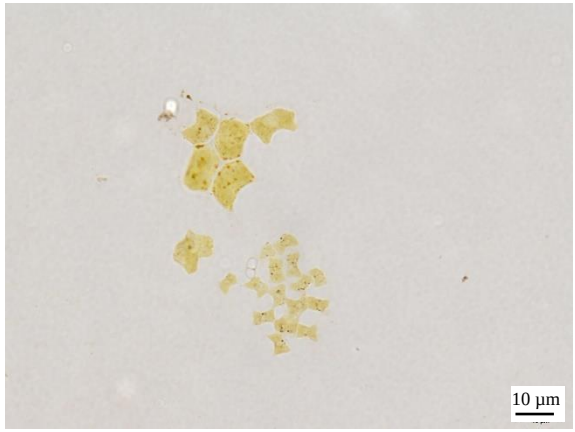

Pediastrum boryanum

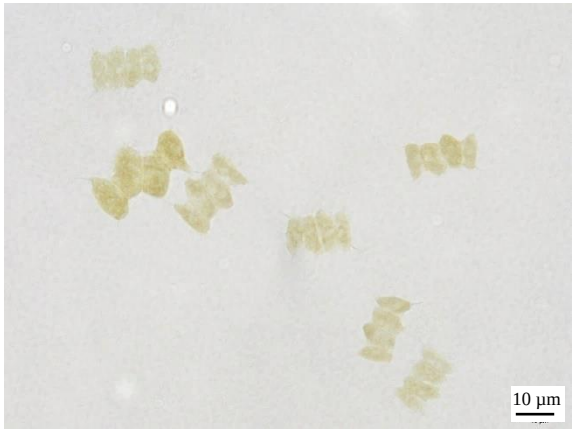

Desmodesmus cf. *armatus*

Figure 4. Examples of control cultures stained with lead sulfide, demonstrating the absence of polyP granules.

This method of staining polyP granules is not quantitative but enables a clear distinction between cells with and without granules, as well as an indication of polyP granule size and abundance. The specificity of the stain has previously been confirmed using energy dispersive X-ray spectroscopy (Plouviez et al., 2021). The cellular phosphorus content (%P) at each time point was calculated for each replicate and the replicates from different experimental runs were pooled for each species (Figure 5). Replicates were excluded where their dry weight measurements indicated a decrease over 24 hours (due to measurement error at low densities).

As can be seen in Figure 5, the kinetics of intracellular P accumulation (and related polyP synthesis) were species-dependent:

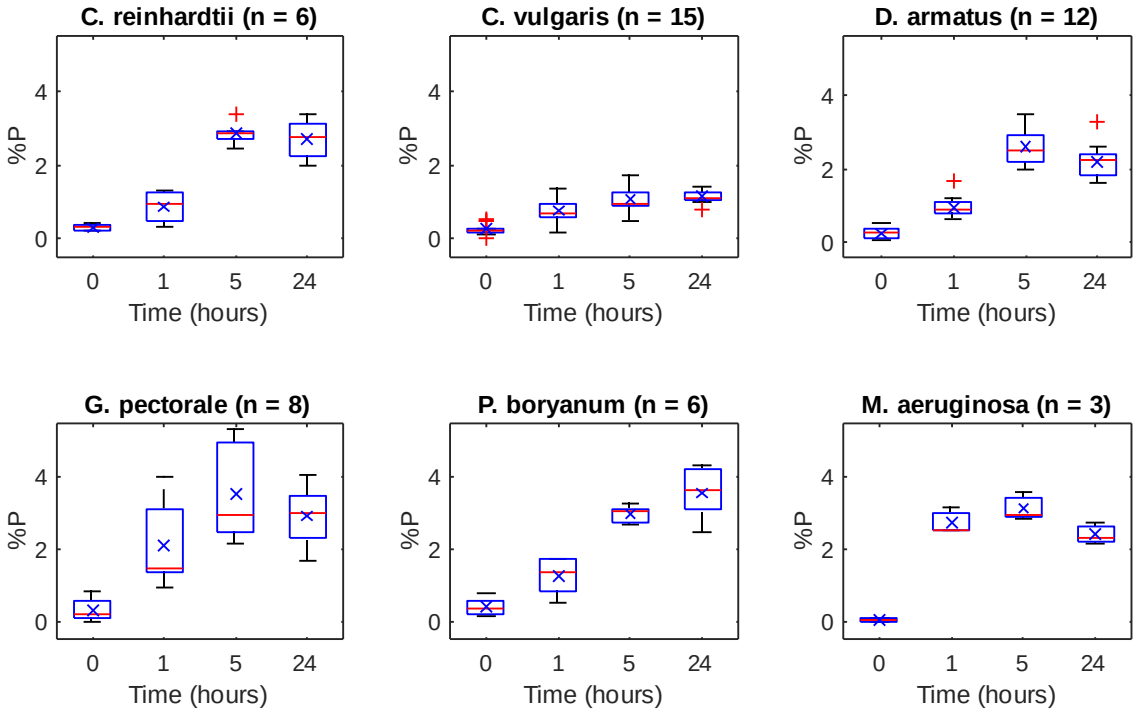

Figure 5. Box-and-whisker plots showing cellular P content as a fraction of dry weight (%P) from n biological replicates of six species of microalgae after P repletion. Mean values are indicated by a blue '×', medians by a red horizontal line, and outliers by a red '+'.

From 0-1 hours after P repletion, cellular phosphorus content (%P) increased significantly in all the tested species. *M. aeruginosa* and *G. pectorale* exhibited the largest changes over this period, increasing to 2.7 ± 0.4% and 2.1 ± 1.2% of dry biomass, respectively, after one hour. This shows

that the response to P repletion occurred rapidly for all the species, as previously evidenced in *C. reinhardtii* (Plouviez et al., 2021).

From 1-5 hours after P repletion, the cellular phosphorus content increased significantly in all the species tested, with the largest increase from 0.9 ± 0.4% to 2.9 ± 0.3% being recorded in *C. reinhardtii*.

Between 5 and 24 hours after P repletion, the cellular phosphorus content only changed significantly in *D. armatus* and *M. aeruginosa*, in both cases decreasing. *D. armatus* grew by 40 ± 12% over this period while the average phosphate concentration of the medium (Figure 6) was not significantly different (t-test, p = 0.18). This combination of cessation of P uptake and continued growth resulted in a decrease of intracellular P relative to dry weight.

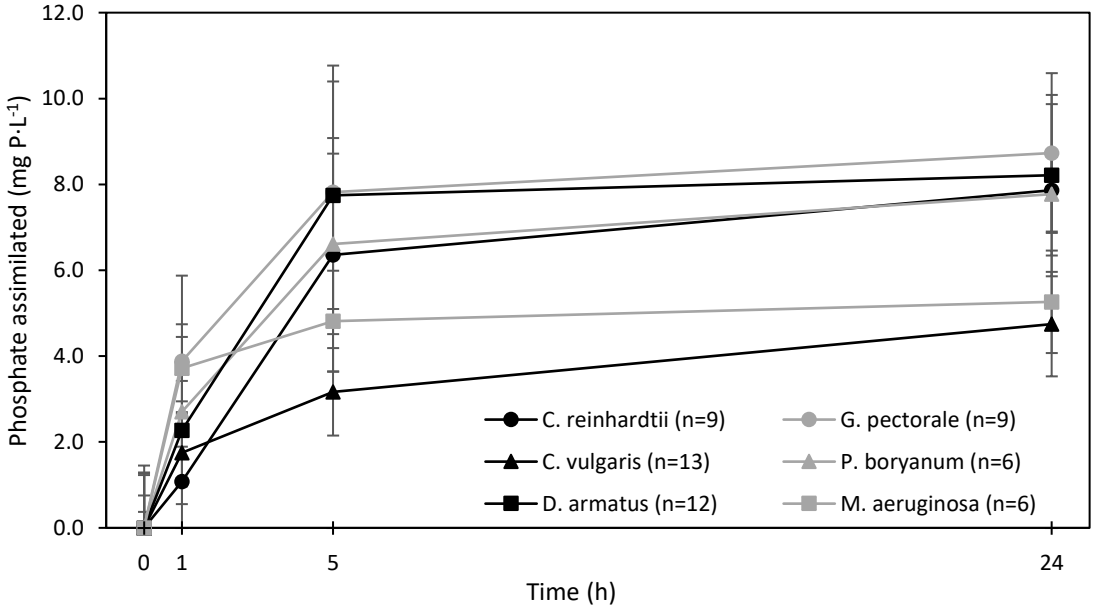

Figure 6. Mean (± standard deviation) cumulative phosphate assimilated by each species. Extracellular phosphate concentrations at 0 h were estimated from the measured concentrations prior to P addition and the quantity of phosphate added, determined by the change in total phosphorus.

The highest cellular P content values recorded ranged from 1.15% (*C. vulgaris*) to 3.55% (*G. pectorale*) (Table 9). These values are in reasonable agreement with values reported in the literature (see Table 7).

Growth rates (μ, day^{-1}) were calculated from the log ratio of dry biomass measurements at the start (DW_i) and end DW_f) of the experiment (Equation 3.1).

$$\mu = \ln\left(\frac{DW_f}{DW_i}\right) \tag{3.1}$$

Table 9. Highest observed %P (mean ± standard deviation) values and the time point at which they were recorded, for each species, observed in the current work.

Species	**Time**	**%P**
Chlamydomonas reinhardtii	5 h	2.9 ± 0.3
Chlorella vulgaris	24 h	1.2 ± 0.2
Desmodesmus cf. *armatus*	5 h	2.6 ± 0.5
Gonium pectorale	5 h	3.6 ± 1.3
Pediastrum boryanum	24 h	3.6 ± 0.8
Microcystis aeruginosa	5 h	3.1 ± 0.4

No significant increase in *P. boryanum* biomass (i.e., no growth) was observed over the 24 hours following P repletion. The other species grew but only *G. pectorale* and *M. aeruginosa* exhibited significantly higher growth in treatment cultures than in control cultures (Figure 7).

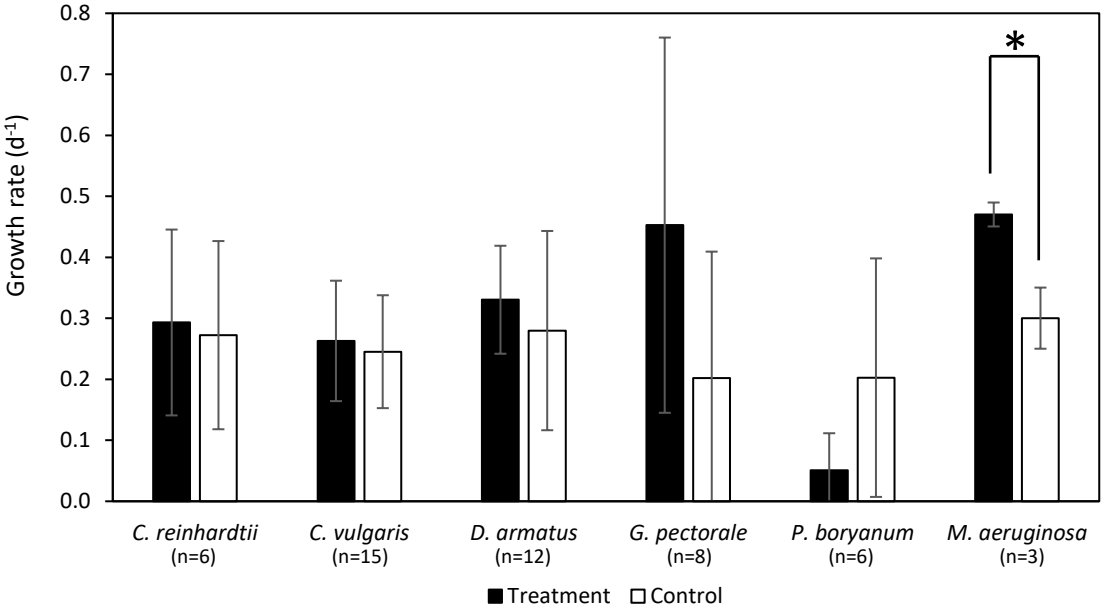

Figure 7. Growth rates (mean ± standard deviation) in P-repleted treatments (T) and controls (C) determined over 24 hours from the P repletion time. Significant differences: * $p < 0.05$

Since growth was not lower when polyP was formed (i.e., in treatment cultures), this suggests that the hypothesized 'energy trade-off' between growth and polyP synthesis had a negligible effect. For all the species tested, except *M. aeruginosa*, the negligible impact of P repletion on growth suggests that the microalgae were not P-limited for growth under the conditions tested. That they still accumulated P as polyP, despite not being P-limited, supports the idea that these stores are used when P becomes limiting and thereby acts as a survival mechanism.

Interestingly, several of the *C. vulgaris* replicates had no visible granules after 24 hours, indicating that the granules formed within the first 5 hours had been consumed. If the P stored in the granules was used for growth, we would expect to see a higher increase in biomass in the treatment cultures but this was not the case.

3.4.3 Protein sequence prediction

RNA extracted from *C. vulgaris* and *D. armatus*[17] was sequenced and transcriptomes assembled. Proteins sequences were predicted from the transcripts and these were searched for homologues of the *C. reinhardtii* VTC4 protein. The results of this process are summarised in Table 10.

Table 10. Results summary for RNA extraction, transcriptome assembly, protein sequence prediction, and BLAST searching for sequence homologues of CrVTC4 in *C. vulgaris* and *D. armatus*.

Species	***C. vulgaris***	***D. armatus***
RNA concentration	48 ng/µL	93 ng/µL
Number of paired-end reads	87,030,946	65,607,216
GC content	62%	56%
Number of assembled transcripts (Trinity)	102,422	268,259
Number of predicted protein sequences (TransDecoder)	99,537	74,681
Number of protein sequences matching CrVTC4	37	17
Sequence length of best match	721 bp	727 bp

[17] The author was unable to extract RNA of sufficient quality for sequencing from *G. pectorale* and *P.boryanum*. The protein sequence for the *C. reinhardtii* VTC4 protein, available from the Phytozome database, was used for the subsequent protein structure prediction.

The resulting predicted protein sequences both contained the three conserved domains found in CrVTC4 (see 3.4.1) and were therefore assumed to have the same polyP polymerase function.

3.4.4 Protein structure prediction and substrate docking

While the involvement of VTC proteins in polyP synthesis has been demonstrated in *C. reinhardtii* (Aksoy et al., 2014; Plouviez et al., 2021; E. Sanz-Luque et al., 2020), this function was only inferred in *C. vulgaris* and *D. armatus* tested based on sequence similarities.

As a first approach to assess potential differences in the polyP synthase activity of VTC complexes, the 3D structures of key VTC4 protein domains (i.e., the VTC polyP polymerase catalytic core and the SPX phosphate sensor domain) from *C. reinhardtii*, *C. vulgaris*, and *D. armatus* were predicted based on the amino acid sequence deduced from their respective putative VTC4 genes. Pairwise similarity between the amino acid sequences was higher between the microalgae than with the yeast (Table 11).

Table 11. Distance matrix showing pairwise sequence similarity (% identity) between the complete VTC4 protein sequences used to generate the structural models, based on a multiple sequence alignment performed using Clustal Omega.

	C. reinhardtii	***C. vulgaris***	***D. armatus***
C. vulgaris	52.9%	n/a	n/a
D. armatus	59.1%	53.7%	n/a
S. cerevisiae	28.8%	29.1%	28.0%

The structure prediction was performed by homology modelling using a classical template-based approach and using the Alphafold2 neural network-based model, followed by molecular dynamics structure equilibration and energy minimization in the presence of a docked polyphosphate (15 residues) in a water box at 25°C.

The three microalgal VTC4 protein structures predicted share a fair structural homology with the VTC4 protein from *Saccharomyces cerevisiae*[18], the experimentally determined structure of which is available in the PDB database (see 3.3.6). Both approaches produced very close structures for the VTC catalytic core and the SPX domain structure. This modelling evidenced that the VTC catalytic core and SPX domain structures are conserved between the microalgae studied and yeast (Figure 8). Furthermore, docking calculations using a pentadecaphosphate (polyP$_{15}$) model showed a similar positioning of the polyP$_{15}$ chain within the catalytic sites (Figure 8), in agreement with the experimental evidence of the polyP catalytic role of VTC4 in *C. reinhardtii* (Plouviez et al., 2021).

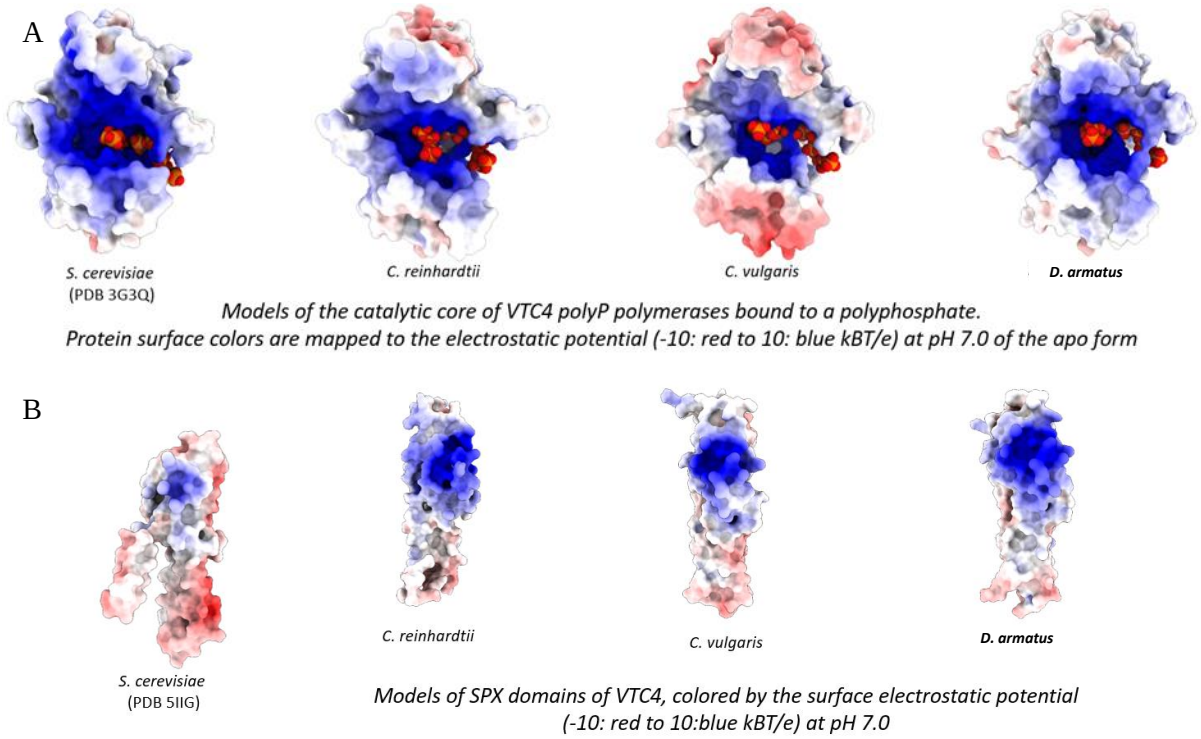

Figure 8. A (top): VTC4 polyP polymerase catalytic core models obtained by homology modelling, using Phyre2 and AlphaFold, for *C. reinhardtii*, *C. vulgaris* and *D. armatus* based on *Saccharomyces cerevisiae* protein crystal structure. Structures were equilibrated in the presence of a docked polyphosphate in a TIP3 water box using NAMD (Nanoscale Molecular Dynamics). B (bottom): VTC4 SPX domain models obtained by homology modelling for *C. reinhardtii*, *C. vulgaris* and *D. armatus* based on *Saccharomyces cerevisiae* protein crystal structure.

[18] 100% probability of homology according to Phyre2 calculations, 38-44% sequence identity with ~60% sequence coverage including the catalytic core.

The structural similarities described above for the predicted VTC4 proteins of *C. vulgaris* and *D. armatus*, identified as such by sequence homology, indicate that these sequences indeed encode VTC4 proteins with similar functionality to that of *C. reinhardtii*.

To the best of our knowledge, the models presented in Figure 8 are the first microalgal VTC protein models currently available. Critically, the predicted structure of VTC4 is confirmed to be compatible with a polyP synthase function in *C. reinhardtii*, *C. vulgaris*, and *D. armatus*. However, further work is needed to understand whether differences in VTC structure can explain the differences in kinetics observed in the bioassays and to unravel how polyP synthesis is regulated at the protein level. Production of these enzymes by heterologous expression and subsequent in vitro characterization may reveal whether the action of these proteins is reversible, as it has recently been shown to be in fungal VTC4 proteins (Nguyen et al., 2022).

3.5 Summary of findings

A BLAST search for protein homologues of the *Chlamydomonas reinhardtii* polyP polymerase CrVTC4 revealed similar protein-encoding sequences in 48 species of microalgae distributed across different phyla. Phylogenetic analysis demonstrated that the similarity between proteins resulted in their organization into clades aligning with their taxonomic relationships. This suggests that the *VTC4* gene represents an ancient ability of microalgae that has evolved with species as the microalgal lineage has spread out over time. Therefore, it is likely that this gene is present within most eukaryotic microalgae and the ability to synthesize polyP is also highly conserved. The evidence to date suggests therefore that polyP synthesis is required in all environments in which microalgae are found but species have evolved unique proteins to suit their needs.

For the first time, six species (including four species known to genetically encode putative VTC4 proteins and one encoding a PPK protein) were assayed under similar conditions for polyP accumulation. All strains accumulated polyP as granules but *Chlorella vulgaris* demonstrated markedly less accumulation than the other species following P repletion in the same conditions.

Growth was not negatively affected by P repletion, suggesting that the energy cost of polyP accumulation does not affect growth. In fact, a positive effect of P repletion on growth in *M. aeruginosa* indicated that P repletion may, in some cases, promote both increasing growth and polyP accumulation.

Protein homology modelling was used to predict VTC4 protein models for *C. reinhardtii*, *C. vulgaris* and *Desmodesmus* cf. *armatus*, based on the structure of the *Saccharomyces cerevisiae* VTC4 protein structure. To the best of our knowledge, these models are the first available for microalgae. Importantly, the models showed structural conservation of the VTC catalytic site and SPX domain, confirming that the structures of CrVTC4 and the predicted VTC4 proteins of *C. vulgaris* and *D. armatus* are compatible with polyP synthase activity.

Further work is needed to understand if differences in VTC structure observed can explain the differences in kinetics observed in the bioassays and to unravel how polyP synthesis is regulated at the protein level in microalgae. However, since it is known that luxury uptake in microalgae is influenced by environmental conditions (see 2.4.2.3), and this knowledge comes largely from studies using mixed populations, further insight can be gained from ascertaining whether these influences are consistent between species observed to display differing kinetics of P uptake and polyP accumulation.

Chapter 4 The species-dependence of environmental influences on luxury uptake in microalgae

4.1 Preface

A review of the relevant literature (Chapter 2) revealed that luxury uptake of phosphorus (P) and its intracellular accumulation as polyphosphate (polyP) have been observed in many species of algae. This mechanism can be triggered 'on demand' and evidence suggests that environmental conditions influence the degree of accumulation.

In Chapter 3, the polyP accumulation abilities of various microalgal species were compared. This involved growing the microalgae on a medium supplied with a low concentration of phosphate for a sufficient time to deplete this extracellular P source, then replenishing it with a high concentration of inorganic phosphate. It was thus demonstrated that, in the same conditions of temperature and light intensity, phosphate was assimilated to maximal concentrations ranging from 1.2 to 5.4 % P (by dry weight) over 24 hours, depending on the species. It was also observed that, over a short period, polyP granules that were formed following P repletion could be subsequently degraded. This degradation may be linked to growth, as the microalgae turn to internal P stores to maintain metabolic processes once the medium again becomes P-depleted.

Although the differences observed in Chapter 3 may reflect differences in the 'abilities' of the species studied, luxury uptake in microalgae is influenced by environmental conditions (see 2.4.2.3) and it is possible that microalgal species respond differently to changes in the various conditions. Environmental conditions known to influence luxury uptake in microalgae were therefore selected as parameters for a screening experiment using two species of microalgae grown axenically. The objective of this experiment was to identify combinations of parameters producing marked differences in the responses of the two species to P repletion, so that their gene expression could be examined (in Chapter 5 and Chapter 6) to determine whether changes in gene expression underly the different responses to P repletion.

4.2 Introduction

The suggested physiological functions of polyP in microalgae are diverse (see Chapter 2, Table 3). However, the circumstances of polyP appearance within cells are somewhat better understood: a rapid change in extracellular phosphate concentration can trigger an 'overplus response' wherein surplus P assimilated from the surroundings is stored as polyP for later use (Harold, 1966). This process requires microalgae to expend energy, first to transport phosphate into and within their cells, and then to form the 'high-energy' phosphoanhydride bonds of polyP. This energy expenditure may impact other cellular processes and, ultimately, growth. Similarly, growth may reduce the energy available for P uptake and polyP synthesis. Furthermore, polyP synthesis may compete with nucleic acid metabolism for available P (Harold, 1966). Therefore, higher polyP accumulation is often evidenced in growth-limiting conditions (Aitchison & Butt, 1973).

Of the environmental conditions known to influence luxury uptake (see 2.4.2.3), five were selected for a factorial experiment to determine effects of changing the parameters on growth and polyP metabolism in *Chlamydomonas reinhardtii* and *Chlorella vulgaris*.

4.3 Methodology

4.3.1 Strains and cultivation conditions

Based on the results obtained in Chapter 3, two species with markedly different responses to changes in P availability were selected. *Chlamydomonas reinhardtii* (CC-1690 wild-type strain) was first selected as it is considered a model organism (Harris, 2001), its genome has been completely sequenced (Merchant et al., 2007) and the P metabolism of this microalga has been widely studied. For comparison, *Chlorella vulgaris* (UTEX 259 strain) was selected based on the low phosphate uptake and kinetics of granule production/consumption observed during the species screening experiments (see Chapter 3).

C. reinhardtii and *C. vulgaris* were cultivated on liquid and solid (agar) media as described in section 3.3.2.1.

4.3.2 Experimental design

The protocol for triggering luxury uptake on demand, described in Chapter 3, was used to screen five parameters of interest (P repletion dose, light supply, P depletion time, temperature, and pH), identified in the literature search (see 2.4.2.3), in a two-level full factorial experimental design. A two-level design (with 'high' and 'low' levels for each factor) allows for identification of statistically significant changes in the response variable associated with changes in one or more parameters.

A total of six two-level factors (including the categorical variable, species) resulted in 64 experiments as well as 10 centre point experiments (5 per species) to confirm consistency across experiments and establish uncertainty values for the response variables. These were ordered semi-randomly (see Appendix B.1.1), such that 2 to 4 experiments could be performed simultaneously in the same conditions of light supply and temperature.

4.3.3 Parameters and response variables

The five environmental factors selected were assigned high, low, and centre point levels (Table 12). Since the species is a categorical variable, centre point experimental runs were performed for each species, using the midpoint values of each of the remaining five parameters.

Table 12. Parameters selected for the factorial experiment.

Parameter	**Units**	**Low level**	**Centre point**	**High level**
P repletion dose [a]	mg $P \cdot L^{-1}$	5	10	15
Light supply [b]	µmol photons$\cdot m^{-2}s^{-1}$	0 ('dark')	80	160 ('light')
P depletion time [c]	Days	3	5	7
Temperature [d]	°C	10	20	30
pH [e]		7.6	8.1	8.6

[a] Standard assay (Chapter 3) dose ± 50%.

[b] Received light on upper surface of Parafilm.

[c] Standard assay P depletion time ± 2 days.

[d] 5 °C below the standard assay temperature ± 10 °C to avoid bleaching observed at 35 °C.

[e] Observed pH in cultivation conditions ± 0.5.

The response variables studied (Table 13) were similar to those used in Chapter 3. However, optical density was used as a proxy for dry weight based on correlations from data collected previously (see Appendix B.1.2) and polyP concentrations were measured directly instead of using cellular P content as an estimate of polyP.

Table 13. Response variables used to assess differences in P assimilation and storage.

Response	**Purpose**
Growth	Identify changes in metabolism linked to the conditions and/or polyP synthesis.
Phosphate uptake	Quantify changes in P assimilation.
PolyP accumulation	Quantify changes in P storage as polyP.
Granule formation	Confirm P storage as vacuolar polyP.

4.3.4 Experimental protocol

To obtain consistent cell densities (measured by optical density) at the start of each experiment, the cell concentration in P-depleted cultures was adjusted either by addition of growth medium without P or by centrifuging and removal of an appropriate volume of supernatant. The target optical density values were approximately 0.80 for *C. reinhardtii* and 1.50 for *C. vulgaris*, to be equivalent to 0.3 g $DW \cdot L^{-1}$ for each species (based on Appendix B.1.2). Samples were taken from the source cultures (three per experiment) for initial measurements (see 4.3.5) and 1 mL of each culture was stored at -80 °C. 7 mL of each source culture, buffered with 20 µM Tris buffer (see Appendix B.1.3), was transferred to two 15.5 mL wells of a six-well flat-bottomed polystyrene microplate (Corning #353046), giving two sets of biological triplicates.

The plates were covered with Parafilm® to minimize moisture loss and contamination without preventing gas transfer (Figure 9). The cultures were mixed by continuous orbital agitation at 150 min^{-1} using benchtop shakers (IKA HS/KS 260). Continuous illumination was provided by fluorescent tubes mounted horizontally above the plates. This consisted of six 18 W T8 5500 K fluorescent tubes (Viva-Lite, Winterbach, Germany) for low light supply (centre points) and nine 36 W T8 5500 K fluorescent tubes (Viva-Lite, Winterbach, Germany) for high light supply. Experiments were conducted at constant temperature in a temperature-controlled room.

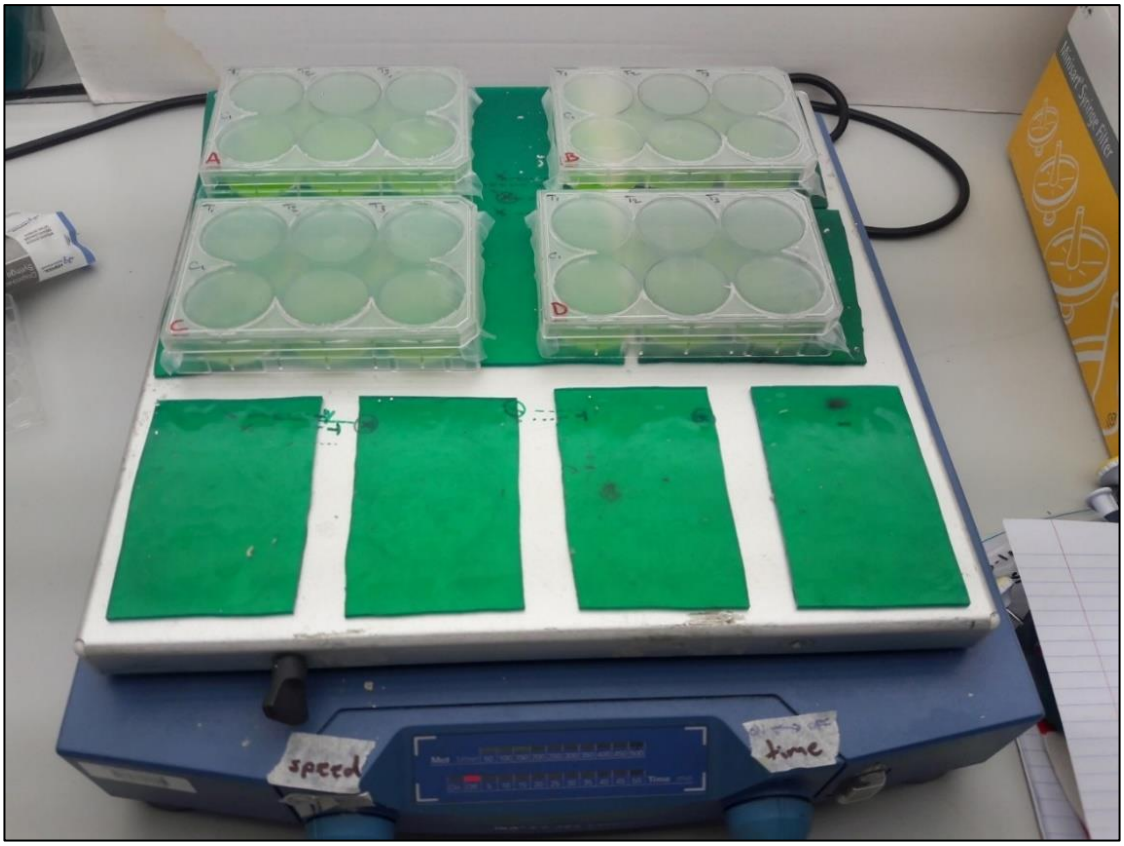

Figure 9. Experimental setup for the factorial experiments. Four experimental plates are shown on the orbital shaker, illuminated from above. Holes have been cut in the lids to allow them to hold the Parafilm in place without inhibiting gas transfer.

At the start of the experiment (0 hours), one set of replicates, henceforth referred to as "treatments", was replenished with 0.1 M phosphate solution (66 mM K_2HPO_4 and 34 mM KH_2PO_4) to obtain the desired phosphate dose. The other set of replicates, henceforth referred to as "controls", received no addition, since the volume of phosphate solution added to the treatments was less than 1% of the total volume and the dilution factor was considered negligible. Additional samples were taken after 6 and 24 hours.

4.3.5 Measurements

Optical density (OD) was measured as absorbance of 683 nm light using a SPECTROstar Nano absorbance plate reader (BMG Labtech). For this purpose, 750 µL samples were mixed with an equal volume of MilliQ water in a 24-well transparent microplate.

The concentration of extracellular free orthophosphate was measured using a microplate assay based on the molybdophosphate colorimetric reaction using ascorbic acid (Murphy & Riley, 1962). A reagent stock solution ('molybdate colour reagent') was prepared from 323 µM potassium antimonyl tartrate and 6.89 mM ammonium molybdate tetrahydrate in 3.5% sulfuric acid. An ascorbic acid solution (50 mM in deionized water) was stored at 4 °C and any unused reagent was discarded after 7 days. Standard phosphate solutions were prepared from potassium dihydrogen phosphate at concentrations ranging from 0.1 to 6.7 $mg \cdot L^{-1}$ in the same buffer used in the experiments. The final reaction mix comprised 135 µL sample, 35 µL molybdate colour reagent, and 30 µL ascorbic acid reagent. This was incubated at room temperature for 10 minutes, before measuring the absorbance at 880 nm using a SPECTROstar Nano absorbance plate reader (BMG Labtech). Standard curves and analysis are shown in Appendix B.1.4.

The relative abundance of polyphosphate (granular or free) was estimated using an in situ fluorometric assay based on methods reported in the literature (Gomes et al., 2013; Kulakova et al., 2011; Martin & Van Mooy, 2013). Frozen samples were thawed at room temperature and transferred to a Nunc 96-well black polystyrene microplate (Thermo Fisher, catalog number 237105) as six aliquots of 117 µL. 33 µL of MilliQ water was added to one of these as autofluorescence control. Polyphosphate standards used as inter-plate controls were prepared from Type 45 sodium phosphate glass (Sigma-Aldrich) at 0.45 and 2.25 mg $P \cdot L^{-1}$. To all wells, except those designated autofluorescence controls (used for measuring fluorescence of the sample matrix, to be deducted from sample measurements), 33 µL of 40 $\mu g \cdot mL^{-1}$ 4′,6-diamidino-2-phenylindole dihydrochloride (DAPI) (Sigma-Aldrich, product number D9542) was added to give a final concentration of 25 µM. The plate was covered with aluminium foil and incubated at room temperature for one hour. Fluorescence intensity was then measured using a Varioskan LUX microplate reader (Thermo Fisher Scientific) using excitation at 415 nm and measuring emission at 550 nm, with 12 nm bandwidth, and 100 ms integration time with automatic dynamic range selection. Values were reported in arbitrary relative fluorescence units (RFU) by SkanIt Software 6.0.1 (Thermo Fisher Scientific). Validation of the protocol for estimating polyP (assuming that

changes in cellular P content mainly represent polyP) from changes in fluorescence intensity is shown in Appendix B.1.5.

Polyphosphate granules were observed using optical light microscopy following cytological staining using lead nitrate and ammonium sulfide (Sells, 2019). Briefly, 200 µL culture was pipetted onto a glass microscope slide, dried at 105 °C in a drying oven, treated with a solution of 25 g lead nitrate·L^{-1} in 5% nitric acid for 5 minutes, rinsed with RO water, treated with 20% ammonium sulfide (aqueous solution) for 10 seconds, rinsed again with RO water, then dried as above. Slides were examined using an Olympus BX53 light microscope fitted with an Olympus XC50 camera and the cellSens Dimension (v. 1.5) software. Granule abundance was ranked from 0 (no granules visible) to 5 (high abundance) as shown in Figure 10 and Figure 11.

pH was measured using an Orion Star A214 pH/ISE meter equipped with an Orion ROSS Ultra pH/ATC Triode (Thermo Scientific) at the start and end of each experimental run.

4.3.6 Analysis

P uptake, polyP accumulation, granule formation, and growth were determined from changes in the response variables (Table 13), from 0-6 h and 6-24 h. Summaries of raw data can be found in Appendix B.1.6 and uncertainty calculations are given in Appendix B.1.7. A five-factor two-level full factorial design for each species subset was implemented in Minitab 18 (www.minitab.com). Data were entered as averages of biological replicates and analyzed using a general linear model. A factorial analysis was performed on each data set (one per species) with up to two-way interaction effects, identified as significant for p-values < 0.05 (Appendix B.1.8). Identified effects were verified using paired t-tests in R (version 3.6.3). Using paired t-tests allows for significant differences in a single parameter to be identified while accounting for concurrent changes in other parameters (data are paired such that only the parameter of interest changes within each pair) and therefore can discern effects more clearly than simply comparing the variabilities of two sets of data in which many parameters are varied. Differences were considered significant where the p-value is less than 0.05, unless otherwise specified.

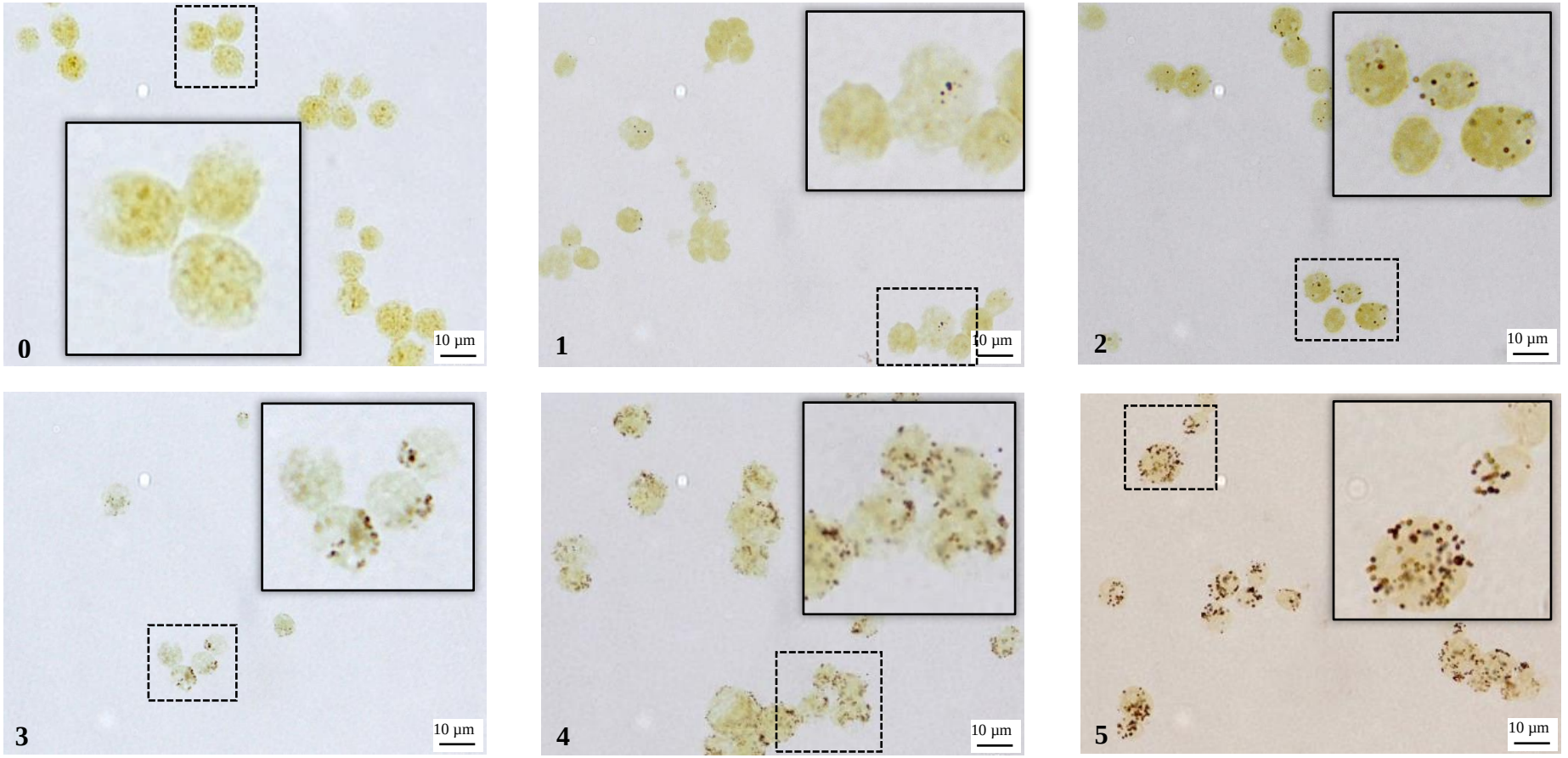

Figure 10. Examples of granule abundance rankings for *C. reinhardtii*. Numbers indicate ranking on a scale of 0 – 5. Scale bars in bottom right indicate 10 µm. Inset images show enlargements of regions surrounded by dashed borders.

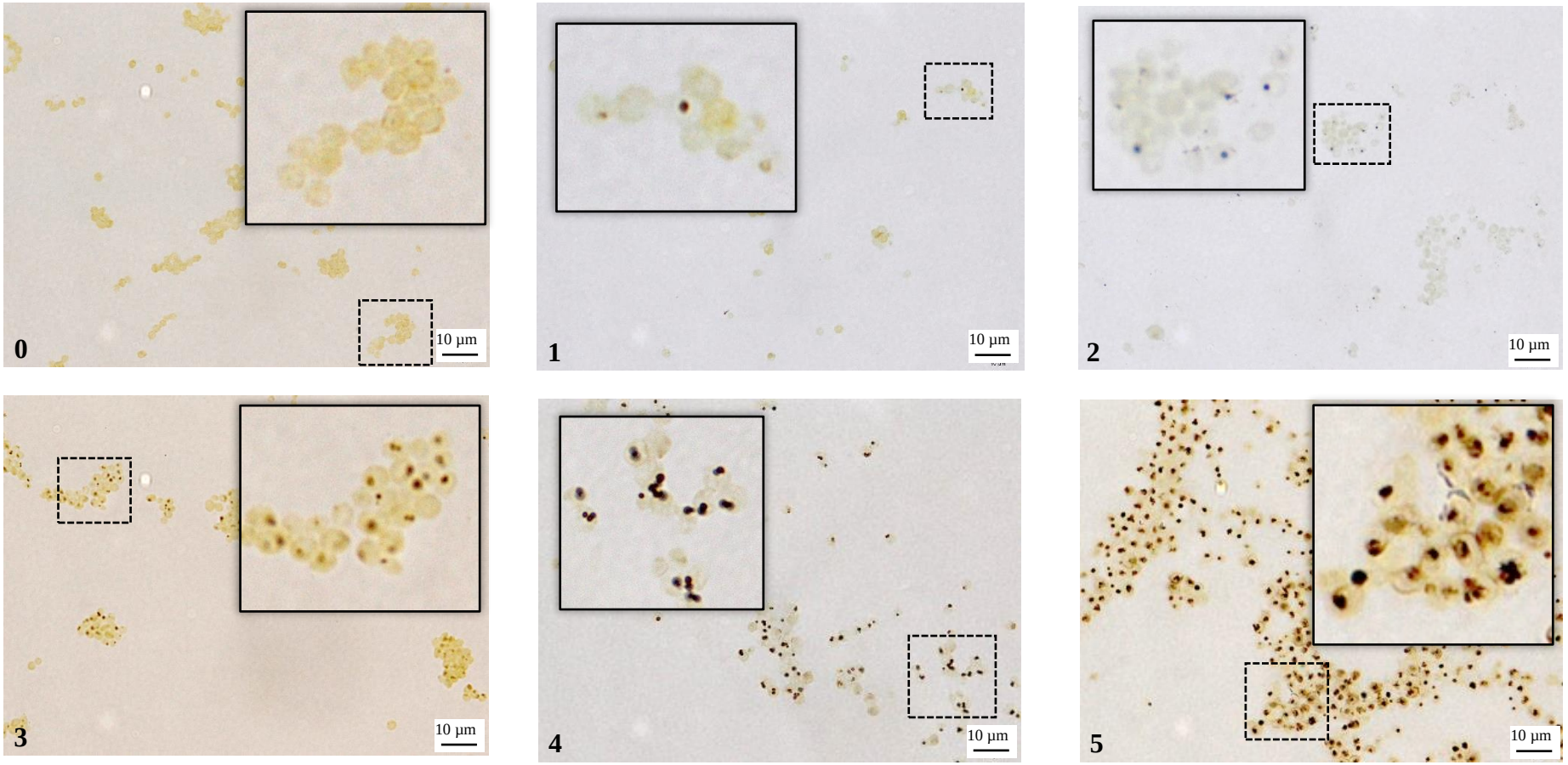

Figure 11. Examples of granule abundance rankings for *C. vulgaris*. Numbers indicate ranking on a scale of 0 – 5. Scale bars in bottom right indicate 10 µm. Inset images show enlargements of regions surrounded by dashed borders.

4.4 Results

In Chapter 3, *Chlamydomonas reinhardtii* and *Chlorella vulgaris* were shown to assimilate P differently in response to P repletion following a period of P depletion. Those experiments were conducted in the same conditions of light intensity, temperature, and pH, the cultures were grown without further P addition (P-depleted) for the same length of time (5 days), and the concentration of extracellular P added after this period was the same (10 mg $P \cdot L^{-1}$). To evaluate how changes in these parameters influence P assimilation and storage, and how the two species might respond differently to environmental changes, a full factorial experiment was carried out.

The following sections (4.4.1 to 4.4.4) present the main effects of the selected parameters on the response variables. Significant effects were identified with respect to each response variable (growth, P uptake, polyP accumulation, and granule formation), firstly by referring to effects matrices (Appendix B.1.8) produced from the results of the factorial analysis, and then by confirming significance using *t*-tests on the collated data (Appendix B.1.6).

4.4.1 The influence of environmental parameters on growth

It was shown in Chapter 3 that *C. reinhardtii* and *C. vulgaris* grew significantly in the conditions tested (Figure 7). There were also no differences in growth between P-repleted treatments and P-depleted controls over 24 hours. This suggested that P repletion did not have a significant effect on growth over this period (i.e., the cells were P-depleted but not P-limited). The effects of P repletion might, however, not be observed if the required threshold of P supply for growth is met and other factors are growth-limiting (Wu et al., 2021).

The 'centre point conditions' used in the present factorial experiment (20 °C, 80 µmol photons$\cdot m^{-2}s^{-1}$, 5 days P depletion) were closer to the conditions used in Chapter 3 (25 °C, 29 µmol photons$\cdot m^{-2}s^{-1}$ light, 5 days P depletion) than the high and low levels of each parameter. While the temperature was 5 °C lower and the light intensity was more than doubled, the P repletion dose given was the same on a volume basis (10 mg $P \cdot L^{-1}$).

In the centre point experiments (5 experimental runs per species, with biological triplicates in each; data are presented in Appendix B.1.6), growth was significantly higher (paired *t*-test, $p < 0.05$) in P-repleted treatment cultures than in controls over 24 hours, for both species (Figure 12).

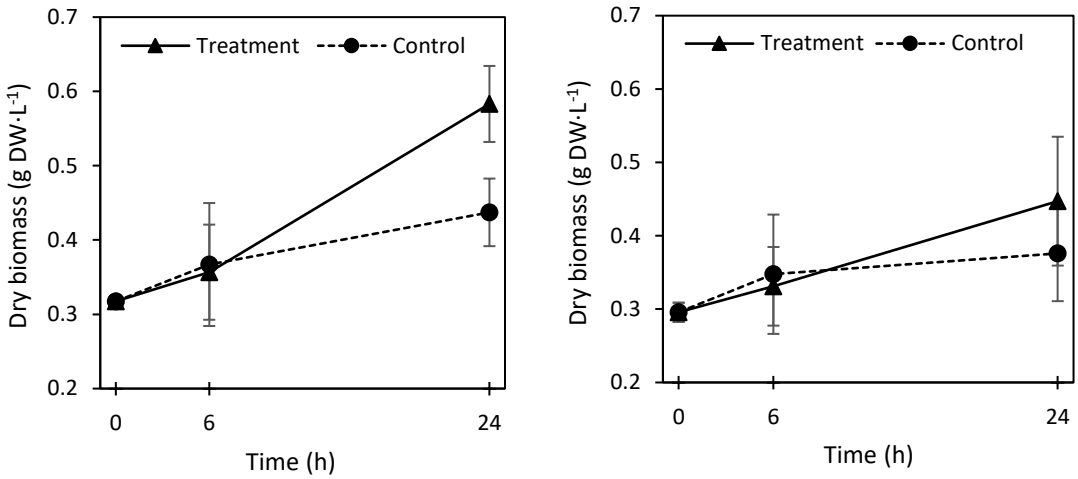

Figure 12. Growth (changes in dry weight) in *C. reinhardtii* (left) and *C. vulgaris* (right) cultures in centre point experimental runs (temperature: 20 °C; light supply: 80 µmol·m^{-2}s^{-1}; P repletion dose: 10 mg P·L^{-1}; pH: 8.1; P depletion time: 5 days).

Since all cultures used in the present work were pre-cultivated in the same conditions used in Chapter 3, the cultures may have been acclimatizing to the changes in light intensity and temperature (increasing light intensity from 29 to 80 µmol photons·m^{-2}s^{-1} and temperature increased from 20 to 25 °C) at the start of the experiment.

Growth rates in the control (P-depleted) cultures were similar between Chapter 3 and Chapter 4 (Table 14) but growth in the treatment (P-repleted) cultures was significantly higher than in the controls only in the Chapter 4 centre point experiments, confirming P limitation and suggesting that growth in the Chapter 3 cultures was limited by light.

Growth was not significantly affected by pH or P repletion dose in either species[19] but was influenced by the other parameters as discussed below.

[19] Although the effects matrices indicate that P repletion dose was associated with *C. reinhardtii* growth in light from 6-24 h (Appendix B.1.8), this effect was determined to be a statistical artefact.

Table 14. Comparison of growth rates (mean ± SD) over 24 hours for *C. reinhardtii* and *C. vulgaris* calculated from the results of Chapter 3 and Chapter 4.

		Growth rate (d^{-1})	
		Chapter 3 [a]	Chapter 4 [b]
C. reinhardtii	Treatments	0.29 ± 0.15 (n = 6)	0.61 ± 0.10 (n = 15)
	Controls	0.33 ± 0.16 (n = 4)	0.32 ± 0.10 (n = 15)
C. vulgaris	Treatments	0.27 ± 0.11 (n = 12)	0.40 ± 0.19 (n = 15)
	Controls	0.25 ± 0.10 (n = 12)	0.23 ± 0.15 (n = 15)

[a] Determined as the log ratio of the final biomass density (DW) to initial density.

[b] Calculated as above, using centre point optical density (OD) data. Assumes a constant DW/OD ratio.

Light supply

Considerable metabolic differences may occur between light and dark conditions. Treating these conditions as levels in the factorial analysis may imply a continuum of response to this parameter. Therefore, the data for each species were split into subsets by light supply for further analysis.

Optical density (OD) (Appendix B.1.6) increased in darkness although growth could not have occurred in the absence of light or an organic carbon source to supply energy. The absence of growth was confirmed by replicating the experiment and directly measuring dry biomass (DW) (Appendix B.1.9). The changes in OD in darkness were therefore assumed to be related to changes in pigmentation due to the transfer from conditions of light sufficiency to darkness (Soeder & Stengel, 1974) or cell clumping. Consequently, only the optical density data from experiments conducted in light conditions were analysed to identify effects of the parameters on growth.

P depletion time

Although Hernandez et al. (2006) found *C. vulgaris* growth declined irreversibly after 5 days of P starvation, the *C. vulgaris* cultures in the present work were able to grow after 7 days P depletion (mean = 0.039 g $DW \cdot L^{-1}$ over 24 h). This growth was however less than the growth of cultures only P-depleted for 3 days (mean = 0.121 g $DW \cdot L^{-1}$ over 24 h). Growth in *C. reinhardtii* was not

impacted by P depletion time. It should be noted that some authors use the term ‘P starvation’ to refer to conditions in which cultures are removed from P-containing media and resuspended in P-free media, causing an abrupt change in extracellular P availability, whereas the term ‘P depletion’ used in the present work refers to a culture inoculated on low-P media and allowed to gradually deplete the P in the medium through growth. This may mean that growth in P-starved cultures is affected by the lack of available P whereas growth in P-depleted cultures is not affected.

Temperature

Since pH, and P repletion dose were not significantly associated with changes in growth, and P depletion time was only associated with changes in *C. vulgaris* growth, the data from experimental runs performed in light were considered to be replicates at either 30 °C (n = 8) or 10 °C (n = 8), with respect to growth. Photosynthetic activity approximately doubles for every 10 °C increase (Davison, 1991), so a significant difference in growth was expected over the experimental range of 20 °C. Although metabolism is expected to be reduced at 10 °C, previous studies have shown that some microalgae can still grow at this temperature (Schmidt et al., 2016).

C. reinhardtii grew significantly under light supply and this growth was significantly ($p < 0.05$) higher at 30 °C than at 10 °C (Figure 13, left), whereas *C. vulgaris* only grew significantly at 30 °C (Figure 13, right).

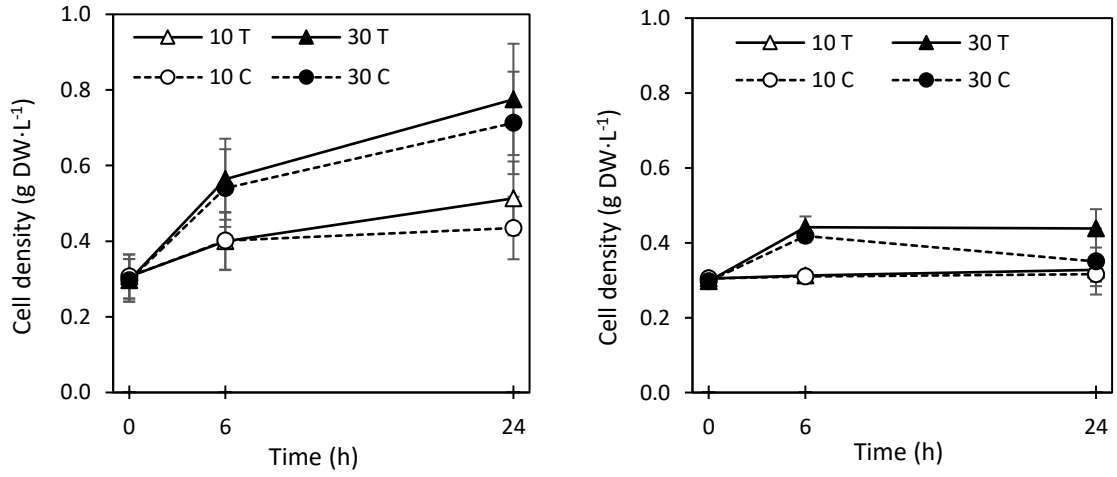

Figure 13: Growth (change in dry weight) of *C. reinhardtii* (left) and *C. vulgaris* (right) P-repleted treatment (T) and P-depleted control (C) cultures at 10 and 30 °C under light supply. Error bars represent standard deviations of 8 replicates for each condition.

4.4.2 The influence of environmental parameters on phosphate uptake

C. reinhardtii

The factorial analysis (Appendix B.1.8, Table 45) indicated that P uptake in *C. reinhardtii* was most strongly impacted by P repletion dose, as can be seen in Figure 14 (left). From 0-6 h (and from 0-24 h), P uptake was significantly ($p < 0.05$) associated with P repletion dose, both in light and darkness.

At the low P repletion dose (5 mg $P \cdot L^{-1}$), *C. reinhardtii* assimilated all the available P in the first six hours after P repletion (Figure 14, top left) and further P uptake was absent due to P depletion in the medium (Figure 14, middle left). At the high P repletion dose (15 mg $P \cdot L^{-1}$), P uptake was more variable and this variation was not accounted for by differences in light supply ($p = 0.08$), temperature ($p = 0.12$), or pH ($p = 0.60$) from 0-6 h. Instead, increasing P depletion time was significantly ($p < 0.05$) associated with increasing P uptake (from 11.0 ± 3.1 to 14.6 ± 4.1 mg $P \cdot L^{-1}$) at the high P repletion dose from 0-6 h as reported for other species (Lavrinovičs et al., 2021). This difference was not significant from 0-24 h, indicating that the initial rate of P uptake, not the total P assimilated, was affected by the change in P repletion dose.

C. vulgaris

P uptake was more variable in *C. vulgaris* than in *C. reinhardtii* from 0-6 h, at both P repletion doses (Figure 14, right). In contrast, P uptake from 6-24 h increased from 0.3 ± 0.1 to 4.3 ± 1.2 mg $P \cdot L^{-1}$ with increasing P repletion dose. P uptake was also positively associated with light supply, at both high and low P repletion doses from 0-6 h, but only at the high dose from 6-24 h. This suggests that *C. vulgaris* has a more limited 'capacity' for P storage than *C. reinhardtii* but its ability to assimilate P is increased in the light when P can also be used for growth.

While P uptake in *C. vulgaris* was on average the highest in the light at the high P repletion dose, it was also the most variable in these conditions. No significant effects involving any of the other tested parameters were able to account for this variability.

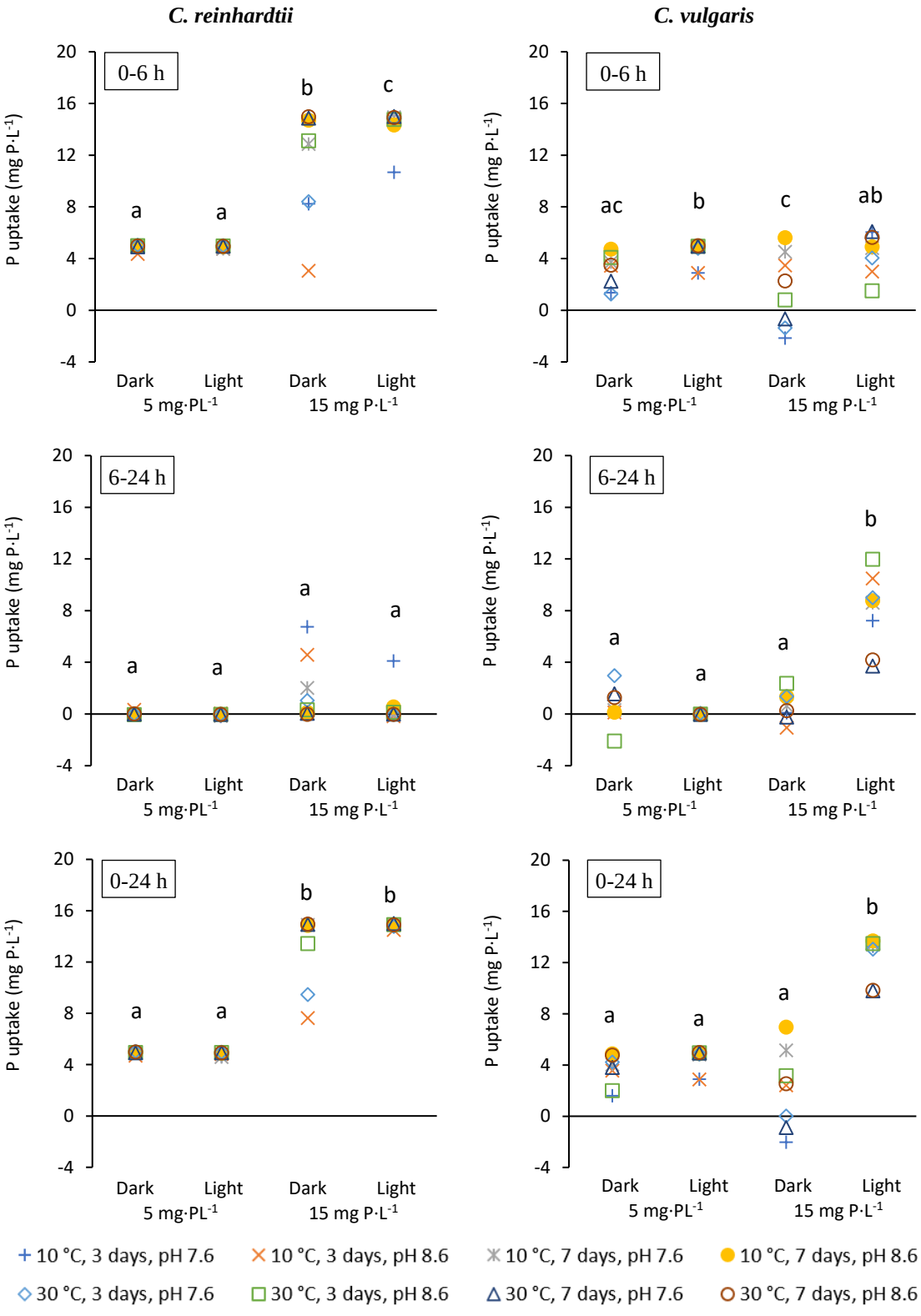

Figure 14. Phosphate uptake (change in extracellular phosphate concentration, mg P·L^{-1}) in the indicated light supply and P repletion dose (mg P·L^{-1}) conditions. n = 8 in all cases. Error bars are not shown for clarity given the high number of data points displayed. Measurements from sets of conditions annotated with different letters were significantly different (paired t-tests, $p < 0.05$).

Higher P uptake in *C. vulgaris* from 0-6 hours was also significantly associated with increased P depletion time, in both light and darkness.

4.4.3 The influence of environmental parameters on polyP accumulation

The polyP content of samples (Figure 15) was estimated semi-quantitatively [20] using a fluorescence assay with the fluorophore DAPI (see 4.3.5). Differences between polyP measurements were evaluated from 0-6 h and from 6-24 h to give estimates of intracellular polyP accumulation over these intervals.

C. reinhardtii

PolyP accumulation in *C. reinhardtii* was strongly associated with P repletion dose (see Appendix B.1.8, Table 47). A positive association between temperature and polyP accumulation from 0-6 h was found only at the low P repletion dose, increasing the change in polyP content from 0.26 ± 0.13 to 0.51 ± 0.25. P depletion time was positively associated with polyP accumulation only at the high P repletion dose and from 6-24 h (increasing from 0.06 ± 0.03 to 0.35 ± 0.17). Decreases in polyP content were only observed in 3-day P-depleted cultures from 6-24 h and were not associated with decreases in granule abundance, suggesting that non-granular polyP formed during the first 6 hours was used for metabolism, but not in the more P-depleted (7 days) cultures.

C. vulgaris

PolyP accumulation in *C. vulgaris* was most strongly associated with light supply from 0-6 h and P repletion dose from 6-24 h (Appendix B.1.8, Table 48). The effect of light supply from 6-24 h (indicated by the factorial analysis) was found to only be significant ($p < 0.05$) at the high repletion dose, as can be seen in Figure 15 (middle, right). The effect of P repletion dose was also not significant in the 3-day P depletion time condition.

[20] Arbitrary relative fluorescence units (RFU) allow quantitative comparison between fluorescence intensity measurements of polyP without reference to physical units.

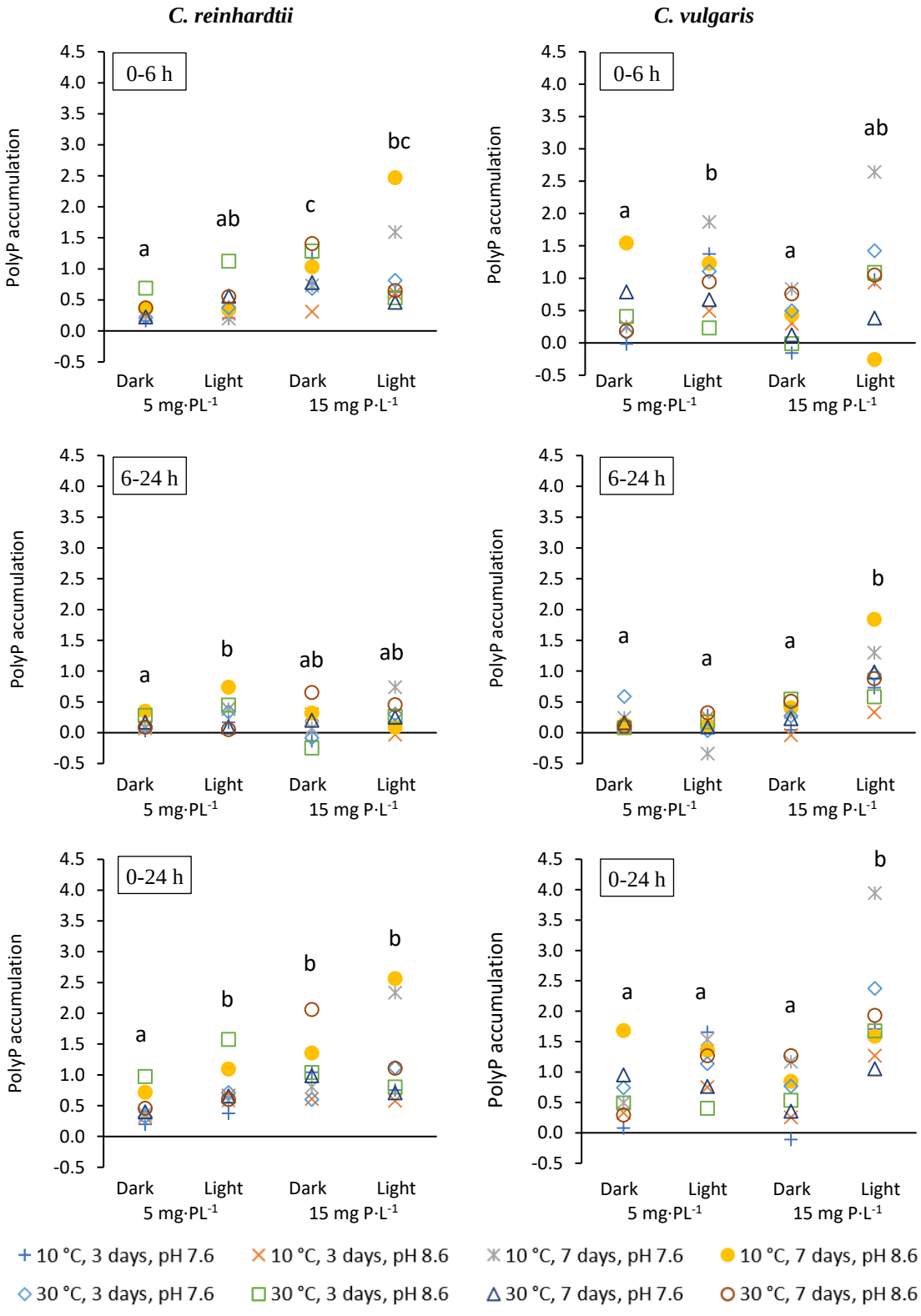

Figure 15. PolyP accumulation (changes in fluorescence intensity) in the indicated light supply and P repletion dose (mg $P \cdot L^{-1}$) conditions. n = 8 in all cases. Error bars are not shown for clarity given the high number of data points displayed. Measurements from sets of conditions annotated with different letters were significantly different (paired t-tests, $p < 0.05$).

Initial measurements of polyP content were consistently higher in *C. vulgaris* than in *C. reinhardtii*. It has been noted in the literature that *Chlorella* spp. can harbour considerable quantities of polyP under normal growth conditions (Harold, 1966) and this might be a point of difference between the two species. However, as evidenced by their OD/DW ratios, the cells of the two species have different spectrochemistry, so it is possible that fluorescence measurements are not directly comparable between species. Within each species, relative changes in fluorescence were used to establish patterns of changes in polyP with respect to the tested conditions and these patterns were compared between the two species.

4.4.4 The influence of environmental parameters on granule formation

Granule formation was not quantitatively compared between the two species because differences in cell sizes and typical numbers of granules per cell (see Chapter 3) potentially introduce a bias. The rankings used reflect the abundance of granules relative to the maximum observed in each species and can be used to compare trends between the two species (Figure 16).

C. reinhardtii

Granule formation in *C. reinhardtii* was positively associated with P repletion dose (increasing from 3.1 ± 1.4 to 4.2 ± 1.9) and light supply (increasing from 3.3 ± 1.5 to 4.1 ± 1.8) from 0-6 h. Temperature and P depletion time were negatively associated with granule formation but only at the low P repletion dose.

From 6-24 h, the only observed effect was a negative association between granule formation and light supply, decreasing the change in abundance ranking from an average of 0.25 ± 0.07 to -1.00 ± 0.45. This suggests that granule consumption occurred due to growth in light in P-limited conditions. This is similar to the pattern of production and degradation of acid-soluble polyP observed by Aitchison and Butt (1973).

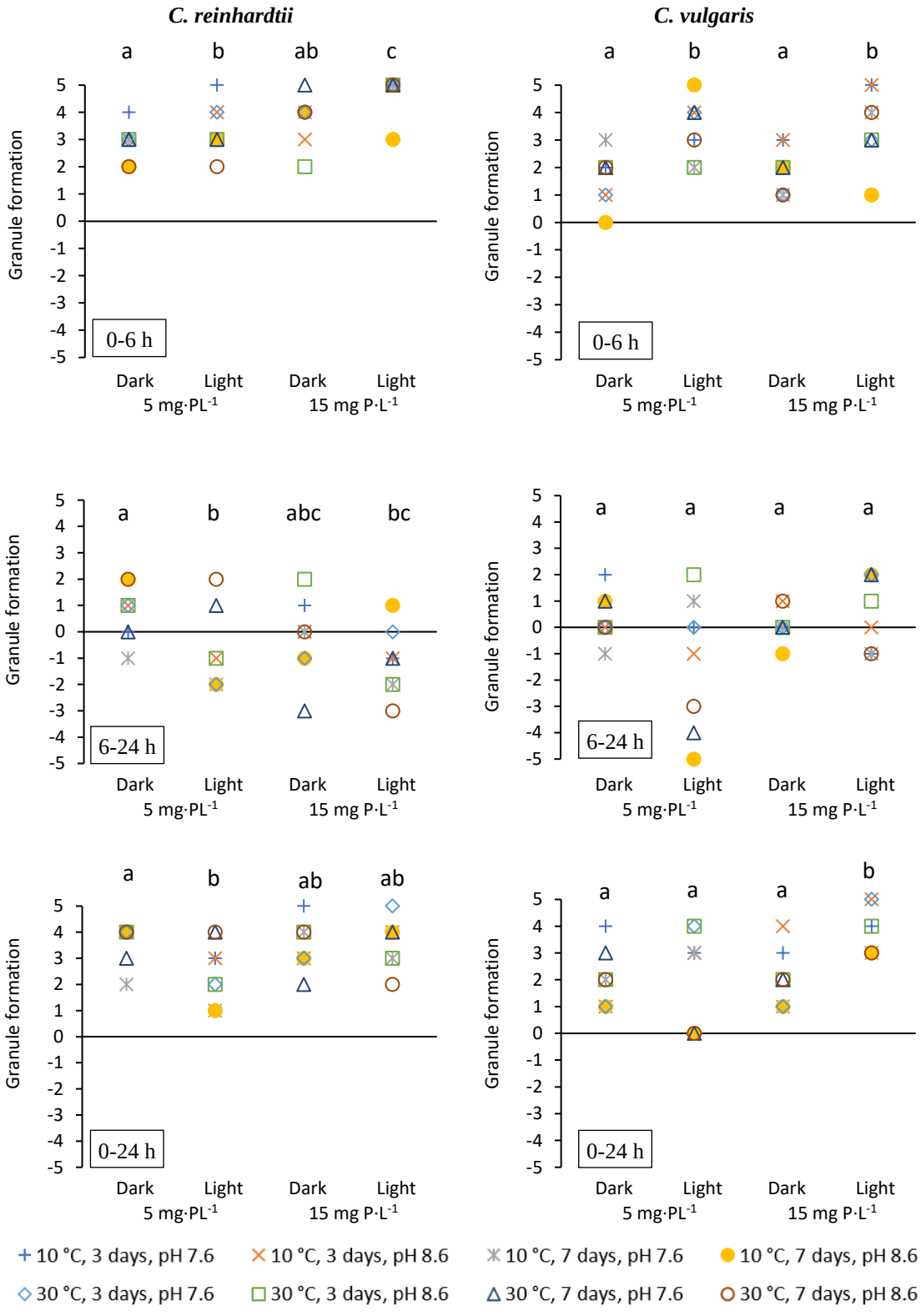

Figure 16. Granule formation (changes in ranked granule abundance in cytologically stained samples) in the indicated light supply and P repletion dose (mg $P \cdot L^{-1}$) conditions. n = 8 in all cases. Error bars are not shown for clarity given the high number of data points displayed. Measurements from sets of conditions annotated with different letters were significantly different (paired t-tests, $p < 0.05$).

C. vulgaris

The results of the factorial analysis (Appendix B.1.8, Table 50) indicated that only light supply was positively associated with granule formation from 0-6 h, increasing from an average of 1.8 ± 0.7 to 3.4 ± 1.4.

There was considerable variation in granule formation/degradation from 6-24 h in the light and at the low P repletion dose (Figure 16, middle right) but this could not be statistically associated with changes in any of the other parameters.

4.5 Discussion

Growth in both species was associated with differences in light supply and temperature, as can be seen in Table 15 and Table 16. This was expected since both these parameters influence photosynthesis (Soeder & Stengel, 1974). Growth was not affected by P repletion in either species, meaning that P uptake and accumulation as polyP were not having a significant energy penalty on growth.

Table 15. Summary of significant effects of the tested parameters on the given response variables in *C. reinhardtii*.

Parameter	**Response variable**			
	Growth	P uptake	PolyP accumulation	Granule formation
Light supply	+	NS	NS	+/- [a]
Temperature	+	NS	+	-
P repletion dose	NS	+	+	+
pH	NS	NS	NS	NS
P depletion time	NS	+	+	-

[a] Positive effect from 0-6 h and negative effect from 6-24 h. Effects are indicated as positive (+), negative (-), or not significant (NS).

All the parameters tested influenced P uptake and polyP accumulation in both species. Clear differences were observed between the two species as discussed further below.

Table 16. Summary of significant effects of the tested parameters on the given response variables in *C. vulgaris*.

Parameter	**Response variable**			
	Growth	P uptake	PolyP accumulation	Granule formation
Light supply	+	+	+	+
Temperature	+	NS	NS	NS
P repletion dose	NS	+	+	NS
pH	NS	NS	NS	NS
P depletion time	- [b]	+	NS	NS

[b] Effect only observed in treatment (+P) cultures. Effects are indicated as positive (+), negative (-), or not significant (ns).

Light supply

P uptake in *C. reinhardtii* was not influenced by light supply, indicating that the lack of light energy in darkness did not inhibit P assimilation, whereas P uptake in *C. vulgaris* was reduced in the absence of light. This suggests that *C. vulgaris* has a more limited ability, compared to *C. reinhardtii*, to utilize other energy sources for P uptake.

PolyP accumulation in *C. vulgaris* was also significantly lower in darkness, but species still synthesized polyP in the absence of external energy (i.e., light) supply. Furthermore, polyP was not accumulated more when growth was absent (in darkness). This indicates that polyP accumulation was not diminished by concurrent growth 'competing' for limited light energy (Plouviez, Oliveira da Rocha, & Guieysse, 2022). The higher polyP accumulation observed in light supply suggests that P uptake and/or polyP synthesis is/are enhanced directly by increased light energy. It is also possible that the fluorescence signal is lower for granular polyP compared to the equivalent amount of 'free' polyP (due to the high density of granules) and that photosynthetic growth results in the mobilization of short-chain polyP (potentially produced from long-chain granular polyP) within the cell.

PolyP granules were formed in both species from 0-6 h and the granule abundance after 6 hours was higher in light than in darkness. From 6-24 h, reductions in granule abundance (assumed to be granule consumption[21]) were observed in both species. In *C. reinhardtii*, this was higher in light than in darkness whereas light supply had no significant effect on granule consumption in *C. vulgaris* over this period. Although P repletion dose did not have a significant effect on granule consumption, it was noted that the majority of granule consumption occurred in experimental runs in which all the extracellular P was assimilated while light was supplied. Therefore, it appears that both species have formed granules and then used them for metabolism when external P sources were exhausted.

Temperature

Increased temperature was associated with increased growth in both species but was only associated with significant changes in polyP metabolism in *C. reinhardtii*. Luxury P uptake has been reported to be enhanced by increased temperature (Powell et al., 2009; Powell et al., 2008) but changes in cellular P content (as a measure of luxury uptake) are the result of changes in both P assimilation and cell growth. For *C. vulgaris*, this means that our observation of higher growth at a higher temperature, without similarly higher P assimilation, results in an overall *decrease* in cellular P content with increasing temperature in this species.

In *C. reinhardtii*, at the low P repletion dose, increased temperature was associated with increased polyP accumulation but decreased granule formation, suggesting that more of the assimilated P was used for growth (resulting in an increase in 'metabolic' polyP, as discussed above with respect to light supply), rather than being stored in granules, at the higher temperature. The high P repletion dose was presumably sufficient to enable a higher rate of growth (at the higher temperature) without impacting on the cells' ability to store polyP as granules. Since increasing

[21] It should be noted that granule abundance was a highly subjective metric and may be influenced by growth, since high levels of growth may reduce the relative abundance of granules.

temperature tends to increase the rate of biochemical processes (up to a point), the absence of a clear effect of temperature on P uptake suggests that enzyme kinetics were not rate limiting for these processes.

pH

The response variables were not significantly affected by changes in pH for either species. Sells et al. (2018) observed an effect of pH on luxury uptake (in mixed populations dominated by *Scenedesmus* spp.) but concluded that this was due to effects on CO_2 limitation and, consequently, growth. Other authors (Cembella et al., 1982; Kuhl, 1962) have noted that P uptake in some species, including *C. vulgaris*, is maximal around pH 6 – 8. The range of pH values tested may therefore have not been sufficient to observe effects on P assimilation.

P repletion dose

In both species, increasing P repletion dose led to increases in P uptake and polyP accumulation, but no change in growth. This finding corroborates evidence in the literature that luxury uptake is positively influenced by the external P concentration (Crimp et al., 2018; Powell et al., 2009; Schmidt et al., 2016).

P repletion dose was positively associated with granule formation in *C. reinhardtii* but not in *C. vulgaris*, despite being positively associated with P uptake and polyP accumulation in both species. This suggests that *C. reinhardtii* has a higher capacity for polyP storage than *C. vulgaris*. The latter was observed to contain only 1 – 3 granules per cell, whereas *C. reinhardtii* had more granules per cell by an order of magnitude. It is not clear whether there are different limits on the number of vacuoles each species can produce or whether the lower number of granules observed in *C. vulgaris* was a result of lower polyP synthesis. Further work could elucidate the process of granule formation and the composition of vacuole contents in different species.

P depletion time

Prior P depletion has been shown to increase the rate of P uptake following P repletion (Hernandez et al., 2006; Lavrinovičs et al., 2021). It has also been shown that some species will not accumulate polyP upon P addition without first being starved of P whereas other species accumulate more polyP *without* prior starvation (Lavrinovičs et al., 2020). Lavrinovičs et al. (2021) found that *C. vulgaris* assimilated P faster after 3 days P depletion than without P depletion, but slower after 5 days than after 3 days, while other algal species followed different patterns. This might indicate that *C. vulgaris* responds to sustained P stress by shutting down metabolism, including P uptake, while other species enhance their P scavenging mechanisms through upregulation of genes related to P metabolism. In the present work, increasing the P depletion time from 3 to 7 days was associated with higher P uptake over the first six hours following P repletion in both *C. reinhardtii* and *C. vulgaris*. This suggests that both species, when grown for a longer time without P addition, were more metabolically prepared to assimilate P (Plouviez et al., 2021). However, changes in P depletion time were not associated with changes in polyP accumulation or granule formation in *C. vulgaris* although P depletion time was positively associated with polyP accumulation in *C. reinhardtii*. Interestingly, P depletion time was also negatively associated with granule formation in *C. reinhardtii* from 0-6 h at the low P repletion dose. This may indicate that a longer P depletion time means that P is needed to restore normal metabolism following austerity measures (P sparing etc.) although it is not clear why the P is first stored as granular polyP, which incurs an energy cost.

The work described here demonstrated that the responses of *C. reinhardtii* and *C. vulgaris* to P repletion following P depletion were affected differently by the environmental conditions, confirming that the tested parameters not only influence luxury uptake but may also be key to understanding species differences. The mechanisms through which they influence luxury uptake are not well understood but may involve changes in the regulation of genes in the P/polyP pathway. Therefore, the next objective sought to determine whether there were in fact gene expressions changes related to changing these parameters.

Chapter 5 Can environmental effects on gene expression explain changes in luxury uptake?

5.1 Preface

In Chapter 4, changes in temperature, light supply, P repletion dose, and P depletion time were shown to be associated with changes in polyP metabolism in *Chlamydomonas reinhardtii* and *Chlorella vulgaris*. The initial objective of subsequent research was to examine the role of gene expression in the two species' different responses to P repletion following P depletion. However, due to poor reproducibility of RNA extraction from *C. vulgaris*, this work focuses on *C. reinhardtii*. This green microalga is also a model species with a fully sequenced genome and with which numerous studies have already been undertaken to elucidate gene expression responses to changes in nutrient status, making it an ideal candidate for study in this context.

The work presented in this Chapter aims to determine whether differences in gene expression might be responsible for observed effects of environmental parameters on luxury uptake. To the best of our knowledge, the effects of these parameters on gene expression in the polyP pathway have not previously been investigated. This knowledge is important to inform future research and development of microalgae-based wastewater treatment technologies and to better understand the ecological implications of increased nutrient availability in waterways.

Since the factorial experiment described in Chapter 4 revealed that changing light supply, temperature, P repletion dose, and P depletion time resulted in clear differences in P uptake and polyP accumulation, selected experiments were repeated with samples taken for gene expression analysis. This enabled confirmation of the parameters which significantly influenced P metabolism and to investigate potential links between the changes observed in Chapter 4 and changes in gene expression.

5.2 Introduction

Algae deprived of phosphorus (P) engage a suite of abiotic stress[22] responses collectively termed the 'P starvation response'. The examination of gene expression can provide insight into these responses. Gene expression refers to the process of using information stores in genes to produce functional proteins through the transcription of genes into mRNA[23] and subsequent translation of mRNA into amino acid sequences.

Microalgae possess numerous enzymes involved in P uptake and polyP accumulation. Under conditions of P sufficiency, free extracellular phosphate is transported across the cellular membrane by constitutive low-affinity [24] phosphate (P_i) transporters (Dyhrman, 2016; Shimogawara et al., 1999). As external P availability decreases, cells respond by activating genes to produce inducible[25] phosphatases as well as high-affinity phosphate transporters (Grossman & Aksoy, 2015). Intracellular P-containing compounds may also be used as a source of P: for example, chloroplast DNA may be recycled (Yehudai-Resheff et al., 2007), membrane phospholipids may be replaced with sulfolipids and galactolipids (Bajhaiya et al., 2016; Riekhof et al., 2003), and polyP stores may be mobilized (Moseley et al., 2009). Metabolic changes (e.g., bypassing reactions that involve the use of P) may also be employed to reduce the demand for P, impacting on glycolysis, photosynthesis, and starch and lipid metabolism (Bajhaiya et al., 2016; Shimogawara et al., 1999). The influence of the environmental parameters affecting luxury P uptake on these gene expression changes is not known.

---

[22] Abiotic stress factors are non-living environmental factors which can have negative impacts on an organism.

[23] Messenger RNA. Individual mRNA sequences are known as 'transcripts' and collectively form the 'transcriptome' of an organism.

[24] Low-affinity transporters have a high Michaelis-Menten constant (K_m), meaning that they have their highest reaction rate in higher substrate concentrations than high-affinity transporters. Constitutive expression refers to the continual transcription of certain genes to maintain the proteins they encode in all conditions.

[25] Inducible genes are expressed, and inducible proteins produced, as needed.

5.2.1 Genetic components of the polyP pathway

The genome of *C. reinhardtii* has been fully sequenced and functions have been suggested for many of the proteins it encodes (Salomé & Merchant, 2019). Numerous genes have been identified as being involved in the pathway from exogenous phosphate-containing compounds to internal stores, including genes involved in polyP synthesis (Figure 17). As discussed in Section 2.7, the proteins encoded by these genes include extracellular phosphatases, phosphate transporters, cation exchangers, components of the vacuolar transporter chaperone (VTC) complex, and the regulatory protein PSR1 (Grossman & Aksoy, 2015).

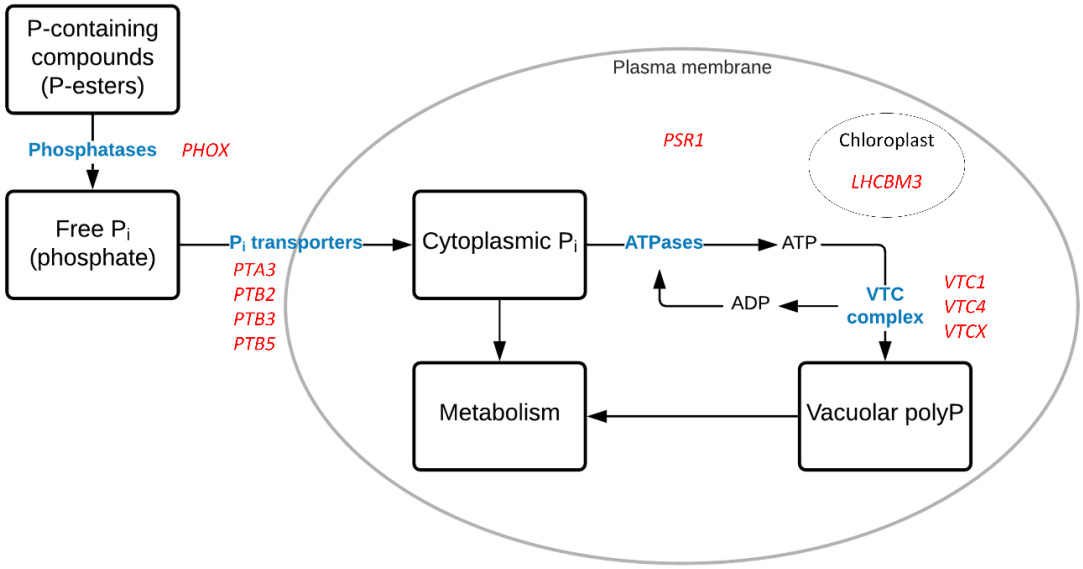

Figure 17. Schematic representation of the polyP synthesis pathway. Key enzyme classes are indicated in blue bold type and genes examined the present study are shown in red italic type.

The regulatory protein PSR1 is a transcription factor responsible for regulating the transcription of other genes involved in P metabolism in the response to changes in P availability (Bajhaiya et al., 2016; Moseley et al., 2006; Shimogawara et al., 1999; Wykoff et al., 1999). The *PSR1* gene is upregulated during P depletion, so we would expect it to be downregulated following P repletion, which has been confirmed experimentally (Plouviez et al., 2021).

The gene encoding the inducible alkaline phosphatase PHOX has been widely reported as being upregulated by P depletion, increasing in expression 1,000 – 30,000 times within 1 – 3 days of P

depletion (Bajhaiya et al., 2016; Moseley et al., 2009; Wang et al., 2020). Alkaline phosphatases are enzymes produced in response to P starvation which liberate orthophosphate from phosphorus-containing compounds to increase extracellular P-scavenging (Quisel et al., 1996) and their relative activity can be used as an indicator of the degree of P depletion (Eixler, Karsten, & Selig, 2006). *PHOX* has also been shown to be downregulated by around 2,000 times during P repletion (Plouviez et al., 2021).

The genome of *C. reinhardtii* encodes four PTA-type (H^+/P_i symporter) and ten PTB-type (Na^+/P_i symporter) phosphate transporters, most of which have been shown to be differentially regulated during changes in P availability and some of which are believed to be under the control of the regulatory protein PSR1 (Moseley et al., 2006). The PTA-type proteins are theorized to be situated on the plasma membrane (Wang et al., 2020) but may also be involved in intracellular phosphate transport (Moseley et al., 2006).

PolyP synthesis in *C. reinhardtii* is catalyzed by the VTC4 protein – a subunit of the vacuolar transporter chaperone (VTC) complex named for its similarity to a protein with homologous function in the yeast *Saccharomyces cerevisiae* (Plouviez et al., 2021; Emanuel Sanz-Luque et al., 2020). VTC4 contains a phosphate-sensing SPX domain which it may use to sense increases in intracellular phosphate concentration through interactions with inositol phosphates (Plouviez et al., 2021). Although protein homologues of the yeast proteins VTC2 and VTC3 have not been found in *C. reinhardtii*, there is a VTC accessory component named VTC1, demonstrated to be essential for polyP synthesis (Aksoy et al., 2014). Genes encoding other putative VTC components have been identified but their function not confirmed yet. Among these is a (Phytozome accession Cre01.g005500) which potentially encodes a putative VTC component with high similarity to VTC4 (Grossman & Aksoy, 2015). Based on its sequence similarity, particularly in regions containing conserved protein domains, it is hypothesized that this may be a second VTC4-type protein, possibly in a separate subcellular location, and should respond to changes in P availability in a manner similar to that of *VTC4*. To avoid confusion, this gene has been termed '*VTCX*' within the present work. Both *VTC4* and *VTCX* have previously been shown

to be downregulated 24 hours after P repletion (Plouviez et al., 2021). The *VTC4* gene also encodes a protein containing an SPX domain, so the VTC4 protein may be able to respond to changes in P availability independently of PSR1 and without being differentially regulated at the gene level.

5.2.2 Potential mechanisms of parameter influences on gene expression

Environmental parameters could potentially affect gene expression during P repletion through different mechanisms:

1. Changes in growth metabolism may alter the demand for P, resulting in changes in intracellular phosphate concentration, to which the cell may respond by changing the expression of genes related to P uptake and scavenging (‘pulling’).

2. The activity of proteins involved in P assimilation (such as P transporters situated on the cell membrane) may be directly affected by changes in environmental parameters, which would impact the rate at which available P is assimilated (‘pushing’). Gene expression may then change in response to changes in the availability of intracellular phosphate.

3. Changes in extracellular P availability (i.e., P repletion dose) may result in different rates of *passive* P uptake, changing the intracellular phosphate concentration and leading to cellular responses as described in (1).

The objective of this work was to determine whether environmental parameters which influence P luxury uptake affect the expression of genes involved in P uptake and polyP accumulation and, if so, which parts of the polyP pathway they affect. This knowledge is needed to better understand how P removal processes can be optimized through manipulation of process parameters.

5.2.3 Quantification of gene expression levels using qPCR

Quantitative real-time PCR following reverse transcription of RNA (RT-qPCR) is a method of estimating gene expression levels. RNA is first extracted from the samples and, since PCR can only amplify DNA, the RNA is converted to complementary DNA (cDNA) by an enzymatic process. In the qPCR reaction, the cDNA is mixed with primers specific to the target transcript sequence and a DNA polymerase enzyme which produces new copies of the target cDNA sequence. With each successive cycle, the number of amplicons (copies of the target sequence) is increased by a factor proportional to the amplification efficiency (ideally doubling). A fluorescent dye incorporated into the reaction mix binds to DNA and its fluorescence intensity is used to quantify the amount of DNA present after each cycle. The number of cycles (interpolated between integer values) taken for fluorescence to reach a predetermined threshold value is estimated (Figure 18); this is referred to as the quantification cycle, or C_q.

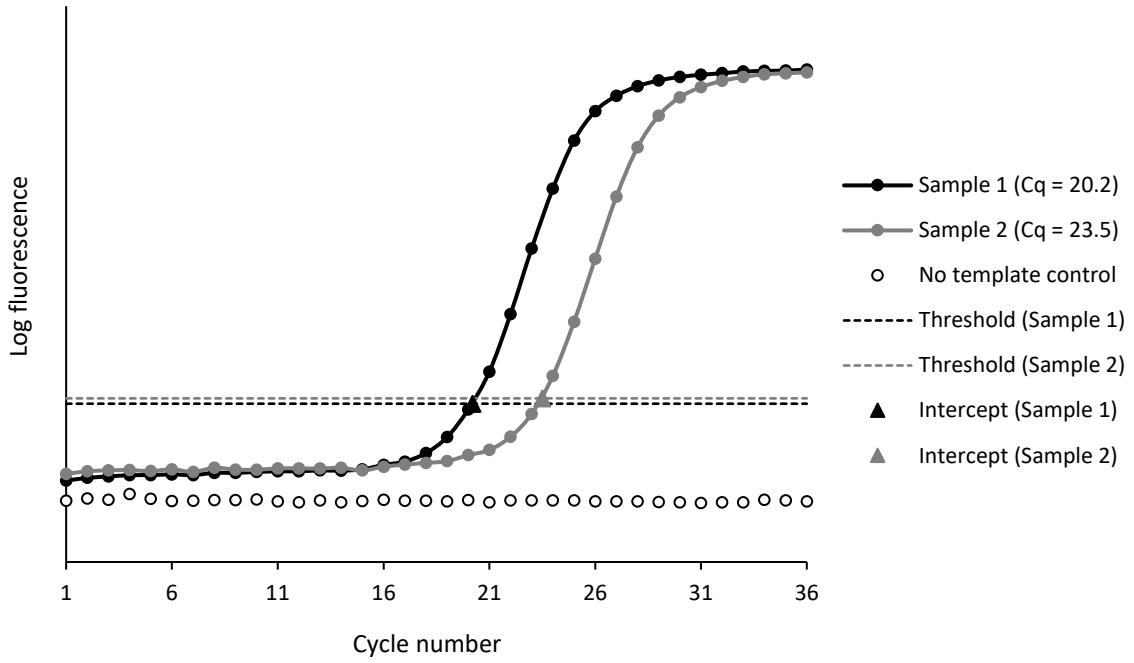

Figure 18. Example data (*PTB2*) showing the fluorescence development within two samples during qPCR. Their C_q values were determined from the point at which the curves intercept their respective threshold values (shown as triangles). The 'no template control' contained all reagents but no cDNA and confirms the specificity of the reaction.

Although the cycle number is an integer value, C_q values are interpolated using a regression fit. Assuming an amplification efficiency of 2, the number of amplicons should be related to the initial number of transcripts by Equation 5.1:

$$N_k = N_0 \cdot 2^{(C_q)} \tag{5.1}$$

where N_0 is the initial number of target sequences (transcripts) and N_k is the total number of transcripts and amplicons when the threshold is passed.

The higher the C_q value, the more cycles were required to reach the threshold value and, therefore, the lower the number of target transcripts initially present.

By rearrangement of Equation 5.1, we can see that C_q values may be used to represent expression changes on a log scale (Eq. 5.2).

$$C_q = \log_2\left(\frac{N_k}{N_0}\right) \tag{5.2}$$

A difference in C_q values of 1 corresponds to one sample having twice the initial number of transcripts, or expression level, of the other, a C_q value of 2 corresponds to a four-fold difference, and so on. Using C_q values circumvents the need to quantify transcript levels by determining only relative levels.

5.2.4 Differential gene expression analysis using qPCR data

Since the number of transcripts present in RNA may be affected by the efficiency of RNA extraction, it is necessary for relative expression levels to be normalized with reference to a gene for which expression levels are known to be unvarying (ubiquitously expressed). Such genes are known as endogenous reference genes, or 'housekeeping' genes, and suitable candidates may vary between organisms. Normalized expression levels can be determined, as $\log_2$-transformed values ($\log_2$ -NE), from the difference in C_q values between the reference and target genes (Eq. 5.3).

$$\log_2 \text{-}NE = C_{q,ref} - C_{q,target} \tag{5.3}$$

To compare the relative expression of a target gene within two samples, the above normalization is incorporated into an equation evaluating the difference between the two normalized C_q values and therefore known as the '$2^{-\Delta\Delta C_T}$ method'[26] (Schmittgen & Livak, 2008). In this way, relative expression may be determined without the need to convert C_q values to absolute expression values.

The relative expression of a target gene in sample B, with respect to sample A,

$$\log_2\left(\frac{N_B}{N_A}\right) = \left(C_{q,ref} - C_{q,target}\right)_B - \left(C_{q,ref} - C_{q,target}\right)_A \quad (5.4)$$

The values of $\Delta\Delta C_q$ itself can be used as log-base-2 transformations of relative expression, or $\log_2$ -RE .

5.2.5 P repletion vs depletion

Investigations to date have largely focused on microalgal gene expression responses to P depletion (reduction in available P, i.e., nutrient limitation) while few have looked at the effects of P repletion (restoring available P to a level that allows for normal metabolism) (e.g., Plouviez et al. (2021); Solovchenko et al. (2019). However, the two approaches essentially address the same transition between the two states of P availability. As P becomes depleted, genes that enhance P uptake/storage are upregulated[27]. Upon P repletion, the same genes are then downregulated. Once the added P has been consumed, the culture will gradually become P-depleted again and its P uptake/storage genes will start to be upregulated again. Therefore, we expect those genes reported to be upregulated during P depletion to be downregulated following P repletion before being upregulated again. The timing of these changes may affect the expression changes we observe during the experimental period. It should be noted that P depletion may be gradual (due to the cessation of P addition, as in the present work) or abrupt; some authors have resuspended cells in

[26] C_q is also sometimes known as C_T (threshold cycle), C_P (crossing point), or TOP (take-off point). C_q is the preferred nomenclature when following MIQE Guidelines (Bustin et al., 2009).

[27] Upregulation refers to the increase in transcription of genes into mRNA (also known as gene expression), which is used to synthesize proteins.

P-free medium to immediately deprive them of extracellular P sources (e.g., Bajhaiya et al. (2016); Moseley et al. (2006). This difference might also be reflected in the timeline of expression changes. Although the influence of environmental conditions on luxury uptake is known, the changes in gene expression taking place in different conditions are not known.

5.2.6 Hypotheses

In Chapter 4, increased P repletion dose and P depletion time were both shown to be associated with increased P uptake and polyP accumulation in *C. reinhardtii*, whereas increased light supply and temperature were associated with increased polyP accumulation but not P uptake.

It was therefore hypothesized that:

- Changes in the expression of genes associated with P uptake and polyP synthesis, following P repletion, will be more pronounced when the P repletion dose is increased.
- The expression of genes upregulated during P depletion (particularly *PSR1* and high-affinity phosphate transporters) will increase over time, resulting in higher expression levels of these genes after 7 days than after 3 days P depletion (prior to P repletion).
- Increased light supply and temperature cause changes in cell metabolism which increases the production of polyP, either by increasing the activity of polyP-synthesizing enzymes or by increasing the mobilization of intracellular P as short-chain polyP or other metabolic intermediates.

5.3 Methodology

5.3.1 Species selection and cultivation conditions

Chlamydomonas reinhardtii (wild-type strain CC-1690) was selected, as discussed in Section 5.1 and maintained on liquid and solid media as described in Section 3.3.2.1.

5.3.2 Selection of conditions for examination

Pairs of experimental runs from Chapter 4 were selected such that one parameter was different between the two sets of conditions but significant differences in P uptake and polyP accumulation were observed in *Chlamydomonas reinhardtii*. Since changes in initial pH resulted in the fewest significant effects, this parameter was removed from the next phase of the experiment. Four parameters (light supply, temperature, P repletion dose, and P depletion time) were selected to be examined using five experiments (Table 17).

Table 17. Conditions selected for experiments to examine gene expression differences at the two levels of four parameters, the experimental run numbers from Chapter 4, and the response variables affected.

Parameter	**Low level**	**Run #**	**High level**	**Run #**	**Effects observed**
Light supply (μmol photons$\cdot m^{-2}s^{-1}$)	0	35	160	15	Growth PolyP
Temperature (°C)	10	35	30	10	Growth
P repletion dose (mg P$\cdot L^{-1}$)	5	35	15	4	P uptake PolyP
P depletion time (days)	3	61	7	4	P uptake

For consistency with the experiments conducted in Chapter 4, the initial pH of experimental cultures was still set by using Tris buffer and all experiments were conducted at pH 8.6.

5.3.3 Gene selection

The genes selected for expression analysis (Table 18) included nine genes related to P metabolism regulation, assimilation, and storage and one gene related to photosynthesis but known to be influenced by changes in P availability.

The *CBLP* gene was selected as the endogenous reference gene. The mRNA encoding this G protein β subunit-like protein is constitutively expressed (Schloss, 1990) and it has been used widely as a reference gene in studies related to P metabolism in *Chlamydomonas* (González-Ballester et al., 2010; Moseley et al., 2006; E. Sanz-Luque et al., 2020).

5.3.4 Primer design

Primer sequences (Appendix C.1) were either obtained from the literature or designed using PrimerQuest software (Integrated DNA Technologies) and sequences from the *C. reinhardtii* v5.5 genome (Merchant et al., 2007) downloaded from the Phytozome database (Goodstein et al., 2012).

Table 18. Genes selected for examination of gene expression in *C. reinhardtii* during P repletion in different conditions.

Gene	Accession	Function	Reason for selection
PSR1	Cre12.g495100	Phosphorus stress response regulator	Encodes a key regulatory protein known to sense P_i levels and control the regulation of other genes.
PHOX	Cre04.g216700	Alkaline phosphatase	Known to be differentially regulated strongly during P depletion/repletion.
VTC4	Cre09.g402775	PolyP polymerase	Essential for polyP synthesis.
VTCX	Cre01.g005500	Unknown	Putative VTC4 homologue.
VTC1	Cre12.g510250	VTC complex component	Essential for polyP synthesis.
PTA3	Cre16.g686750	H^+/P_i symporter	Putative high-affinity phosphate transporter (Grossman & Aksoy, 2015)
PTB2	Cre07.g325741	Na^+/P_i symporter	Putative high-affinity P_i transporter (Grossman & Aksoy, 2015).
PTB3	Cre07.g325740	Na^+/P_i symporter	PSR1-controlled P_i transporter.
PTB5	Cre02.g144700	Na^+/P_i symporter	PSR1-controlled P_i transporter.
LHCBM3	Cre04.g232104	Light harvesting complex component (Photosystem II)	Involved in photosynthesis but differentially regulated following P repletion (Plouviez et al., 2021).

5.3.5 Experimental design

C. reinhardtii was cultivated as previously described (see 4.3.1) and inoculated in triplicate. Following the growth period (3 or 7 days, as dictated by the particular experimental parameters), optical density (OD) was adjusted to approximately 0.8 as described previously. 10 mL samples

of each replicate were collected in 15 mL centrifuge tubes and frozen at -80 °C to be used for RNA extraction.

The remaining culture was transferred to six-well microplates in 5 mL aliquots such that each plate contained two aliquots of each replicate culture (see Figure 19). These aliquots were adjusted to pH 8.6 by addition of Tris buffer to a final concentration of 20 mM.

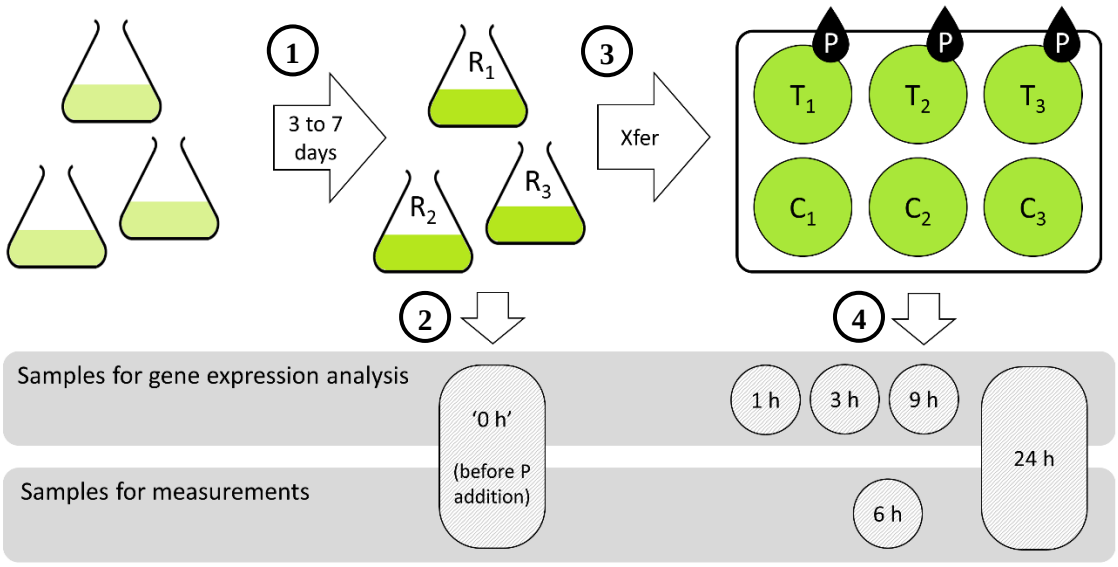

Figure 19. Overview of the experimental procedure. Cells were inoculated on a low-P medium and grown for 3 to 7 days (1). At the beginning of the experiment, '0 hour' samples were taken (2), cultures were designated as numbered replicates and transferred to six-well microplates (3) as pairs of 'treatments' (T_x) or 'controls' (C_x). Further samples were taken after 1, 3, 6, 9, and 24 hours (4).

The microplates were covered with Parafilm and moved to a temperature-controlled room previously set to the required temperature. Once the temperature of the cultures was the same as the room temperature, pH was measured and the microplates were moved to benchtop shakers where they were kept mixed by orbital agitation at 150 min^{-1} beneath the same lights used for the 'light' condition described in Section 4.3.

Half the wells were P-repleted with phosphate as previously described. At 1, 3, 9, and 24 hours after P repletion, two plates were removed and stored at -80 °C for RNA extraction.

5.3.6 RNA extraction

Samples were thawed at room temperature. Samples from pairs of plates frozen simultaneously were combined (2 × 5 mL) in 15 mL centrifuge tubes to make up 10 mL of each. All the tubes were then centrifuged for 2 minutes at 3000 × *g*. The supernatant was discarded and the pellet was stored at -80 °C until extraction.

RNA was extracted from two out of each set of biological triplicates following a modified procedure using PureLink RNA Mini Kit (Thermo Fisher) with 1 mL TRIzol Reagent in place of the supplied lysis buffer. Cells were homogenized with 10 to 20 2.3 mm zirconium silica beads using a Roche MagNAlyser for 60 seconds at 5000 min^{-1}. The remainder of the procedure followed the manufacturer's instructions. Potential DNA contamination was eliminated using DNase Max (Qiagen).

5.3.7 cDNA library preparation (reverse transcription)

RNA was reverse transcribed to cDNA by first-strand synthesis using qScript cDNA SuperMix (Quantabio, cat. no. 95048-100). Approximately 500 ng total RNA was used from each sample.

5.3.8 Quantitative real-time PCR (qPCR)

Primer stock solutions were prepared from lyophilized oligonucleotides by addition of RNase- and DNase-free water to a concentration of 1 mM and working solution were prepared from these by diluting to 10 µM. Both stock and working solutions were stored at -80 °C.

qPCR reactions (10 µL in 96-well microplates) were prepared using 5x HOT FIREPol SolisGreen qPCR Mix (Solis Biodyne, catalog number 08-46-00001), 2 µL template (diluted 10× in RNAse/DNAse-free water), and 0.25 – 0.5 µL (0.25 – 0.5 pmol) of each (forward and reverse) primer.

qPCR was performed on a LightCycler 480 using software version 1.5.1 (Roche) and following the following protocol: 10 min pre-incubation at 95 °C, followed by ≤ 40 cycles of 10 s

denaturation at 95 °C, 20 s annealing at 58 °C, and 20 s extension at 72 °C. Melt curve analysis was performed at the conclusion of quantification.

For each gene examined, two plates were prepared, one containing 0- and 24-hour samples and the other containing 1-hour samples. Each plate included three no-template controls and three positive controls using *LHCBM3* primers. Samples were tested for genomic DNA (gDNA) contamination by running a PCR reaction (using the VTC4 primers (which bind to gDNA on either side of an intron sequence) and the following conditions:

Reaction mixture (per sample): 5 µLEmeraldAmp GT PCR Master Mix (Takara Bio Inc., code number RR310A); 0.5 µL forward primer (CrVTC4_F1); 0.5 µL reverse primer (CrVTC4_R1); 3 µL RNAse/DNAse-free water; 1 µL cDNA template.

Reaction conditions: 3 min at 94 °C, followed by 35 cycles of 10 s at 94 °C, 30 s at 58 °C, and 1 min at 72 °C, then 5 min final extension at 72 °C.

The PCR products were electrophoresed (30 min at 100 V on 2% agarose gel) and deemed to be free of gDNA contamination since no band was visible at around 600 bp, whereas a band at around 100 bp confirmed the presence of VTC4 mRNA in the extracted samples. *C. reinhardtii* gDNA was used as a positive control.

5.3.9 Analysis

Raw qPCR data were extracted from the software output using LC480Conversion, and C_q values and primer efficiencies calculated using LinRegPCR. Both programmes were downloaded from https://medischebiologie.nl/files/.

The data were normalized using the *CBLP* gene and changes in expression levels were calculated as described in Section 5.2.4.

Significance thresholds for changes in gene expression are discussed in Section 5.4.3.

5.4 Results

The five experiments (A – E) were performed in the same manner as the experiments described in Chapter 4 except as noted in Table 19.

Table 19. Summary of conditions used in the experiments.

Parameter	**Experiment**				
	A	B	C	D	E
Light supply (µmol photons·$m^{-2}s^{-1}$)	0	160	0	0	0
Temperature (°C)	10	10	30	10	10
P repletion dose (mg P·L^{-1})	5	5	5	15	15
P depletion time (days)	7	7	7	7	3

Underlined entries indicate differences compared to experiment A.

5.4.1 Phosphate uptake

The observed P uptake was in reasonable agreement with the results from Chapter 4 (Table 20). No effects of light supply or temperature on P uptake were observed, which agrees with the findings reported in Chapter 4 for *C. reinhardtii*. However, since all the available phosphate was assimilated within six hours in both experiments (Table 20), it is possible that differences in uptake rate could have been observed with a higher sampling temporal resolution (i.e., samples taken within the first six hours). P uptake was, however, found to be influenced by P repletion dose and P depletion time since, at the higher P repletion dose, extracellular P was not exhausted within 6 hours.

P repletion dose (A vs D)

P uptake over 24 hours was higher in cells repleted at 15 mg P·L^{-1} than at 5 mg P·L^{-1}, which was expected given the results reported in Chapter 4. A difference in 0-6 h uptake between the experiments of Chapter 4 and the present results, at the high P repletion dose, may indicate a different P uptake rate but the total P uptake over 24 h was not significantly different (Table 20, $p = 0.51$).

Table 20. Phosphate uptake (mean ± standard deviation of three biological replicates) , determined as the change in the concentration in the medium over the given period, from the present (Chapter 5) experiments compared with the Chapter 4 experiments which were conducted in the same conditions.

	Light supply	**Temperature**	**P repletion dose**	**P depletion time**	**Phosphate uptake (mg P·L^{-1})**					
					Chapter 4			Chapter 5		
	(µmol·m^{-2}s^{-1})	(°C)	(mg P·L^{-1})	(days)	0-6 h	6-24 h	0-24 h	0-6 h	6-24 h	0-24 h
A	0	10	5	7	4.97 ± 0.02	0.00 ± 0.02	4.97 ± 0.01	4.90 ± 0.02	0.03 ± 0.02	4.93 ± 0.00
B	160	10	5	7	4.90 ± 0.05	-0.02 ± 0.02	4.88 ± 0.03	4.88 ± 0.02	0.02 ± 0.03	4.90 ± 0.01
C	0	30	5	7	4.98 ± 0.01	-0.02 ± 0.01	4.96 ± 0.01	4.99 ± 0.01	0.00 ± 0.01	4.99 ± 0.01
D	0	10	15	7	14.71 ± 0.27	0.13 ± 0.25	14.84 ± 0.02	3.57 ± 0.31	11.1 ± 0.06	14.67 ± 0.37
E	0	10	15	3	3.05 ± 1.29	4.58 ± 0.78	7.63 ± 0.51	3.01 ± 0.32	4.80 ± 0.77	7.82 ± 0.76

Table 21. Comparison of polyP accumulation measurements (mean ± standard deviation of three biological replicates) from the present (Chapter 5) experiments compared with the Chapter 4 experiments which were conducted in the same conditions.

	Light supply	**Temperature**	**P repletion dose**	**P depletion time**	**PolyP accumulation**					
					Chapter 4			Chapter 5		
	(µmol·m^{-2}s^{-1})	(°C)	(mg P·L^{-1})	(days)	0-6 h	6-24 h	0-24 h	0-6 h	6-24 h	0-24 h
A	0	10	5	7	0.39 ± 0.11	0.38 ± 0.17	0.77 ± 0.06	0.18 ± 0.04	0.03 ± 0.07	0.21 ± 0.07
B	160	10	5	7	0.04 ± 0.03	0.41 ± 0.06	0.45 ± 0.06	0.17 ± 0.04	0.22 ± 0.04	0.39 ± 0.03
C	0	30	5	7	0.12 ± 0.03	0.05 ± 0.04	0.17 ± 0.03	0.32 ± 0.05	0.03 ± 0.05	0.35 ± 0.01
D	0	10	15	7	1.15 ± 0.02	0.36 ± 0.06	1.51 ± 0.05	0.17 ± 0.10	0.17 ± 0.15	0.34 ± 0.06
E	0	10	15	3	0.33 ± 0.06	0.32 ± 0.02	0.65 ± 0.05	0.20 ± 0.03	0.18 ± 0.09	0.38 ± 0.11

P depletion time (D vs E)

The total P uptake from 0-6 h was not appreciably impacted by P depletion time but, from 6-24 h, P uptake was significantly higher ($p < 0.05$) following 7 days of P depletion. The total amount of P assimilated over 24 hours was therefore considerably lower after only 3 days of P depletion.

5.4.2 PolyP accumulation

Although the measurements of polyP accumulation (changes in DAPI fluorescence, indicating changes in polyP content between time points) showed little agreement with the results from Chapter 4, they confirmed that polyP increased following P repletion in all the conditions tested (Table 21).

In the present work, polyP was accumulated in both light and dark conditions but was higher in the light. PolyP accumulation was not significantly influenced by temperature, P repletion dose, or P depletion time as found in Chapter 4.

Although the present results show some differences in polyP accumulation compared with the results from Chapter 4, they confirmed that there were differences in P uptake and polyP accumulation between experiments conducted in different conditions.

5.4.3 Gene expression

Given that experiments A and D were both performed in the same conditions of light supply, temperature, and P depletion time, the variability in the control (P-depleted) cultures' gene expression gives an estimate of 'noise' and is used here as a threshold for significance of differences in gene expression. The variability in $\log_2$-transformed gene expression within these control cultures ($n = 4$) varied by gene, with standard deviations ranging from 0.7 to 2.7. The upper 95% confidence limit of 2.0 (a four-fold difference in expression) was therefore used as a threshold value for significance. While this threshold is similar to that used in other studies (for example, a threshold of ±1.5 was used by González-Ballester et al. (2010) for $\log_2$-tranformed

data), increasing variability in gene expression between the experiment A and D controls over 24 hours suggested that the change in conditions of light and temperature had caused disruption in cell metabolism. This high level of 'noise' may obscure effects on gene expression; therefore, another experiment was designed to eliminate changes in conditions and will be discussed in Chapter 6.

5.4.3.1 Gene expression during P depletion

The transcript abundance levels of *PHOX* and *PTA3* were significantly higher after 7 days than after 3 days of P depletion (Table 22), indicating that these genes had been upregulated over the additional four days of P depletion.

Table 22. Normalized mean C_q values (log_2-transformed relative transcript abundance in control cultures[a]) after 3 days (experiment E) and 7 days (mean of experiments A – D) growth in standard conditions.

	P scavenging		**PolyP synthesis**			**Phosphate transport**				**PSII**
	PSR1	*PHOX*	*VTC4*	*VTCX*	*VTC1*	*PTA3*	*PTB2*	*PTB3*	*PTB5*	*LHCBM3*
3 days	-1.8	-3.7	0.1	-2.8	-6.5	-6.4	-0.6	1.9	-2.7	5.1
7 days	-1.2	1.0	0.9	-1.7	-5.6	-4.3	1.7	2.3	-2.1	5.3

[a] *CBLP* was used as the endogenous reference gene for normalization. Shading intensity indicates degree of relative transcript abundance. PSII: photosystem II-related activity.

This evidence supports the hypothesis, at least with respect to some P-related genes, that the degree of upregulation is linked to the duration of P depletion. Genes which were not significantly differently expressed after 3 days or 7 days may have already reached an upper limit for their expression.

5.4.3.2 Gene expression following P repletion

Transcriptional responses to P repletion can be evaluated by comparing the gene expression levels between P-repleted treatment cultures and P-depleted controls. Previous studies have shown that most of the studied genes are downregulated following P repletion (see 5.2.1), but it is not known whether this change in regulation is influenced by environmental conditions.

After 1 hour from P repletion, *PSR1*, *PHOX*, *VTCX*, *PTB5*, and *LHCBM3* were downregulated, while *PTA3* was upregulated in some conditions. Notably, these changes were not evidenced in experiments at 10 °C in darkness (Table 23: rows A, D, and E).

Table 23. Log_2-transformed relative gene expression [a] 1 hour after P repletion.

	P scavenging		**PolyP synthesis**			**Phosphate transport**				**PSII**
	PSR1	*PHOX*	*VTC4*	*VTCX*	*VTC1*	*PTA3*	*PTB2*	*PTB3*	*PTB5*	*LHCBM3*
A	-0.35	-0.43	-0.36	-1.48	-1.12	-0.11	0.43	-0.30	-0.49	-1.41
B	**-2.21**	-1.63	-0.34	**-3.09**	-0.48	**2.88**	0.84	0.23	0.45	-1.86
C	-1.78	**-6.33**	-1.95	-0.55	-0.27	**5.75**	-0.58	-0.37	**-2.82**	**-2.71**
D	-1.44	-0.57	-1.09	-1.21	0.39	0.80	1.02	0.70	-0.61	-1.16
E	-0.70	0.63	0.38	0.03	0.87	1.85	1.96	1.00	0.50	-0.58

[a] Positive values (green) indicate upregulation of genes in treatment cultures (+P) relative to controls (-P) and negative values (red) indicate downregulation. Bold type indicates greater than four-fold expression changes.

After 24 hours, expression of the tested genes in the treatment cultures was predominantly lower than in the controls (Table 24), confirming the expected downregulation of genes related to P assimilation and storage following P repletion (see 2.7.6).

Table 24. Log_2-transformed relative gene expression [a] 24 hours after P repletion.

	P scavenging		**PolyP synthesis**			**Phosphate transport**				**PSII**
	PSR1	*PHOX*	*VTC4*	*VTCX*	*VTC1*	*PTA3*	*PTB2*	*PTB3*	*PTB5*	*LHCBM3*
A	**-2.42**	**-14.62**	**-4.71**	**-5.50**	**-2.15**	**-4.26**	**-2.97**	**-5.01**	**-5.79**	**-2.52**
B	**-2.53**	**-11.43**	**-2.39**	**-3.97**	**-2.48**	**-5.43**	**-2.06**	**-5.80**	**-7.27**	**2.33**
C	-1.56	**-7.62**	**-2.40**	-1.20	-1.91	**-5.76**	**-3.82**	-0.55	-1.95	-1.71
D	**-2.32**	**-12.12**	**-4.25**	-1.89	0.23	-1.16	**-3.36**	**-4.61**	**-5.82**	-0.85
E	**-3.27**	**-4.78**	**-3.56**	-1.99	-0.78	-0.23	-0.42	**-3.07**	**-3.21**	-1.91

[a] Positive values (green) indicate upregulation of genes in treatment cultures (+P) relative to controls (-P) and negative values (red) indicate downregulation. Bold type indicates greater than four-fold expression changes.

The photosynthesis-related gene *LHCBM3*, previously shown to be downregulated following P repletion (Plouviez et al., 2021), was only significantly downregulated ($\Delta\Delta C_q$ = -2.52) in

experiment A, and was upregulated ($\Delta\Delta C_q$ = 2.33) in the increased light condition (experiment B), which suggests a more complex interaction between P status and light availability and therefore might warrant further investigation.

Analysis of relative gene expression, as above, assumes that expression levels stay relatively constant in control cultures while expression changes in treatment cultures are due to changes in conditions such as P repletion. Since the experimental design involved growing the cultures initially in standard conditions, then transferring them to the different experimental conditions, changes in metabolism were expected. In particular, following transfer from 25 °C to 10 °C and light to darkness, we would expect metabolism to be appreciably reduced (Raven & Geider, 1988). On the other hand, 30 °C is well below the range of temperatures initiating a heat stress response in *C. reinhardtii* (Schroda, Hemme, & Mühlhaus, 2015), so we would expect to see an increase in endogenous metabolism[28] (rather than a stress response), which might have influenced the expression of the genes studied here. Indeed, *PSR1*, *PHOX*, *LHCBM3*, and *VTCX* were all significantly downregulated during the first hour after the temperature was reduced to 10 °C (in both light and darkness; see Table 25, rows A, B, D, and E). On the other hand, *VTC1*, *PTA3*, and *PTB2* were upregulated during the first hour at 30 °C (in darkness; row C).

Table 25. Changes in $\log_2$-transformed normalized gene expression [a] in control cultures (P-depleted) from 0-1 hours.

	P scavenging		**PolyP synthesis**			**Phosphate transport**				**PSII**
	PSR1	*PHOX*	*VTC4*	*VTCX*	*VTC1*	*PTA3*	*PTB2*	*PTB3*	*PTB5*	*LHCBM3*
A	**-3.77**	**-3.80**	-0.59	**-3.29**	1.60	0.24	0.58	0.31	0.32	**-2.03**
B	**-4.70**	**-6.09**	**-4.77**	**-3.40**	**2.02**	**-3.27**	-1.05	**-2.79**	**-3.25**	**-4.60**
C	0.27	1.45	0.41	0.52	**3.57**	**2.24**	**4.41**	0.88	**2.36**	0.56
D	**-3.42**	**-2.91**	-1.12	**-4.95**	1.31	-1.96	**2.98**	-0.13	1.33	**-2.27**
E	**-4.79**	-1.89	-1.29	**-4.37**	**2.79**	-1.75	**2.21**	-0.99	0.63	**-2.37**

[a] Positive values (green) indicate upregulation of genes and negative values (red) indicate downregulation. Bold type indicates greater than four-fold expression changes.

[28] The only experiment conducted at 30 °C was in darkness, so we would not expect to see any impact on growth metabolism, which might be observed by increasing temperature in the light.

Similarly, the increased light supply in experiment B (relative to the prior growth conditions) appears to have caused the downregulation of *VTC4*, *PTB3*, and *PTB5*, as well as increased downregulation of *LHCBM3* ($\Delta\Delta C_q$ = -4.60, compared to $\Delta\Delta C_q$ = -2.03 in darkness at the same temperature).

Table 26 shows the differences in normalized gene expression changes in control cultures, from 0-24 hours, between pairs of experiments differing in one parameter but otherwise performed in identical conditions. The data suggest that genes related to polyP synthesis and P transport were still differentially expressed in response to the changes in conditions even 24 hours after the change in conditions. However, the observed differences in expression between experiments A and D, in which only the treatment cultures received a different P repletion dose, indicate that there may have been gene expression differences between the cultures used in different experiments.

Table 26. Differences between $\log_2$-transformed normalized gene expression [a] in control cultures (P-depleted), from 0-24 hours, in pairs of experiments differing in one parameter.

Parameter change	**PolyP synthesis**			**Phosphate transport**			
	VTC4	*VTCX*	*VTC1*	*PTA3*	*PTB2*	*PTB3*	*PTB5*
Increased light supply (B-A)	**-2.9**	**-4.1**	1.8	-1.9	**-4.8**	**-4.7**	**-4.9**
Increased temperature (C-A)	-1.8	**-2.9**	1.8	0.4	**4.2**	-1.6	-0.2
Increased P repletion dose (D-A)	**-2.1**	**-4.3**	**-2.5**	-1.5	1.6	**-2.5**	**-2.9**
Increased P depletion time (D-E)	1.9	0.8	-1.9	-1.9	1.1	0.5	1.1

[a] Positive values (green) indicate upregulation of genes with the given parameter change and negative values (red) indicate downregulation. Bold type indicates greater than four-fold expression changes.

On the other hand, the 0-24 h changes in the expression of polyP synthesis-related genes in treatment cultures were affected much less by changes in light supply and temperature than in the controls (Table 27). Therefore, the observed higher polyP synthesis in increased light supply (at 10 °C) and in increased temperature (in darkness) were not accompanied by changes in the expression of polyP synthesis genes 24 hours after P repletion. It was also observed that P uptake

was not affected by differences in light supply and temperature, although the tested transporter genes showed clear differences in expression after 24 hours.

Table 27. Differences between log_2-transformed normalized gene expression [a] in treatment cultures, from 0-24 hours, in pairs of experiments differing in one parameter.

Parameter change	**PolyP synthesis**			**Phosphate transport**			
	VTC4	*VTCX*	*VTC1*	*PTA3*	*PTB2*	*PTB3*	*PTB5*
Increased light (B-A)	-0.6	**-2.6**	1.4	**-3.1**	**-3.9**	**-5.5**	**-6.4**
Increased temperature (C-A)	0.5	1.4	**2.0**	-1.1	**3.4**	**2.9**	**3.6**
Increased P repletion dose (D-A)	-1.7	-0.7	-0.1	1.6	1.2	**-2.1**	**-3.0**
Increased P depletion time (D-E)	1.2	0.9	-0.9	**-2.9**	-1.8	-1.0	-1.5

[a] Positive values (green) indicate upregulation of genes with the given parameter change and negative values (red) indicate downregulation. Bold type indicates greater than four-fold expression changes.

Higher downregulation of some of the P transporter genes over 24 hours (Table 27) may reflect the higher P uptake observed (as downregulation is a response to increased intracellular P concentration) when P repletion dose and P depletion time were increased. However, differences in gene expression which might be responsible for observed differences in P uptake and polyP metabolism are more likely to be observed at an earlier time (e.g., 1 hour), since P repletion resulted in strong downregulation of P transporter genes after 24 hours. *PTB2* expression increased more from 0-1 h at the high P repletion dose than at the low dose (Table 28). This gene may have been upregulated in response. However, in both experiments A and D, *PTB2* expression levels in treatment cultures were not significantly higher than in the controls (Table 23), so the difference in expression between the two experiments is unlikely to be related to the difference in P repletion dose but some other, uncontrolled, factor.

PTB2 was also more upregulated when temperature was increased and no difference in P uptake was observed. There were also no significant differences in P transporter gene expression between experiments D and E, which were conducted after different P depletion times.

Table 28. Differences between log_2-transformed normalized gene expression [a] in treatment cultures, from 0-1 hours, in pairs of experiments differing in one parameter.

	PolyP synthesis			**Phosphate transport**			
	VTC4	*VTCX*	*VTC1*	*PTA3*	*PTB2*	*PTB3*	*PTB5*
Increased light supply (B-A)	**-4.2**	-1.7	1.1	-0.5	-1.2	**-2.6**	**-2.6**
Increased temperature (C-A)	-0.6	**4.7**	**2.8**	**7.9**	**2.8**	0.5	-0.3
Increased P repletion dose (D-A)	-1.3	-1.4	1.2	-1.3	**3.0**	0.6	0.9
Increased P depletion time (D-E)	-1.3	-1.8	**-2.0**	-1.3	-0.2	0.6	-0.4

[a] Positive values (green) indicate upregulation of genes with the given parameter change and negative values (red) indicate downregulation. Bold type indicates greater than four-fold expression changes.

5.5 Discussion

Growth was not examined in the present chapter since optical density was shown to be influenced by changes in light and temperature (Chapter 4) and therefore not useful as a proxy for growth in the conditions tested in this experiment (direct measurement of biomass concentration was not possible considering the small volumes cultivated).

5.5.1 Phosphate transport

There was no observable difference in P uptake between cells P repleted in light and darkness. Perry (1976) also reported no change in P uptake rate in the marine diatom *Thalassiosira pseudonana* over a range of light intensities equivalent to 0 – 90% of ocean surface illumination. This is a surprising finding given that P uptake is known to require energy (Brown & Shilton, 2014), so we would expect P uptake to be absent, or at least lower, in darkness. The energy requirement for P uptake in the dark may be satisfied by the use of stored carbohydrates as an energy source (de Winter et al., 2013). Accumulation of starch and lipids is induced by P starvation under the control of PSR1 (Bajhaiya et al., 2016) so P-depleted cells could be expected to have accumulated carbohydrates which they could use as an energy source upon P-repletion in darkness. The use of these internal energy reserves is normally associated with biomass loss but

the methods of assessing growth used in the present work may not be sensitive enough to detect these relatively small changes.

Light and temperature are known to influence ion transport across membranes (Soeder & Stengel, 1974) so they could impact phosphate uptake. Alternatively, increases in cellular metabolism might reduce the intracellular phosphate concentration, thereby either increasing passive P uptake via a higher P concentration gradient across the cell membrane or increasing active P transport through upregulation of transporter-encoding genes (see 2.7.6). P uptake is related to external P concentration following Michaelis-Menten kinetics (Rhee, 1973) and reported kinetics suggest the presence of both high- and low-affinity phosphate transporters in *C. reinhardtii* (Shimogawara et al., 1999). However, Kuhl (1962) observed that P uptake was dependent on external P concentration in the light but not in the dark. Powell et al. (2008) similarly demonstrated a positive interaction effect between P concentration and light intensity, indicating that increased light enhanced the effect of P concentration on P uptake. Although the results in Chapter 4 demonstrated that P repletion dose had a significant effect on P uptake both in light and darkness (Table 15; Figure 14), the effect was weaker in darkness.

In the present study, P uptake over 24 hours (in darkness at 10 °C) increased with P repletion dose (between experiments A and D) but the difference could not be attributed to differences in expression of P transporter genes.

P uptake over 24 hours was also higher with increased P depletion time. The present findings corroborate other studies reporting that increased P depletion time was positively associated with P uptake (Aitchison & Butt, 1973; Lavrinovičs et al., 2020; Lavrinovičs et al., 2021).

Despite the higher P uptake observed with increased P depletion time, there were no differences in the expression levels of the tested transporter genes between experiments D and E following P repletion. Although this means that the gene expression response to P repletion was not affected by P depletion time, the higher initial (prior to P repletion) expression of the phosphate transporter

gene *PTA3* after 7 days of P depletion suggests a more ‘active’ than ‘reactive’ strategy for preparing cells to assimilate P upon repletion.

5.5.2 PolyP synthesis

PolyP in microalgae is synthesized by the vacuolar transporter chaperone (VTC) complex, specifically by the polymerase protein VTC4. The VTC component VTC1 is also required for polyP synthesis (Aksoy et al., 2014; Plouviez et al., 2021). The gene herein described as *VTCX* also encodes a protein similar to VTC4, which may also be a polyP polymerase but this function has not yet been confirmed. The expression of *VTC4*, *VTC1*, and *VTCX* was therefore examined to determine their responses to P repletion in the different conditions.

In the present work, polyP accumulation was higher in the light than in darkness (at 10°C) and higher at 30 °C than at 10 °C (in darkness). The change in gene expression in the treatment cultures from 0-1 hours (Table 28) showed that the expression of *VTC4* decreased more during the first hour following P repletion in the light than in darkness. This difference was also seen in the control cultures so it is likely due solely to the changing conditions of light supply and temperature rather than a response to P repletion. Regardless, this difference would not support the hypothesis that increased gene expression is the cause of higher polyP synthesis since the greater decrease in expression would instead result in a reduced capacity for polyP synthesis.

At 30 °C, however, *VTCX* and *VTC1* were both expressed more 1 hour after P repletion than at 10 °C. This higher expression might have resulted in a higher abundance of VTCX and VTC1 proteins, which could have increased polyP synthesis. Alternatively, the higher temperature may have directly increased the activity of proteins already present.

Interestingly, the total P uptake was the same in each of the experiments used to compare these parameters (see Table 20, rows A – C). Differences in polyP content (at similar intracellular P contents) may indicate that the form of the polyP present varied between conditions. In more metabolically active cells, we might see more phosphorylated metabolic intermediates such as

short-chain polyP (Powell et al., 2009) and inositol phosphates, which are involved in signalling and P homeostasis (Emanuel Sanz-Luque et al., 2020). Inositol phosphates are known to interfere with the estimation of polyP using the DAPI fluorescence assay (Kolozsvari et al., 2014). These compounds, associated with metabolism, may have increased in abundance through mobilization of existing cellular P reserves, which could explain why the total increase in polyP content was not consistent with the total P assimilation[29] in each of the conditions tested. Powell et al. (2008) noted that the concentration of acid-soluble polyP within algal cells was lower in high light supply. Further metabolomics study into changes in the compartmentation of P-containing compounds following P repletion may confirm that the inconsistency mentioned above was due to the transformation of granular polyP.

The higher polyP accumulation observed at the higher P repletion dose (compare A and D in Table 21) agrees with findings from Aitchison and Butt (1973) but there were no significant differences in expression of VTC genes in cells from experiments A and D. The upregulation of VTC genes during P depletion (see 2.7.6) and the low turnover of VTC proteins (Plouviez et al., 2021) mean that the proteins could be expected to have already been abundant at the time of P repletion and the higher polyP accumulation in D compared to A was therefore likely a consequence of higher P uptake.

5.5.3 Conclusion

The expression changes (upregulation) of *VTCX* and *VTC1* over the first hour may be linked to differences in polyP synthesis with respect to temperature but increased polyP synthesis observed in light, compared to darkness, was not associated with greater upregulation of VTC genes.

Although there was a difference in P uptake associated with changing the P depletion time, there were no observed differences in P transporter gene expression which might account for this

[29] Assuming no significant change in biomass concentration, the total increase in intracellular P content should be similar, after 6 hours, between experiments A, B, and C.

difference in P uptake. On the other hand, upregulation of *PTB2* at the higher P repletion dose suggests that differential expression of P transporter genes could be responsible for the difference in P uptake in that case.

Although the tested genes responded to P repletion in the expected manner (downregulation of treatments relative to controls) after 24 hours, the changing conditions at the start of the experiment also caused changes in gene expression, making comparisons between different experiments difficult. Therefore, another experiment was performed to reduce 'noise' in gene expression and confirm the observed differences in gene expression.

Chapter 6 The influence of P repletion dose and P depletion time on P assimilation and accumulation in unchanged growth conditions

6.1 Preface

The experimental designs used in Chapter 4 and Chapter 5 caused a shift in light supply and temperature in both treatment and controls, which produced drift in gene expression in addition to the condition-specific responses to P repletion. New experiments were therefore performed to examine changes in gene expression associated with changes in P repletion dose and P depletion time (the parameters having the most significant effects on P metabolism) under constant light supply and temperature.

6.2 Methodology

6.2.1 Selection of conditions for examination

Since the results disclosed in Chapter 5 showed that changing light supply and temperature at the start of the experiment had a significant impact on gene expression, a new experiment was designed where light and temperature are kept constant throughout both the pre-cultivation and experimental periods. This simpler design (only 2 parameters) allowed for the replicates in four conditions (two levels each of P repletion dose and P depletion time) to be cultivated simultaneously, instead of inoculating experimental cultures at different times which introduced additional variation.

6.2.2 Gene selection

The list of genes selected for examination in Section 5.3.3 (see Table 18) was reduced to seven genes related to P metabolism regulation, assimilation, and storage. These genes encode the P starvation response regulator PSR1, the VTC complex (polyP synthesis) components VTC4, VTCX, and VTC1, and the phosphate transporters PTA3, PTB2, and PTB5.

6.2.3 Experimental protocol

C. reinhardtii was cultivated on low phosphorus (1 mg $P \cdot L^{-1}$) minimal medium (low-P MM) in a Minitron incubator (Infors, Bottmingen, Switzerland) at 25 °C, with 29 µmol photons$\cdot m^{-2}s^{-1}$ light supplied by 2 Cool White 15 W fluorescent tubes (General Electric, U.S.A.) and orbital agitation at 150 min^{-1}. A 250 mL culture thus grown for five days was reinoculated on 550 mL low-P MM with 20 mM pH 8.6 Tris buffer. This culture, containing approximately 0.5 million cells$\cdot mL^{-1}$, was transferred to six-well microplates in 7 mL aliquots, creating 102 replicate cultures. The plates were covered with Parafilm M plastic film to minimize moisture loss, then returned to the incubator (Figure 20) to grow in the same conditions (except that addition of the plastic film reduced light reaching the cultures to approximately 25 µmol photons$\cdot m^{-2}s^{-1}$) as the pre-culture.

P-repletion experiments were started after 3 and 7 days of continuous growth in these conditions. Six plates were arbitrarily selected for each experiment. In each of these plates, two wells were repleted with approximately 5 mg $P \cdot L^{-1}$ (using a stock solution containing 0.66 M K_2HPO_4 and 0.34 M KH_2PO_4), two with 15 mg $P \cdot L^{-1}$, and two were kept as no-P controls. The volume of phosphate solution added was calculated based on a volume of 7 mL. However, due to inconsistent volume losses, the actual initial concentrations were determined by sampling immediately after adding P. Measurements at different time points were from different replicates.

At 1 and 24 hours after P repletion, four samples each were taken from wells repleted at the high P dose (15 mg $P \cdot L^{-1}$), the low P dose (5 mg $P \cdot L^{-1}$), and the no-P controls. From each of these 12 samples, 5 mL was frozen at -80 °C to be later thawed, concentrated (by centrifugation), and refrozen prior to RNA extraction. The remainder of the samples was used to measure optical density, dissolved phosphate concentration using a microplate assay (following filtration), and microscopic observation with slides prepared for cytological staining (all as described in 4.3.5). Additional samples were taken 2 and 5 days after P repletion for measurements of optical density and gene expression.

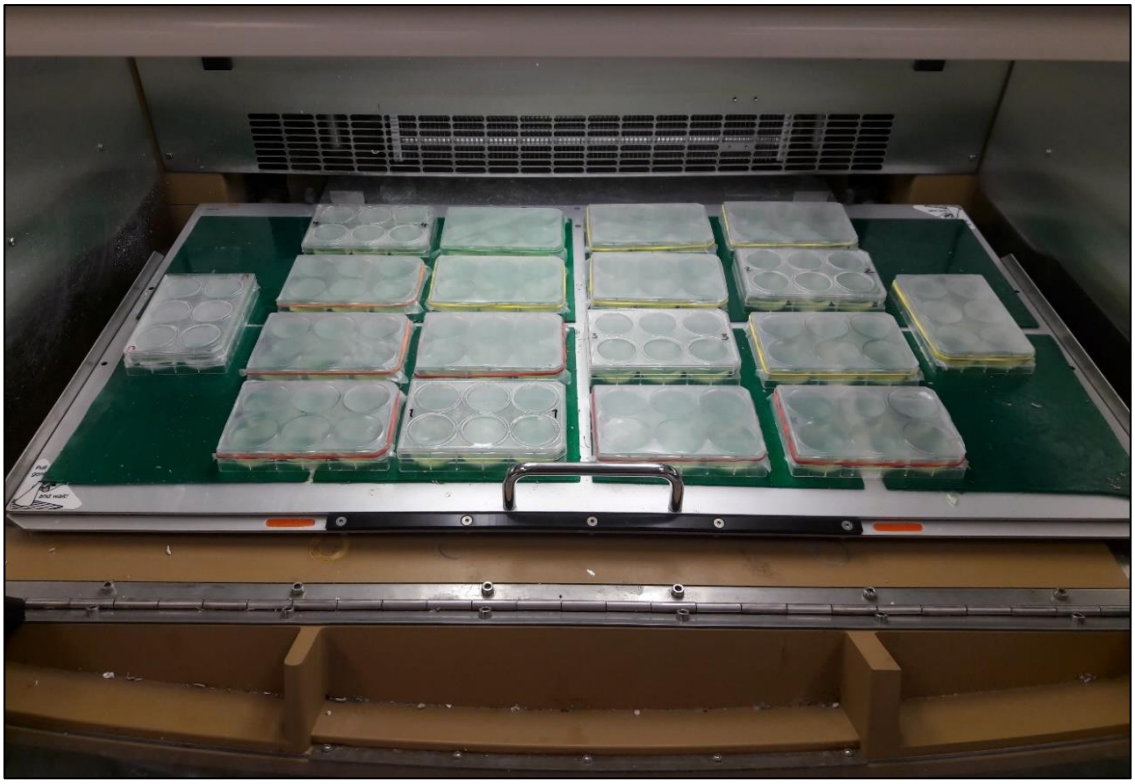

Figure 20. Microplates containing algal culture, covered with Parafilm, set up for the experiment.

Table 29. Schedule of sampling and analyses performed on each set of samples.

Time	**Analyses performed**			
	Optical density	Dissolved phosphate	Cytological staining	Gene expression
2 days	●			●
3 days (pre-P)	●	●		●
3 days 0 hours [a]		●		
3 days 1 hour		●	●	●
3 days 6 hours	●	●	●	
4 days (3d + 24 h)	●	●		●
5 days	●			●
7 days (pre-P)	●	●		●
7 days 0 hours [a]		●		●
7 days 1 hour		●	●	●
7 days 6 hours	●	●	●	
8 days (7d + 24 h)	●	●		●

[a] Samples taken immediately after addition of phosphate.

6.2.4 Analysis

Data for P uptake and polyP accumulation were analysed as described in Chapter 5, except that the changes in extracellular phosphate were evaluated from 0-1 hours and 1-6 hours, instead of only from 0-6 hours. RNA was extracted from samples (5 mL per sample) and processed as described in Sections 5.3.6, 5.3.7, and 5.3.8.

Changes in growth, P uptake, polyP accumulation were considered statistically significant where $p < 0.05$, unless otherwise specified. The significance of changes in gene expression was evaluated using the same significance threshold established in Section 5.4.3.

6.3 Results and Discussion

P repletion experiments were performed in the same conditions of light supply (i.e., same intensity and cultivation vessel geometry) and temperature as used during the pre-cultivation period. Optical density was used as a proxy for growth, since light supply and temperature did not change (i.e., we did not expect strong changes in pigment content impacting the OD/cell mass ratio). P uptake, polyP accumulation, and granule formation were analyzed as in the previous chapter.

6.3.1 Growth

Changes in optical density over 8 days followed zero-order kinetics (see Appendix C.3.1). Considering this clear trend, the day 7 (0 hour) data were assumed to be erroneous and replaced with a value linearly interpolated between adjacent points. Treatment and control cultures were assumed to have the same optical density at 0 hours.

There was no significant difference in growth between the P-repleted treatment cultures and P-depleted controls (Figure 21), which is consistent with the finding in Chapter 3 (also in constant light supply and temperature).

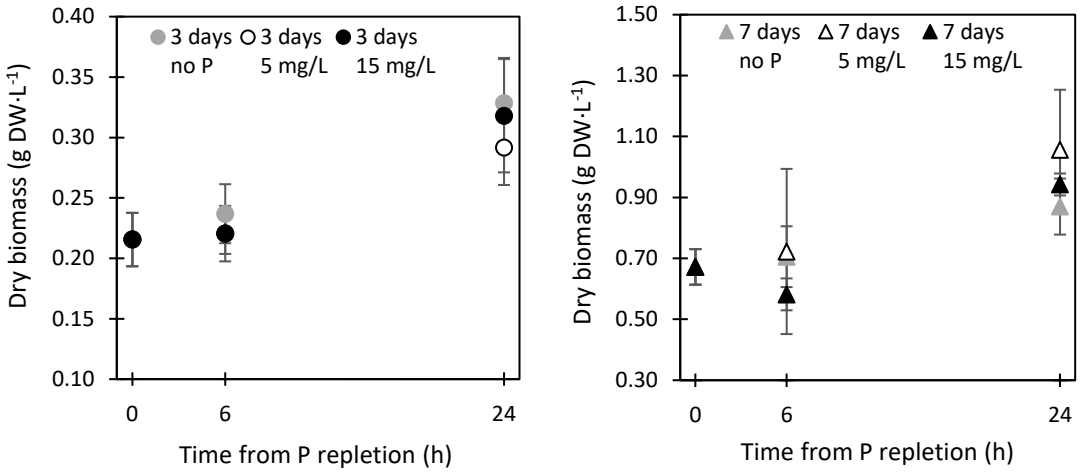

Figure 21. Mean (± SD) estimated dry biomass densities of arbitrarily selected replicate cultures (4 per data point) in the 3-day (left) and 7-day (right) P depletion time experiments. Cultures were given approximately 5 mg $P \cdot L^{-1}$ or 15 mg $P \cdot L^{-1}$ as phosphate, or no P addition.

The P-repleted treatment cultures were assumed to harbour the same cell density as the controls at 0 hours although the apparent decrease in biomass concentration from 0-6 hours in one sample highlights the high variability between biological replicates after several days of growth. No effects of P repletion dose or P depletion time on growth were evidenced (Table 30).

Table 30. Estimated growth rates from optical density data, calculated over the 24 hours following P repletion, by P depletion time and P repletion dose (mg $P \cdot L^{-1}$). Errors were calculated from the confidence intervals for log-transformed optical density measurements (n = 12, $\alpha = 0.05$).

P depletion time	**Growth rate (day^{-1})**		
	15 mg $P \cdot L^{-1}$	5 mg $P \cdot L^{-1}$	No-P control
3 days	0.39 ± 0.11	0.30 ± 0.10	0.42 ± 0.10
7 days	0.34 ± 0.09	0.45 ± 0.14	0.26 ± 0.09

6.3.2 P uptake

The initial rate of P uptake following P repletion (evidenced by the decrease in extracellular phosphate concentration from 0-1 h, as shown in Figure 22 and Table 31) was higher in cells repleted at 15 mg $P \cdot L^{-1}$ than cells repleted at 5 mg $P \cdot L^{-1}$, which was expected given the results reported in Chapter 5.

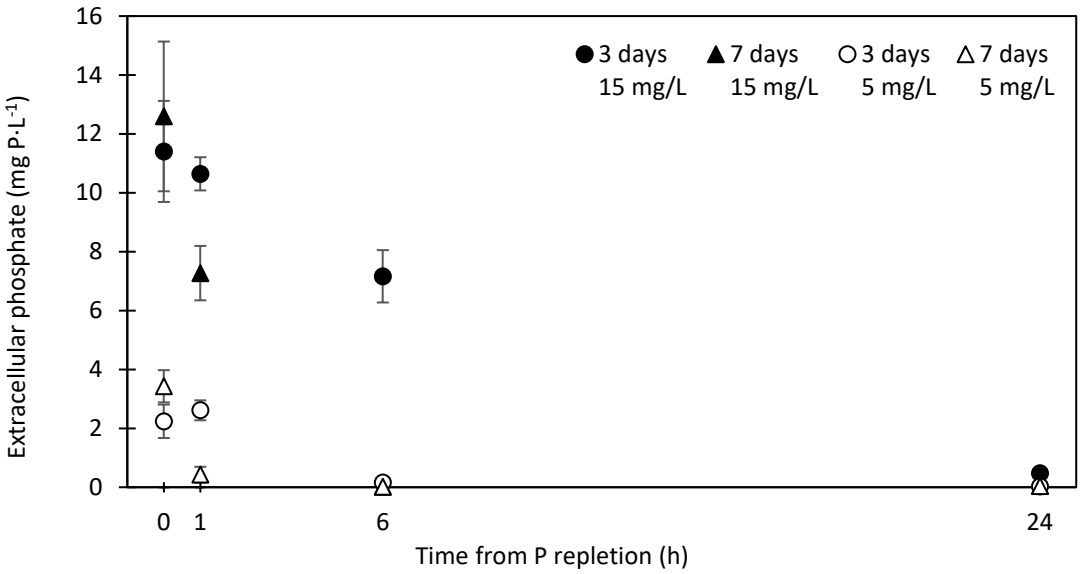

Figure 22. Mean (± SD) extracellular phosphate concentrations in arbitrarily selected replicate cultures at the indicated P repletion doses and P depletion times.

The cultures grew significantly between 3 and 7 days, meaning that the cell densities were different at the start of experiments conducted after different P depletion times. Assuming that the DW/OD ratio[30] was stable and approximately 0.80 g DW·L^{-1}, the specific average P uptake rate over the first hour (i.e., normalized by dry weight) was higher in the cultures P-depleted during for 7 days than in the cultures P-depleted for 3 days (Table 31). The rate of P uptake also increased with P repletion dose.

Table 31. Average P uptake rates in cultures given different P repletion doses after either 3 or 7 days of P depletion. Errors shown were calculated on the assumption of 21% relative error (see Appendix B.1.4).

P depletion time	**P repletion dose**	**P uptake (mg P·g DW^{-1}·h^{-1})**		
		0 – 1 h	1 – 6 h	6 – 24 h
3 days	5 mg P·L^{-1}	NS	≥ 0.7 ± 0.2	NA
	15 mg P·L^{-1}	1.1 ± 0.2	1.0 ± 0.2	0.6 ± 0.1
7 days	5 mg P·L^{-1}	≥ 1.4 ± 0.3	NA	NA
	15 mg P·L^{-1}	2.5 ± 0.5	≥ 0.7 ± 0.1	NA

NS: not significant

NA: not applicable since all available P has already been assimilated by the start of the given interval.

[30] Measurements taken from the source culture at the time of inoculation (0 days) produced a mean dry biomass density of 0.07 ± 0.01 g·L^{-1} and mean optical density of 0.089 ± 0.000.

These results provide the first evidence that increased P depletion time influences the P uptake rate in *C. reinhardtii*. A similar trend has been reported for other microalgae (Lavrinovičs et al., 2021), suggesting a similar evolutionary adaption to P availability (Chapter 2).

6.3.3 PolyP accumulation

Changes in the polyP content of the treatment cultures confirmed that polyP was accumulated, following P repletion, in cultures P-depleted for 3 days (Figure 23), as previously shown in Chapter 5. At both P repletion doses, polyP content increased significantly ($p < 0.05$) from 0-1 hours and 1-6 hours but decreased from 6-24 hours. There was no significant difference between the amount of polyP accumulated at the two doses. There were also no statistically significant changes in cultures P-depleted for 7 days, possibly due to high variability between replicates, but polyP was accumulated from 0-6 h in cultures supplied 5 mg $P \cdot L^{-1}$ and from 0-24 h in cultures supplied 15 mg $P \cdot L^{-1}$.

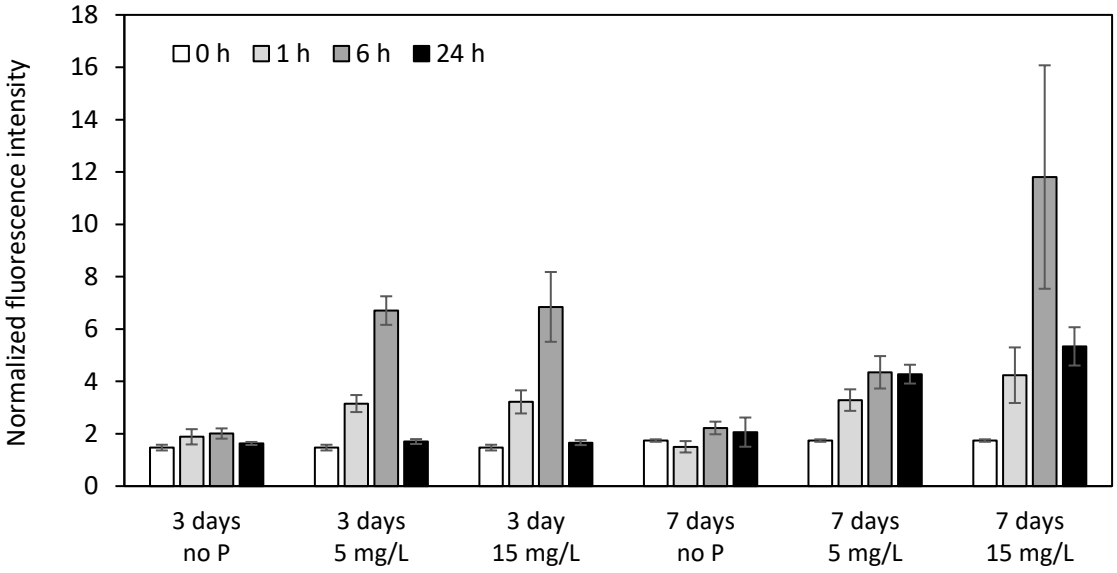

Figure 23. Estimates of polyP content by relative fluorescence intensity of bound DAPI in arbitrarily selected replicate cultures at the indicated P repletion doses and P depletion times. Error bars represent standard deviations of three technical replicates.

6.3.4 Granule formation

Granule formation from 0-1 h was higher after 7 days P depletion than after 3 days (Table 32),

but the trends in granule formation were different to the trends of polyP accumulation, suggesting different kinetics of granular and non-granular polyP formation from 0-6 h.

Table 32. Qualitative granule abundance following P repletion after 3 days or 7 days P depletion.

P depletion time	**P repletion dose**	**Mean granule abundance ranking [a]**		
		1 h	6 h	24 h
3 days	Control (no P)	0.0	0.3	0.0
	5 mg $P \cdot L^{-1}$	1.0	2.8	0.0
	15 mg $P \cdot L^{-1}$	2.4	3.8	0.0
7 days	Control (no P)	0.0	0.0	0.5
	5 mg $P \cdot L^{-1}$	4.5	3.4	1.4
	15 mg $P \cdot L^{-1}$	4.8	3.5	2.8

[a] Granule abundance was ranked qualitatively from 0 (no granules) to 5 (highest abundance observed), as described in Section 4.3.5.

After 3 days of P depletion, increased P repletion dose was associated with increased granule formation whereas, after 7 days of P repletion, granule formation was similar at both P repletion doses, except for a greater decrease in granule abundance from 6-24 h at the low P repletion dose. The decreases in granule abundance from 6-24 h confirmed that the reduction in polyP, evidenced by decreased DAPI fluorescence, was associated with granule consumption and this suggests that cells P-depleted for a longer time retain polyP granules less due to the increased pressure on intracellular P reserves. The cultures P-depleted for 7 days assimilated all the extracellular phosphate within the first six hours following P repletion, which suggests that the cultures given the high P repletion dose stored more P in forms besides granular polyP, and this may explain why the granules in that case were degraded less once the medium was P depleted.

6.3.5 Changes in gene expression

RNA yields varied between samples (Appendix C.3.2, Table 53) and were noticeably higher 24 hours after P repletion in cultures P-depleted for 7 days. Therefore, the data may have been affected by limitations on RNA extraction from P-depleted cultures. The expression levels in control cultures were assumed to remain stable over the first hour after 3 days P depletion.

P starvation response

The gene encoding the P starvation response regulator PSR1 was downregulated over the first hour following P repletion but more so in cultures P depleted for 7 days (Figure 24, right). This suggests that P depletion time impacted the 'preparedness' of cells to respond transcriptomically to P repletion. The 7-day P-depleted cultures also showed a positive association between the P repletion dose and the magnitude of downregulation after 1 hour. In the 3-day P-depleted cultures (Figure 24, left), *PSR1* was downregulated in both P-repleted conditions but more so at the low P repletion dose, indicating that the effect of P repletion dose was not the same in cultures P-depleted for a shorter time.

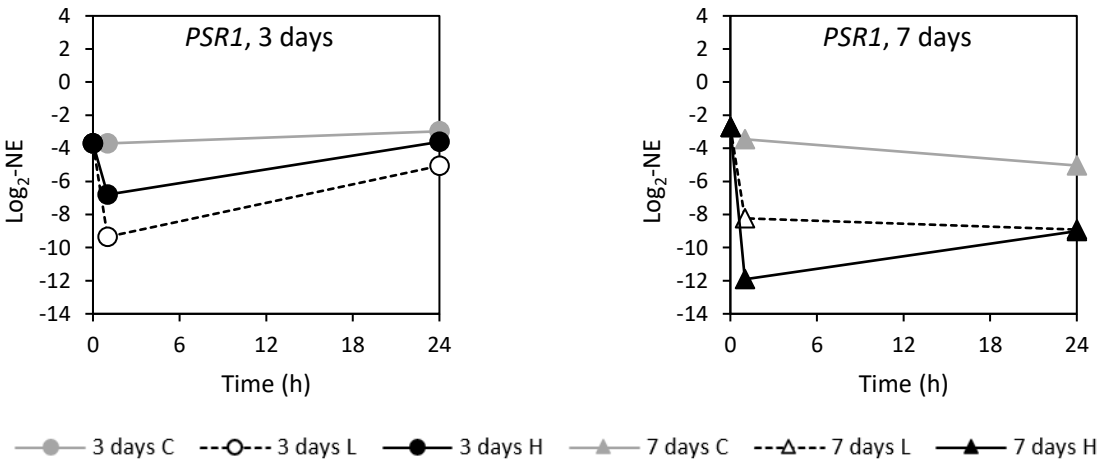

Figure 24. Changes in log_2-transformed normalized gene expression (log_2-NE) of *PSR1* in low P-repleted (L), high P-repleted (H), and no-P control (C) cultures following 3 days (left) or 7 days (right) P depletion.

Phosphate transport

The P transporter genes *PTA3*, *PTB2*, and *PTB5* did not exhibit clear patterns of expression changes in cultures P-depleted for 3 days (Figure 25, left) and, in cultures P-depleted for 7 days, the patterns of *PTA3* and *PTB2* gene expression were similar between treatment and control cultures. However, *PTB5* was only downregulated significantly (from 0-1 h) after 7 days P depletion and this downregulation was associated with P repletion dose (Figure 25, right).

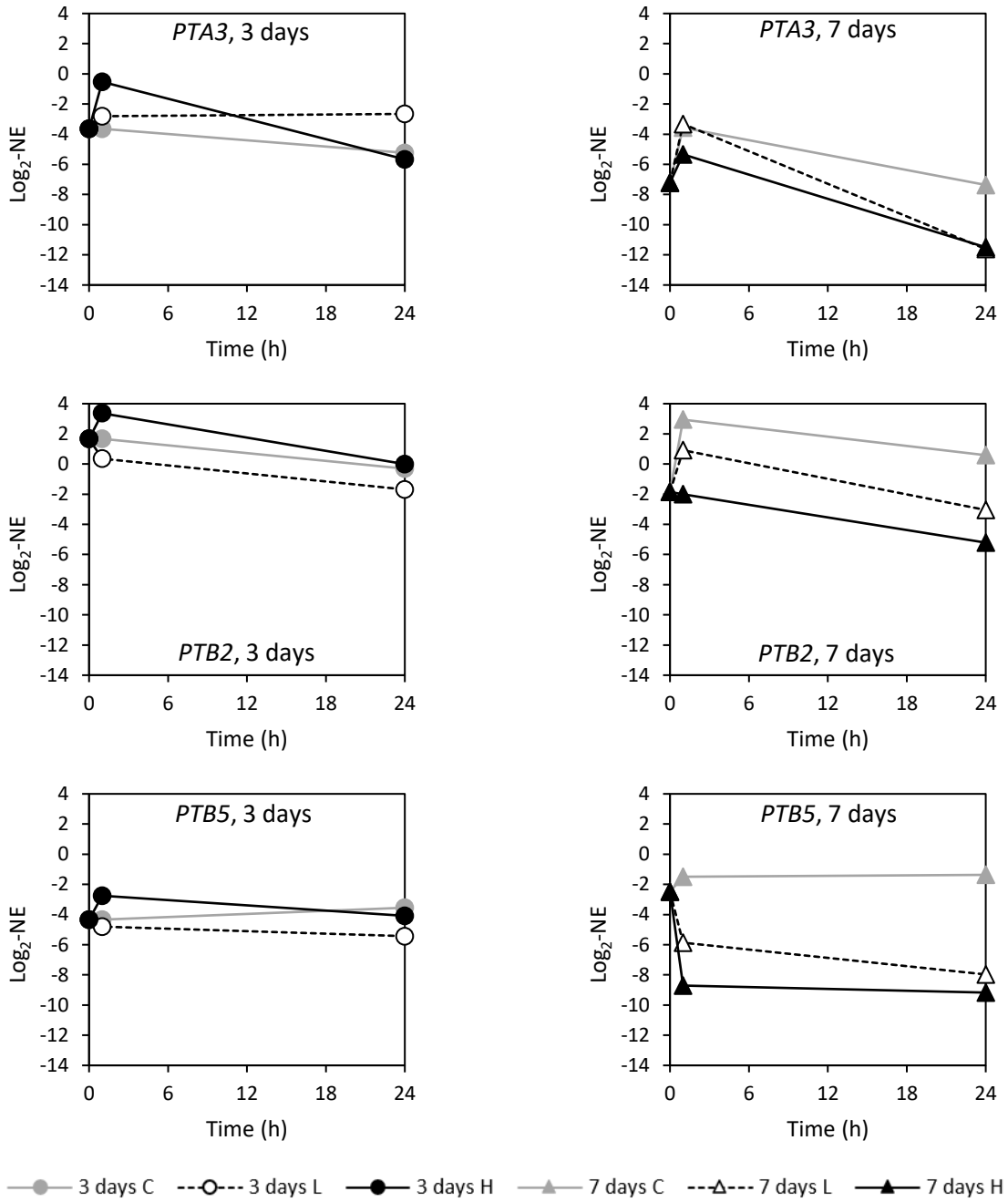

Figure 25. Changes in log_2-transformed normalized gene expression (log_2-NE) of *PTA3*, *PTB2*, and *PTB5* (top to bottom) in low P-repleted (L), high P-repleted (H), and no-P control (C) cultures following 3 days (left) or 7 days (right) P depletion.

PolyP synthesis

In the 7-day P-depleted condition, *VTC4* and *VTCX* were upregulated in control cultures over the first hour, but the expression of *VTC4* and *VTCX* decreased significantly from 0-1 h in both treatment conditions, and this downregulation was associated with P repletion dose (Figure 26,

right). In the 3-day P-depleted condition, *VTC4* and *VTCX* expression changes were smaller and not associated with P repletion dose.

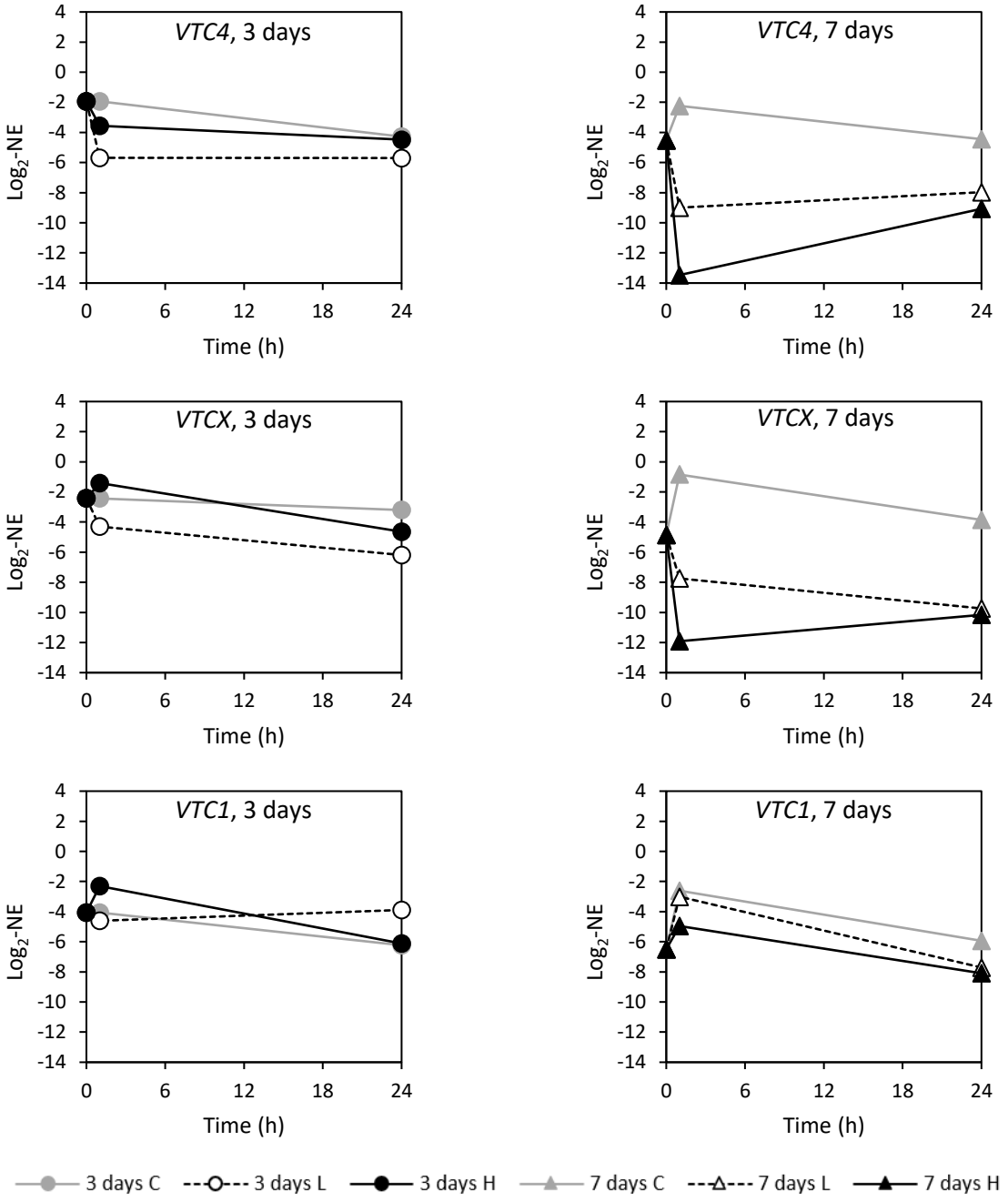

Figure 26. Changes in log_2-transformed normalized gene expression (log_2-NE) of *VTC4*, *VTCX*, and *VTC1* (top to bottom) in low P-repleted (L), high P-repleted (H), and no-P control (C) cultures following 3 days (left) or 7 days (right) P depletion.

Although unexpected changes in gene expression were still observed in the controls, the expression of *PSR1*, *VTC4*, *VTCX*, and *PTB5* in treatment cultures evidenced significant

decreases over the first hour following P repletion in cultures previously P-depleted for 7 days (Figure 25). The magnitude of downregulation of these genes was also correlated with the P repletion dose. This response is expected as cells no longer experiencing P deprivation can save resources by reducing the production of proteins that are no longer needed when intracellular P is plentiful.

The downregulation pattern described above was not as clearly evidenced in cultures P-depleted for only 3 days: changes in expression over the first hour were smaller than after 7 days depletion and P repletion was not consistently associated with downregulation. This result is however consistent with the previously mentioned finding that polyP accumulation was associated with P repletion dose only after 7 days P depletion.

Table 33. Changes in log_2-normalized gene expression [a] ($\Delta\Delta C_q$) of *PSR1*, *VTC4*, *VTCX*, and *PTB5* in treatment cultures, relative to P-depleted controls, from 0-1 h after addition of P.

P repletion dose	**$\Delta\Delta C_q$ (0-1 h)**							
	3 days P depletion				7 days P depletion			
	PSR1	*VTC4*	*VTCX*	*PTB5*	*PSR1*	*VTC4*	*VTCX*	*PTB5*
5 mg P·L^{-1}	**-5.6**	**-3.8**	-1.9	-0.5	**-5.5**	**-4.5**	**-2.9**	**-3.4**
15 mg P·L^{-1}	**-3.1**	-1.6	1.0	1.6	**-9.2**	**-8.9**	**-7.1**	**-6.2**

[a] Positive values (green) indicate upregulation of genes, and negative values (red) indicate downregulation, in P-repleted treatment cultures, relative to controls. Bold type indicates greater than four-fold (i.e., significant) expression changes.

Overall, the trends reported above indicate that the strength of the downregulation of genes involved in both P uptake (*PTA3*, *PTB2*, and *PTB5*) and polyP synthesis (*VTC4*, *VTCX*, and *VTC1*) induced by P repletion was influenced by P repletion dose but only after the longer (7 days) P depletion time.

6.3.6 Conclusions

The new experiment confirmed findings reported in Chapter 4 and Chapter 5 (albeit in different conditions of light supply and temperature) that increased P repletion dose and P depletion time

were associated with increased P uptake but had no effect on growth. Increased polyP accumulation was not associated with increased P repletion dose, whereas granule formation was associated with P repletion dose but only after 3 days P depletion. However, granule formation was significantly higher from 0-1 h after 7 days P depletion.

These findings suggest that the synthesis of granular and non-granular polyP pools have different kinetics and that the assimilated P is allocated to these pools differently depending on the duration of prior P depletion.

A stronger transcriptional response to P repletion (downregulation of *PSR1*, *VTC4*, *VTCX*, and *PTB5*) after 1 hour was evidenced after 7 days P depletion, and this downregulation was stronger at the high P repletion dose. PolyP accumulation from 0-6 h was also higher at the high P repletion dose, after 7 days P depletion, despite the greater downregulation of *VTC4* and *VTCX*.

Overall, the changes in gene expression evidenced here provided little support for the hypothesis that environmental influences on gene expression are responsible for differences in P uptake and polyP accumulation. Instead, the results suggest that P-depleted cells are 'conditioned' to be ready to assimilate P and synthesize polyP when P becomes available. Further studies into the activity of P-related proteins, their affinities for P substrates, and post-translational modifications may provide insight into the processes which prepare cells for P uptake and how these are influenced by duration of P depletion.

Chapter 7 Conclusions

7.1 Implications for ecology and evolution

The ability to store excess phosphorus (P) as polyphosphate (polyP) has been widely reported in microalgae but this trait had not previously been established as common and genetically 'hardwired' in microalgae. In the present work, a search of genomic databases identified 48 species of microalgae harbouring genes encoding proteins similar to the known polyP polymerase in *Chlamydomonas reinhardtii*. Although microalgal genetic data is currently limited, these genes were found in multiple phyla and their protein sequence similarity aligned phylogenetically with their taxonomy, suggesting that the *VTC4* gene is ancient and widely conserved among microalgae.

Results of previous studies have indicated that microalgal species may differ in their responses to changes in P availability. Putative VTC4 protein sequences were obtained using RNA extracted from laboratory cultures of *Chlorella vulgaris* and *Desmodesmus* cf. *armatus* in conditions of P-deficiency. These sequences and the *C reinhardtii* VTC4 protein sequence (Cre09.g402775) were used to generate structural models of the VTC4 protein by homology modelling and showed that the key catalytic and phosphate-sensing domains of these proteins are conserved and similar to that of the well-studied yeast *Saccharomyces cerevisiae*. Therefore, we are confident that these proteins indeed have polyP polymerase functionality. Further study of the protein models may reveal aspects of their structure engendering differences in their activation or efficiencies that could explain the observed differences in P accumulation kinetics described below.

To examine phenotypic variation in P responses, six species of microalgae – *C. reinhardtii*, *C. vulgaris*, *D. armatus*, *Gonium pectorale*, *Pediastrum boryanum*, and *Microcystis aeruginosa* were selected based on their relevance to New Zealand ecology and use in waste stabilization ponds. Each microalga was assayed by replenishing their growth medium with phosphate after a period of P depletion. This showed that the cellular P content increased significantly in all six species and the accumulation of P as granular polyP was confirmed by cytological staining. *C. vulgaris*

assimilated less P than the other species, attaining a maximum cellular P content of 1.15 ± 0.17 % within 24 h, whereas the others ranged from 2.60 ± 0.49 % (*D. armatus*) to 3.57 ± 0.77 % (*P. boryanum*).

C. reinhardtii and *C. vulgaris*, displaying clearly different responses to P repletion, were used to examine changes in their responses in different conditions of light supply, temperature, pH, P repletion dose, and P depletion time as these parameters had previously been shown to influence luxury uptake. Overall, *C. reinhardtii* assimilated significantly more P than *C. vulgaris* in the conditions tested. Both species were capable of P uptake and polyP accumulation in darkness and light supply only influenced P uptake in *C. vulgaris*. The energy requirement for P transport and polyP synthesis in darkness might be met by using intracellular energy reserves accumulated during P depletion. Increasing temperature (within the range tested) had a positive effect on polyP accumulation in *C. reinhardtii* only. P repletion dose and P depletion time had significant effects on P uptake in both species, but only impacted polyP accumulation in *C. reinhardtii*.

For the first time, changes in gene expression were examined to investigate whether transcriptional changes might be responsible for the differences in polyP metabolism observed. Experiments in conditions in which differences in P uptake and polyP accumulation had been demonstrated were repeated using *C. reinhardtii* and samples taken for RNA extraction and gene expression analysis by RT-qPCR. The effects of P repletion dose (5 or 15 mg $P \cdot L^{-1}$) and P depletion time (3 or 7 days) on P uptake were confirmed but differences in gene expression were complicated by changes in light and temperate before and after P repletion. Additional experiments were conducted under constant light and temperature conditions to more specifically assess the effects of P repletion dose and P depletion time. The results again confirmed that these increasing P repletion dose and P depletion time was associated with increasing P uptake. Differences in total polyP accumulation and granule formation were both associated with differences in P repletion dose but the effect on each polyP pool was dependent on P depletion time and suggests that the kinetics of granular and non-granular polyP formation are different.

As expected, most of the genes examined were downregulated following P repletion, but the higher polyP synthesis observed after 7 days of P depletion (compared to 3 days) could not be associated with upregulation of VTC genes, which suggests that the differences observed were not due to gene regulation following P repletion. Changes in enzyme activity might be responsible for the observed differences in P metabolism. Differences between species may be due to their specific enzymes and the changes in their activity in response to environmental conditions.

7.2 Implications for process optimization

Enhanced P removal by microalgae offers a potential low-cost solution to the problem of P pollution from insufficiently treated wastewater discharge (Slocombe et al., 2020; Solovchenko et al., 2016). P-laden microalgal biomass can be used as fertilizer to recover and reuse P, reducing the demand for P fertilizer in agriculture. Maximum P removal is attained when both the degree of polyP accumulation and biomass productivity are maximal (Brown & Shilton, 2014). In waste stabilization ponds (WSP), P availability is typically not growth-limiting so the potential for enhanced uptake is limited. Designing 'luxury uptake pond' systems (Brown & Shilton, 2014; Sells, 2019), where P-limitation conditions change between stages, can create an environment in which P uptake is promoted by transitioning microalgae from conditions of P-depletion to P-sufficiency. However, the present work has shown that responses to changes in P availability vary between species and this knowledge is important for selecting species for treatment processes.

Chlamydomonas reinhardtii and *Chlorella vulgaris* were compared and it was confirmed that *C. reinhardtii* was able to assimilate far more phosphate than *C. vulgaris* in the conditions tested. The reasons for this are not clear but may be due to a physiological limitation on the amount of P that can be accumulated as, for example, granular polyP in *C. vulgaris*. Both species were able to assimilate P and synthesize polyP in the absence of light, which is an important consideration in WSP undergoing natural diurnal light fluctuations and where mutual shading at high biomass concentrations could limit light availability. Process design should also seek to optimize the recycling of algal biomass to take advantage of the effects of P repletion dose and P depletion

time on P uptake. P-depleted cells exposed to high P concentrations in the right conditions could rapidly accumulate polyP, resulting in P-rich biomass, some of which could be harvested, and the remainder transferred to growth conditions where they would become P-depleted again before being returned to high P.

7.3 Future prospects

The following areas of research are recommended to advance the present knowledge:

7.3.1 Gene conservation

Although the genes required for polyP synthesis are clearly conserved in microalgae, there is still a limited amount of genomic data available for microalgae. To our knowledge, only *Chattonella antiqua* has been reported as being unable to synthesize polyP (Watanabe, Kohata, & Kimura, 1991). The absence of reported polyP synthesis, however, does not necessarily mean that a species does not have the ability, so identification of potential genes/proteins (or confirmation of the lack thereof) would provide strong evidence that it does.

7.3.2 Protein activity

Now that we have structural models of microalgal VTC4 proteins, we can begin to look at structural features which may explain why/how these proteins have different efficiencies and activities in different physiological conditions (Chapter 3).

Heterologous expression, extraction, and in vitro characterization of proteins may also help to better understand the influences of the parameters tested on the activity and post-translational regulation of polyP polymerases and phosphate transporters. This could help to identify potential chemical triggers (or inhibitors) for polyP synthesis.

The enzymes responsible for polyP degradation in microalgae have not yet been identified. Identifying these enzymes and being able to study their activities would help to better understand how microalgae can be manipulated to retain accumulated polyP.

In the present study, regulatory changes in the genes encoding the phosphatase PHOX were confirmed but the influence of PHOX was not determined since the only P substrate supplied was orthophosphate. In wastewater stabilization ponds, there is likely to be a significant portion of bioavailable P in the form of P-esters and changes in phosphatase activity may affect P uptake efficiency. Therefore, studies into the influence of different P substrates could confirm the importance of phosphatases in polyP metabolism.

7.3.3 Further gene studies

While the present work focuses on gene expression in the model microalga *Chlamydomonas reinhardtii*, the original intention was to compare expression patterns in *C. reinhardtii* with those in *Chlorella vulgaris*, as the latter microalga demonstrated a more limited capacity for polyP accumulation. This comparative study was hindered by inconsistent RNA extraction from *C. vulgaris* but this comparative analysis, if analytical challenges could be overcome, may identify critical transcriptional differences between the two species.

The *VTCX* gene was identified as potentially encoding a homologue of the polyP polymerase VTC4 and was shown here to be differentially regulated similarly to *VTC4*. However, the involvement of VTCX during polyP accumulation has not been confirmed. Using a mutant strain lacking the *VTCX* gene from the Chlamydomonas Library Project (e.g., LMJ.RY0402.210215), biochemical assays could be used to determine whether this protein is essential for polyP accumulation and the potential effects of its absence on polyP metabolism, particularly with respect to those changes in conditions in which *VTCX* was shown to be differently regulated.

7.3.4 Source of energy for polyP metabolism in darkness

Carbohydrate metabolism may be an important factor influencing P uptake and polyP synthesis, since these processes can take place in the absence of light. Starch and lipids accumulate during P depletion (Bajhaiya et al., 2016) and differences between species may affect their abilities to utilize these stores as energy source following P repletion in the dark. This could be investigated further by quantifying carbohydrates stored during P depletion and following P repletion and comparing against constantly P-repleted conditions.

7.3.5 Influences of other factors

Various factors potentially influencing luxury uptake have not been considered in the present work. Factors especially worth investigating may be inferred from the hypothetical functions of polyP in microalgae (see 2.4.4). Among these, abiotic factors include the presence of high concentrations of heavy metals, osmotic stress, and alkaline stress, while biotic factors include competition and cooperation (between microalgae and other organisms or between species of microalgae) and the influence of growth cycle stages. A similar set of experiments to the one used during this study could be designed to determine the influence of the abiotic factors on P assimilation and accumulation in microalgae.

7.4 Results dissemination

Aspects of the work described in Chapters 3 and 4 have been presented at conferences:

The results of the biochemical assays discussed in Chapter 3 were presented at Plant Science Central (Palmerston North, NZ) on 7 July 2021 as ‘Comparison of polyphosphate accumulation between six species of microalgae’.

The results of the factorial analysis discussed in Chapter 4 were presented at Physiomar & ANZMBS 2021 (Nelson, NZ) on 9 September 2021 as ‘The phosphate overplus response in *Chlamydomonas reinhardtii* and *Chlorella vulgaris*: Different strategies and the influence of environmental factors on polyphosphate accumulation’.

A manuscript is presently in preparation based on the work described in Chapter 3.

References

Achbergerová, L., & Nahálka, J. (2011). Polyphosphate - An ancient energy source and active metabolic regulator. *Microbial Cell Factories, 10*(1), 63. doi:10.1186/1475-2859-10-63

Afgan, E., Baker, D., Batut, B., van den Beek, M., Bouvier, D., Čech, M., . . . Blankenberg, D. (2018). The Galaxy platform for accessible, reproducible and collaborative biomedical analyses: 2018 update. *Nucleic acids research, 46*(W1), W537-W544. doi:10.1093/nar/gky379

Ahn, K., & Kornberg, A. (1990). Polyphosphate kinase from *Escherichia coli*. Purification and demonstration of a phosphoenzyme intermediate. *The Journal Of Biological Chemistry, 265*(20), 11734-11739.

Aitchison, P. A., & Butt, V. S. (1973). The relation between the synthesis of inorganic polyphosphate and phosphate uptake by *Chlorella vulgaris*. *Journal of Experimental Botany, 24*(3), 497-510. doi:10.1093/jxb/24.3.497

Akiyama, M., Crooke, E., & Kornberg, A. (1992). The polyphosphate kinase gene of *Escherichia coli*. Isolation and sequence of the ppk gene and membrane location of the protein. *The Journal Of Biological Chemistry, 267*(31), 22556-22561.

Akiyama, M., Crooke, E., & Kornberg, A. (1993). An exopolyphosphatase of *Escherichia coli*. The enzyme and its *ppx* gene in a polyphosphate operon. *The Journal Of Biological Chemistry, 268*(1), 633-639.

Aksoy, M., Pootakham, W., & Grossman, A. R. (2014). Critical function of a *Chlamydomonas reinhardtii* putative polyphosphate polymerase subunit during nutrient deprivation. *The Plant Cell, 26*(10), 4214-4229.

Allan, R. A., & Miller, J. J. (1980). Influence of S-adenosylmethionine on DAPI-induced fluorescence of polyphosphate in the yeast vacuole. *Canadian Journal of Microbiology, 26*(8), 912-920. doi:10.1139/m80-158

Altschul, S. F., Gish, W., Miller, W., Myers, E. W., & Lipman, D. J. (1990). Basic local alignment search tool. *Journal of Molecular Biology, 215*(3), 403-410. doi:https://doi.org/10.1016/S0022-2836(05)80360-2

Angelova, P. R., Agrawalla, B. K., Elustondo, P. A., Gordon, J., Shiba, T., Abramov, A. Y., . . . Pavlov, E. V. (2014). In situ investigation of mammalian inorganic polyphosphate localization using novel selective fluorescent probes JC-D7 and JC-D8. *ACS chemical biology, 9*(9), 2101-2110. doi:10.1021/cb5000696

Aschar-Sobbi, R., Abramov, A. Y., Diao, C., Kargacin, M. E., Kargacin, G. J., French, R. J., & Pavlov, E. (2008). High sensitivity, quantitative measurements of polyphosphate using a new DAPI-based approach. *Journal of Fluorescence, 18*(5), 859-866. doi:10.1007/s10895-008-0315-4

Ashford, A., Ryde, S., & Barrow, K. (1994). Demonstration of a short chain polyphosphate in *Pisolithus tinctorius* and the implications for phosphorus transport. *New Phytologist, 126*(2), 239-247.

Ault-Riché, D., Fraley, C. D., Tzeng, C. M., & Kornberg, A. (1998). Novel assay reveals multiple pathways regulating stress-induced accumulations of inorganic polyphosphate in *Escherichia coli*. *Journal of bacteriology, 180*(7), 1841-1847.

Bajhaiya, A. K., Dean, A. P., Zeef, L. A. H., Webster, R. E., & Pittman, J. K. (2016). PSR1 is a global transcriptional regulator of phosphorus deficiency responses and carbon storage metabolism in *Chlamydomonas reinhardtii*. *Plant Physiology, 170*(3), 1216-1234.

Ballance. (2022, 06/04/22). Product price list. Retrieved from https://ballance.co.nz/medias/Price-List-effective-06-April-2022-SuperPlus.pdf?context=bWFzdGVyfHJvb3R8NjA0Mzk0NnxhcHBsaWNhdGlvbi9wZGZ8aDZkL2hjZC9oMDAvOTM5NzA1OTIyMzU4Mi5wZGZ8NjBkOGY0MzFjZmNi

OWUxMTc3MDc1MzdlNDkwNTIxODQxNzAxNzYzMTAzZTU3N2U3ZmMxZDc0MjIyNTZjZmFiYw

Barcytė, D., Pilátová, J., Mojzeš, P., & Nedbalová, L. (2020). The arctic *Cylindrocystis* (Zygnematophyceae, Streptophyta) green algae are genetically and morphologically diverse and exhibit effective accumulation of polyphosphate. *Journal of Phycology, 56*(1), 217-232. doi:10.1111/jpy.12931

Bental, M., Pick, U., Avron, M., & Degani, H. (1991). Polyphosphate metabolism in the alga *Dunaliella salina* studied by 31P-NMR. *Biochimica et Biophysica Acta (BBA) - Molecular Cell Research, 1092*(1), 21-28. doi:https://doi.org/10.1016/0167-4889(91)90173-U

Blaby-Haas, C. E., & Merchant, S. S. (2017). Regulating cellular trace metal economy in algae. *Current Opinion in Plant Biology, 39*, 88-96. doi:https://doi.org/s10.1016/j.pbi.2017.06.005

Blackburn, S. (2004). Water pollution and bioremediation by microalgae: Eutrophication and water poisoning. *Handbook of Microalgal Culture: Biotechnology and Applied Phycology*, 417-429.

Blank, L. M. (2012). The cell and P: From cellular function to biotechnological application. *Current Opinion in Biotechnology, 23*(6), 846-851. doi:https://doi.org/10.1016/j.copbio.2012.08.002

Bock, C., Jacob, A., Kirst, G. O., Leibfritz, D., & Mayer, A. (1996). Metabolic changes of the Antarctic green alga *Prasiola crispa* subjected to water stress investigated by in vivo 31P NMR. *Journal of Experimental Botany, 47*(2), 241-249. doi:10.1093/jxb/47.2.241

Bolier, G., de Koningh, M. C. J., Schmale, J. C., & Donze, M. (1992). Differential luxury phosphate response of planktonic algae to phosphorus removal. *Hydrobiologia, 243*(1), 113-118. doi:10.1007/bf00007026

Brown, N., & Shilton, A. (2014). Luxury uptake of phosphorus by microalgae in waste stabilisation ponds: current understanding and future direction. *Reviews in Environmental Science and Biotechnology, 13*(3), 321-328. doi:10.1007/s11157-014-9337-3

Bru, S., Jiménez, J., Canadell, D., Ariño, J., & Clotet, J. (2017). Improvement of biochemical methods of polyP quantification. *Microbial Cell, 4*(1), 6.

Bruna, R. E., Kendra, C. G., Groisman, E. A., & Pontes, M. H. (2021). Limitation of phosphate assimilation maintains cytoplasmic magnesium homeostasis. *Proceedings of the National Academy of Sciences, 118*(11), e2021370118. doi:10.1073/pnas.2021370118

Bustin, S. A., Benes, V., Garson, J. A., Hellemans, J., Huggett, J., Kubista, M., . . . Wittwer, C. T. (2009). The MIQE guidelines: *M*inimum *I*nformation for publication of *Q*uantitative real-time PCR *E*xperiments. *Clinical Chemistry, 55*(4), 611-622. doi:10.1373/clinchem.2008.112797

Callow, J. A., Capaccio, L. C. M., Parish, G., & Tinker, P. B. (1978). Detection and estimation of polyphosphate in vesicular ‐ arbuscular mycorrhizas. *New Phytologist, 80*(1), 125-134.

Cembella, A. D., Antia, N. J., & Harrison, P. J. (1982). The utilization of inorganic and organic phosphorous compounds as nutrients by eukaryotic microalgae: A multidisciplinary perspective: Part I. *CRC Critical Reviews in Microbiology, 10*(4), 317-391. doi:10.3109/10408418209113567

Cembella, A. D., Antia, N. J., Harrison, P. J., & Rhee, G. Y. (1984). The utilization of inorganic and organic phosphorous compounds as nutrients by eukaryotic microalgae: A multidisciplinary pherspective: Part 2. *CRC Critical Reviews in Microbiology, 11*(1), 13-81. doi:10.3109/10408418409105902

Chang, C.-W., Moseley, J. L., Wykoff, D., & Grossman, A. R. (2005). The LPB1 gene is important for acclimation of *Chlamydomonas reinhardtii* to phosphorus and sulfur deprivation. *Plant Physiology, 138*(1), 319-329. doi:10.1104/pp.105.059550

Christ, J. J., & Blank, L. M. (2018a). Analytical polyphosphate extraction from *Saccharomyces cerevisiae*. *Analytical Biochemistry, 563*, 71-78. doi:https://doi.org/10.1016/j.ab.2018.09.021

Christ, J. J., & Blank, L. M. (2018b). Enzymatic quantification and length determination of polyphosphate down to a chain length of two. *Analytical Biochemistry, 548*, 82-90. doi:https://doi.org/10.1016/j.ab.2018.02.018

Christ, J. J., Smith, S. A., Willbold, S., Morrissey, J. H., & Blank, L. M. (2020). Biotechnological synthesis of water‐soluble food‐grade polyphosphate with *Saccharomyces cerevisiae*. *Biotechnology and Bioengineering*.

Clark, J. E., Beegen, H., & Wood, H. G. (1986). Isolation of intact chains of polyphosphate from "*Propionibacterium shermanii*" grown on glucose or lactate. *Journal of bacteriology, 168*(3), 1212-1219.

Cordeiro, C. D., Ahmed, M. A., Windle, B., & Docampo, R. (2019). NUDIX hydrolases with inorganic polyphosphate exo- and endopolyphosphatase activities in the glycosome, cytosol and nucleus of *Trypanosoma brucei*. *Bioscience reports, 39*(5), BSR20190894. doi:10.1042/BSR20190894

Cordell, D., Drangert, J.-O., & White, S. (2009). The story of phosphorus: Global food security and food for thought. *Global Environmental Change, 19*(2), 292-305. doi:https://doi.org/10.1016/j.gloenvcha.2008.10.009

Craggs, R. (2006). Nutrients. In A. Shilton (Ed.), *Pond treatment technology* (pp. 77-99). London, UKh: IWA Publishing.

Crimp, A., Brown, N., & Shilton, A. (2018). Microalgal luxury uptake of phosphorus in waste stabilization ponds – Frequency of occurrence and high performing genera. *Water Science and Technology, 78*(1), 165-173.

Crimp, A. J. (2015). *Luxury uptake of phosphorus by microalgae in New Zealand waste stabilisation ponds : A thesis presented in partial fulfilment of the requirements for the degree of Masters in Engineering at Massey University, Manawatu, New Zealand.* (Doctor of Philosophy (Ph.D.) Doctoral). Massey University, Retrieved from http://hdl.handle.net/10179/7535

Crooke, E., Akiyama, M., Rao, N. N., & Kornberg, A. (1994). Genetically altered levels of inorganic polyphosphate in *Escherichia coli*. *The Journal Of Biological Chemistry, 269*(9), 6290-6295.

Davison, I. R. (1991). Environmental effects on algal photosynthesis: temperature. *Journal of Phycology, 27*(1), 2-8. doi:https://doi.org/10.1111/j.0022-3646.1991.00002.x

de Mazancourt, C., & Schwartz, M. W. (2012). Starve a competitor: Evolution of luxury consumption as a competitive strategy. *Theoretical Ecology, 5*(1), 37-49. doi:10.1007/s12080-010-0094-9

de Winter, L., Klok, A. J., Cuaresma Franco, M., Barbosa, M. J., & Wijffels, R. H. (2013). The synchronized cell cycle of *Neochloris oleoabundans* and its influence on biomass composition under constant light conditions. *Algal Research, 2*(4), 313-320. doi:https://doi.org/10.1016/j.algal.2013.09.001

Desfougeres, Y., Gerasimaite, R., Jessen, H. J., & Mayer, A. (2016). Vtc5, a novel subunit of the vacuolar transporter chaperone complex, regulates polyphosphate synthesis and phosphate homeostasis in yeast. *The Journal Of Biological Chemistry, 291*(42), 22262-22275. doi:10.1074/jbc.M116.746784

Diaz, J. M., & Ingall, E. D. (2010). Fluorometric quantification of natural inorganic polyphosphate. *Environmental Science & Technology, 44*(12), 4665-4671. doi:10.1021/es100191h

Dick, R. P., & Tabatabai, M. A. (1986). Hydrolysis of polyphosphates in soils. *Soil Science, 142*(3), 132-140.

Docampo, R. (2006). Acidocalcisomes and polyphosphate granules. In *Inclusions in prokaryotes* (pp. 53-70): Springer.

Docampo, R., & Huang, G. (2016). Acidocalcisomes of eukaryotes. *Current Opinion in Cell Biology, 41*, 66-72. doi:https://doi.org/10.1016/j.ceb.2016.04.007

Docampo, R., & Moreno, S. N. J. (2011). Acidocalcisomes. *Cell Calcium, 50*(2), 113-119. doi:https://doi.org/10.1016/j.ceca.2011.05.012

Docampo, R., Ulrich, P., & Moreno Silvia, N. J. (2010). Evolution of acidocalcisomes and their role in polyphosphate storage and osmoregulation in eukaryotic microbes. *Philosophical Transactions of the Royal Society B: Biological Sciences, 365*(1541), 775-784. doi:10.1098/rstb.2009.0179

Dodds, W. K., Bouska, W. W., Eitzmann, J. L., Pilger, T. J., Pitts, K. L., Riley, A. J., . . . Thornbrugh, D. J. (2009). Eutrophication of U.S. freshwaters: analysis of potential economic damages. *Environmental Science & Technology, 43*(1), 12-19. doi:10.1021/es801217q

Donald, K. M., Scanlan, D. J., Carr, N. G., Mann, N. H., & Joint, I. (1997). Comparative phosphorus nutrition of the marine cyanobacterium *Synechococcus* WH7803 and the marine diatom *Thalassiosira weissflogii*. *Journal of Plankton Research, 19*(12), 1793-1813. doi:10.1093/plankt/19.12.1793

Droop, M. R. (1973). Some thoughts on nutrient limitation in algae. *Journal of Phycology, 9*(3), 264-272. doi:10.1111/j.1529-8817.1973.tb04092.x

Dueñas, J. F., Alonso, J. R., Rey, À. F., & Ferrer, A. S. (2003). Characterisation of phosphorous forms in wastewater treatment plants. *Journal of Hazardous Materials, 97*(1), 193-205. doi:https://doi.org/10.1016/S0304-3894(02)00260-1

Dyhrman, S. T. (2016). Nutrients and their acquisition: Phosphorus physiology in microalgae. In *The physiology of microalgae* (pp. 155-183): Springer.

Dyhrman, S. T., Chappell, P. D., Haley, S. T., Moffett, J. W., Orchard, E. D., Waterbury, J. B., & Webb, E. A. (2006). Phosphonate utilization by the globally important marine diazotroph *Trichodesmium*. *Nature, 439*(7072), 68-71. doi:10.1038/nature04203

Dyhrman, S. T., Jenkins, B. D., Rynearson, T. A., Saito, M. A., Mercier, M. L., Alexander, H., . . . Heithoff, A. (2012). The transcriptome and proteome of the diatom *Thalassiosira pseudonana* reveal a diverse phosphorus stress response. *PLOS ONE, 7*(3), e33768. doi:10.1371/journal.pone.0033768

Egle, L., Rechberger, H., Krampe, J., & Zessner, M. (2016). Phosphorus recovery from municipal wastewater: An integrated comparative technological, environmental and economic assessment of P recovery technologies. *Science of The Total Environment, 571*, 522-542. doi:https://doi.org/10.1016/j.scitotenv.2016.07.019

Eixler, S., Karsten, U., & Selig, U. (2006). Phosphorus storage in *Chlorella vulgaris* (Trebouxiophyceae, Chlorophyta) cells and its dependence on phosphate supply. *Phycologia, 45*, 53-60. doi:10.2216/04-79.1

Elgavish, A., & Elgavish, G. A. (1980). 31P-NMR differentiation between intracellular phosphate pools in *Cosmarium* (Chlorophyta). *Journal of Phycology, 16*(3), 368-374. doi:10.1111/j.1529-8817.1980.tb03047.x

Fisher, K. A. (1971). Polyphosphate in a chlorococcalean alga. *Phycologia, 10*(2-3), 177-182. doi:10.2216/i0031-8884-10-2-177.1

Fitzgerald, G. P., & Nelson, T. C. (1966). Extractive and enzymatic analyses for limiting or surplus phosphorus in algae. *Journal of Phycology, 11*, 32-37.

Gaxiola, R. A., Edwards, M., & Elser, J. J. (2011). A transgenic approach to enhance phosphorus use efficiency in crops as part of a comprehensive strategy for sustainable agriculture. *Chemosphere, 84*(6), 840-845. doi:https://doi.org/10.1016/j.chemosphere.2011.01.062

Gerasimaitė, R., Sharma, S., Desfougères, Y., Schmidt, A., & Mayer, A. (2014). Coupled synthesis and translocation restrains polyphosphate to acidocalcisome-like vacuoles and prevents its toxicity. *Journal of Cell Science, 127*(23), 5093. doi:10.1242/jcs.159772

Gezelius, K. (1974). Inorganic polyphosphates and enzymes of polyphosphate metabolism in the cellular slime mold *Dictyostelium discoideum*. *Archives of Microbiology, 98*(1), 311-329. doi:10.1007/BF00425292

Gilbert, N. (2009). The disappearing nutrient: Phosphate-based fertilizers have helped spur agricultural gains in the past century, but the world may soon run out of them. Natasha Gilbert investigates the potential phosphate crisis. *Nature*(7265), 716. doi:10.1038/461716a

Gomes, F. M., Ramos, I. B., Wendt, C., Girard-Dias, W., De Souza, W., Machado, E. A., & Miranda, K. (2013). New insights into the in situ microscopic visualization and quantification of inorganic polyphosphate stores by 4',6-diamidino-2-phenylindole (DAPI)-staining. *European Journal of Histochemistry, 57*(4). doi:10.4081/ejh.2013.e34

González-Ballester, D., Casero, D., Cokus, S., Pellegrini, M., Merchant, S. S., & Grossman, A. R. (2010). RNA-seq analysis of sulfur-deprived *Chlamydomonas* cells reveals aspects of acclimation critical for cell survival. *The Plant Cell, 22*(6), 2058-2084.

González-Gil, S., Keafer, B. A., Jovine, R. V., Aguilera, A., Lu, S., & Anderson, D. M. (1998). Detection and quantification of alkaline phosphatase in single cells of phosphorus-starved marine phytoplankton. *Marine Ecology Progress Series, 164*, 21-35.

Goodstein, D. M., Shu, S., Howson, R., Neupane, R., Hayes, R. D., Fazo, J., . . . Rokhsar, D. S. (2012). Phytozome: a comparative platform for green plant genomics. *Nucleic acids research, 40*(Database issue), D1178-D1186. doi:10.1093/nar/gkr944

Grabherr, M. G., Haas, B. J., Yassour, M., Levin, J. Z., Thompson, D. A., Amit, I., . . . Regev, A. (2011). Full-length transcriptome assembly from RNA-Seq data without a reference genome. *Nature Biotechnology, 29*(7), 644-652. doi:10.1038/nbt.1883

Grobbelaar, J. U. (2004). Algal nutrition: Mineral nutrition. In A. Richmond (Ed.), *Handbook of Microalgal Culture: Biotechnology and Applied Phycology* (pp. 97-115). Oxford, UK: Blackwell Science Ltd.

Grossman, A. R., & Aksoy, M. (2015). Algae in a phosphorus‐limited landscape. *Annual Plant Reviews, 48*, 337-374. doi:10.1002/9781118958841.ch12

Guiry, M. D. G., G. M. (2022). AlgaeBase. Retrieved from https://www.algaebase.org

Günther, S., Trutnau, M., Kleinsteuber, S., Hause, G., Bley, T., Röske, I., . . . Müller, S. (2009). Dynamics of polyphosphate-accumulating bacteria in wastewater treatment plant microbial communities detected via DAPI (4′, 6′-diamidino-2-phenylindole) and tetracycline labeling. *Applied and Environmental Microbiology, 75*(7), 2111-2121.

Haas, B. J., Papanicolaou, A., Yassour, M., Grabherr, M., Blood, P. D., Bowden, J., . . . Regev, A. (2013). De novo transcript sequence reconstruction from RNA-seq using the Trinity platform for reference generation and analysis. *Nature Protocols, 8*(8), 1494-1512. doi:10.1038/nprot.2013.084

Harold, F. M. (1960). Accumulation of inorganic polyphosphate in mutants of *Neurospora crassa*. *Biochimica et Biophysica Acta, 45*, 172-188. doi:https://doi.org/10.1016/0006-3002(60)91438-4

Harold, F. M. (1963). Accumulation of inorganic polyphosphate in *Aerobacter aerogenes*. I. Relationship to growth and nucleic acid synthesis. *Journal of bacteriology, 86*(2), 216.

Harold, F. M. (1964). Enzymic and genetic control of polyphosphate accumulation in *Aerobacter aerogenes*. *Microbiology, 35*(1), 81-90. doi:https://doi.org/10.1099/00221287-35-1-81

Harold, F. M. (1966). Inorganic polyphosphates in biology: Structure, metabolism, and function. *Bacteriological Reviews, 30*(4), 772.

Harris, E. H. (2001). *Chlamydomonas* as a model organism. *Annual Review of Plant Physiology and Plant Molecular Biology, 52*(1), 363-406. doi:10.1146/annurev.arplant.52.1.363

Healey, F. P. (1973). Inorganic nutrient uptake and deficiency in algae. *CRC Critical Reviews in Microbiology, 3*(1), 69-113. doi:10.3109/10408417309108746

Hemens, J., & Mason, M. H. (1968). Sewage nutrient removal by a shallow algal stream. *Water Research, 2*(4), 277-287. doi:https://doi.org/10.1016/0043-1354(68)90020-1

Hernandez, J.-P., de-Bashan, L. E., & Bashan, Y. (2006). Starvation enhances phosphorus removal from wastewater by the microalga *Chlorella* spp. co-immobilized with *Azospirillum brasilense*. *Enzyme and Microbial Technology, 38*(1), 190-198. doi:https://doi.org/10.1016/j.enzmictec.2005.06.005

Hessen, D. O., Færøvig, P. J., & Andersen, T. (2002). Light, nutrients, and P:C ratios in algae:grazer performance related to food quality and quantity. *Ecology, 83*(7), 1886-1898. doi:10.1890/0012-9658(2002)083[1886:LNAPCR]2.0.CO;2

Hill, T. W., & Kafer, E. (2001). Improved protocols for Aspergillus minimal medium: trace element and minimal medium salt stock solutions. *Fungal Genetics Reports, 48*(1), 20-21.

Hothorn, M., Neumann, H., Lenherr, E. D., Wehner, M., Rybin, V., Hassa, P. O., . . . Mayer, A. (2009). Catalytic core of a membrane-associated eukaryotic polyphosphate polymerase. *Science, 324*(5926), 513-516.

Hürlimann, H. C., Pinson, B., Stadler-Waibel, M., Zeeman, S. C., & Freimoser, F. M. (2009). The SPX domain of the yeast low-affinity phosphate transporter Pho90 regulates transport activity. *EMBO reports, 10*(9), 1003-1008. doi:10.1038/embor.2009.105

Hutching, G. (2018). The ethical element to fertiliser - push for NZ co-ops to stop buying phosphate from Morocco. Retrieved from https://www.stuff.co.nz/business/farming/101920354/nz-fertiliser-coops-under-growing-pressure-to-stop-buying-phosphate-from-morocco?rm=m

Hutchinson, G. E. (1961). The paradox of the plankton. *The American Naturalist, 95*(882), 137-145. doi:10.1086/282171

Jacobson, L., & Halmann, M. (1982). Polyphosphate metabolism in the blue-green alga *Microcystis aeruginosa*. *Journal of Plankton Research, 4*(3), 481-488. doi:10.1093/plankt/4.3.481

Jacobson, L., Halmann, M., & Yariv, J. (1982). The molecular composition of the volutin granule of yeast. *Biochemical Journal, 201*(3), 473. doi:10.1042/bj2010473

Jensen, T. E., & Sicko, L. M. (1974). Phosphate metabolism in blue-green algae. I. Fine structure of the "polyphosphate overplus" phenomenon in *Plectonema boryanum*. *Canadian Journal of Microbiology, 20*(9), 1235-1239. doi:10.1139/m74-190

Jumper, J., Evans, R., Pritzel, A., Green, T., Figurnov, M., Ronneberger, O., . . . Potapenko, A. (2021). Highly accurate protein structure prediction with AlphaFold. *Nature, 596*(7873), 583-589.

Juni, E., Kamen, M. D., Spiegelman, S., & Wiame, J. M. (1947). Physiological heterogeneity of metaphosphate in yeast. *Nature, 160*(4073), 717-718. doi:10.1038/160717b0

Kanai, R., Aoki, S., & Miyachi, S. (1965). Quantitative separation of inorganic polyphosphates in *Chlorella* cells. *Plant and Cell Physiology, 6*(3), 467-473. doi:10.1093/oxfordjournals.pcp.a079116

Keasling, J., Van Dien, S., Trelstad, P., Renninger, N., & McMahon, K. (2000). Application of polyphosphate metabolism to environmental and biotechnological problems. *Biochemistry (Moscow), 65*(3), 324-331.

Keasling, J. D. (1997). Regulation of intracellular toxic metals and other cations by hydrolysis of polyphosphate. *Annals of the New York Academy of Sciences, 829*(1), 242-249. doi:10.1111/j.1749-6632.1997.tb48579.x

Keck, K., & Stich, H. (1957). The widespread occurrence of polyphosphate in lower plants. *Annals of Botany, 21*(4), 611-619. doi:10.1093/oxfordjournals.aob.a083588

Kelley, L. A., Mezulis, S., Yates, C. M., Wass, M. N., & Sternberg, M. J. (2015). The Phyre2 web portal for protein modeling, prediction and analysis. *Nature Protocols, 10*(6), 845-858.

Klauth, P., Pallerla, S. R., Vidaurre, D., Ralfs, C., Wendisch, V. F., & Schoberth, S. M. (2006). Determination of soluble and granular inorganic polyphosphate in *Corynebacterium glutamicum*. *Applied Microbiology and Biotechnology, 72*(5), 1099-1106. doi:10.1007/s00253-006-0562-8

Kolozsvari, B., Parisi, F., & Saiardi, A. (2014). Inositol phosphates induce DAPI fluorescence shift. *Biochemical Journal, 460*(3), 377-385. doi:10.1042/BJ20140237

Komine, Y., Eggink, L. L., Park, H., & Hoober, J. K. (2000). Vacuolar granules in *Chlamydomonas reinhardtii*: polyphosphate and a 70-kDa polypeptide as major components. *Planta, 210*(6), 897-905.

Kornberg, A. (1995). Inorganic polyphosphate: Toward making a forgotten polymer unforgettable. *Journal of bacteriology, 177*(3), 491-496.

Kornberg, A., Rao, N. N., & Ault-Riche, D. (1999). Inorganic polyphosphate: a molecule of many functions. *Annual Review of Biochemistry*, 89.

Kuhl, A. (1962). Inorganic phosphorus uptake and metabolism. In R. A. Lewin (Ed.), *Physiology and biochemistry of algae* (pp. 211-229). New York: Academic Press Inc.

Kuhl, A. (1974). Phosphorus. In W. D. P. Stewart (Ed.), *Algal physiology and biochemistry* (pp. 636-654). Oxford: Blackwell Scientific.

Kulaev, I., & Kulakovskaya, T. (2000). Polyphosphate and phosphate pump. *Annual Review of Microbiology, 54*(1), 709. doi:10.1146/annurev.micro.54.1.709

Kulaev, I., Vagabov, V., & Kulakovskaya, T. (1999). New aspects of inorganic polyphosphate metabolism and function. *Journal of Bioscience and Bioengineering, 88*(2), 111-129. doi:https://doi.org/10.1016/S1389-1723(99)80189-3

Kulaev, I. S., & Vagabov, V. M. (1983). Polyphosphate metabolism in micro-organisms. In A. H. Rose, J. G. Morris, & D. W. Tempest (Eds.), *Advances in microbial physiology* (Vol. 24, pp. 83-171): Academic Press.

Kulaev, I. S., Vagabov, V. M., & Kulakovskaya, T. V. (2004). *The biochemistry of inorganic polyphosphates* (2nd ed.): Wiley Online Library.

Kulakova, A. N., Hobbs, D., Smithen, M., Pavlov, E., Gilbert, J. A., Quinn, J. P., & McGrath, J. W. (2011). Direct quantification of inorganic polyphosphate in microbial cells using 4′ -6-diamidino-2-phenylindole (DAPI). *Environmental Science & Technology, 45*(18), 7799-7803. doi:10.1021/es201123r

Kulakovskaya, T., Pavlov, E., & Dedkova, E. N. (2016). *Inorganic polyphosphates in eukaryotic cells*: Springer.

Kumble, K. D., & Kornberg, A. (1995). Inorganic polyphosphate in mammalian cells and tissues. *The Journal Of Biological Chemistry, 270*(11), 5818-5822. doi:10.1074/jbc.270.11.5818

Lander, N., Cordeiro, C., Huang, G., & Docampo, R. (2016). Polyphosphate and acidocalcisomes. *Biochemical Society Transactions, 44*(1), 1. doi:10.1042/BST20150193

Lander, N., Ulrich, P. N., & Docampo, R. (2013). *Trypanosoma brucei* vacuolar transporter chaperone 4 (TbVtc4) is an acidocalcisome polyphosphate kinase required for in vivo infection. *Journal of Biological Chemistry, 288*(47), 34205-34216. doi:10.1074/jbc.M113.518993

Lavrinovičs, A., Mežule, L., & Juhna, T. (2020). Microalgae starvation for enhanced phosphorus uptake from municipal wastewater. *Algal Research, 52*, 102090. doi:https://doi.org/10.1016/j.algal.2020.102090

Lavrinovičs, A., Murby, F., Zīverte, E., Mežule, L., & Juhna, T. (2021). Increasing phosphorus uptake efficiency by phosphorus-starved microalgae for municipal wastewater post-treatment. *Microorganisms, 9*(8). doi:10.3390/microorganisms9081598

Lee, W. D., Gawri, R., Shiba, T., Ji, A.-R., Stanford, W. L., & Kandel, R. A. (2017). Simple silica column–based method to quantify inorganic polyphosphates in cartilage and other tissues. *CARTILAGE, 9*(4), 417-427. doi:10.1177/1947603517690856

Leitão, J. M., Lorenz, B., Bachinski, N., Wilhelm, C., Müller, W. E. G., & Schröder, H. C. (1995). Osmotic-stress-induced synthesis and degradation of inorganic polyphosphates in the alga *Phaeodactylum tricornutum*. *Marine Ecology Progress Series, 121*, 279-288.

Levin, G. V., & Shapiro, J. (1965). Metabolic uptake of phosphorus by wastewater organisms. *Journal (Water Pollution Control Federation)*, 800-821.

Lindegren, C. C. (1947). Function of volutin (metaphosphate) in mitosis. *Nature, 159*(4028), 63-64. doi:10.1038/159063a0

Loppes, R., & Matagne, R. (1973). Acid phosphatase mutants in *Chlamydomonas*: Isolation and characterization by biochemical, electrophoretic and genetic analysis. *Genetics, 75*(4), 593-604.

Lorenz, B., & Schröder, H. (1999). Methods for investigation of inorganic polyphosphates and polyphosphate-metabolizing enzymes. In H. C. Schröder & W. E. G. Müller (Eds.), *Inorganic polyphosphates: Biochemistry, biology, biotechnology* (pp. 217-239): Springer.

Martin, P., Dyhrman, S. T., Lomas, M. W., Poulton, N. J., & Van Mooy, B. A. S. (2014). Accumulation and enhanced cycling of polyphosphate by Sargasso Sea plankton in response to low phosphorus. *Proceedings of the National Academy of Sciences, 111*(22), 8089. doi:10.1073/pnas.1321719111

Martin, P., & Van Mooy, B. A. S. (2013). Fluorometric quantification of polyphosphate in environmental plankton samples: Extraction protocols, matrix effects, and nucleic acid interference. *Applied and Environmental Microbiology, 79*(1), 273-281. doi:10.1128/AEM.02592-12 %J Applied and Environmental Microbiology

McDowell, R. W., & Nash, D. (2012). A review of the cost-effectiveness and suitability of mitigation strategies to prevent phosphorus loss from dairy farms in New Zealand and Australia. *Journal of Environmental Quality, 41*(3), 680-693. doi:10.2134/jeq2011.0041

Merchant, S. S., Prochnik, S. E., Vallon, O., Harris, E. H., Karpowicz, S. J., Witman, G. B., . . . Maréchal-Drouard, L. (2007). The *Chlamydomonas* genome reveals the evolution of key animal and plant functions. *Science, 318*(5848), 245-250.

Miyachi, S., Kanai, R., Mihara, S., Miyachi, S., & Aoki, S. (1964). Metabolic roles of inorganic polyphosphates in *Chlorella* cells. *Biochimica et Biophysica Acta (BBA) - General Subjects, 93*(3), 625-634. doi:https://doi.org/10.1016/0304-4165(64)90345-9

Miyachi, S., & Tamiya, H. (1961). Distribution and turnover of phosphate compounds in growing *Chlorella* cells. *Plant and Cell Physiology, 2*(4), 405-414. doi:10.1093/oxfordjournals.pcp.a077695

Monaghan, R. M., Hedley, M. J., Di, H. J., McDowell, R. W., Cameron, K. C., & Ledgard, S. F. (2007). Nutrient management in New Zealand pastures— recent developments and future issues. *New Zealand Journal of Agricultural Research, 50*(2), 181-201. doi:10.1080/00288230709510290

Moreno, S. N., & Docampo, R. (2013). Polyphosphate and its diverse functions in host cells and pathogens. *PLoS pathogens, 9*(5), e1003230.

Moseley, J. L., Chang, C.-W., & Grossman, A. R. (2006). Genome-based approaches to understanding phosphorus deprivation responses and PSR1 control in *Chlamydomonas reinhardtii*. *Eukaryotic cell, 5*(1), 26-44.

Moseley, J. L., Gonzalez-Ballester, D., Pootakham, W., Bailey, S., & Grossman, A. R. (2009). Genetic interactions between regulators of *Chlamydomonas* phosphorus and sulfur deprivation responses. *Genetics, 181*(3), 889-905.

Moudříková, Š., Sadowsky, A., Metzger, S., Nedbal, L., Mettler-Altmann, T., & Mojzeš, P. (2017). Quantification of polyphosphate in microalgae by raman microscopy and by a reference enzymatic assay. *Analytical Chemistry, 89*(22), 12006-12013. doi:10.1021/acs.analchem.7b02393

Mühlroth, A., Winge, P., El Assimi, A., Jouhet, J., Maréchal, E., Hohmann-Marriott, M. F., . . . Bones, A. M. (2017). Mechanisms of phosphorus acquisition and lipid class remodeling under P limitation in a marine microalga *Plant Physiology, 175*(4), 1543-1559. doi:10.1104/pp.17.00621

Mullan, A., Quinn, J. P., & McGrath, J. W. (2002). A nonradioactive method for the assay of polyphosphate kinase activity and its application in the study of polyphosphate metabolism in *Burkholderia cepacia*. *Analytical Biochemistry, 308*(2), 294-299. doi:https://doi.org/10.1016/S0003-2697(02)00249-X

Murphy, J., & Riley, J. P. (1962). A modified single solution method for the determination of phosphate in natural waters. *Analytica Chimica Acta, 27*, 31-36. doi:https://doi.org/10.1016/S0003-2670(00)88444-5

Nagasaka, S., & Yoshimura, E. (2008). External iron regulates polyphosphate content in the acidophilic, thermophilic alga *Cyanidium caldarium*. *Biological Trace Element Research, 125*(3), 286. doi:10.1007/s12011-008-8177-9

Nagel, L. (1948). Volutin. *The Botanical Review, 14*(3), 174-184.

Nazari-Sharabian, M., Ahmad, S., & Karakouzian, M. (2018). Climate change and eutrophication: A short review. *Engineering, Technology & Applied Science Research, 8*(6), 3668-3672.

Nguyen, C. T., Ezawa, T., & Saito, K. (2022). Polyphosphate polymerizing and depolymerizing activity of VTC4 protein in an arbuscular mycorrhizal fungus. *Soil Science and Plant Nutrition*, 1-12. doi:10.1080/00380768.2022.2029220

Niemeyer, R. (1976). Cyclic condensed metaphosphates and linear polyphosphates in brown and red algae. *Archives of Microbiology, 108*(3), 243-247. doi:10.1007/BF00454848

Nishikawa, K., Machida, H., Yamakoshi, Y., Ohtomo, R., Saito, K., Saito, M., & Tominaga, N. (2006). Polyphosphate metabolism in an acidophilic alga *Chlamydomonas acidophila* KT-1 (Chlorophyta) under phosphate stress. *Plant Science, 170*(2), 307-313. doi:https://doi.org/10.1016/j.plantsci.2005.08.025

Nishikawa, K., Yamakoshi, Y., Uemura, I., & Tominaga, N. (2003). Ultrastructural changes in *Chlamydomonas acidophila* (Chlorophyta) induced by heavy metals and polyphosphate metabolism. *FEMS Microbiology Ecology, 44*(2), 253-259. doi:10.1016/S0168-6496(03)00049-7

Noegel, A., & Gotschlich, E. C. (1983). Isolation of a high molecular weight polyphosphate from *Neisseria gonorrhoeae*. *The Journal of Experimental Medicine, 157*(6), 2049. doi:10.1084/jem.157.6.2049

Ogawa, N., DeRisi, J., & Brown, P. O. (2000). New components of a system for phosphate accumulation and polyphosphate metabolism in *Saccharomyces cerevisiae* revealed by genomic expression analysis. *Molecular biology of the cell, 11*(12), 4309-4321.

Oh-hama, T., Siebelt, F., Furihata, K., Seto, H., Miyachi, S., & Ohmori, M. (1986). ^{31}P-NMR studies on inorganic polyphosphates in microalgae. *Journal of Phycology, 22*(4), 485-490. doi:10.1111/j.1529-8817.1986.tb02492.x

Omelon, S., Georgiou, J., & Habraken, W. (2016). A cautionary (spectral) tail: Red-shifted fluorescence by DAPI–DAPI interactions. *Biochemical Society Transactions, 44*(1), 46. doi:10.1042/BST20150231

Oshima, Y. (1997). The phosphatase system in *Saccharomyces cerevisiae*. *Genes & Genetic Systems, 72*(6), 323-334. doi:10.1266/ggs.72.323

Ota, S., & Kawano, S. (2017). Extraction and molybdenum blue-based quantification of total phosphate and polyphosphate in *Parachlorella*. *Bio-protocol, 7*(17), e2539-e2539. doi:10.21769/BioProtoc.2539

Park, J. B. K., Craggs, R. J., & Shilton, A. N. (2011). Recycling algae to improve species control and harvest efficiency from a high rate algal pond. *Water Research, 45*(20), 6637-6649. doi:https://doi.org/10.1016/j.watres.2011.09.042

Park, J. B. K., Craggs, R. J., & Shilton, A. N. (2015). Algal recycling enhances algal productivity and settleability in *Pediastrum boryanum* pure cultures. *Water Research, 87*, 97-104. doi:https://doi.org/10.1016/j.watres.2015.09.013

Patni, N. J., Dhawale, S. W., & Aaronson, S. (1977). Extracellular phosphatases of *Chlamydomonas reinhardi* and their regulation. *Journal of bacteriology, 130*(1), 205. Retrieved from http://jb.asm.org/content/130/1/205.abstract

Pearson, H. (2006). Microbiology of waste stabilisation ponds. In A. Shilton (Ed.), *Pond treatment technology* (pp. 14-48). London, UK: IWA Publishing.

Perry, M. J. (1976). Phosphate utilization by an oceanic diatom in phosphorus-limited chemostat culture and in the oligotrophic waters of the central North Pacific. *Limnology and Oceanography, 21*(1), 88-107. doi:https://doi.org/10.4319/lo.1976.21.1.0088

Pettersen, E. F., Goddard, T. D., Huang, C. C., Meng, E. C., Couch, G. S., Croll, T. I., . . . Ferrin, T. E. (2021). UCSF ChimeraX: Structure visualization for researchers, educators, and developers. *Protein Science, 30*(1), 70-82.

Peverly, J. H., Adamec, J., & Parthasarathy, M. V. (1978). Association of potassium and some other monovalent cations with occurrence of polyphosphate bodies in *Chlorella pyrenoidosa*. *Plant Physiology, 62*(1), 120. doi:10.1104/pp.62.1.120

Phillips, J. C., Hardy, D. J., Maia, J. D., Stone, J. E., Ribeiro, J. V., Bernardi, R. C., . . . Jiang, W. (2020). Scalable molecular dynamics on CPU and GPU architectures with NAMD. *The Journal of chemical physics, 153*(4), 044130.

Pick, U., Zeelon, O., & Weiss, M. (1991). Amine accumulation in acidic vacuoles protects the halotolerant alga *Dunaliella salina* against alkaline stress. *Plant Physiology, 97*(3), 1226. doi:10.1104/pp.97.3.1226

Plouviez, M., Fernández, E., Grossman, A. R., Sanz-Luque, E., Sells, M., Wheeler, D., & Guieysse, B. (2021). Responses of *Chlamydomonas reinhardtii* during the transition from P-deficient to P-sufficient growth (the P-overplus response): The roles of the vacuolar transport chaperones and polyphosphate synthesis. *Journal of Phycology, n/a*(n/a). doi:https://doi.org/10.1111/jpy.13145

Plouviez, M., Oliveira da Rocha, C. S., & Guieysse, B. (2022). Intracellular polyphosphate is a P reserve in Chlamydomonas reinhardtii. *Algal Research, 66*, 102779. doi:https://doi.org/10.1016/j.algal.2022.102779

Plouviez, M., Wheeler, D., Shilton, A., Packer, M. A., McLenachan, P. A., Sanz‐Luque, E., . . . Guieysse, B. (2017). The biosynthesis of nitrous oxide in the green alga *Chlamydomonas reinhardtii*. *The Plant Journal, 91*(1), 45-56.

Powell, N., Shilton, A., Chisti, Y., & Pratt, S. (2009). Towards a luxury uptake process via microalgae – Defining the polyphosphate dynamics. *Water Research, 43*(17), 4207-4213. doi:https://doi.org/10.1016/j.watres.2009.06.011

Powell, N., Shilton, A., Pratt, S., & Chisti, Y. (2011a). Luxury uptake of phosphorus by microalgae in full-scale waste stabilisation ponds. *Water Science and Technology, 63*(4), 704-709. doi:10.2166/wst.2011.116

Powell, N., Shilton, A., Pratt, S., & Chisti, Y. (2011b). Phosphate release from waste stabilisation pond sludge: Significance and fate of polyphosphate. *Water Science and Technology, 63*(8), 1689-1694. doi:10.2166/wst.2011.336

Powell, N., Shilton, A. N., Pratt, S., & Chisti, Y. (2008). Factors influencing luxury uptake of phosphorus by microalgae in waste stabilization ponds. *Environmental Science & Technology, 42*(16), 5958-5962. doi:10.1021/es703118s

Pratt, C., Parsons, S. A., Soares, A., & Martin, B. D. (2012). Biologically and chemically mediated adsorption and precipitation of phosphorus from wastewater. *Current Opinion in Biotechnology, 23*(6), 890-896. doi:https://doi.org/10.1016/j.copbio.2012.07.003

Pruitt, K. D., Tatusova, T., & Maglott, D. R. (2007). NCBI reference sequences (RefSeq): a curated non-redundant sequence database of genomes, transcripts and proteins. *Nucleic acids research, 35*(suppl_1), D61-D65. doi:10.1093/nar/gkl842

Qi, W., Baldwin, Stephen A., Muench, Stephen P., & Baker, A. (2016). Pi sensing and signalling: from prokaryotic to eukaryotic cells. *Biochemical Society Transactions, 44*(3), 766-773. doi:10.1042/BST20160026

Quisel, J. D., Wykoff, D. D., & Grossman, A. R. (1996). Biochemical characterization of the extracellular phosphatases produced by phosphorus-deprived *Chlamydomonas reinhardtii*. *Plant Physiology, 111*(3), 839. doi:10.1104/pp.111.3.839

Rao, N. N., Gómez-García, M. R., & Kornberg, A. (2009). Inorganic polyphosphate: Essential for growth and survival. *Annual Review of Biochemistry, 78*(1), 605-647. doi:10.1146/annurev.biochem.77.083007.093039

Rao, N. N., & Kornberg, A. (1996). Inorganic polyphosphate supports resistance and survival of stationary-phase *Escherichia coli*. *Journal of bacteriology, 178*(5), 1394-1400.

Rao, N. N., & Kornberg, A. (1999). Inorganic polyphosphate regulates responses of *Escherichia coli* to nutritional stringencies, environmental stresses and survival in the stationary phase. In H. C. Schröder & W. E. G. Müller (Eds.), *Inorganic polyphosphates: Biochemistry, biology, biotechnology* (pp. 183-195). Berlin, Heidelberg: Springer Berlin Heidelberg.

Rashid, M. H., Rumbaugh, K., Passador, L., Davies, D. G., Hamood, A. N., Iglewski, B. H., & Kornberg, A. (2000). Polyphosphate kinase is essential for biofilm development, quorum sensing, and virulence of *Pseudomonas aeruginosa*. *Proceedings of the National Academy of Sciences, 97*(17), 9636. doi:10.1073/pnas.170283397

Raven, J. A., & Geider, R. J. (1988). Temperature and algal growth. *New Phytologist, 110*(4), 441-461. doi:https://doi.org/10.1111/j.1469-8137.1988.tb00282.x

Ravensdown. (2022, 01/05/22). Fertiliser prices. Retrieved from https://www.ravensdown.co.nz/media/5846/price-list-may-01-2022.pdf

Reusch, R. N. (1999). Polyphosphate/poly-(R)-3-hydroxybutyrate) ion channels in cell membranes. In H. C. Schröder & W. E. G. Müller (Eds.), *Inorganic polyphosphates: Biochemistry, biology, biotechnology* (pp. 151-182): Springer.

Rhee, G. Y. (1972). Competition between an alga and an aquatic bacterium for phosphate. *Limnology and Oceanography, 17*(4), 505-514.

Rhee, G. Y. (1973). A continuous culture study of phosphate uptake, growth rate and polyphosphate in *Scenedesmus* sp. *Journal of Phycology, 9*(4), 495-506. doi:10.1111/j.1529-8817.1973.tb04126.x

Ried, M. K., Wild, R., Zhu, J., Pipercevic, J., Sturm, K., Broger, L., . . . Hothorn, M. (2021). Inositol pyrophosphates promote the interaction of SPX domains with the coiled-coil motif of PHR transcription factors to regulate plant phosphate homeostasis. *Nature Communications, 12*(1), 384. doi:10.1038/s41467-020-20681-4

Riekhof, W. R., Ruckle, M. E., Lydic, T. A., Sears, B. B., & Benning, C. (2003). The sulfolipids 2′ -*O*-acyl-sulfoquinovosyldiacylglycerol and sulfoquinovosyldiacylglycerol are absent from a *Chlamydomonas reinhardtii* mutant deleted in *SQD1 Plant Physiology, 133*(2), 864-874. doi:10.1104/pp.103.029249

Romans, K. M., Carpenter, E. J., & Bergman, B. (1994). Buoyancy regulation in the colonial diazotrophic cyanobacterium *Trichodesmium tenue*: Ultrastructure and storage of carbohydrate, polyphosphate, and nitrogen. *Journal of Phycology, 30*(6), 935-942. doi:10.1111/j.0022-3646.1994.00935.x

Ruiz, F. A., Lea, C. R., Oldfield, E., & Docampo, R. (2004). Human platelet dense granules contain polyphosphate and are similar to acidocalcisomes of bacteria and unicellular eukaryotes. *The Journal Of Biological Chemistry, 279*(43), 44250-44257. doi:10.1074/jbc.M406261200

Ruiz, F. A., Marchesini, N., Seufferheld, M., Govindjee, & Docampo, R. (2001). The polyphosphate bodies of *Chlamydomonas reinhardtii* possess a proton-pumping pyrophosphatase and are similar to acidocalcisomes. *The Journal Of Biological Chemistry, 276*(49), 46196-46203. doi:10.1074/jbc.M105268200

Ruiz, F. A., Rodrigues, C. O., & Docampo, R. (2001). Rapid changes in polyphosphate content within acidocalcisomes in response to cell growth, differentiation, and environmental stress *inTrypanosoma cruzi*. *The Journal Of Biological Chemistry, 276*(28), 26114-26121. doi:10.1074/jbc.M102402200

Salomé, P. A., & Merchant, S. S. (2019). A series of fortunate events: introducing *Chlamydomonas* as a reference organism. *The Plant Cell, 31*(8), 1682-1707. doi:10.1105/tpc.18.00952

Samadani, M., & Dewez, D. (2018a). Cadmium accumulation and toxicity affect the extracytoplasmic polyphosphate level in *Chlamydomonas reinhardtii*. *Ecotoxicology and Environmental Safety, 166*, 200-206. doi:https://doi.org/10.1016/j.ecoenv.2018.09.094

Samadani, M., & Dewez, D. (2018b). Effect of mercury on the polyphosphate level of alga *Chlamydomonas reinhardtii*. *Environmental Pollution, 240*, 506-513. doi:https://doi.org/10.1016/j.envpol.2018.04.141

Sanz-Luque, E., Bhaya, D., & Grossman, A. R. (2020). Polyphosphate: A multifunctional metabolite in cyanobacteria and algae. *Frontiers in Plant Science, 11*(938). doi:10.3389/fpls.2020.00938

Sanz-Luque, E., Saroussi, S., Huang, W., Akkawi, N., & Grossman, A. R. (2020). Metabolic control of acclimation to nutrient deprivation dependent on polyphosphate synthesis. *Science Advances, 6*(40), eabb5351. doi:10.1126/sciadv.abb5351

Schindler, D. W., & Vallentyne, J. R. (2008). *The algal bowl: overfertilization of the world's freshwaters and estuaries*: University of Alberta Press.

Schloss, J. A. (1990). A Chlamydomonas gene encodes a G protein β subunit-like polypeptide. *Molecular and General Genetics MGG, 221*(3), 443-452. doi:10.1007/BF00259410

Schmidt, J. J., Gagnon, G. A., & Jamieson, R. C. (2016). Microalgae growth and phosphorus uptake in wastewater under simulated cold region conditions. *Ecological Engineering, 95*, 588-593. doi:https://doi.org/10.1016/j.ecoleng.2016.06.114

Schmittgen, T. D., & Livak, K. J. (2008). Analyzing real-time PCR data by the comparative CT method. *Nature Protocols, 3*(6), 1101-1108. doi:10.1038/nprot.2008.73

Schroda, M., Hemme, D., & Mühlhaus, T. (2015). The *Chlamydomonas* heat stress response. *The Plant Journal, 82*(3), 466-480. doi:https://doi.org/10.1111/tpj.12816

Secco, D., Wang, C., Arpat, B. A., Wang, Z., Poirier, Y., Tyerman, S. D., . . . Whelan, J. (2012). The emerging importance of the SPX domain-containing proteins in phosphate homeostasis. *New Phytologist, 193*(4), 842-851. doi:10.1111/j.1469-8137.2011.04002.x

Sells, M. (2019). *Elevating phosphorus accumulation in waste stabilisation pond algae: A thesis presented in partial fulfilment of the requirements for the degree of Doctor of Philosophy in Environmental Engineering at Massey University, Palmerston North, New Zealand.* (Doctor of Philosophy). Massey University, Palmerston North, NZ.

Sells, M. D., Brown, N., & Shilton, A. N. (2018). Determining variables that influence the phosphorus content of waste stabilization pond algae. *Water Research, 132*, 301-308. doi:https://doi.org/10.1016/j.watres.2018.01.013

Serafim, L. s. S., Lemos, P. C., Levantesi, C., Tandoi, V., Santos, H., & Reis, M. A. M. (2002). Methods for detection and visualization of intracellular polymers stored by

polyphosphate-accumulating microorganisms. *Journal of Microbiological Methods, 51*(1), 1-18. doi:https://doi.org/10.1016/S0167-7012(02)00056-8

Serrano, A., Perez-Castiñeira, J. R., Baltscheffsky, H., & Baltscheffsky, M. (2004). Proton-pumping inorganic pyrophosphatases in some archaea and other extremophilic prokaryotes. *Journal of Bioenergetics and Biomembranes, 36*(1), 127-133. doi:10.1023/B:JOBB.0000019604.49875.b3

Sethuraman, A., Rao, N. N., & Kornberg, A. (2001). The endopolyphosphatase gene: Essential in *Saccharomyces cerevisiae*. *Proceedings of the National Academy of Sciences, 98*(15), 8542. doi:10.1073/pnas.151269398

Seufferheld, M., Lea, C. R., Vieira, M., Oldfield, E., & Docampo, R. (2004). The H^+-pyrophosphatase of *Rhodospirillum rubrum* is predominantly located in polyphosphate-rich acidocalcisomes. *The Journal Of Biological Chemistry, 279*(49), 51193-51202. doi:10.1074/jbc.M406099200

Seufferheld, M. J., & Curzi, M. J. (2010). Recent discoveries on the roles of polyphosphates in plants. *Plant Molecular Biology Reporter, 28*(4), 549-559. doi:10.1007/s11105-010-0187-z

Shilton, A. N., Powell, N., & Guieysse, B. (2012). Plant based phosphorus recovery from wastewater via algae and macrophytes. *Current Opinion in Biotechnology, 23*(6), 884-889. doi:https://doi.org/10.1016/j.copbio.2012.07.002

Shimogawara, K., Wykoff, D. D., Usuda, H., & Grossman, A. R. (1999). *Chlamydomonas reinhardtii* mutants abnormal in their responses to phosphorus deprivation. *Plant Physiology, 120*(3), 685-694.

Shirahama, K., Yazaki, Y., Sakano, K., Wada, Y., & Ohsumi, Y. (1996). Vacuolar function in the phosphate homeostasis of the yeast *Saccharomyces cerevisiae*. *Plant and Cell Physiology, 37*(8), 1090-1093. doi:10.1093/oxfordjournals.pcp.a029058 %J Plant and Cell Physiology

Sianoudis, J., Küsel, A. C., Mayer, A., Grimme, L. H., & Leibfritz, D. (1986). Distribution of polyphosphates in cell-compartments of *Chlorella fusca* as measured by 31P-NMR-spectroscopy. *Archives of Microbiology, 144*(1), 48-54. doi:10.1007/BF00454955

Siderius, M., Musgrave, A., van den Ende, H., Koerten, H., Cambier, P., & van der Meer, P. (1996). *Chlamydomonas eugametos* (Chlorophyta) stores phosphate in polyphosphate bodies together with calcium. *Journal of Phycology, 32*(3), 402-409. doi:10.1111/j.0022-3646.1996.00402.x

Sievers, F., Wilm, A., Dineen, D., Gibson, T. J., Karplus, K., Li, W., . . . Higgins, D. G. (2011). Fast, scalable generation of high-quality protein multiple sequence alignments using Clustal Omega. *Molecular systems biology, 7*, 539-539. doi:10.1038/msb.2011.75

Slocombe, S. P., Zúñiga-Burgos, T., Chu, L., Wood, N. J., Camargo-Valero, M. A., & Baker, A. (2020). Fixing the broken phosphorus cycle: wastewater remediation by microalgal polyphosphates. *Frontiers in Plant Science, 11*.

Smith, B. T., & Davis, R. H. (2012). Sedimentation of algae flocculated using naturally-available, magnesium-based flocculants. *Algal Research, 1*(1), 32-39. doi:https://doi.org/10.1016/j.algal.2011.12.002

Soeder, C., & Stengel, E. (1974). Physico-chemical factors affecting metabolism and growth rate. In W. D. P. Stewart (Ed.), *Algal physiology and biochemistry*. Oxford: Blackwell Scientific.

Solovchenko, A., Khozin-Goldberg, I., Selyakh, I., Semenova, L., Ismagulova, T., Lukyanov, A., . . . Gorelova, O. (2019). Phosphorus starvation and luxury uptake in green microalgae revisited. *Algal Research, 43*, 101651. doi:https://doi.org/10.1016/j.algal.2019.101651

Solovchenko, A., Verschoor, A. M., Jablonowski, N. D., & Nedbal, L. (2016). Phosphorus from wastewater to crops: An alternative path involving microalgae. *Biotechnology Advances, 34*(5), 550-564. doi:https://doi.org/10.1016/j.biotechadv.2016.01.002

Sommer, A. L., & Thomas, E. B. (1938). Meta- and pyrophosphate within the algal cell. *Plant Physiology, 13*(1), 199-205.

Sommer, U. (1996). Nutrient competition experiments with periphyton from the Baltic Sea. *Marine Ecology Progress Series, 140*, 161-167.

Stats NZ. (2021a, 15/04/21). Agricultural and horticultural land use. Retrieved from https://www.stats.govt.nz/indicators/agricultural-and-horticultural-land-use

Stats NZ. (2021b, 15/04/21). Fertilisers - nitrogen and phosphorus. Retrieved from https://www.stats.govt.nz/indicators/fertilisers-nitrogen-and-phosphorus

Stewart, W. M., & Roberts, T. L. (2012). Food security and the role of fertilizer in supporting it. *Procedia Engineering, 46*, 76-82. doi:https://doi.org/10.1016/j.proeng.2012.09.448

Streichan, M., Golecki, J. R., & Schön, G. (1990). Polyphosphate-accumulating bacteria from sewage plants with different proceses for biological phosphorus removal. *FEMS Microbiology Ecology, 6*(2), 113-124.

Susser, J. R., Pelini, S. L., & Weintraub, M. N. (2020). Can we reduce phosphorus runoff from agricultural fields by stimulating soil biota? *Journal of Environmental Quality, 49*(4), 933-944. doi:https://doi.org/10.1002/jeq2.20104

Talboys, P. J., Heppell, J., Roose, T., Healey, J. R., Jones, D. L., & Withers, P. J. A. (2016). Struvite: a slow-release fertiliser for sustainable phosphorus management? *Plant and Soil, 401*(1), 109-123. doi:10.1007/s11104-015-2747-3

Tchobanoglous, G., Burton, F. L., & Stensel, H. (1991). Wastewater engineering. *Management, 7*, 1-4.

Titman, D. (1976). Ecological competition between algae: Experimental confirmation of resource-based competition theory. *Science, 192*(4238), 463. doi:10.1126/science.192.4238.463

Torriani, A. (1960). Influence of inorganic phosphate in the formation of phosphatases by *Escherichia coli*. *Biochimica et Biophysica Acta, 38*, 460-469. doi:https://doi.org/10.1016/0006-3002(60)91281-6

Trott, O., & Olson, A. J. (2010). AutoDock Vina: improving the speed and accuracy of docking with a new scoring function, efficient optimization, and multithreading. *Journal of computational chemistry, 31*(2), 455-461.

Tsednee, M., Castruita, M., Salomé, P. A., Sharma, A., Lewis, B. E., Schmollinger, S. R., . . . Merchant, S. S. (2019). Manganese co-localizes with calcium and phosphorus in *Chlamydomonas* acidocalcisomes and is mobilized in manganese-deficient conditions. *J Biol Chem, 294*(46), 17626-17641. doi:10.1074/jbc.RA119.009130

Twiss, M. R., & Nalewajko, C. (1992). Influence of phosphorus nutrition on copper toxicity to three strains of *Scenedesmus acutus* (Chlorophyceae). *Journal of Phycology, 28*(3), 291-298. doi:10.1111/j.0022-3646.1992.00291.x

USGS. (2019). Phosphate rock statistics ad information. Retrieved from https://www.usgs.gov/centers/nmic/phosphate-rock-statistics-and-information

Van Mooy, B. A. S., Hmelo, L. R., Sofen, L. E., Campagna, S. R., May, A. L., Dyhrman, S. T., . . . Mincer, T. J. (2012). Quorum sensing control of phosphorus acquisition in *Trichodesmium consortia*. *The Isme Journal, 6*(2), 422-429. doi:10.1038/ismej.2011.115

Wang, L., Xiao, L., Yang, H., Chen, G., Zeng, H., Zhao, H., & Zhu, Y. (2020). Genome-wide identification, expression profiling, and evolution of phosphate transporter gene family in green algae. *Frontiers in Genetics, 11*(1170). doi:10.3389/fgene.2020.590947

Wang, X., Schröder, H. C., & Müller, W. E. (2018). Amorphous polyphosphate, a smart bioinspired nano-/bio-material for bone and cartilage regeneration: towards a new paradigm in tissue engineering. *Journal of Materials Chemistry B, 6*(16), 2385-2412.

Watanabe, M., Kohata, K., & Kimura, T. (1991). Diel vertical migration and nocturnal uptake of nutrients by *Chattonella antiqua* under stable stratification. *Limnology and Oceanography, 36*(3), 593-602.

Werner, T. P., Amrhein, N., & Freimoser, F. M. (2007). Inorganic polyphosphate occurs in the cell wall of *Chlamydomonas reinhardtii* and accumulates during cytokinesis. *BMC Plant Biology, 7*(1), 51. doi:10.1186/1471-2229-7-51

Whitehead, M. P., Hooley, P., & Brown, M. R. (2013). Horizontal transfer of bacterial polyphosphate kinases to eukaryotes: Implications for the ice age and land colonisation. *BMC research notes, 6*(1), 221.

Wiame, J. M. (1949). The occurrence and physiological behavior of two metaphosphate fractions in yeast. *The Journal Of Biological Chemistry, 178*(2), 919-929.

Widra, A. (1959). Metachromatic granules of microorganisms. *Journal of bacteriology, 78*(5), 664.

Wild, R., Gerasimaite, R., Jung, J.-Y., Truffault, V., Pavlovic, I., Schmidt, A., . . . Mayer, A. (2016). Control of eukaryotic phosphate homeostasis by inositol polyphosphate sensor domains. *Science, 352*(6288), 986. doi:10.1126/science.aad9858

Wu, Q., Guo, L., Li, X., & Wang, Y. (2021). Effect of phosphorus concentration and light/dark condition on phosphorus uptake and distribution with microalgae. *Bioresource Technology, 340,* 125745. doi:https://doi.org/10.1016/j.biortech.2021.125745

Wykoff, D. D., Grossman, A. R., Weeks, D. P., Usuda, H., & Shimogawara, K. (1999). Psr1, a nuclear localized protein that regulates phosphorus metabolism in *Chlamydomonas*. *Proceedings of the National Academy of Sciences, 96*(26), 15336. doi:10.1073/pnas.96.26.15336

Yehudai-Resheff, S., Zimmer, S. L., Komine, Y., & Stern, D. B. (2007). Integration of chloroplast nucleic acid metabolism into the phosphate deprivation response in *Chlamydomonas reinhardtii*. *The Plant Cell, 19*(3), 1023. doi:10.1105/tpc.106.045427

Yuan, Z., Pratt, S., & Batstone, D. J. (2012). Phosphorus recovery from wastewater through microbial processes. *Current Opinion in Biotechnology, 23*(6), 878-883. doi:https://doi.org/10.1016/j.copbio.2012.08.001

Zhou, D., Zhang, C., Fu, L., Xu, L., Cui, X., Li, Q., & Crittenden, J. C. (2017). Responses of the microalga *Chlorophyta* sp. to bacterial quorum sensing molecules (N-acylhomoserine lactones): Aromatic protein-induced self-aggregation. *Environmental Science & Technology, 51*(6), 3490-3498. doi:10.1021/acs.est.7b00355

Zhou, J., Lyu, Y., Richlen, M. L., Anderson, D. M., & Cai, Z. (2016). Quorum sensing is a language of chemical signals and plays an ecological role in algal-bacterial idnteractions. *Critical Reviews in Plant Sciences, 35*(2), 81-105. doi:10.1080/07352689.2016.1172461

Appendix A

A.1 Summary of parameters tested and analyses performed.

Table 34. Summary of environmental parameters tested and analyses performed within each chapter.

Parameters tested	Chapter			
	3	4	5	6
Species	●	●		
Light supply		●	●	
Temperature		●	●	
P repletion dose		●	●	●
P depletion time		●	●	●
pH		●		
Analyses performed				
P uptake	●	●	●	●
PolyP accumulation		●	●	●
Granule formation		●		●
Growth	●	●		●
Gene expression			●	●

Appendix B

B.1 0 supporting information

B.1.1 Factorial experimental design

Table 35. Full factorial experimental design (semi-randomized).

Light supply ($\mu mol \cdot m^{-2}s^{-1}$)	Temperature (°C)	P depletion time (days)	P repletion dose ($mg\ P \cdot L^{-1}$)	pH	Run # (*C. reinhardtii*)	Run # (*C. vulgaris*)
0	10	3	5	7.6	52	64
160	10	3	5	7.6	53	1
0	30	3	5	7.6	56	46
160	30	3	5	7.6	26	21
0	10	7	5	7.6	34	36
160	10	7	5	7.6	14	25
0	30	7	5	7.6	31	33
160	30	7	5	7.6	41	29
0	10	3	15	7.6	51	63
160	10	3	15	7.6	60	9
0	30	3	15	7.6	49	13
160	30	3	15	7.6	47	43
0	10	7	15	7.6	3	37
160	10	7	15	7.6	22	24
0	30	7	15	7.6	11	32
160	30	7	15	7.6	18	28
0	10	3	5	8.6	62	54
160	10	3	5	8.6	59	2
0	30	3	5	8.6	50	12
160	30	3	5	8.6	27	42
0	10	7	5	8.6	35	5
160	10	7	5	8.6	15	16
0	30	7	5	8.6	10	38
160	30	7	5	8.6	40	58
0	10	3	15	8.6	61	55
160	10	3	15	8.6	7	8
0	30	3	15	8.6	44	45
160	30	3	15	8.6	48	20
0	10	7	15	8.6	4	6
160	10	7	15	8.6	23	17
0	30	7	15	8.6	30	39
160	30	7	15	8.6	19	57

B.1.2 DW/OD correlations used for initial target OD

Ratios of dry biomass weight to optical density (DW/OD) were established by performing linear regressions on data collected during the Objective 1 experiments (Chapter 3) and trials. Measurements were performed as described in Section 3.3.2.3.

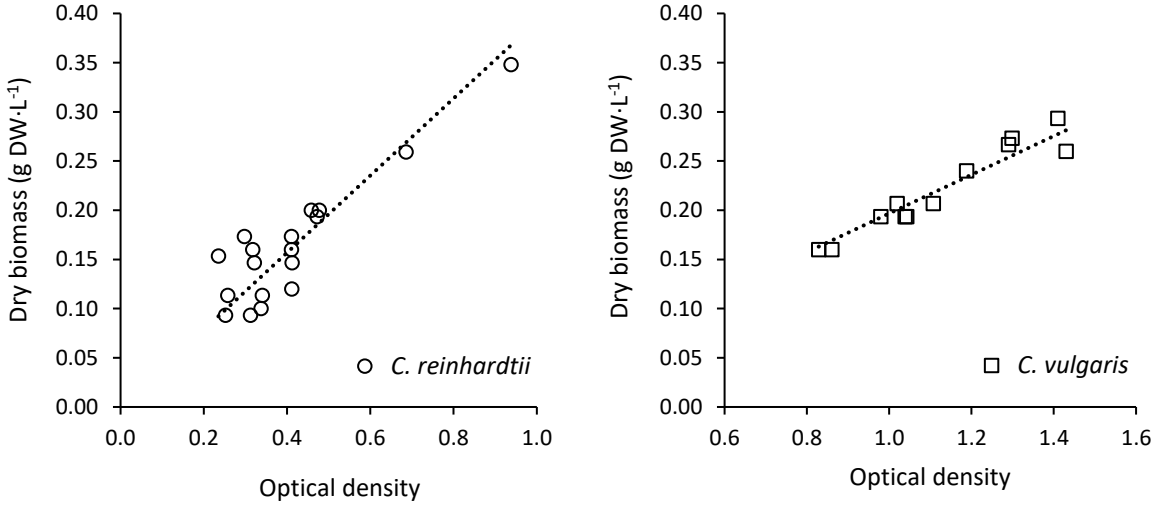

Figure 27. Dry weight vs optical density in *C. reinhardtii* (n = 18; R^2 = 0.39) (left) and *C. vulgaris* (n = 24; R^2 = 0.99) (right). Dotted lines show best fit.

DW/OD ratios:

C. reinhardtii: 0.39 g DW·L^{-1}

C. vulgaris: 0.20 g DW·L^{-1}

B.1.3 Tris buffer formulation

Data from SigmaAldrich Technical Bulletin No. 106B[31] provided the concentrations of tris base and tris-HCl required to prepare 0.05 M solutions of tris buffer for desired pH values at 25 °C. These data were plotted (Figure 28) and fitted with third degree polynomial equations.

The required concentrations (g·L^{-1}) of Tris-HCl and Tris base, for a given pH at 25 °C, are given by Equations B.1 (R^2 = 0.9999) and B.2 (R^2 = 0.9999), respectively.

$$[Tris\text{-}HCl] = 1.347pH^3 - 32.964pH^2 + 262.72pH - 683.7 \quad \text{(B.1)}$$

$$[Tris\ base] = -1.0542pH^3 + 25.722pH^2 - 205.7pH + 541.75 \quad \text{(B.2)}$$

[31] https://www.sigmaaldrich.com/deepweb/assets/sigmaaldrich/product/documents/301/225/106bbul.pdf

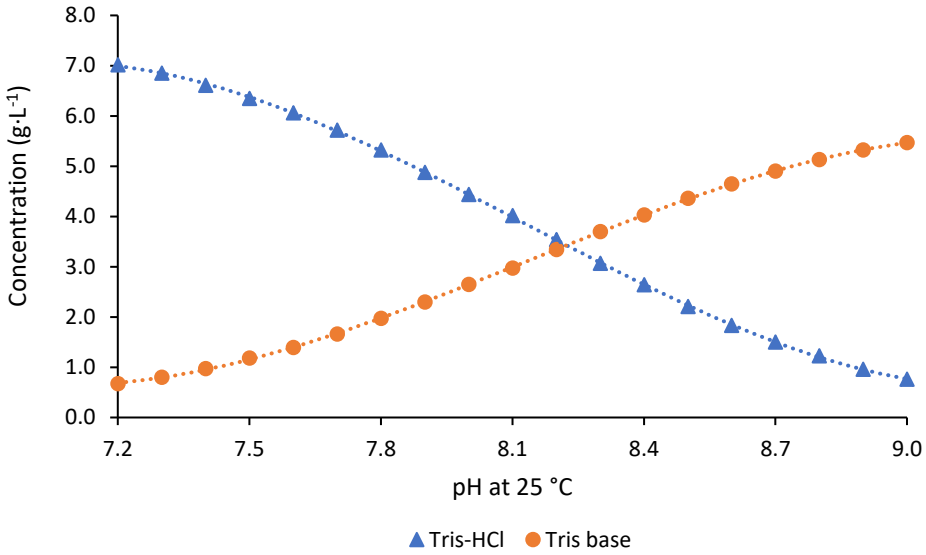

Figure 28. Concentrations of tris base and tris-HCl recommended to achieve the given pH in a 0.05 M buffer solution at 25 °C. Dotted lines indicate third degree polynomial fits.

Due to the temperature effects on pH described in the Technical Bulletin, a solution with a target pH of pH_T (at target temperature T °C) will have a pH value of pH_{25} (at 25 °C) according to Equation B.3.

$$pH_{25} = \begin{cases} pH_T - 0.03(25 - T) \text{ for } 5\ ^\circ C \leq T < 25\ ^\circ C \\ pH_T + 0.025(T - 25) \text{ for } 25\ ^\circ C < T \leq 37\ ^\circ C \end{cases} \quad \text{(B.3)}$$

The desired concentrations of the components were calculated using the above cubic equations and multiplied by a factor of 40 to produce 2 M stock solutions (Table 36).

Table 36. Concentrations of Tris-HCl and Tris base required to produce 2 M buffer stock solutions with the target pH at the given temperatures.

Target pH	**Concentration of Tris-HCl (g·L^{-1})**			**Concentration of Tris base (g·L^{-1})**		
	10 °C	20 °C	30 °C	10 °C	20 °C	30 °C
7.6	7.02	n/a	5.59	0.63	n/a	1.71
8.1	n/a	4.65	n/a	n/a	2.44	n/a
8.6	3.75	n/a	1.41	3.13	n/a	4.93

n/a: Not required by the factorial design.

B.1.4 Phosphate microplate assay standard curves

A standard curve was included on each plate (one per experiment). Standards were prepared in the same Tris buffer as used in the experiment.

For each pH level, the mean absorbances from all the standard curves were transformed by natural log and plotted against the log-transformed standard concentrations. Power laws were formulated to determine phosphate concentration from absorbance using the slope and intercept of a linear regression for each pH value (Equation A.4).

$$\ln[P_i] = m \cdot \ln A + c \tag{A.4}$$

Where $[P_i]$ is the concentration of phosphate in the medium A is the absorbance of light with a wavelength of 880 nm.

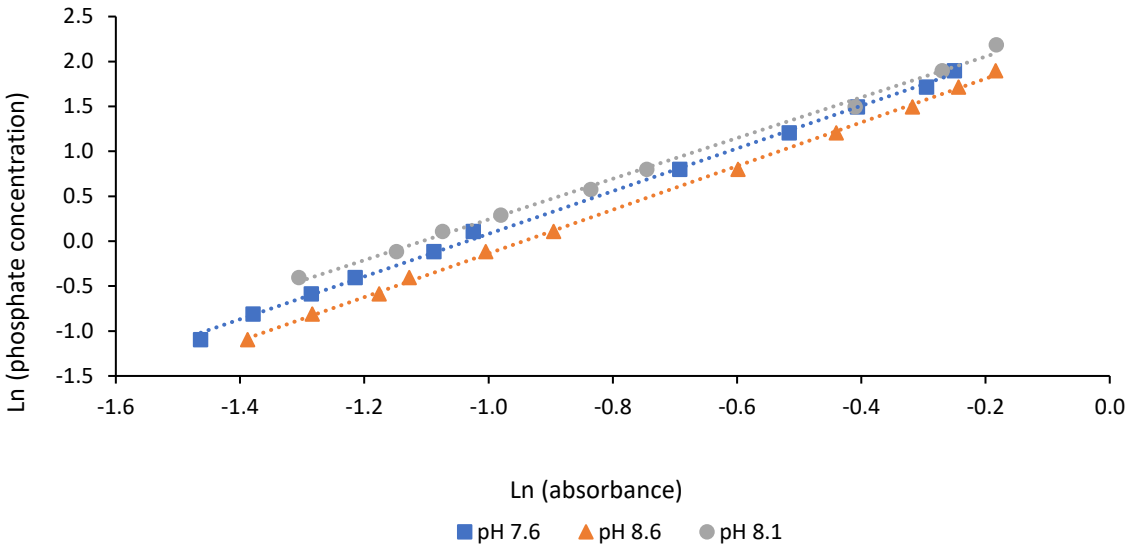

Figure 29. Log-log plot of phosphate standard concentrations vs measured absorbances using the microplate assay.

The phosphate concentration (mg·L^{-1}) can therefore be predicted from the absorbance measurements using Equation B.4:

$$[PO_4^{3-}] = \begin{cases} 11.68A^{2.38} & \text{for pH 7.6} \\ 12.27A^{2.51} & \text{for pH 8.1} \\ 9.92A^{2.43} & \text{for pH 8.6} \end{cases} \tag{B.4}$$

A proportional estimate of uncertainty for phosphate measurements was determined based on data from standard curves performed at pH 8.1 (n = 14).

The uncertainty in the absorbance measurements was determined (for each standard concentration) using 95% confidence $\left(U_A = \pm\frac{2.16\sigma_A}{\sqrt{14}}\right)$.

Since the standard curve data were fit to a power law curve ($P = e^c \cdot A^m$, where P is the estimated phosphate concentration in mg·L^{-1} and A is the absorbance measurement), the absolute uncertainty of P, $U_P = e^c \cdot m \cdot \bar{A}^{m-1} \cdot U_A$

Therefore, the fractional uncertainty of P, $F_P = m \cdot \frac{U_A}{\bar{A}}$

This ranged between 7 – 15%, except at $P = 0$ (32%).

For changes in phosphate concentration, $\Delta P = P_a - P_b$, the fractional uncertainty $F_{\Delta P} = \sqrt{F_a^2 + F_b^2}$.

In the worst case ($F_P = 15\%$), this is approximately ± 21%

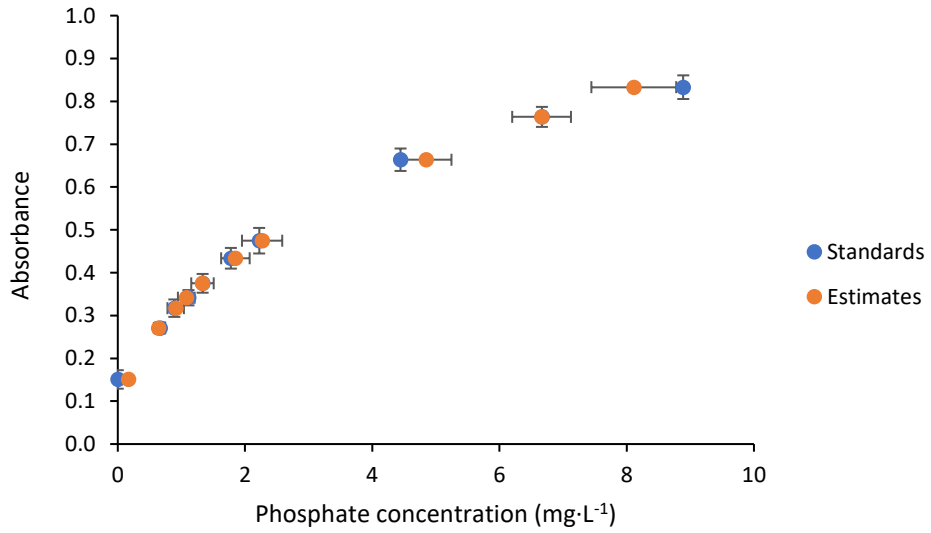

Figure 30. Absorbances at 880 nm from standard curves used in measurements of phosphate in centre point experiments (n = 12) and corresponding phosphate concentrations estimated from the measured absorbances using a power law fit. Vertical error bars indicate 95% confidence limits for absorbance and horizontal error bars indicate the calculated uncertainties of the estimated concentrations.

B.1.5 Validation of DAPI microplate assay for in situ determination of polyP

Four E-flasks containing 100 mL low-P minimal medium were inoculated with 20 mL each of *C. reinhardtii* CC-1690 and grown as in Section 3.3.2 for 7 days.

After taking samples for P_{tot}, P_{ext}, DW, and lead-sulfide staining, phosphate was added to final concentrations of 5, 10, and 20 mg P·L^{-1} (with one flask kept as no-P control).

Samples were again taken further measurements, as above, after 24 h, and additional samples stored at -180 °C to determine polyP content through DAPI fluorescence (see 4.3.5).

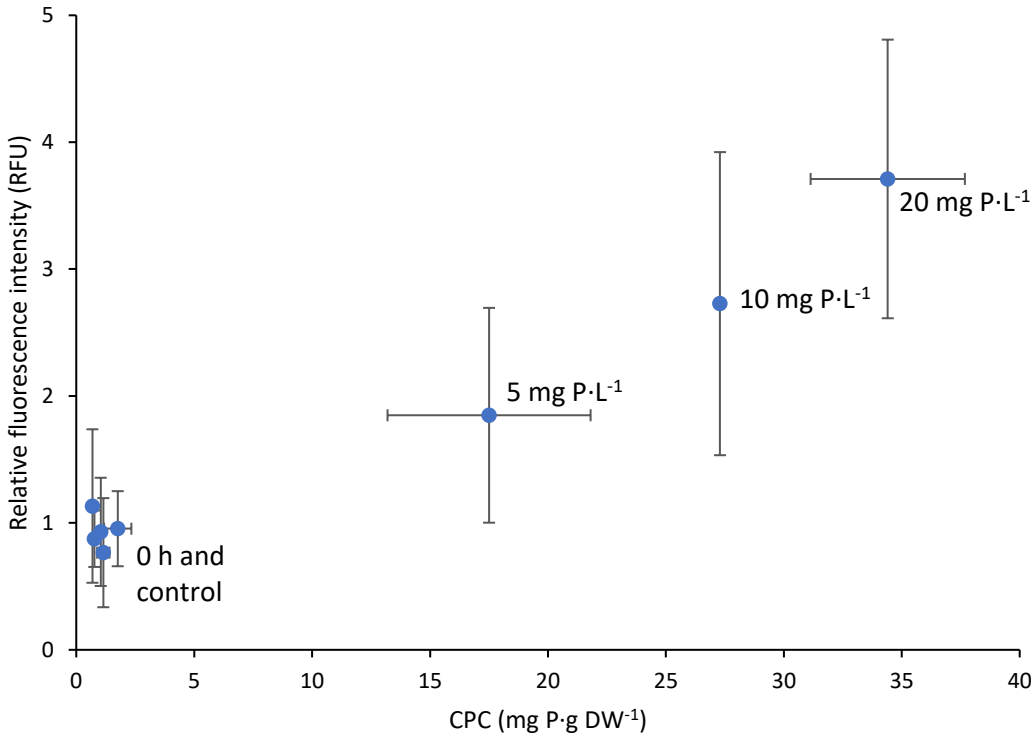

Figure 31. Comparison of fluorescence measurements and estimated cellular phosphorus content (CPC) of *C. reinhardtii* cultures 24 hours after addition of phosphate doses from 0 – 20 mg P·L^{-1}.

B.1.6 Factorial experiment data summary

See B.1.1 for experimental conditions (by run number).

Table 37. Collated data for *C. reinhardtii* experiments (Treatment cultures).

Run	Mean optical density			Mean pH change	Granule abundance (rank)			Extracellular phosphate-P (mg $P \cdot L^{-1}$)			PolyP (normalized fluorescence intensity)		
	0 h	6 h	24 h		0 h	6 h	24 h	0 h	6 h	24 h	0 h	6 h	24 h
3	0.73	0.90	0.91	-0.04	0	4	4	0.03	2.17	0.14	0.21	0.94	1.01
4	0.73	0.94	0.91	-0.10	0	4	3	0.03	0.32	0.19	0.34	1.38	1.70
7	0.87	1.04	1.69	0.70	0	5	4	0.04	0.39	0.56	0.15	0.76	0.73
10	0.81	1.24	1.25	0.07	0	2	4	0.05	0.09	0.07	0.12	0.49	0.58
11	0.81	1.38	1.35	-0.08	0	5	2	0.05	0.18	0.12	0.12	0.90	1.11
14	0.71	1.16	1.20	0.30	0	3	1	0.06	0.32	0.47	0.28	0.47	0.86
15	0.71	1.17	1.11	0.41	0	3	1	0.06	0.15	0.17	0.28	0.63	1.37
18	0.73	1.34	1.85	0.25	0	5	4	0.04	0.05	0.05	0.13	0.59	0.84
19	0.73	1.49	2.13	0.87	0	5	2	0.04	0.14	0.16	0.13	0.78	1.24
22	0.81	0.96	1.18	-0.05	0	5	3	0.04	0.12	0.14	0.37	1.97	2.71
23	0.81	0.95	1.32	0.44	0	3	4	0.04	0.71	0.16	0.36	2.83	2.92
26	0.78	1.53	1.61	-0.06	NA	4	2	0.04	0.05	0.08	0.25	0.62	0.96
27	0.78	1.70	1.77	0.71	NA	3	2	0.04	0.07	0.08	0.34	1.46	1.91
30	0.80	1.02	1.11	-0.12	0	4	4	0.04	0.08	0.09	0.52	1.92	2.58
31	0.80	1.05	1.21	0.09	0	3	3	0.04	0.12	0.12	0.31	0.53	0.71
34	0.79	0.79	0.76	0.15	0	3	2	0.04	0.06	0.07	0.53	0.80	0.89
35	0.79	0.72	0.80	0.01	0	2	4	0.04	0.07	0.07	0.62	0.98	1.33
40	0.77	1.36	1.62	0.53	0	2	4	0.04	0.09	0.11	0.50	1.05	1.10
41	0.77	1.36	2.01	0.20	0	3	4	0.04	0.09	0.10	0.46	1.02	1.12
44	0.84	0.99	1.15	0.03	0	2	4	0.03	1.92	1.60	0.69	1.97	1.73
47	0.76	1.36	2.22	0.13	0	5	5	0.03	0.21	0.26	0.44	1.25	1.56
48	0.76	1.42	2.68	0.72	0	5	3	0.03	0.27	0.12	0.35	0.89	1.16
49	0.78	1.24	1.35	-0.14	0	4	3	0.03	6.63	5.58	0.49	1.17	1.09
50	0.78	1.37	1.28	0.13	0	3	4	0.03	0.04	0.08	0.45	1.14	1.42
51	0.77	0.95	0.78	0.03	0	4	5	0.03	6.79	0.03	0.32	1.49	1.36
52	0.77	0.83	0.85	0.04	0	4	4	0.03	0.04	0.04	0.31	0.47	0.51
53	0.77	1.07	1.17	0.37	0	5	3	0.03	0.19	0.37	0.28	0.49	0.66
56	0.81	1.33	1.20	-0.01	0	3	4	0.07	0.03	0.04	0.54	0.76	0.86
59	0.81	0.96	1.39	0.33	0	4	3	0.03	0.27	0.22	0.44	0.71	1.10
60	0.81	0.88	1.48	0.32	0	5	4	0.03	4.37	0.25	0.45	1.07	1.20
61	0.73	0.77	0.77	-0.18	1	3	3	0.06	12.01	7.43	0.38	0.70	0.99
62	0.73	0.71	0.69	-0.10	1	3	4	0.06	0.71	0.37	0.41	0.66	0.74

NA: data not available.

Table 38. Collated data for C. reinhardtii experiments (Control cultures).

Run	Mean optical density			Mean pH change	Granule abundance (rank)			Extracellular phosphate-P (mg $P \cdot L^{-1}$)			PolyP (normalized fluorescence intensity)		
	0 h	6 h	24 h		0 h	6 h	24 h	0 h	6 h	24 h	0 h	6 h	24 h
3	0.73	0.89	0.90	-0.20	0	0	0	0.03	0.13	0.16	0.21	0.31	0.33
4	0.73	0.89	0.91	-0.03	0	0	0	0.03	0.15	0.18	0.34	0.33	0.35
7	0.87	1.18	1.45	-0.02	0	0	0	0.04	0.38	0.45	0.15	0.16	0.18
10	0.81	1.07	1.21	-0.10	0	0	0	0.05	0.11	0.08	0.12	0.28	0.32
11	0.81	1.20	1.31	-0.07	0	0	0	0.05	0.17	0.13	0.12	0.18	0.19
14	0.71	1.10	0.99	0.14	0	0	0	0.06	0.29	0.31	0.28	0.25	0.26
15	0.71	1.15	1.00	0.09	0	0	0	0.06	0.14	0.17	0.28	0.36	0.44
18	0.73	1.25	1.89	0.02	0	0	0	0.04	0.04	0.04	0.13	0.18	0.22
19	0.73	1.29	1.97	0.23	0	0	0	0.04	0.14	0.17	0.13	0.18	0.24
22	0.81	0.94	1.10	-0.33	0	0	0	0.04	0.11	0.09	0.37	0.56	0.54
23	0.81	0.95	1.07	-0.03	0	0	0	0.04	0.12	0.13	0.36	0.49	0.55
26	0.78	1.51	1.46	0.28	NA	0	0	0.04	0.06	0.10	0.25	0.31	0.41
27	0.78	1.70	1.54	0.25	NA	0	0	0.04	0.06	0.08	0.34	0.64	0.81
30	0.80	1.14	1.12	-0.24	0	0	0	0.04	0.06	0.10	0.52	0.52	0.62
31	0.80	1.20	1.16	0.09	0	0	0	0.04	0.08	0.12	0.31	0.34	0.44
34	0.79	0.74	0.73	0.07	0	0	0	0.04	0.07	0.06	0.53	0.44	0.45
35	0.79	0.80	0.97	-0.02	0	0	0	0.04	0.06	0.08	0.62	0.56	0.72
40	0.77	1.47	1.50	0.23	0	0	0	0.04	0.07	0.07	0.50	0.53	0.51
41	0.77	1.38	1.39	0.04	0	0	0	0.04	0.09	0.08	0.46	0.45	0.57
44	0.84	0.98	1.13	-0.81	0	0	0	0.03	0.13	0.14	0.69	0.69	0.67
47	0.76	1.23	2.27	0.09	0	0	0	0.03	0.25	0.19	0.44	0.40	0.42
48	0.76	1.27	2.60	0.34	0	0	0	0.03	0.28	0.17	0.35	0.38	0.40
49	0.78	1.30	1.28	-0.25	0	0	0	0.03	0.04	0.08	0.49	0.46	0.52
50	0.78	1.35	1.17	0.09	0	0	0	0.03	0.05	0.06	0.45	0.51	0.57
51	0.77	1.47	0.84	-0.05	0	0	0	0.03	0.02	0.03	0.32	0.29	0.31
52	0.77	1.22	0.87	-0.06	0	0	0	0.03	0.03	0.04	0.31	0.29	0.33
53	0.77	1.05	0.88	0.14	0	0	0	0.03	0.23	0.18	0.28	0.30	0.38
56	0.81	1.22	1.12	-0.06	0	0	0	0.07	0.03	0.04	0.54	0.50	0.51
59	0.81	0.91	1.33	0.14	0	0	0	0.03	0.04	0.04	0.44	0.44	0.51
60	0.81	0.95	1.12	0.07	0	0	0	0.03	0.03	0.04	0.45	0.41	0.51
61	0.73	0.81	0.83	-0.34	1	0	0	0.06	0.04	0.05	0.38	0.41	0.43
62	0.73	0.69	0.74	-0.04	1	0	0	0.06	0.02	0.03	0.41	0.42	0.45

NA: data not available.

Table 39. Collated data for *C. vulgaris* experiments (Treatment cultures).

Run	Mean optical density			Mean pH change	Granule abundance (rank)			Extracellular phosphate-P (mg P·L^{-1})			PolyP (normalized fluorescence intensity)		
	0 h	6 h	24 h		0 h	6 h	24 h	0 h	6 h	24 h	0 h	6 h	24 h
1	1.57	1.58	1.61	-0.17	0	3	3	0.03	2.15	2.14	1.54	2.92	3.20
2	1.57	1.62	1.77	-0.20	0	4	3	0.03	2.15	2.16	2.44	2.94	3.19
5	1.56	1.51	1.42	-0.06	0	0	1	0.04	0.32	0.18	0.97	2.51	2.64
6	1.56	1.49	1.36	-0.03	0	2	1	0.04	9.43	8.08	2.23	2.66	3.07
8	1.49	1.60	1.78	0.41	0	5	5	0.04	12.05	1.55	0.42	1.35	1.69
9	1.49	1.56	1.94	0.51	0	5	4	0.04	8.99	1.76	0.42	1.39	2.12
12	1.38	1.87	1.98	-0.18	0	2	2	0.06	2.92	3.07	0.54	0.95	1.03
13	1.38	1.84	1.87	-0.11	0	1	1	0.06	16.43	15.05	0.54	1.04	1.31
16	1.60	1.55	1.65	0.19	0	5	0	0.08	0.16	0.17	0.84	2.07	2.20
17	1.60	1.57	1.57	0.09	0	1	3	0.08	10.17	1.38	0.84	1.77	2.43
20	1.50	2.48	2.34	0.29	0	3	4	0.04	13.54	1.56	0.59	1.68	2.27
21	1.50	2.46	2.46	0.10	0	4	4	0.04	0.26	0.19	0.59	1.69	1.73
24	1.49	1.48	1.45	0.26	0	4	3	0.04	10.25	1.64	1.28	3.92	5.22
25	1.49	1.53	1.35	0.17	0	2	3	0.04	0.16	0.22	1.17	3.04	2.70
28	1.51	2.09	2.17	0.00	NA	3	5	0.04	8.96	5.24	1.73	2.09	2.74
29	1.51	2.25	2.12	0.01	NA	4	0	0.04	0.09	0.11	0.13	0.80	0.89
32	1.45	1.69	1.52	0.03	0	2	2	0.04	15.71	15.94	2.43	2.56	2.79
33	1.45	1.60	1.56	0.01	0	2	3	0.04	2.80	1.24	1.64	2.43	2.59
36	1.46	1.27	1.70	0.18	0	3	2	0.04	1.33	1.01	2.02	2.27	2.51
37	1.46	1.24	1.40	0.19	0	1	1	0.04	10.54	9.90	2.58	3.41	3.74
38	1.51	1.83	1.82	-0.06	0	2	2	0.04	1.55	0.26	0.80	0.98	1.09
39	1.51	1.74	1.81	-0.04	0	1	2	0.04	12.77	12.50	2.58	3.34	3.85
42	1.43	2.10	2.37	0.19	0	2	4	0.04	0.09	0.09	2.19	2.42	2.60
43	1.43	2.08	2.56	0.18	0	3	5	0.04	11.01	2.00	1.98	3.41	4.36
45	1.46	1.56	1.68	-0.04	0	2	2	0.04	14.24	11.87	1.38	1.37	1.92
46	1.46	1.56	1.75	0.00	0	1	1	0.04	3.78	0.80	1.67	1.82	2.41
54	1.52	1.44	1.27	-0.02	0	1	1	0.05	1.61	1.48	1.13	1.37	1.46
55	1.52	1.65	1.35	-0.04	0	3	4	0.05	11.58	12.63	0.97	1.27	1.23
57	1.53	2.07	1.80	0.02	0	4	3	0.05	9.42	5.22	1.81	2.86	3.74
58	1.53	2.12	1.71	-0.10	0	3	0	0.05	0.05	0.07	1.55	2.49	2.82
63	1.38	1.25	1.45	0.19	0	3	3	0.06	17.21	17.10	1.38	1.23	1.27
64	1.38	1.40	1.53	0.21	0	2	4	0.06	3.71	3.47	1.37	1.36	1.45

NA: data not available.

Table 40. Collated data for C. vulgaris experiments (Control cultures).

Run	Mean optical density			Mean pH change	Granule abundance (rank)			Extracellular phosphate-P (mg $P \cdot L^{-1}$)			PolyP (normalized fluorescence intensity)		
	0 h	6 h	24 h		0 h	6 h	24 h	0 h	6 h	24 h	0 h	6 h	24 h
1	1.57	1.55	1.64	-0.06	0	0	0	0.03	0.04	0.04	1.54	2.53	2.78
2	1.57	1.61	1.75	-0.10	0	0	0	0.03	0.08	0.06	2.44	2.76	3.02
5	1.56	1.46	1.38	-0.03	0	0	0	0.04	0.14	0.19	0.97	1.70	2.00
6	1.56	1.46	1.39	-0.02	0	NA	0	0.04	0.25	0.26	2.23	1.95	2.38
8	1.49	1.60	1.77	0.27	0	0	0	0.04	0.33	0.38	0.42	0.96	1.07
9	1.49	1.57	1.84	0.42	0	0	0	0.04	0.29	0.36	0.42	0.81	0.96
12	1.38	1.87	1.96	-0.15	0	0	0	0.06	0.14	0.11	0.54	0.87	0.99
13	1.38	1.74	1.90	-0.12	0	0	0	0.06	0.33	0.49	0.54	0.99	1.13
16	1.60	1.46	1.44	-0.03	0	0	0	0.08	0.18	0.18	0.84	1.63	1.70
17	1.60	1.44	1.37	-0.08	0	0	0	0.08	0.41	0.20	0.84	1.32	1.39
20	1.50	2.24	2.15	-0.02	0	0	0	0.04	0.21	0.21	0.59	1.24	1.24
21	1.50	2.18	2.14	0.01	0	0	0	0.04	0.22	0.23	0.59	1.25	1.30
24	1.49	1.63	1.47	0.07	0	0	0	0.04	0.18	0.21	1.28	2.13	2.29
25	1.49	1.51	1.36	-0.03	0	0	0	0.04	0.18	0.19	1.17	2.12	2.23
28	1.51	2.17	2.08	-0.08	NA	0	0	0.04	0.07	0.07	1.73	1.52	1.58
29	1.51	2.02	1.87	-0.14	NA	0	0	0.04	0.08	0.10	0.13	0.44	0.45
32	1.45	1.69	1.79	-0.02	0	0	0	0.04	0.12	0.15	2.43	1.99	2.43
33	1.45	1.84	1.57	0.05	0	0	0	0.04	0.10	0.07	1.64	1.84	2.02
36	1.46	1.31	1.64	0.12	0	0	0	0.04	0.07	0.08	2.02	1.89	2.12
37	1.46	1.28	1.45	0.13	0	0	0	0.04	0.10	0.07	2.58	2.58	2.78
38	1.51	1.87	1.80	-0.12	0	0	0	0.04	0.16	0.17	0.80	0.83	0.82
39	1.51	1.77	1.78	-0.09	0	0	0	0.04	0.41	0.50	2.58	2.33	2.67
42	1.43	2.08	1.79	0.01	0	0	0	0.04	0.07	0.08	2.19	2.03	2.06
43	1.43	1.96	2.12	-0.04	0	0	0	0.04	0.10	0.12	1.98	1.79	1.61
45	1.46	1.59	1.60	-0.06	0	0	0	0.04	0.15	0.14	1.38	1.30	1.45
46	1.46	1.58	1.65	0.03	0	1	0	0.04	0.16	0.20	1.67	1.66	1.77
54	1.52	1.52	1.24	-0.07	0	0	0	0.05	0.21	0.25	1.13	1.27	1.22
55	1.52	1.18	1.33	-0.11	0	0	0	0.05	0.31	0.23	0.97	0.93	1.05
57	1.53	2.08	0.97	-0.18	0	0	0	0.05	0.04	0.03	1.81	1.99	1.98
58	1.53	2.00	0.88	-0.18	0	0	0	0.05	0.05	0.04	1.55	1.84	1.87
63	1.38	1.27	1.41	0.18	0	0	0	0.06	0.03	0.03	1.38	1.22	1.23
64	1.38	1.47	1.63	0.16	0	0	0	0.06	0.04	0.05	1.37	1.32	1.35

NA: data not available.

Table 41. Raw data (means of biological triplicates, except for granule abundance) for *C. reinhardtii* centre points.

Run	Optical density					Extracellular P (mg PO_4^{3-}-P·L^{-1})					PolyP (normalized fluorescence)					Granule abundance (rank)					pH	
	0	T_6	C_6	T_{24}	C_{24}	0	T_6	C_6	T_{24}	C_{24}	0	T_6	C_6	T_{24}	C_{24}	0	T_6	C_6	T_{24}	C_{24}	T_{24}	C_{24}
	0.80	0.88	0.83	1.65	0.97		0.1	n/a	n/a	n/a		0.73	0.19	0.86	0.27						8.58	8.36
1	0.90	0.81	0.85	1.65	1.09	n/a	0.1	0.0	n/a	n/a	0.00	0.69	0.19	0.96	0.22	0	3	0	3	0	8.64	8.41
	0.77	0.86	0.91	1.65	1.02		0.0	0.0	n/a	n/a		0.65	0.18	0.74	0.24						8.63	8.42
	0.82	0.99	1.11	1.45	1.23		0.0	0.0	0.0	0.0		0.40	0.19	0.49	0.21						8.56	8.33
2	0.82	0.95	1.20	1.36	1.14	0.1	0.0	0.0	0.0	0.0	0.21	0.44	0.19	0.56	0.23	0	2	0	2	0	8.60	8.25
	0.82	1.11	1.03	1.56	1.14		0.0	0.0	0.0	0.0		0.50	0.19	0.48	0.20						8.42	8.18
	0.82	1.19	1.27	1.33	1.39		0.2	0.2	0.1	0.2		0.34	0.18	0.47	0.22						8.60	8.14
3	0.82	1.11	0.95	1.34	1.24	0.0	0.1	0.1	0.1	0.2	0.22	0.44	0.15	0.52	0.22	0	4	0	4	0	8.64	8.08
	0.82	0.98	1.19	1.41	1.15		0.1	0.2	0.1	0.2		0.40	0.17	0.52	0.23						8.62	8.00
	0.78	0.73	0.71	1.39	0.98		0.0	0.0	0.0	0.0		0.75	0.35	0.94	0.40						8.61	8.35
4	0.79	0.79	0.73	1.46	1.16	0.1	0.1	0.0	0.0	0.1	0.36	0.79	0.36	0.97	0.44	0	5	0	4	0	8.61	8.40
	0.80	0.85	0.87	1.71	1.07		0.0	0.0	0.0	0.0		0.80	0.35	1.00	0.43						8.72	8.39
	0.82	0.86	0.90	1.45	1.00		1.0	0.0	1.1	0.0		0.74	0.35	0.94	0.40							
5	0.81	0.83	0.77	1.35	1.23	0.1	0.9	0.0	1.3	0.1	0.35	0.87	0.32	0.87	0.40	0	4	0	3	0	n/a	n/a
	0.81	0.79	0.79	1.66	1.00		1.2	0.0	1.2	0.1		0.85	0.33	0.89	0.45							

0: 0 hours (prior to P repletion)
T_6, T_{24}: Treatment (+P) cultures at 6, 24 hours
C_6, C_{24}: Control (-P) cultures at 6, 24 hours
n/a: Data not available

Table 42. Raw data (means of biological triplicates, except for granule abundance) for *C. vulgaris* centre points.

Run	Optical density					Extracellular P (mg PO_4^{3-}-P·L^{-1})					PolyP (normalized fluorescence)					Granule abundance (rank)					pH	
	0	T_6	C_6	T_{24}	C_{24}	0	T_6	C_6	T_{24}	C_{24}	0	T_6	C_6	T_{24}	C_{24}	0	T_6	C_6	T_{24}	C_{24}	T_{24}	C_{24}
	0.69	0.97	1.10	1.35	0.93		n/a	n/a	0.0	0.0		1.63	1.00	1.65	1.30						8.47	8.23
1	0.69	0.98	1.23	1.11	0.94	n/a	0.1	0.0	0.0	0.0	0.94	1.50	0.96	1.46	1.29	0	5	0	2	0	8.50	8.28
	0.71	1.04	1.12	1.12	0.86		0.0	0.0	0.0	0.0		1.58	1.05	1.55	1.29						8.52	8.27
	0.75	0.78	0.78	0.94	0.79		1.5	0.0	0.0	0.0		2.34	1.12	1.97	1.67						8.56	8.29
2	0.77	0.77	0.76	0.95	0.78	0.0	1.3	0.0	0.0	0.0	1.57	2.27	1.27	1.92	1.50	0	3	0	3	0	8.54	8.28
	0.77	0.79	0.72	1.02	0.77		1.3	0.0	0.0	0.0		2.57	1.26	1.94	1.50						8.49	8.32
	0.76	0.74	0.81	1.02	1.00		2.5	0.1	1.6	0.2		1.51	1.38	1.77	1.58						8.51	8.36
3	0.76	0.71	0.71	0.90	0.89	0.0	2.4	0.1	2.0	0.2	1.61	1.48	1.24	1.65	1.42	0	4	0	4	0	8.47	8.30
	0.75	0.72	0.73	1.17	0.99		2.3	0.1	0.2	0.2		1.53	1.26	1.97	1.31						8.53	8.26
	0.75	0.76	0.77	0.89	0.89		4.9	0.0	0.0	0.0		1.54	1.15	1.70	1.25							8.27
4	0.75	0.77	0.79	1.01	0.92	0.1	4.7	0.0	0.1	0.0	1.11	1.49	1.12	1.66	1.21	0	5	0	2	0	n/a	8.24
	0.75	0.77	0.94	1.10	0.91		5.2	0.0	0.1	0.1		1.53	1.17	1.77	1.30							8.25
	0.73	0.84	0.84	1.39	1.13		4.2	0.1	1.3	0.1		1.82	1.27	1.77	1.45							
5	0.73	0.88	0.86	1.36	1.13	0.0	3.6	0.0	1.2	0.1	1.18	1.79	1.30	1.71	1.49	0	4	0	3	0	n/a	n/a
	0.73	0.91	0.88	1.43	1.16		3.4	0.1	1.2	0.1		1.82	1.33	1.75	1.60							

0: 0 hours (prior to P repletion)
T_6, T_{24}: Treatment (+P) cultures at 6, 24 hours
C_6, C_{24}: Control (-P) cultures at 6, 24 hours
n/a: Data not available

B.1.7 Calculation of uncertainties

Uncertainties for growth and polyP measurements were calculated using the standard errors of centre point measurements and the appropriate *t*-statistic ($\alpha = 0.05$, n-1 degrees of freedom).

Uncertainties for P uptake measurements were calculated as described in Appendix B.1.4.

B.1.8 Effects Matrices

Statistically significant effects ($\alpha = 0.05$) in bold. Positive effects highlighted in green; negative effects in red; intensity of colour indicates relative strength of effect. The main effects for each factor are shown as values on the diagonal of each table. A positive main effect indicates that setting the factor to its high level was associated with an *increase* in the response variable. A negative main effect indicates that setting the factor to its low level was associated with a *decrease* in the response variable. The remaining values in the tables indicate two-way interaction effects between factors. Statistically significant effects ($p < 0.05$) are shown in bold type).

Abbreviations:

PHOS = P repletion dose

LIGHT = light supply

TEMP = temperature

TIME = P depletion time

PH = pH

Colour scale for strength of effects:

Growth (change in optical density) (Light only)

Table 43. Effects matrices for growth in *C. reinhardtii* (in light only) from 0-6 h (left) and 6-24 h (right).

0-6 hours

	PHOS	TEMP	TIME	PH
PHOS	-0.134			
TEMP	0.070	**0.448**		
TIME	0.025	-0.113	0.021	
PH	0.035	0.052	-0.004	0.039

6-24 hours

	PHOS	TEMP	TIME	PH
PHOS	**0.445**			
TEMP	0.113	0.250		
TIME	-0.234	0.123	-0.181	
PH	0.113	-0.360	-0.125	0.072

Table 44. Effects matrices for growth in *C. vulgaris* (in light only) from 0-6 h (left) and 6-24 h (right).

0-6 hours

	PHOS	TEMP	TIME	PH
PHOS	-0.008			
TEMP	-0.062	**0.683**		
TIME	-0.037	-0.077	-0.120	
PH	0.112	-0.027	-0.035	-0.009

6-24 hours

	PHOS	TEMP	TIME	PH
PHOS	0.107			
TEMP	0.004	-0.093		
TIME	-0.007	-0.062	**-0.275**	
PH	-0.192	-0.152	0.012	-0.094

Table 45. Effects matrices for phosphate uptake (mg P·L^{-1}) in *C. reinhardtii* from 0-6 h (left) and 6-24 h (right).

0-6 h

	PHOS	LIGHT	TIME	TEMP	PH
PHOS	**7.867**				
LIGHT	**1.496**	**1.482**			
TIME	**1.776**	**-1.300**	**1.831**		
TEMP	1.009	-0.475	-0.776	1.161	
PH	0.332	0.157	-0.077	0.320	0.258

6-24 h

	PHOS	LIGHT	TIME	TEMP	PH
PHOS	**1.222**				
LIGHT	-0.605	**-0.688**			
TIME	**-0.859**	0.451	**-0.897**		
TEMP	**-1.021**	0.516	**0.725**	**-1.037**	
PH	-0.570	0.088	0.324	0.405	-0.480

Table 46. Effects matrices for phosphate uptake (mg P·L^{-1}) in *C. vulgaris* from 0-6 h (left) and 6-24 h (right).

0-6 h

	PHOS	LIGHT	TIME	TEMP	PH
PHOS	-0.431				
LIGHT	0.525	**1.892**			
TIME	0.419	-0.068	**1.452**		
TEMP	**-0.872**	**0.956**	-0.421	-0.627	
PH	-0.357	**-1.279**	0.102	-0.022	0.571

6-24 h

	PHOS	LIGHT	TIME	TEMP	PH
PHOS	**3.953**				
LIGHT	**4.049**	**3.212**			
TIME	**-0.938**	-0.731	**-0.965**		
TEMP	-0.602	-0.799	**-1.160**	0.036	
PH	0.784	0.520	-0.156	-0.137	0.338

Polyphosphate accumulation

Table 47. Effects matrices for polyP accumulation in *C. reinhardtii* from 0-6 h (left) and 6-24 h (right).

0-6 h

	PHOS	LIGHT	TIME	TEMP	PH
PHOS	**0.5608**				
LIGHT	-0.0464	0.0906			
TIME	0.2187	0.1168	0.1679		
TEMP	-0.2477	-0.1636	-0.2573	0.0062	
PH	-0.0193	0.0167	0.0975	0.1115	0.2009

6-24 h

	PHOS	LIGHT	TIME	TEMP	PH
PHOS	-0.0329				
LIGHT	-0.0192	**0.1583**			
TIME	0.1333	-0.0527	0.1512		
TEMP	0.0611	-0.296	-0.0811	-0.0210	
PH	-0.0446	-0.0839	0.0069	-0.0073	0.0852

Table 48. Effects matrices for polyP accumulation in *C. vulgaris* from 0-6 h (left) and 6-24 h (right).

0-6 h

	PHOS	LIGHT	TIME	TEMP	PH
PHOS	-0.029				
LIGHT	0.069	**0.614**			
TIME	-0.160	-0.164	0.276		
TEMP	0.133	-0.115	-0.275	-0.181	
PH	-0.094	-0.382	-0.001	0.148	-0.209

6-24 h

	PHOS	LIGHT	TIME	TEMP	PH
PHOS	**0.447**				
LIGHT	**0.346**	**0.278**			
TIME	**0.217**	0.069	0.126		
TEMP	-0.063	-0.126	-0.157	0.024	
PH	0.025	0.059	0.163	-0.016	0.042

Table 49. Effects matrices for granule formation in *C. reinhardtii* from 0-6 h (left) and 6-24 h (right).

0-6 h

	PHOS	LIGHT	TIME	TEMP	PH
PHOS	**1.125**				
LIGHT	0.250	**0.875**			
TIME	**0.625**	**-0.625**	-0.250		
TEMP	0.375	-0.125	0.250	0.000	
PH	0.000	0.250	0.125	0.125	**-0.875**

6-24 h

	PHOS	LIGHT	TIME	TEMP	PH
PHOS	-0.625				
LIGHT	0.375	**-1.250**			
TIME	-0.750	0.625	-0.125		
TEMP	-0.875	0.250	0.125	0.250	
PH	-0.375	-0.500	0.375	0.000	0.750

Table 50. Effects matrices for granule formation in *C. vulgaris* from 0-6 h (left) and 6-24 h (right).

	PHOS	LIGHT	TIME	TEMP	PH
PHOS	0.188				
LIGHT	-0.063	**1.688**			
TIME	-0.563	-0.062	-0.312		
TEMP	-0.313	-0.062	0.688	-0.312	
PH	0.063	0.063	-0.188	0.063	-0.187

	PHOS	LIGHT	TIME	TEMP	PH
PHOS	0.750				
LIGHT	1.000	-0.625			
TIME	0.750	-0.625	-0.875		
TEMP	0.375	0.250	-0.250	0.250	
PH	0.375	-0.250	-0.250	0.125	-0.250

B.1.9 Verification of DW/OD ratio

These experiments were performed in the same manner as described above but with one full six-well microplate per time point (apart from 0 hours) to provide sufficient volume for OD and DW measurements (as described in Part 1).

The first of these was a 'positive control' in which the cultures were grown for 8 days on 'standard' minimal medium (309 mg $P \cdot L^{-1}$) to maintain P sufficiency throughout this period. The experiment was conducted in high light (160 µmol photons$\cdot m^{-2}s^{-1}$) and high temperature (30 °C) conditions, with a P repletion dose of 50.0 mg $P \cdot g\ DW^{-1}$.

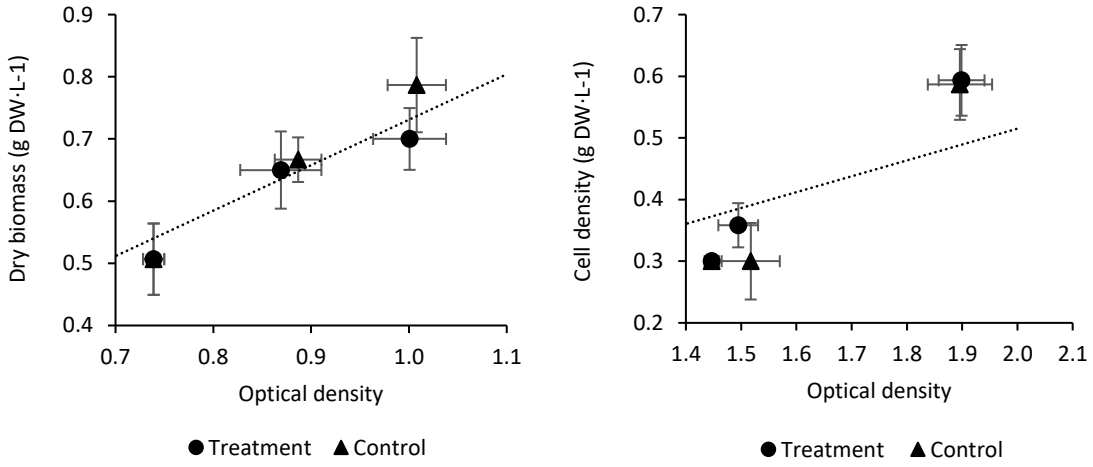

Figure 32. Dry weight vs optical density for P-replete cultures of *C. reinhardtii* (left) and *C. vulgaris* (right) in light at 30 °C.

Numbers indicate hours since phosphate addition (treatments). Dotted lines indicate the mean DW/OD ratio of the combined treatment and control groups.

For the second experiment, the cultures were P-depleted for 7 days and the experiment carried out in the same conditions as above (160 µmol photons$\cdot m^{-2}s^{-1}$, 30 °C, 7 days P depletion), effectively replicating the procedure used in the factorial experiments but with additional dry weight measurements.

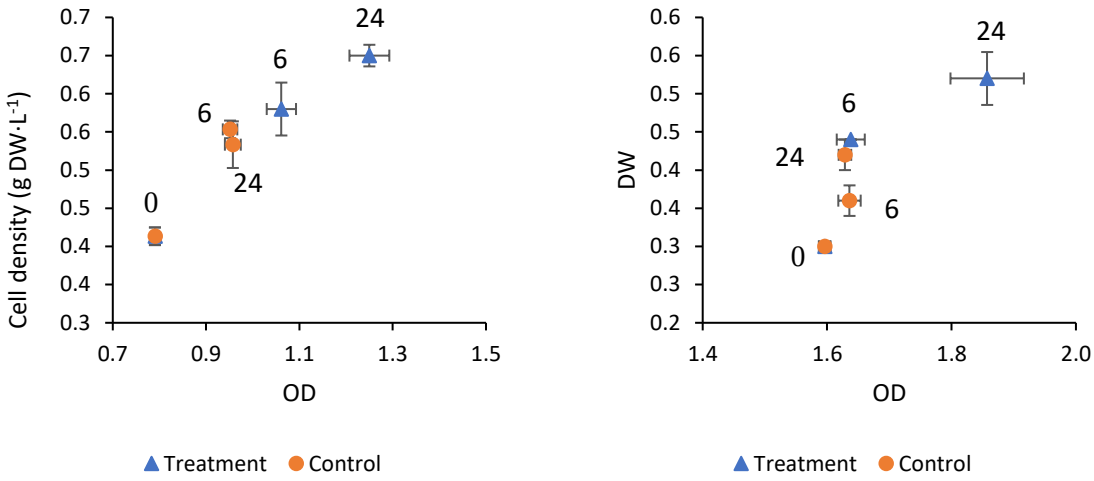

Figure 33. Dry weight vs optical density for P-depleted cultures of *C. reinhardtii* (left) and *C. vulgaris* (right) in light at 30 °C.

The third control experiment was conducted as above but in darkness. Growth was negligible (observed increases may be attributable to phosphate uptake) and optical density did not change appreciably in either treatments or controls.

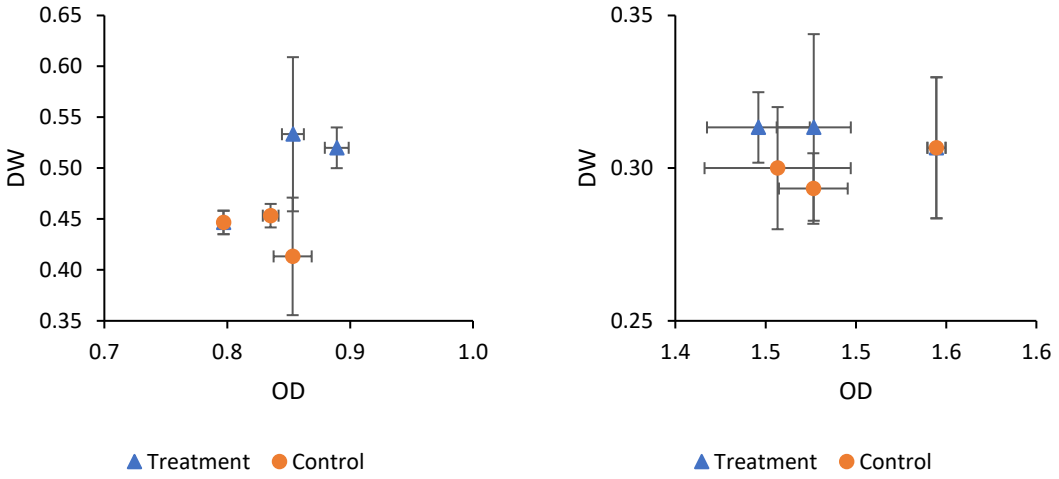

Figure 34. Dry weight vs optical density for P-replete cultures of *C. reinhardtii* (left) and *C. vulgaris* (right) in darkness at 30 °C.

Appendix C

C.1 RT-qPCR primers

Table 51. Primers used for RT-qPCR in Chapter 5 and Chapter 6.

Gene	Forward primer		Reverse primer		Source
	Name	Sequence (5′ to 3′)	Name	Sequence (5′ to 3′)	
PSR1	CrPSR1_F1	CAACAGCAGCAACAAGAGCA	CrPSR1_R1	ATCACCGAAGTCAAAGTCCC	Chang et al. (2005)
PHOX	CrPHOX_F1	TTCCGTTTCCGTTCTCTGAC	CrPHOX_R1	CCCTGCATCTTGTTCTCCAG	Chang et al. (2005)
LHCBM3	LHCBM3_2F	GCGTCGCGTCGTGATGGAGTT	LHCBM3_2R	CGGGACCGCGTAAACCACAAAC	González-Ballester et al. (2010)
VTC4	CrVTC4_F1	GACCAGGACAAGAAGGATGAC	CrVTC4_R1	GCCCAGGTAGTTGATGTTGA	This study
VTCX	CrVTCX_F2	GTCAACTAGGTCCTCCGAAATG	CrVTCX_R2	CTCTTGGTTGGCTGCTAGATAA	This study
VTC1	VTC1-1F	TAAGTCATATTTCGCCAACGAG	VTC1-1R	TGAACAGAGCGTAGCCCATGAT	Aksoy et al. (2014)
PTB2	CrPTB2_F1	TGTGCTCGTGCATTCTCTTC	CrPTB2_R1	CCCTTGGTGAACACGAAGTAA	Moseley et al. (2006)
PTB3	CrPTB3_F1	GCGAGAACTCCTACGTCCTG	CrPTB3_R1	AGTCCAGTCGCTGTTGGAAG	Moseley et al. (2006)
PTB5	CrPTB5_F1	CTCAACCCAGTTGGCAATTTACTTT	CrPTB4/5_R1	GCCTTGTTCGAGTCCCAGT	Moseley et al. (2006)
PTA3	PTA3-2F	TCGCATGGATGTTTGTTCTGTTC	PTA3-2R	GAACTGGAAGGTGTGGATGTACT	Plouviez et al. (2021)
CBLP	CBLP_2F	AAGATGGTCAAGGTCTGGAACCT	CBLP_2R	GTACAGGCGCTTGCCCTCAGCC	Aksoy et al. (2014)

C.2 Chapter 5 supporting information

C.2.1 RT-qPCR data

Table 52. Mean C_q values from 3 technical replicates except (a) only 2 replicates used and (b) only 1 replicate used.

#	Expt	Sample	*CBLP*	*PSR1*	*VTC4*	*VTCX*	*VTC1*	*PHOX*	*PTA3*	*PTB2*	*PTB3*	*PTB5*	*LHCBM3*
16	A	$R_1$0	30.64	31.09	29.18	32.06	33.81	28.63	35.03 [a]	27.94	28.48	32.77	24.46
30	A	$R_3$0	27.92	29.10	27.14	30.06	34.28 [a]	26.75	33.33	25.40	26.10	31.01	23.03
46	A	$C_1$1	27.21	31.17	26.05	31.13 [a]	29.50	29.15	30.84	23.52	24.47	29.55	22.64
52	A	$C_2$1	23.43	28.66	23.52	29.65	27.47	25.92	29.13	20.75	21.57	25.67	20.98
58	A	$T_1$1	24.27	30.27	24.25	30.85	28.73	27.10	29.27	20.87	22.27	27.86	22.47
64	A	$T_2$1	24.11	28.00	23.79	30.62	28.22	26.57 [a]	28.66	20.27	22.12	26.08	21.71
17	A	$C_1$24	32.78	32.34	30.50	30.50	35.82 [a]	27.71	36.47	30.43	28.52	32.06	24.48
35	A	$C_3$24	31.54	31.54	29.14	29.16	35.00	26.40	34.22	28.93	27.11	31.64	23.20
21	A	$T_1$24	26.14	28.34	28.07	28.87	30.74	35.52	32.81	26.03	26.51	31.09	19.85
26	A	$T_2$24	26.61	28.81	29.40	30.21	32.80	36.76	34.81 [a]	27.69	27.57	32.60	21.29
24	B	$R_1$0	29.55	29.35	27.86 [a]	29.97	37.32	26.86	32.16	25.99	25.39	28.85	22.47
33	B	$R_3$0	29.61	30.28	28.53	30.74	33.50	27.85	33.11	26.48	26.20	30.53	23.56
44	B	$C_1$1	27.15	31.58	29.35	30.60	29.93	30.63	33.10	24.60	26.01	30.44	24.32
50	B	$C_2$1	22.77	28.21	27.35	27.66	27.60	27.02	29.47	20.73	21.93	26.19	21.67
56	B	$T_1$1	23.26	29.45	26.20	30.18	27.42	28.83	27.14	19.89	21.87	25.54	22.75
62	B	$T_2$1	24.54	32.63	29.06	32.13	28.94	29.95	27.55	21.63	23.48	28.08	24.84
9	B	$C_1$24	32.18	34.78 [a]	33.27 [a]	33.05	33.62	31.28	35.23 [b]	34.14 [a]	31.09	34.98	30.53
32	B	$C_3$24	29.16	30.36	28.67 [a]	29.86	32.82	27.16	32.56	30.45	27.31	30.51	28.74
20	B	$T_1$24	23.91	28.46	26.82	28.79	29.25	32.67	32.66	27.83	28.15	33.48	20.57
25	B	$T_2$24	23.94	28.26	26.42	28.57	28.66	35.14	32.50	27.38	28.36	33.04	20.55
6	C	$R_2$0	27.84 [a]	30.16 [a]	28.27 [a]	30.76	34.67	28.75	34.29	27.60	26.45	31.00 [a]	23.75
34	C	$R_3$0	27.90 [a]	30.73	28.26 [a]	31.17	34.64	28.04	33.82	27.50	27.20	31.85 [a]	24.57 [a]
47	C	$C_1$1	23.75	25.29	23.60	26.16	27.00	22.16	27.45	18.70	21.26	24.29	18.96
53	C	$C_2$1	23.91	26.98	24.04	26.66	27.10	23.64	28.11	19.49	22.55	25.76	20.16
59	C	$T_1$1	23.19	27.55 [a]	24.87	26.72	26.95	29.05	21.31	19.19	21.60	26.93	21.35

#	Expt	Sample	*CBLP*	*PSR1*	*VTC4*	*VTCX*	*VTC1*	*PHOX*	*PTA3*	*PTB2*	*PTB3*	*PTB5*	*LHCBM3*
65	C	$T_2$1	25.94	29.75	28.13	28.66	29.16	30.89	24.22	21.64	24.41	30.24	24.66
8	C	$C_2$24	27.23	27.63	28.21 [a]	29.08	30.71	30.73	31.31	22.81	25.44	28.10	20.65
14	C	$C_3$24	35.75	35.59 [b]	34.96 [a]	33.76	33.55	34.71 [a]	46.68 [b]	30.88	31.33	35.90 [a]	28.32
28	C	$T_1$24	26.05	28.25	29.84	29.70	31.09	24.37	37.97	25.57	25.11	29.18 [a]	21.66
36	C	$T_3$24	26.93	28.65	29.91 [a]	29.39	32.68	39.71 [b]	34.69	26.22	25.39 [a]	29.45 [a]	21.59
11	D	$R_1$0	31.83	33.32	30.74	32.87	35.67	31.94	33.91 [b]	31.99	29.55	33.75 [a]	26.53
2	D	$R_2$0	30.97	31.81	29.45	32.39	37.22	29.76	34.88 [a]	29.85	28.86	33.44	25.64
67	D	$C_3$1	27.73	30.71	26.19	33.21 [a]	30.49	28.71	32.13	23.50	24.82	28.17	24.15
49	D	$C_2$1	23.49	29.70	24.68	30.39	28.20	27.24	29.02	20.80	22.27	24.79	20.98
55	D	$T_1$1	22.90	29.00	24.28	30.89	26.41	25.41	26.61	18.36	20.13	24.34	21.10
61	D	$T_2$1	24.14	30.11	24.59	30.95	27.32	27.51	28.76	19.72	21.38	25.66	22.18
12	D	$C_1$24	31.24	31.84	29.01	30.62	38.65	27.19	33.39	28.09	27.71 [a]	32.28	22.11
13	D	$C_2$24	25.69	29.21	27.14	29.18	31.94	24.74	29.17	24.88	25.08	29.08	19.81
3	D	$T_1$24	26.38	28.98	28.78	28.56	31.25	35.53 [a]	32.94	28.35	28.38	33.46	18.63
4	D	$T_2$24	25.19	31.36	30.51	29.67	31.92	35.29 [a]	26.59	25.98	28.29	34.19	19.63
23	E	$R_1$0	26.91	29.95	27.93	30.24	34.11	31.44	33.76	28.23	25.77	30.52	23.18
29	E	$R_2$0	28.84	29.40	27.61	31.09	34.58	31.65	34.74	28.68	26.17	30.65	22.27
48	E	$C_1$1	24.00	30.11	24.85	31.29	26.84	29.14	31.44	22.11	22.74	26.14	20.67
54	E	$C_2$1	24.03	31.10	25.55	31.06	28.55	30.01	32.84	22.64	23.47	26.05	21.80
60	E	$T_1$1	23.23	30.59	23.34	30.31	25.62	27.72	29.42	19.37	21.19	24.56	21.25
66	E	$T_2$1	24.30	31.52	25.80	31.49	27.53	29.67	30.66	20.95	22.52	26.15	21.90
19	E	$C_1$24	25.32	28.73	28.93	30.23	31.13	34.03	30.45	26.78	24.72	29.49	23.20
10	E	$C_2$24	26.86	29.12	28.69	29.52	32.24	35.07	30.25	25.75	24.94	30.27	23.28
22	E	$T_1$24	24.46	30.22	30.84	30.40	31.06	37.90 [b]	29.07	24.76	26.09	31.24	23.56
27	E	$T_2$24	24.48	30.93	30.68	30.09	30.62	37.51 [b]	28.86	25.36	26.46	31.71	23.51
Mean primer efficiency[32]			1.74	1.88	1.89	1.90	1.87	1.87	1.92	1.90	1.91	1.89	1.91

[32] Calculated by the software (LinRegPCR) using data from the linear region of the log-fluorescence curve.

C.3 Chapter 6 supporting information

C.3.1 Optical density

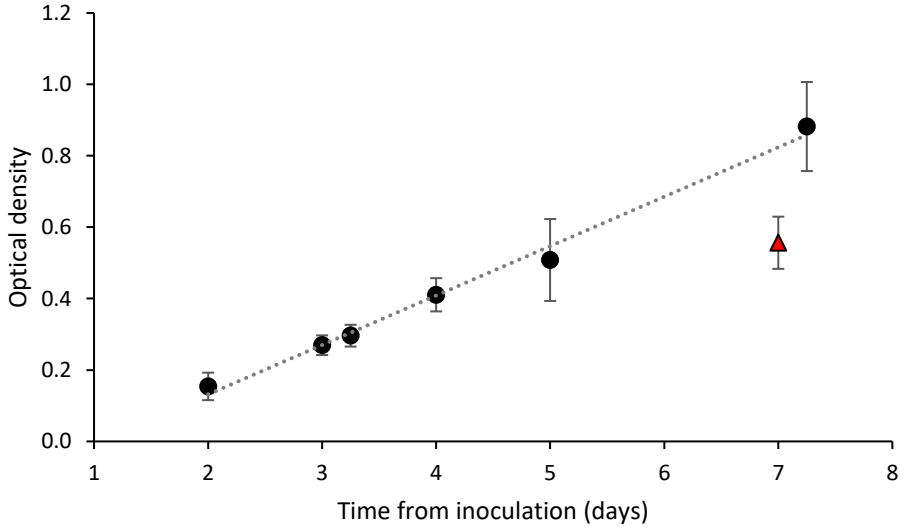

Figure 35. Mean optical density (± standard deviation) of replicate control cultures (n = 4) measured in triplicate. The point represented by a red triangle was assumed to be erroneous. A linear best fit (R^2 = 0.992) is shown for the remaining points.

C.3.2 RT-qPCR data

Table 53. Samples extracted, RNA yields and quality ratios, and raw (mean) C_q data from the Chapter 6 experiment.

#	Sample [a]	Extracted RNA (DNAsed)			Raw C_q data (means of 2 technical replicates, except ones in red = 1 only)							
		Yield (ng) [b]	A_{260}/A_{280} [c]	A_{260}/A_{230} [d]	*CBLP*	*PSR1*	*VTC4*	*VTCX*	*VTC1*	*PTA3*	*PTB2*	*PTB5*
1	3d $R_3$0	268	1.96	1.85	26.96	30.81	28.45	29.50	30.63	30.09	24.87	31.64
2	3d $R_4$0	176	1.83	1.57	26.46	30.02	28.84	28.78	30.91	30.61	25.21	30.45
10	7d $L_3$1	606	1.76	1.41	26.28	34.24	33.60	31.83	27.71	27.51	23.00	30.52
11	7d $H_1$24	12915	2.08	2.16	17.76	26.83	27.53	28.68	26.59	29.96	23.71	27.36
13	7d $H_4$24	11690	1.93	2.34	18.28	27.18	26.67	27.89	26.11	29.10	23.01	27.19
14	7d $L_2$24	7880	1.96	2.16	17.78	26.79	25.93	27.74	25.06	30.02	20.26	25.59
15	7d $L_4$24	11640	2.06	2.14	19.02	27.37	26.99	28.43	27.25	30.04	22.23	27.52
17	3d $L_3$1	666	1.91	1.67	28.98	n/d	31.43	29.99	30.73	27.96	25.55	31.69
18	3d $H_3$1	726	1.98	2.02	27.59	34.80	29.99	29.03	29.05	26.49	23.16	29.96
19	3d $L_3$24	54	2.13	0.73	28.53	30.76	29.84	30.84	32.42	31.19	26.10	30.46
20	3d $H_4$24	160	1.98	1.79	25.70	29.66	28.86	29.87	30.66	30.44	24.55	29.66
21	7d $H_3$1	442	1.90	2.18	25.85	*35.35*	35.59	33.02	27.15	26.74	23.22	30.97
24	7d $L_4$1	282	1.72	2.42	26.19	31.13	32.90	30.78	27.79	27.70	22.92	30.51
26	7d $C_2$24	189	1.85	2.13	22.37	27.78	27.76	28.29	28.31	29.74	22.24	23.73
28	2d R_2	615	1.88	1.18	30.30	32.03	29.83	30.99	32.47	31.05	26.30	32.97
29	2d R_3	708	1.91	1.90	29.63	31.87	31.68	30.73	32.86	32.40	28.41	34.00
30	3d $C_2$1	1065	1.88	1.78	22.33	27.82	28.27	28.81	28.11	29.96	24.83	26.62
31	5d R_1	78	1.91	1.16	26.02	29.14	31.27	29.16	30.77	32.13	26.57	26.98
35	7d $L_1$24	9050	1.92	2.29	18.00	27.38	25.81	27.85	25.63	29.59	21.45	25.61
36	7d $H_2$24	9695	1.97	2.26	18.48	27.53	27.56	28.45	26.11	29.96	23.44	27.50
37	7d $H_4$1	1102	1.79	1.43	19.25	33.58	34.83	34.03	25.12	26.10	22.96	29.60
38	7d $L_2$1	1594	1.85	1.74	20.11	31.92	33.06	33.24	26.12	27.35	23.92	29.15
39	7d $C_4$1	1368	1.74	1.03	28.66	33.10	32.70	30.66	32.58	32.14	27.37	30.58
40	7d $R_1$0	1050	1.99	1.84	25.22	27.38	31.34	*30.94*	32.30	33.09	*28.04*	27.71

#	Sample [a]	Extracted RNA (DNAsed)			Raw C_q data (means of 2 technical replicates, except ones in red = 1 only)							
		Yield (ng) [b]	A_{260}/A_{280} [c]	A_{260}/A_{230} [d]	*CBLP*	*PSR1*	*VTC4*	*VTCX*	*VTC1*	*PTA3*	*PTB2*	*PTB5*
42	3d $L_4$24	530	1.90	1.64	24.17	32.08	34.26	34.26	n/d	n/d	29.98	33.11
43	3d $C_2$24	1652	1.91	1.74	24.45	28.05	29.93	27.22	32.14	30.04	25.74	28.41
46	3d $L_4$1	1992	1.76	1.71	22.75	34.87	32.40	31.86	30.57	29.40	25.94	31.49
49	7d $C_3$1	726	1.92	1.55	27.33	30.04	28.24	26.99	29.03	30.87	23.04	28.47
50	7d $C_1$24	828	1.80	1.36	20.24	26.36	26.64	28.52	20.61	22.28	22.86	24.03
51	3d $C_4$24	582	1.93	1.98	26.76	29.11	29.84	30.40	31.53	31.65	26.08	29.90
52	3d $H_2$24	732	1.89	1.61	24.62	27.89	30.42	29.74	31.89	31.22	25.79	28.81
54	5d R_4	650	1.84	1.54	26.21	28.80	33.34	28.99	31.58	33.17	*27.66*	27.53
55	3d $L_2$1	1754	1.91	1.86	25.91	32.49	30.88	28.71	30.18	28.69	25.09	28.88
56	3d $H_2$1	1426	1.96	1.91	25.95	32.34	30.67	27.34	29.10	28.12	23.66	29.09
57	7d $R_4$0	528	1.89	1.06	25.09	28.37	*28.01*	29.09	31.01	31.64	*25.97*	27.55
58	7d $H_2$1	1046	1.73	1.42	22.27	n/d	*37.35*	*36.06*	29.97	30.56	27.21	32.94
59	7d $C_4$24	1080	1.76	1.13	29.92	34.60	33.43	31.73	n/d	33.43	28.91	31.30
60	7d $C_1$1	538	1.90	1.67	26.97	30.20	28.72	27.85	29.17	30.65	23.72	28.41
Mean primer efficiency[33]					1.74	1.86	1.72	1.87	1.83	1.89	1.89	1.88

[a] Naming convention: Xd A_bC, where X is the P depletion time (days), A is the P treatment (R: replicate; C: control; L: low; H: high), b is the replicate number, and C is the time (hours) from P repletion.

[b] Yield calculated from the volume after DNAsing and concentration measured using Nanodrop.

[c,d] Spectrophotometric ratios used to evaluate RNA purity.

n/d: Not detected.

Note: Several samples were removed from the analysis due to low primer efficiency and the melt curve analysis indicating the presence of off-products with a low melting point, possibly indicating reagent carry-over interfering with the binding of the fluorescent dye.

[33] Calculated by the software (LinRegPCR) using data from the linear region of the log-fluorescence curve.